Pathogenesis of Malignant Catarrhal Fever in Cattle

Thesis submitted in accordance with the requirements of the University of Liverpool for the degree of Doctor in Philosophy

By

Mohammed Hamzah Abdulkadhim Al-Saadi

September 2018

Author's Declaration

Apart from the help and advice acknowledged, this thesis represents the unaided work of the author

……

Mohammed Hamzah Abdulkadhim Al-Saadi

September 2018

This research was carried out in the Department of Infection Biology and School of Veterinary Science, University of Liverpool.

Supervisor’s Certification

We certify that the thesis entitled “Pathogenesis of Malignant Catarrhal Fever in Cattle" was prepared under our supervision at the Department of Infection Biology, Institute of Infection and Global Health, Faculty of Health and Life Sciences, University of Liverpool as partial fulfilment of the requirements of University of the Liverpool for the degree of Doctor in Philosophy.

Signature:

Name: Prof James Stewart

Title: Chair of Molecular Virology

Address: Department of Infection Biology

Institute of Infection and Global Health

University of Liverpool

Liverpool Science Park IC2

146 Brownlow Hill

Liverpool L3 5RF

E-mail: j.p.stewart@liverpool.ac.uk

Date:

Acknowledgements

I would first like to thank Allah for his grace upon me and guidance throughout my life to reach this point. It was big challenge for me. However, many people have been supporting me in this intensive journey. Therefore, I would like to reflect my gratitude to those who helped and stand with me in my PhD.

I would like to express my sincere gratitude to my supervisors; Professors James Stewart and Anja Kipar for their scientific supervision and support. I shall never forget the favour for opportunities you have given me to finish my PhD. Your supervisions supported me during my research and writing of this thesis; Many appreciations for you.

Special thanks to Dr George Russell, David Griffiths and Mara Rocchi of the Moredun Research Institute for providing LGL cells, DNA samples and MCF serum. These were really helpful for me to achieve my targets. Also, big thanks to Dr Piotr Kubi´ of National Veterinary Research Institute, Department of Biochemistry, Poland for providing a reconstructed BoHV-6 plasmid.

I would like to acknowledge the members of my department, the Infection Biology of IGH, at the University of Liverpool for their help and support. I am also grateful to the staff senior technician: Mrs Catherine Hartley that provided a prosperous work environment in our laboratory.

Many sincere thanks to my sponsor, University of Al-Qadisiyah, Ministry of Higher Education and Scientific Research in Iraq (MOHESR), the Iraqi Cultural Attaché, London for providing this opportunity and supporting me financially and enabling me to obtain this degree.

Last but not least, I wish to exhibit my gratitude to my family that without their help I could not have such a successful study.

Thank you very much everyone!

Pathogenesis of Malignant Catarrhal Fever in Cattle

Mohammed Hamzah Abdulkadhim Al-Saadi

Abstract

Malignant Catarrhal Fever (MCF) is a fatal disease of cattle. The principal aetiological agent is ovine herpesvirus 2 (OvHV-2). It is carried by sheep that act as an asymptomatic reservoir host. The disease is characterised by complicated pathogenesis with no preventive vaccine.

Previous studies in our laboratory have shown that cattle without MCF can carry OvHV-2, indicating other factors, possibly herpesviruses are involved in MCF. Therefore, the aim of this study was to investigate OvHV-2 and other related ungulate herpesviruses. To do this, we investigate γ-herpesviruses in both asymptomatic and MCF hosts by recruitment of two PCR formats (PAN-herpesvirus consensus and Real time PCR) as qualitative and quantitative approaches. The results showed for the first time that, although the related bovine herpesvirus 6 and ovine herpesvirus 1 are endemic commensals of cattle, they could afford cross-protection from infection with OvHV-2 and development MCF.

OvHV-2 latency could also act a key factor in MCF-triggering. Therefore, a toolkit including antisera against OvHV-2 latency-associated nuclear antigen (oLANA) was produced in this study to demonstrate the latency *in situ* in cells of OvHV2-infected sheep, cattle without MCF, and cattle with MCF, using immunohistochemistry (IHC). The results demonstrated abundant OvHV-2- latency in epithelial and endothelial cells as well as leukocytes, regardless of species and disease. This finding could open new areas for the diagnosis and pathogenesis of MCF- latency.

Modified vaccinia Ankara (MVA) is an attenuated virus derived from vaccinia that was developed during the smallpox eradication programme. The technology for producing recombinant MVA expressing foreign proteins is available. It has a known safety profile and recombinant MVAs expressing proteins from other pathogens are already being used as vaccines/vaccination candidates in man and other animals. We have generated MVA recombinants expressing OvHV-2 gB and gH/L as vaccine candidates for protection against the development of MCF in ungulates. These vectored-subunits generated antibodies to the native proteins after infection of mice. Therefore, they could represent logical vaccines in the future. Our results give critical insight into the pathogenesis and prevention of MCF.

List of contents

Table of Contents

List of Figures

List of Tables

List of Abbreviation

APC	Antigen presenting cells
AP	Ammonium persulfate
BALT	Bronchus associated lymphoid tissue
Bison LHV	Bison lymphotropic herpesvirus
bp	Base pair
BoHV-6	Bovine herpesvirus-6
BSA	Bovine serum albumin
CpHV-2	Caprine herpesvirus-2
DAB	3,3'-diaminobenzidine
DABI	4, 6 diamindino-2-phenylindole HCl
ddH_2O	Distilled de-ionized water
DMEM	Dulbecco's modified Eagle's medium
DNA	Deoxyribonucleic acid
DTT	Dithiothreitol
ELISA	Enzyme linked immunosorbent assay
EBV	Epstein-Barr virus
EDTA	Ethylenediaminetetraacetic acid
FBS	Fetal bovine serum
FITC	Fluoroscein isothiocyanate
GFP	Green fluorescent protein
HRP	Horseradish peroxidase
h	Hour
IF	immunofluorescent
Ig	Immunoglobulin
IHC	immunohistochemistry
IF	Interferon
IL	Interleukin
IPTG	Isopropyl-ß-D-thiogalactopyranoside
KSHV	Kaposi's sarcoma-associated herpesvirus
KB	Kilo base
KDa	Kilo Dalton
LGL	Large granular lymphocyte
LANA	Latency Associated Nuclear Antigen
LB	Luria Bertani
M	Molar
MAb	Monoclonal antibody

MCF	Malignant catarrhal fever
MEM	Minimum Essential Medium
MHC	Major histocompatibility complex
MOI	Multiplicity of infection
mRNA	Messenger ribonucleic acid
µl	Microliter
µm	Micrometer
ml	Milliliter
Mm	Millimole
min	Minute
n	Sample number
ORF	Open reading frame
OD	Optical density
oLANA	OvHV-2-Latency associated nuclear antigen
OvHV-1	Ovine Herpesvirus-1
OvHV-2	Ovine Herpesvirus-2
PBS	Phosphate buffered saline
PFU	Plaque forming unite
PAGE	Polyacrylamide gel electrophoresis
PAb	Polyclonal antibody
PCR	Polymerase chain reaction
qPCR	Quantitative polymerase chain reaction
PVDF	Polyvinylidene difluoride
RNA	Ribonucleic acid
RT	Room temperature (25 °C)
SPA	Sheep Pulmonary Adenomatosis
SMC	Smooth muscle cells
SDS	Sodium dodecyl sulphate
TAE	Tris acetate EDTA
TBE	Tris borate EDTA
TBS	Tris boric saline
TEB	Tris EDTA buffer
TBST	Tris-buffered sulphate tween
U	Unite
v/v	Volume per volume
w/v	Weight per volume
x *g*	x gravity

1. Chapter one: Introduction

1.1 Herpesviruses

Herpesviruses are enveloped double stranded DNA viruses that are responsible for numerous human and veterinary diseases. All herpesvirus members share similar biological structure. However, their pathological effect and tropism are variable due to viral- host interactions by which herpesviruses have evolved a sophisticated mechanism to control host cells and switch between lytic and latent cycles for life-long viral survival (Griffin *et al.*, 2010).

1.1.1 Herpesvirus classification

Herpesviruses have characteristic epidemiological, biological and genetic features (Kimura, 2018). The order herpesvirales is split into three main families according to their pathogenicity and host-replication behaviour: *Alloherpesviridae*, *Herpesviridae* and *Malacoherpesviridae.* The Herpesviridae family is divided into three subfamilies: *Alphaherpesvirinae*, *Betaherpesvirinae*, and *Gammaherpesvirinae*. Nowadays, developments of

the molecular and biochemical techniques have helped in determining herpesvirus taxonomy. However, numerous species within the family, subfamily, and genus are still unassigned (Davison, 2010).

1.1.2 Biological properties of Herpesviridae

1.1.2.1 Alpha-herpesviruses

Alpha-herpesviruses can infect many of hosts including mammals (human and animal), birds, and reptiles. This subfamily has wide cell type tropism (neuronal and epithelial cells). Establishment of latency occurs inside sensory nerve ganglia. Alpha-herpesviruses are subdivided into Simplexvirus and Varicellovirus genera of which Herpes simplex virus-1 (HSV-1) and Varicella zoster virus are well presented prototypes respectively (Modrow *et al.*, 2013).

1.1.2.2 Beta-herpesviruses

Beta-herpesviruses have narrow cell type spectrum (lymphoid cells, kidney, and secretory glands). These viruses replicate in vitro slowly. Beta-herpesviruses can induce cytomegaly inside infected cells (appear enlarged). Importantly, these viruses can establish the latency inside immune cells associated with monocyte series (Modrow *et al.*, 2013).

1.1.2.3 Gamma-herpesviruses

Gamma-herpesviruses have a very restricted host tropism, related within a family or order of a natural host. The period of replication cycle is variable according to the virus type. These viruses have a specific cell type tropism (either B or T lymphocytes). For instance, Epstein-Barr virus (EBV) can establish latency inside B lymphocytes whereas saimiriine herpesvirus infects T lymphocytes latently. Lytic replication occurs in other cell types such as fibroblast, epithelial, and endothelial cells (Modrow *et al.*, 2013).

1.1.3 Herpesvirus structure

Herpesvirus particles have a diameter of 150-200 nm, composed of three structural parts: nucleocapsid that has icosahedral geometry that encloses the viral genome, which is large (120-230 kb in size); an envelope that consists lipid bilayer carrying glycosylated proteins. The space between them that is filled with a proteinaceous matrix known as tegument (Figure 1-1) (Modrow *et al.*, 2013). The genome of herpesviruses is complex with unique and repeated regions. The DNA is double-stranded and linear, but during latency, it circularized as an episome. This episome remains inside the nucleus and maintains itself by tethering into host chromosome during genomes segregation into daughter cells during cell division (Stenglein *et al.*, 2009).

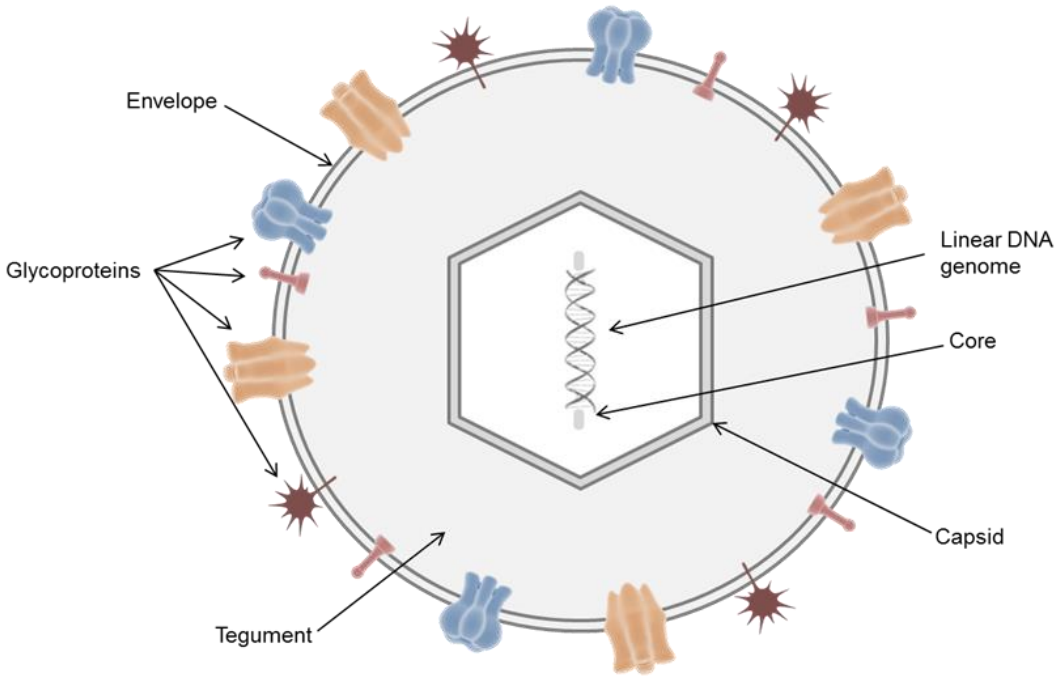

Figure 1-1. Schematic diagram depicts the structural components of herpes simplex virus, adopted from (Modrow *et al.*, 2013).

1.1.4 Herpesvirus genomes

Herpesvirus DNA genomes are constituted of linear and double stranded DNA that organised in number of ORFs which encode proteins ranging from about 70 to more than 200. All herpesvirus members contain unique and repeated sequences. These repeats are variably organised according to the genera of the herpesviruses. In herpesvirus simplex 1 and 2 (a prototypes of α-herpesviruses), the genome contains long and short segment. Each one constitutes of a long and a short unique sequence region. These are flanked by inverted repeats. In gamma-herpesviruses, the identical terminal sequence is repeated at both ends of the genome such in KSHV. In some members such as EBV, additional internal unrelated repeat sequences (internal repeats) are present within the genome (Modrow *et al.*, 2013).

1.1.5 Herpesvirus infection

The most characteristic feature in herpesvirus biology is their ability to form lytic and latent infection through complex interactions within host cells. These two biological forms are controlled by numerous enzymes that effect viral nucleic acid metabolism and replication (Minarovits *et al.*, 2007). Herpesviruses have also numerous evasive strategies to avoid the host immune system. This mainly occurs by suppression of the MHC class I and II which is responsible for processing and presentation of virus-derived antigens on the surface of infected cells (Griffin *et al.*, 2010; Zuo & Rowe, 2012). Recently, it has been shown that herpesviruses can also utilise the

host exosomes as a pathway to infect host cells (Sadeghipour & Mathias, 2017).

The infection is initiated by viral attachment and binding to specific host receptors then the viral entry is initiated (Spear *et al.*, 2000). The capsid structure translocated via the microtubules into the host nuclear pores where viral genome can be injected into the nucleus (Cohen *et al.*, 2011). After that viral DNA enters the nucleus, a highly controlled cascade of gene expression occurs in three kinetic stages: immediate early, early, and late. These stages are linked to viral DNA replication and viral encapsidation. The latter induced via covering the capsid by shell originated from the inner nuclear membrane then replaced by the vesicular membrane of the *trans*-Golgi apparatus. This leads to modify the envelop proteins by enzymes produced within these organelles. All these complicated steps resulted finally to enveloped the viral particle to egress from host cell membrane by cell to cell and exocytosis. Consequently infect other cells (Stenglein *et al.*, 2009). Viral transmission occurs in numerous ways, including direct contact of infected mucosal secretions, tissue transplantation, and blood transfusion (Münz, 2016).

1.1.5.1 Human herpesviruses

Human herpesviruses can cause symptoms ranging from neuropathy to cancer (Britton & Jones, 2014). Humans are susceptible to infection by eight species of herpesviruses (Table 1-1) and have been extensively studied. The severity of pathogenesis and duration are variable according to the viral species. For instance, HSV-1 can cause cold sores and keratitis, while Human cytomegalovirus induces systematic symptoms. In contrast,

EBV is ubiquitous in humans. It replicates in lymphoid tissues and persists in a latent form inside memory B cells. Also, it can cause several types of human malignancy (Bouvard *et al.*, 2009). The aim of this section is to review what is known about human herpesviruses with emphasis on HSV and KSHV as prototypes for the lytic and latent infection.

Table 1-1. List of human herpesviruses with their relevant diseases, adapted from (Jha *et al.*, 2016; Sadeghipour & Mathias, 2017).

Herpesvirus		Disease
Alpha-herpesviruses	Herpes simplex-1	Cold sores
	Herpes simplex-2	Genital infection
	Varicella zoster virus	Chicken pox
Beta-herpesviruses	Human cytomegalovirus	Systemic disease
	Human herpesvirus-6	Fever and rash in young and mononucleosis in old
	Human herpesvirus-7	Pityriasis rosea
Gamma-herpesviruses	Epstein-Barr virus	Infectious mononucleosis T-cell lymphoma T/NK cell lymphoma Gastric carcinoma Breast cancer Burkitt's lymphoma Hodgkin's lymphoma
	Kaposi's sarcoma herpesvirus	Kaposi sarcoma Primary effusion lymphoma AIDS-related lymphoproliferative disorder

1.1.5.1.1 Lytic infection

One of the best studied alpha-herpesvirus for lytic infection is herpes simplex virus (HSV). Initial infection normally occurs at an early age and by close contact. It results in the establishment of sensory neuronal latency from which the virus can replicate and cause recrudescent disease whenever the immune system is suppressed (Tabery, 2010). The initial infection is normally localised within the oral or genital mucosa, then the viral particles pass along the neuronal axons into ganglionic nuclei where latency is established as an extrachromosomal episome. At this stage, it can stay dormant till viral reactivation (Whitley, 2014).

There is a wide range of viral proteins that are encoded by the huge genomic coding capacity for herpesvirus biology. As in all other viruses, these proteins can be categorised as structural and non-structural that are necessary for successful replication (Adler *et al.*, 2017).

In the structural proteins, unlike some other viruses, herpesviruses have more than one glycoprotein embedded in its envelope. These glycoproteins play an important role in host cell entry (endocytosis or fusion of plasma membrane). The common glycoproteins found in all herpesviruses members are gB, gH, gL, and gM. However, some herpesviruses have additional unique glycoproteins present in the host cell membrane and/or embedded within the virus envelope (Modrow *et al.*, 2013). Importantly, some glycoproteins are expressed as heterodimers such as gH/gL, to induce remodelling in host cell fusion activity and thus viral internalisation (Spear *et al.*, 2000). Additional glycoproteins such as gD are also recruited to perform

particular roles such as cell tropism specification, receptor binding and/or enhancing gH/gL binding (Eisenberg *et al.*, 2012).

The tegument component is another structural protein. This protein-rich layer is localised between the viral envelope and capsid structures. This layer contains many proteins which are thought to play important roles in the late, lytic, and immediate early gene expression after viral internalisation. The mechanisms of this perspective was reviewed by (Owen *et al.*, 2015) in HSV-1, where modulation of specific host cell factors involved in host innate immunity by Infected Cell Protein 0 (ICP0), which is an immediate-early protein. Another role of tegument includes delivering the viral capsid to the cell nucleus by directing microtubules through the retrograde mediation pathway, and also during envelopment of cytoplasmic capsids with host membrane at the final assembly stage (Cohen *et al.*, 2011).

1.1.5.1.2 Latent infection

Establishment of latency is characteristic in all herpesviruses, but host cell tropism and latency encoding-genes or proteins are variable. For instance, alphaherpesvirinae can establish latency in neuronal cells while betaherpesvirinae are harboured by monocytes; gammaherpesvirinae form latent infection in lymphocytes (Brunson *et al.*, 2016).

Human herpesvirus 8 (HHV-8) or Kaposi's sarcoma- associated herpesvirus (KSHV) has an efficient latency strategy (Purushothaman *et al.*, 2016). After early infection, the herpesvirus genome circularizes inside the nucleus and shuts off virus/host gene expression to avoid the host immune

response. However, specific virus/host proteins are still expressed to maintain viral activity for later steps.

Latency associated nuclear antigen (LANA) is one of the most abundantly expressed proteins that has a leading role in latency during infection (Minarovits *et al.*, 2007). LANA is encoded by Open Reading Frame 73 (ORF73) of γ-herpesviruses. It consists of three domains: N terminal domain, central domain and C terminal domain (Figure1-2) (Kelley-Clarke *et al.*, 2009). Because γ-herpesviruses are highly related, the amino acid sequence of the corresponding LANA protein exhibits a strong evolutionary relationship (Figure 1-3). The OvHV-2 LANA (oLANA) shows similar features to other related γ-herpesviruses. For instance, the C terminal domain is highly similar, while the central domain is highly acidic with variable length due to multiple tandem repeats. The N terminal region is highly polymorphic (Figures 1-4) (Hart *et al.*, 2007).

Latency maintenance in KSHV in host cells was reported by tethering the viral genome to the host mitotic chromosomes via binding the N terminal domain of LANA with host chromosomes while the C domain binds with the Terminal Region of the viral DNA (Kelley-Clarke *et al.*, 2009). LANA has been shown to be localised around the chromosomal centromeres, which is thought to assure equal viral genome segregation into each new daughter cell upon cell division (Kelley-Clarke *et al.*, 2007; Xiao *et al.*, 2010). However, super-resolution laser confocal and correlative fluorescence electron image analyses have also shown that the LANA of KSHV is localised randomly on the bodies of condensed chromosomes for efficient virus segregation during the mitotic phase (Rahayu *et al.*, 2016).

KSHV LANA contains nuclear localisation signals (NLS) (Figure 1-2); these unique sequences are responsible for LANA transport into the nucleus. This occurs through the phosphorylation by protein kinase A and cdc2- type kinase. Phosphorylation within the NLS leads to the nuclear import system to re-localise LANA protein to the nucleus (Verma *et al.*, 2007).

In KSHV latency, it was shown that LANA possibly modulates many of cellular factors. For instance, LANA can cause accumulation of a transcription factor known as β-catenin. This occurs by interaction of LANA with Glycogen Synthase Kinase 3 beta (GSK-3β) that is necessary for the phosphorylation of β-catenin. Thus, the degradation of this molecule leads to translocation of the cytoplasmic GSK-3β to the nucleus and consequently depletion of phosphorylated cytoplasmic β-catenin (Figure 1-5) (He *et al.*, 2010; Verma *et al.*, 2007). Moreover, KSHV also encodes a G-protein coupled receptor (vGPCR) homologue. This deregulates the expression of Wnt/β-catenin to support its nuclear accumulation then induce malignancy (Angelova *et al.*, 2014).

Latency can also be induced by repression of the transcriptional activity of Replication and Transcription Activator (RTA) which is encoded by ORF50 of KSHV. Interestingly, RTA is found to be self-regulating and thereby activates transcription for lytic cycle switching. Thus, inhibition of this pathway likely leads to induction of the persistency cycle (Deng *et al.*, 2000; Lan *et al.*, 2004).

A further strategy was found in LANA expressed by *Herpesvirus Saimiri* via modulating cell cycle regulatory proteins such as retinoblastoma protein (pRb) that is modulates the host cell cycle into the synthesis phase (s

phase) in which host DNA replication occurs to induce cell immortalisation by degradation of P53 (Borah *et al.*, 2004). In this case, host P53 plays a role as a tumour suppression factor. Therefore, LANA-P53 interaction in KSHV leads to oncogenesis due to down-regulation of P53 transcription. This occurs thorough ubiquitylation (Suzuki *et al.*, 2010) or phosphorylation and ubiquitylation of P53 (Cai *et al.*, 2012).

Recently, it has been found that LANA can also recruit host Polycomb Repressive Complexes (PRC1 and PRC2) to suppress lytic genes through after initial attachment to the viral genome (Toth *et al.*, 2016). Furthermore, LANA modulates cellular factors that are involved in cell cycle control such as: RING3/Brd2 and Brd4, that are commonly expressed in mammalian cells and have transcriptional roles (You *et al.*, 2006); other cellular factors are thought to have similar roles such as: Interferon-Inducible Protein, Acetyl Transferase pCBP and p300, and Id Proteins (Verma *et al.*, 2007). The mechanisms by which γ-herpesviruses can establish latency are sophisticated and not fully clarified.

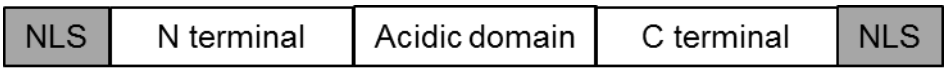

Figure 1-2. Schematic diagram shows the structure of LANA protein in KSHV. The nuclear localisation signals (NLS) are found in the N and C terminal domains which have a role in LANA-nuclear transportation. The acidic domain constitutes of several tandem repeats. The N terminal domain is highly polymorphic whereas the C terminal domain is highly conserved among gamma-herpesviruses.

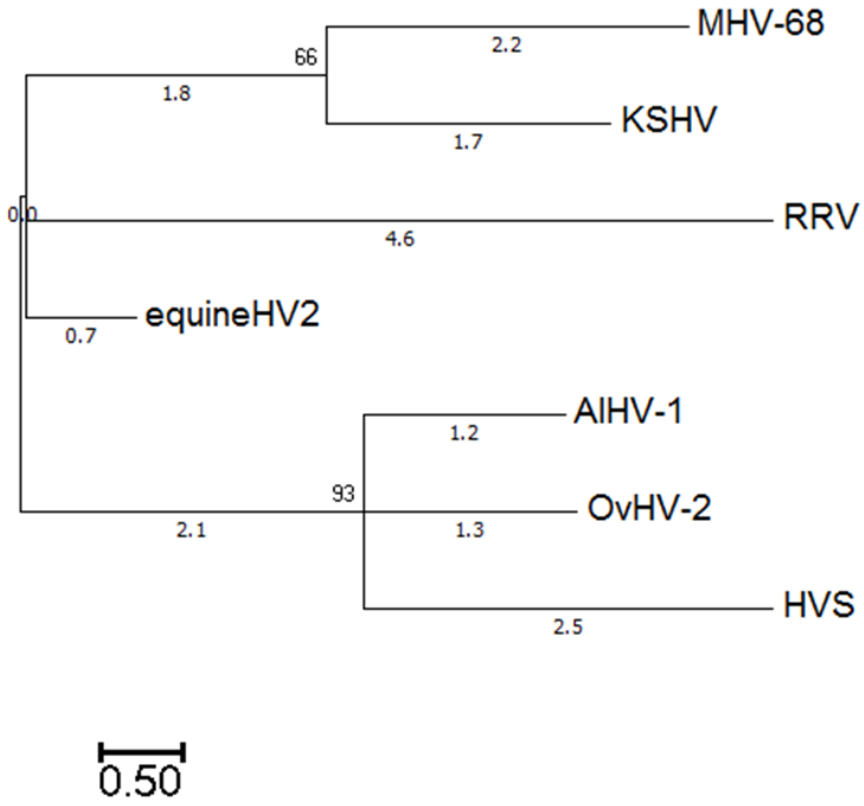

Figure 1-3. Diagram shows the evolutionary relationship of OvHV-2 AIHV-1, HVS, KSHV, RRV, MHV-68, and equine HV2. The sequences of LANA amino acid are deposited at gene bank under (AF410847.1, APB09494, AAC55944, AFQ99213, AAF60071, NP_044913, and AIU39518) accession number respectively. Maximum Likelihood method phylogram with Bootstrap analysis (1,000 replicates) to provide support for individual nodes was conducted by MEGA7 software, version 7.0.21 (Kumar *et al.*, 2016).

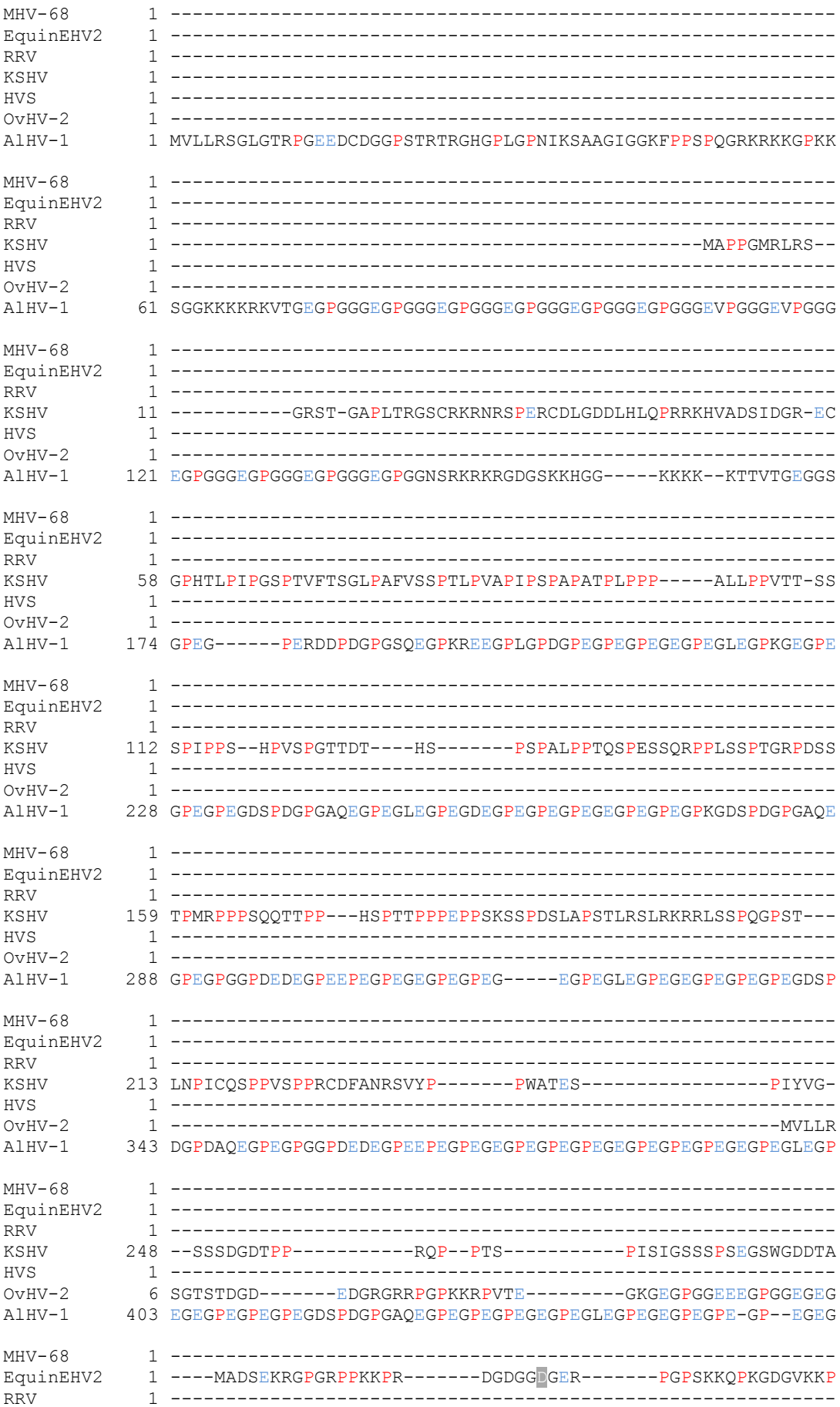
MHV-68 1 ----------
EquinEHV2 1 ----------
RRV 1 ----------
KSHV 1 ----------
HVS 1 ----------
OvHV-2 1 ----------
AlHV-1 1 MVLLRSGLGTRPGEEDCDGGPSTRTRGHGPLGPNIKSAAGIGGKFPPSPQGRKRKKGPKK
MHV-68 1 ----------
EquinEHV2 1 ----------
RRV 1 ----------
KSHV 1 ----------MAPPGMRLRS--
HVS 1 ----------
OvHV-2 1 ----------
AlHV-1 61 SGGKKKKRKVTGEGPGGGEGPGGGEGPGGGEGPGGGEGPGGGEGPGGGEVPGGGEVPGGG
MHV-68 1 ----------
EquinEHV2 1 ----------
RRV 1 ----------
KSHV 11 ----------GRST-GAPLTRGSCRKRNRSPERCDLGDDLHLQPRRKHVADSIDGR-EC
HVS 1 ----------
OvHV-2 1 ----------
AlHV-1 121 EGPGGGEGPGGGEGPGGGEGPGGNSRKRKRGDGSKKHGG-----KKKK--KTTVTGEGGS
MHV-68 1 ----------
EquinEHV2 1 ----------
RRV 1 ----------
KSHV 58 GPHTLPIPGSPTVFTSGLPAFVSSPTLPVAPIPSPAPATPLPPP-----ALLPPVTT-SS
HVS 1 ----------
OvHV-2 1 ----------
AlHV-1 174 GPEG------PERDDPDGPGSQEGPKREEGPLGPDGPEGPEGPEGEGPEGLEGPKGEGPE
MHV-68 1 ----------
EquinEHV2 1 ----------
RRV 1 ----------
KSHV 112 SPIPPS--HPVSPGTTDT----HS-------PSPALPPTQSPESSQRPPLSSPTGRPDSS
HVS 1 ----------
OvHV-2 1 ----------
AlHV-1 228 GPEGPEGDSPDGPGAQEGPEGLEGPEGDEGPEGPEGPEGEGPEGPEGPKGDSPDGPGAQE
MHV-68 1 ----------
EquinEHV2 1 ----------
RRV 1 ----------
KSHV 159 TPMRPPPSQQTTPP---HSPTTPPPEPPSKSSPDSLAPSTLRSLRKRRLSSPQGPST---
HVS 1 ----------
OvHV-2 1 ----------
AlHV-1 288 GPEGPGGPDEDEGPEEPEGPEGEGPEGPEG-----EGPEGLEGPEGEGPEGPEGPEGDSP
MHV-68 1 ----------
EquinEHV2 1 ----------
RRV 1 ----------
KSHV 213 LNPICQSPPVSPPRCDFANRSVYP-------PWATES----------PIYVG-
HVS 1 ----------
OvHV-2 1 ----------MVLLR
AlHV-1 343 DGPDAQEGPEGPGGPDEDEGPEEPEGPEGEGPEGPEGPEGEGPEGPEGPEGEGPEGLEGP
MHV-68 1 ----------
EquinEHV2 1 ----------
RRV 1 ----------
KSHV 248 --SSSDGDTPP----------RQP--PTS----------PISIGSSSPSEGSWGDDTA
HVS 1 ----------
OvHV-2 6 SGTSTDGD-------EDGRGRRPGPKKRPVTE---------GKGEGPGGEEEGPGGEGEG
AlHV-1 403 EGEGPEGPEGPEGDSPDGPGAQEGPEGPEGEGPEGLEGPEGEGPEGPE-GP--EGEG
MHV-68 1 ----------
EquinEHV2 1 ----MADSEKRGPGRPPKKPR-------DGDGGDGER-------PGPSKKQPKGDGVKKP
RRV 1 ----------

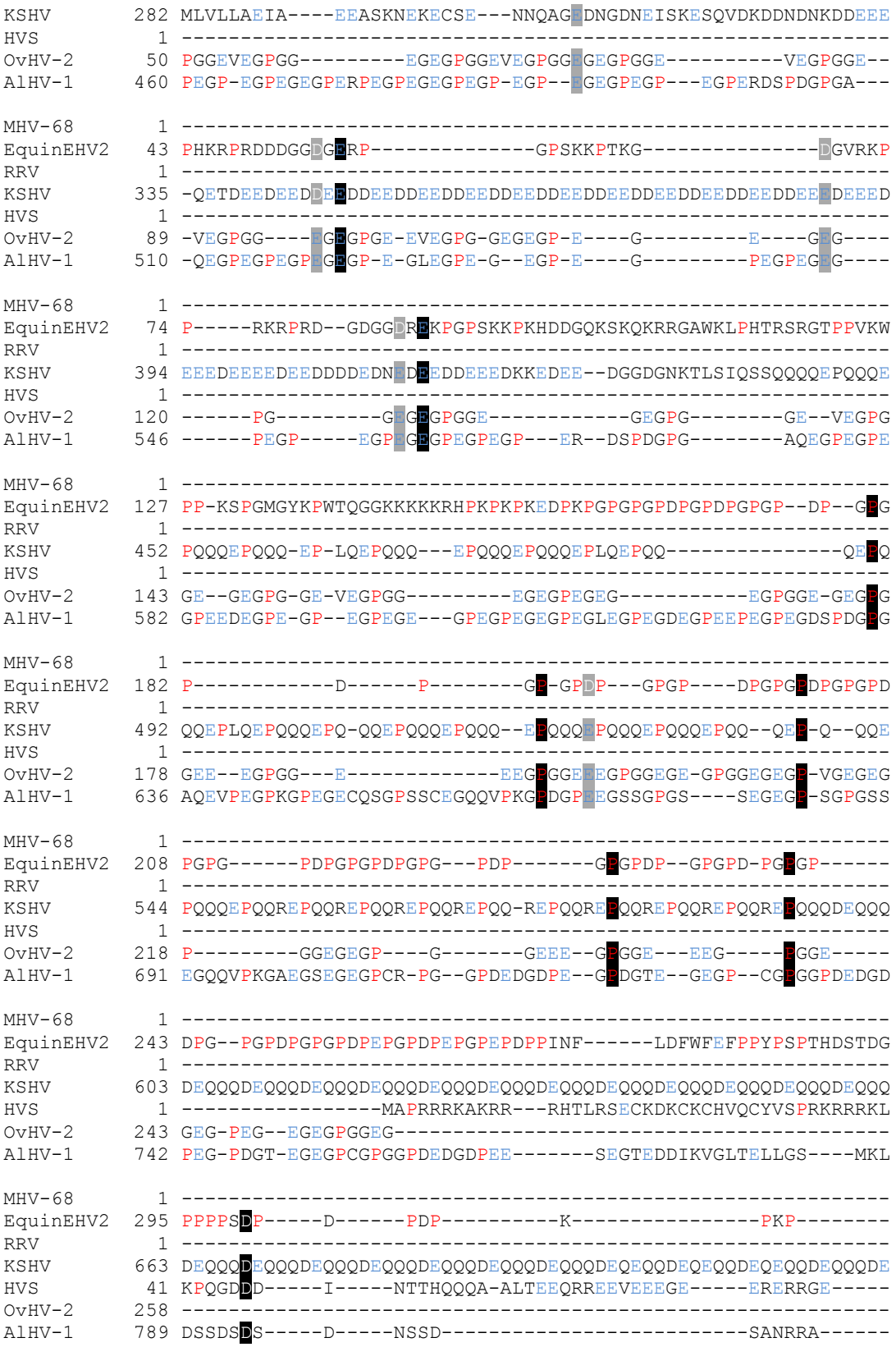

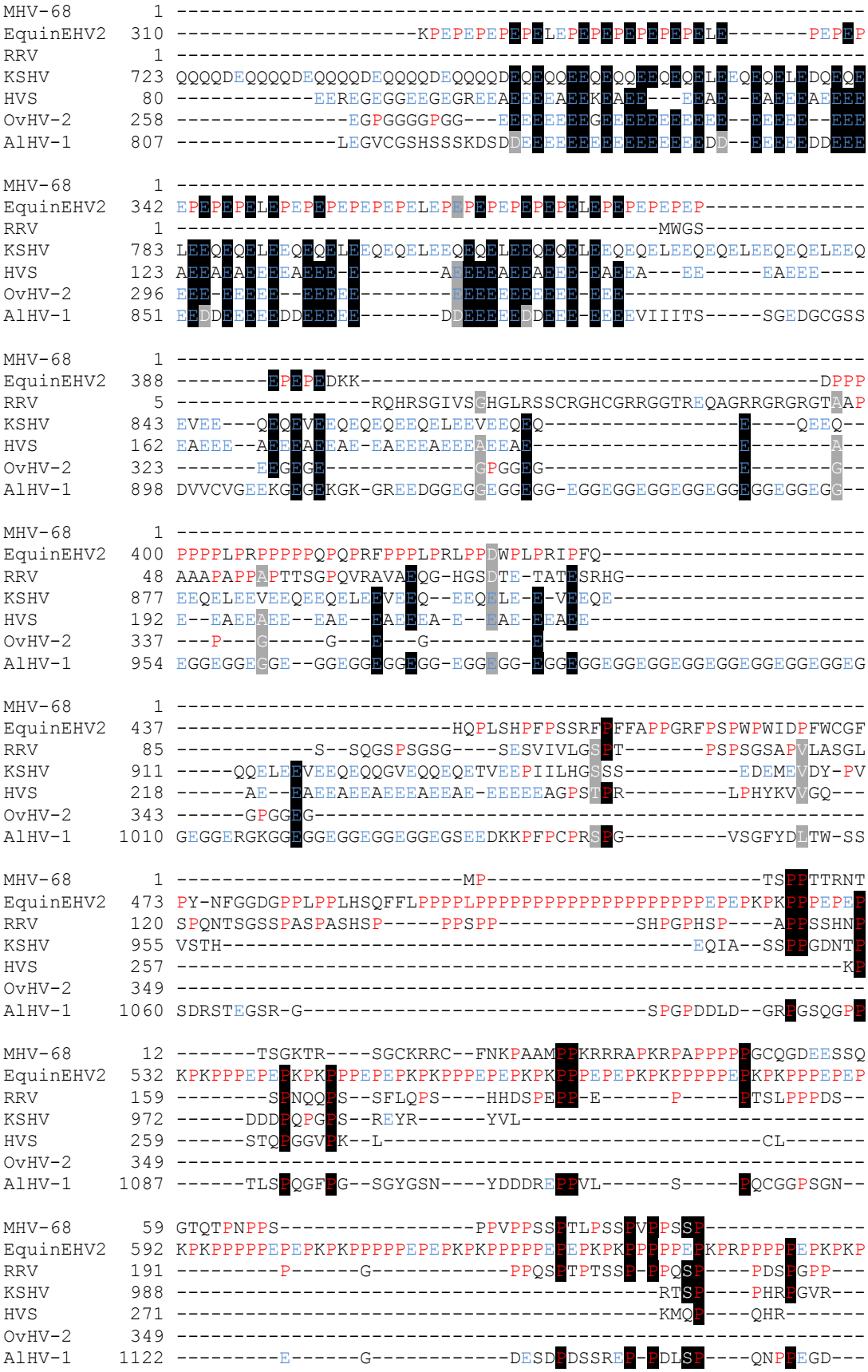
MHV-68
EquinEHV2
RRV
KSHV
HVS
OvHV-2
AlHV-1

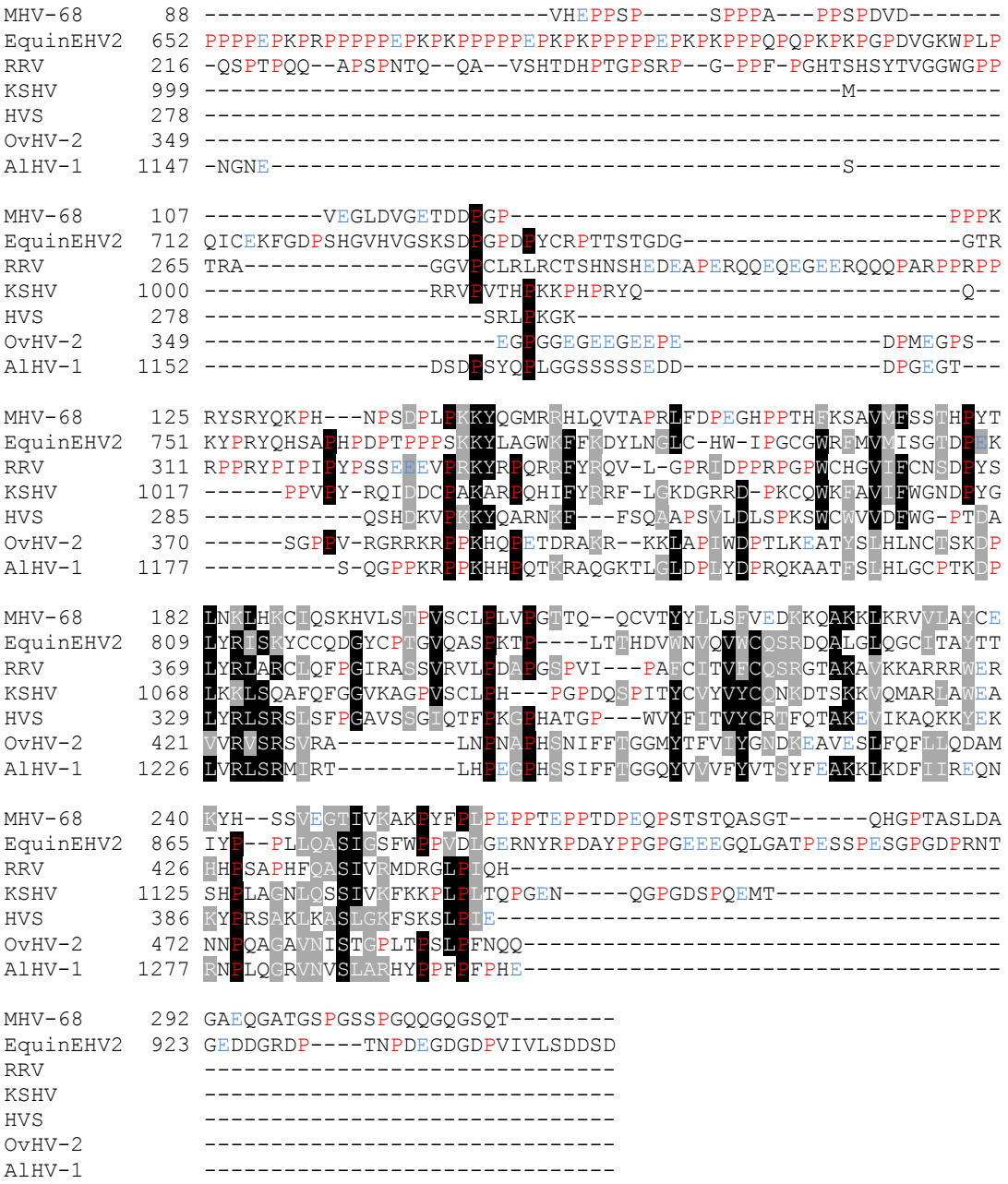

Figure 1-4. Alignment analysis of LANA amino acids homologue of different γ-herpesviruses including: MHV-68, Equine HV2, RRV, KSHV, HVS, OvHV-2, and AIHV-1, corresponded with GenBank accession numbers (NP_044913, AIU39518, NP_570820, ACY00477, NP_040275, AAL05844, and NP_065570) respectively. This was performed using “Clustal Omega” program and displayed by the “BOXSHADE” server. This highlights sequence diversity of LANA in which the highly identical residues (can be seen predominantly within C terminal homologue) are depicted in black. Similar residues are depicted in grey (appear mostly within N terminal homologue). The predominant tandem repeats appear within the central domain of LANA. The Glutamic acid is coloured in blue while the Proline are highlighted red.

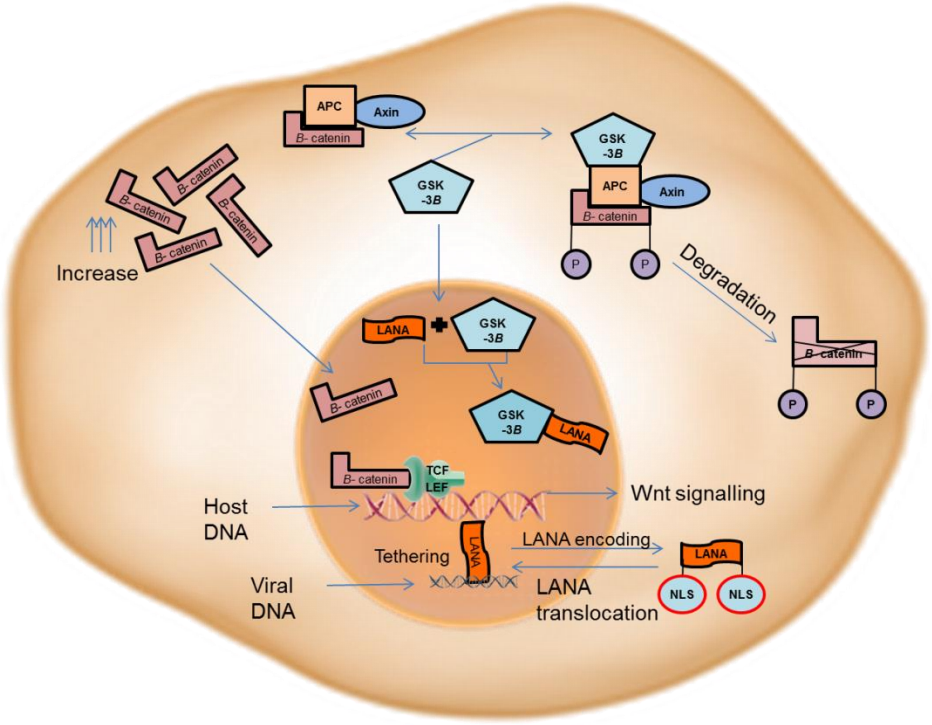

Figure 1-5. Schematic diagram shows tethering of viral genome with host chromatin. The stable expression of LANA into host cytoplasm leads to translocate into nucleus by NLS to maintain viral latency, at the same time LANA modulates Wnt signals by binding to GSK-3B, moving it into the nucleus. Thus, the level of cytoplasmic GSK-3B declined, resulting in accumulation of non-phosphorylated *B*- catenin, leading to translocate it to the nucleus to associate with LEF and TCF family protein of transcription agents. This is one example of how LANA maintains viral latency and modulates host gene transcription. Adopted from (Verma *et al.*, 2007).

1.2 Herpesvirus infection in ruminants

There is wide range of herpesviruses belonging to alpha- and gamma herpesvirinae that can cause variety of syndromes in ruminants. Some herpesviruses can target neuronal cells to cause neuropathy and establish latency. Others however, target lymphoid tissue in their lytic and latent forms and induce immuno-deregulation. In both strategies, viral cycles can persist for life within their hosts (Engels & Ackermann, 1996). Herein, examples of closely related ruminant *alphaherpesviruses* and *gammaherpesvirus* are reviewed with emphasis on their enzootic, pathology, and diagnosis.

1.2.1 Infectious Bovine Rhinotracheitis/Vulvovaginitis

BoHV-1 is classified as an *α-herpesvirus* within *varicellovirus* genus. Its genome consists of double-stranded DNA, 135,301 kb in length (Davison, 2010). To date, there are five strains that can cause disease in cattle. Commonly, it causes two forms of clinical disease: the genital syndrome called “Infectious Pustular Vulvovaginitis” (IPV) in female as well as “Infectious Pustular Balanoposthitis” (IPB) in male; and a respiratory form known as “infectious bovine rhinotracheitis” (IBR) (Muylkens *et al.*, 2007). The disease is wide spread in many countries (Raaperi *et al.*, 2014).

The severity of the disease is variable according to age. For instance, in adults, severity ranges from mild clinical signs with reduction in milk yield to abortion and infertility (Muylkens *et al.*, 2007). However, in younger aged cattle, it can cooperate with other agents to cause a state known as bovine respiratory disease (BRD) complex or “shipping fever”. The agents related to

this include: bovine viral diarrhea virus (BVDV), bovine parainfluenzavirus-3 and bovine respiratory syncytial virus. As a result of this, other opportunistic bacterial infections such as *Mannheimia haemolytica* and *Haemophilus somnus* can lead to increased morbidity and mortality rate (van Drunen Littel-van den Hurk, 2006).

The mode of BoHV-1 transmission includes invading the mucosal membrane of the upper respiratory tract or the conjunctival mucus through the direct contact of contaminated aerosol, also by means of the genital tract membrane during animal mating or infected semen. At this point, the virus causes a lytic infection in epithelia (Muylkens *et al.*, 2007).

The virus can be highly pathogenic during the acute infection. It can cause upper respiratory tract immune suppression by expression of three viral genes (bICP0, UL41, US4) that cause inhibition of interferon transcription, by the bICP0 hindering viral peptide presentation to $CD8^+$ T-cells and by expressing gG that acts as a chemokine- binding protein and interferes with the chemo-attraction of lymphocytes (Jones & Chowdhury, 2007).

Although, sensory neurons are the main sites for latent infection, BoHV-1 can also form persistency and reactivation in other tissues such as lymphoid tonsil, suggesting a possible role of the pharyngeal tonsil in transmission of the virus during reactivation (Winkler *et al.*, 2000). In the central nervous system where the virus establishes latency, expression of bICP0 is repressed (Jones *et al.*, 2006). However, during viral reactivation, expression of this protein increases. The bICP0 is a trans-activator of viral

promoters and its main function is to activate viral gene expression and suppress host cell mediated immunity (Biswas *et al.*, 2013).

Maintaining latency is also achieved by expression of two viral genes, the latency related (LR) gene and ORF-E (Jones *et al.*, 2006, 2011). Expression of bICP0 is antagonised by LR gene transcripts when BoHV-1 becomes latent (Biswas *et al.*, 2013).

The disease has been tackled using effective attenuated or inactivated vaccines, as well as live and killed gE-deleted marker vaccines in Europe that distinguish between infection with the vaccine and virulent virus. However, viral latency and the isolation of virulent virus from diseased animals or from aborted foetuses that were previously vaccinated make the control strategies more difficult (van Drunen Littel-van den Hurk, 2006; Fulton *et al.*, 2016; Mahan *et al.*, 2016).

Recently, a polymerase spiral reaction (PSR) has been developed to detect BoHV-1 by (Malla *et al.*, 2018). This technique provides accuracy, cost, and time effectiveness for diagnosis (Liu *et al.*, 2015).

1.2.2 Bovine herpesvirus 5

BoHV-5 is belonging to the *α-herpesvirinae* subfamily within the *varicellovirus* genus. The virus is commonly named ‘’Bovine encephalitis virus”. Genetically, it is closely related to BoHV-1 (Davison, 2010). However, BoHV-5 and BoHV-1 have different pathogenesis. The central nervous system is the target for BoHV-5 latency especially in young cattle (Delhon *et al.*, 2003) whereas BoHV-1 causes infectious rhinotracheitis in cattle. A recent study has suggested that unique microRNAs encoded by both viral

species possibly play an important role in this pathological discrepancy. Fundamentally, these microRNAs interfere with RNA translation and stability to control protein expression. These microRNAs detected in locus within or near the bICP0 and LR genes that are expressed abundantly in lytic and latent infection, respectively. These have been found in BoHV-1 but not in same locus of BoHV-5 genomes, these miRNAs are likely to be involved in the regulation of viral and host genes during infection and may also play a role in pathology (Tang *et al.*, 2014).

Interestingly, BoHV-5 and BoHV-1 co-infection was demonstrated in a high percentage of cattle in Brazil (75.9 %). All of these cases were infected latently (Campos *et al.*, 2009).

BoHV-5 is considered as a neuro-virulent species. Experimentally, it was reported to latently-infect calf brains. However, systemic infection was reported during reactivation (Vogel *et al.*, 2003). It has also been reported that establishment of latency and reactivation occur not only in CNS but also in non- neuronal tissue such as tonsillar lymphoid tissue (Favier *et al.*, 2014).

Both BoHV-1 and BoHV-5 were detected in bull's semen by PCR (Oliveira *et al.*, 2011) but BoHV-5 was isolated and sequenced from healthy bull's semen. Therefore, in artificial insemination, precautions should be taken to avoid viral transmission (Rodríguez *et al.*, 2012). Other economic and epidemiologic aspects of BoHV-5 infection includes cross-infection into sheep which seem to be susceptible to both acute and latent forms combined with high pathological impact (Silva.M *et al.*, 1999).

Previously, numerous efforts to produce a vaccine using BoHV-1 have failed to show cross protection against BoHV-5. However, a recombinant

BoHV-5 live vaccine has been developed by deleting thymidine kinase and glycoprotein E genes. This has successfully protected cattle from disease against both viral species with observed reduction in viral shedding (Anziliero *et al.*, 2011). A similar reduction in viral shedding was also demonstrated by using a vaccine where glycoprotein I (gI), glycoprotein E (gE) and membrane protein US9 (BoHV-5 gI/gE/US9-) were deleted. Nevertheless, this model did not protect against establishment of latency and virus reactivation (Campos *et al.*, 2011).

The diagnosis of BoHV-5 was reported in several studies such as *in situ* PCR hybridisation assay to detect the virus DNA (Cardoso *et al.*, 2010) and multiplex q-PCR assay that was developed by (Diallo *et al.*, 2011) to differentiate between BoHV-5 and BoHV-1. This technique was combined with a restriction length polymorphism assay to provide simple, and fast viral subtyping identification (Maidana *et al.*, 2013). Another q-PCR assay based on reference control with SYBR-Green fluorescence was used to detect this species reliably, specifically with less time consumption (Cardoso *et al.*, 2013).

Recently, development of an indirect ELISA as a serological diagnostic assay based on recombinant glycoprotein D viral antigen has been used to detect BoHV-5 in less laborious procedures (Dummer *et al.*, 2016). In addition, a latex agglutination test for rapid detection of BoHV-5 and BoHV-1 antibodies has been developed (Fan *et al.*, 2012).

1.2.3 Caprine herpesvirus 1

CpHV-1 is classified as *alphaherpesvirus*, clustered within *varicellovirus* genus; commonly named “goat herpesvirus” (Davison, 2010). It is closely related to BoHV-1 (Engels *et al.*, 1992). This species is widely distributed in several European countries and sometimes causes occasional major outbreaks (Piper *et al.*, 2008; Thiry *et al.*, 2008) while in Poland it was not identified (Czopowicz *et al.*, 2010).

The severity of the clinical signs are age-dependent as in young kids, it is characterised by fatal gastro-enteric infection whereas in aged goats, infection appeared as a mild respiratory syndrome (Keuser *et al.*, 2004b, a; McCoy *et al.*, 2007; Tempesta *et al.*, 1999). As in BoHV-1, there are genital signs within infected females characterised by vesicular-ulcerative vulvo-vaginitis and abortion while in male signs involve ulcerative balanoposthitis (Camero *et al.*, 2015; McCoy *et al.*, 2007). CpHV-1 targets the genital system that acts as the main port for viral transmission. Therefore, it can affect pregnancy, especially during the second phase of gestation (Tempesta *et al.*, 2000, 2004).

There are numerous infection risk factors that lead to CpHV-1 spreading but the venereal method seems to be the most important one as it happens seasonally during the oestrus cycle and natural mating or in any other stressful factors (Silva *et al.*, 2013); However, the airborne and oral-faecal mode of transmission are still unknown. Nevertheless, respiratory and digestive system histological changes have been observed in naturally

infected kids, suggesting that CpHV-1 might be transmitted through these pathways (Roperto *et al.*, 2000).

The diagnosis of CpHV-1 includes using serological, biological, and molecular methods as used by (Keuser *et al.*, 2002, 2004a). Previously, it was diagnosed by PCR after reactivation from the latent phase of the sacral ganglia (Tempesta *et al.*, 1999). However, due to the fact that there is a need to discriminate diagnosis of BoHV-1, BoHV-5, CpHV-1, cervine herpesvirus 1 (CvHV-1) and CvHV-2 which are closely, antigenically and genetically, related to each other, murine monoclonal antibodies (MAbs) have been developed against each of these species and used in several immunological techniques such as ELISA, IFA, and radio-immuno-precipitation (Keuser *et al.*, 2004b). An ELISA test was also developed by using CpHV-1 specific IgG1 and IgG2 (Marinaro *et al.*, 2009).

Numerous studies have been conducted to provide a successful vaccine against CpHV-1, such as using inactivated virus (Camero *et al.*, 2007; Tempesta *et al.*, 2001) or recombinant, using BoHV-1 live attenuated virus without glycoprotein E vaccine (Thiry *et al.*, 2006a, b). Inactivated CpHV-1 vaccine with heat-labile enterotoxin of *Escherichia coli* adjuvant (LTK63) as leads to a strong immune response and protection against fatal CpHV-1 (Tempesta *et al.*, 2007).

1.2.4 Cervid herpesvirus 2

CvHV-2 is a member of the *alphaherpesvirinae*, within *varicellovirus* genus. It is commonly named Reindeer herpesvirus (Davison, 2010). Like other ruminant-specific members of the subfamily: such as CvHV-1 and Elk

herpesvirus (ElkHV), CvHV-2 is related to BoHV-1 as well (Deregt *et al.*, 2005; Kautto *et al.*, 2012; Lillehaug *et al.*, 2003; Vanderplasschen *et al.*, 1993). The sero-prevalence of these members has been demonstrated in several regions including: Alaska, Canada, Greenland, Finland, Sweden, and Norway in which it is widely distributed (das Neves *et al.*, 2010). Recently, an outbreak of infectious keratoconjunctivitis (IKC) has been recorded in semi-domesticated reindeer in Norway, this demonstrating the economic importance of this virus (Tryland *et al.*, 2009) in which viral isolation from naturally infected deer has been reported for the first time.

The clinical signs of CvHV-2 in experimentally infected cattle were noticed as mild rhinitis with possibility of natural transmission. However, isolation and reactivation of this species from its natural host “reindeer” by therapeutic immuno-suppressors, “dexamethasone” leads to severe systemic viremia combined with abortion, that suggest vertical transmission (das Neves *et al.*, 2009a). Furthermore, CvHV-2 appears to be endemic latently in the semi-domesticated reindeer and as in most alphaherpesviruses, the trigeminal ganglia are likely to be the target tissue for latency. Importantly, this species can also cause fatal respiratory syndrome due to the respiratory transmission pathway (das Neves *et al.*, 2009b, c).

A commercial BoHV-1-blocking ELISA has been used to detect CvHV-1 antibodies. This assay is likely useful to screen α-herpesviruses in different hosts (das Neves *et al.*, 2009e, d).

1.2.5 Bovine herpesvirus 2

BoHV-2 is classified within the *alphaherpesvirinae* subfamily, *simplexvirus* genus. It is closely related to Ateline herpesvirus 1, Cercopithecine herpesvirus 2, and human herpes simplex virus type 1 (Davison, 2010). Commonly, it is known as bovine mammillitis virus or Allerton virus or pseudo-lumpy skin disease virus.

It causes vesicular, erosive and necrotic lesions of the teat and udder of the infected cow. These lesions seem to be a way to infect suckling calves or even to spread the virus by any direct skin contact (Ehlers *et al.*, 1999a). The udder lesions possibly also predispose cattle to mastitis. This is due to the fact that BoHV-2 supress immune defences, particularly the physical skin barrier, thus it allows opportunistic pathogens to proliferate and cause inflammation. To date, there is no available commercial vaccine to reduce the occurrence of BoHV-2 cases (Wellenberg *et al.*, 2002).

Interestingly, a novel herpesvirus, closely related to BoHV-2, was detected in naturally infected rabbits with acute clinical disease. This virus was classified as a new member of the simplex virus genus (Jin *et al.*, 2008).

The pathogenesis of BoHV-2 is still unclear. The subclinical infection of heifer cows can develop into acute disease during the first period of lactation, which is considered as a predisposing factor (Torres *et al.*, 2009). Cattle are naturally susceptible to the disease with acute and latent forms of infection observed (Torres *et al.*, 2009, 2010). In the natural infection of cattle, latency is thought to be in the trigeminal ganglia, which seems to be the target site not only for BoHV-2 but also for BoHV-4 co-infection (Campos

et al., 2014). However BoHV-2 can also persist in the inguinal nerves of cattle (Torres *et al.*, 2009).

Further evidence of BoHV-2 infection was reported in Hungary as roe, red, fallow, and mouflon deer species as well as domestic sheep were diagnosed to be positive by PCR for BoHV-2 with variable infection percentage ranging (3-50 %). However, there was no report of positive cases in goats (Kálmán & Egyed, 2005).

In BoHV-2 diagnosis, although PCR has been available since 2002 to detect this virus (De-Giuli *et al.*, 2002; Imai *et al.*, 2002), few recent epidemiological studies have been conducted (Imai *et al.*, 2005). Nevertheless, BoHV-2 was successfully isolated from systemic infections of cattle in the United Kingdom (Woods *et al.*, 1996) and Egypt (Iman, 2012). It was also isolated from milk of cattle that suffered from teat and ductus papillaris ulcer (Wellenberg *et al.*, 2002).

1.2.6 Bovine herpesvirus 4

BoHV-4 belongs to the gammaherpesvirus subfamily (Davison, 2010). The virus has worldwide distribution and has been isolated from healthy and infected cattle with signs of reproductive disorders (Verna *et al.*, 2012). Interestingly, BoHV-4 can naturally and experimentally infect a wide range of hosts including ruminant and non-ruminant species. In this respect, BoHV-4 differs from other γ-herpesviruses that require a specific natural host to infect (Verna *et al.*, 2016).

BoHV-4 has been successfully isolated from dairy herds with evidence of metritis (Bilge-Dağalp *et al.*, 2010; Dubuisson *et al.*, 1991). It is also

reported to be reactivated by stress conditions (Peshev & Christova, 2013) or isolated from cattle with neurological signs (Costa *et al.*, 2011). The frequent occurrence of BoHV-4 in the genital tract indicates in some ways its role in causing reproductive disorders (Verna *et al.*, 2016). Thus, BoHV-4 is tropic for bovine endometrial cells and induces a cytopathic effect by modulating the expression of host cyclooxygenase 2 and prostaglandin estradiol (Donofrio *et al.*, 2007).

BoHV-4 can be propagated in different animal cell lines such bovine, mice, cats, rabbits, monkey, and guinea pigs (Donofrio *et al.*, 2002; Donofrio & Van Santen, 2001; Egyed *et al.*, 1997; Vanderplasschen *et al.*, 1995); interestingly also in human cell lines such as embryonic lung cell line and giant cell glioblastoma (Egyed, 1998).

BoHV-4 has been detected in a high percentage (87.1 %) of cattle with endometritis, vaginitis, and mastitis. However, there was no evidence for its role as a primary causative agent within these cases and it has been suggested that viral cooperation with other opportunistic pathogens could be the main factor for these cases (Chastant-Maillard, 2015; Fabian *et al.*, 2008).

The ORF73 in BoHV-4, as in other gammaherpesviruses, is necessary for viral latency but is non-essential for replication *in vitro* when was deleted. This finding led to the propose a development of a vaccine using BoHV-4 as a vector (Thirion *et al.*, 2010). Other authors have demonstrated the feasibility of using BoHV-4 as a vector to deliver foreign genes because of the genetic properties of BoHV-4 as well as the wide range of hosts that

infects, and the variety of cell lines that allow viral replication (Donofrio *et al.*, 2002; Franceschi *et al.*, 2015; Jacca *et al.*, 2016).

PCR and ELISA assays have been used to diagnose BoHV-4 infection (de Boer *et al.*, 2014; Donofrio *et al.*, 2000).

1.2.7 Bovine herpesvirus 6

BoHV-6, previously known as Bovine lymphotropic herpesvirus (BLHV), is a member of the *Gammaherpesvirinae* subfamily and *Macavirus* genus (Davison, 2010). It has novel complement of genes that are unique in the subfamily including: Bov2, Bov4.5, Bov5, Bov6, Bov7, Bov8 and Bov9. One of these (Bov2.b2) encodes an ornithine decarboxylase (ODC) that controls the cellular proliferation and enhances viral replication (Jia *et al.*, 2014).

This virus was firstly identified in the USA from peripheral blood cells of cattle infected with Bovine leukaemia virus (BLV); at that time, its role as a co-factor in causing BLV- associated disease was proposed (Rovnak *et al.*, 1998). Also, it was detected in paraffin-embedded tissues of bison and cattle infected with MCF (Collins *et al.*, 2000). Interestingly, BoHV-6 has been reported in cattle abortion in Canada (Gagnon *et al.*, 2008) and in lymphoproliferative disease in buffaloes that were negative for bovine leukaemia virus (BLV) (de Oliveira *et al.*, 2015). Other studies have confirmed the presence of BoHV-6 in the UK and other European countries in cows suffering from non-responsive postpartum metritis (PPM), suggesting a role in reproductive system disorders (Banks *et al.*, 2008; Cobb *et al.*, 2006;

Garigliany *et al.*, 2013). PAN-herpesvirus PCR and antibody serological tests were used to identify this species in dairy cattle suffering from metritis in New Zealand (de Boer *et al.*, 2014). However, numerous studies have reported that BoHV-6 is ubiquitous in healthy cattle as viral DNA was detected in peripheral blood of these animals, suggesting infection at a young age (Banks *et al.*, 2008; Kubiś *et al.*, 2013; Rovnak *et al.*, 1998).

Recently, viral meta-genomic analysis has been used to fill the knowledge gap in aetiological agents- associated with Bovine Respiratory Disease (BRD) (Ng *et al.*, 2015) and non-suppurative encephalitis in cattle (Wüthrich *et al.*, 2016); interestingly, BoHV-6 seems to be one of the viruses that could cause these syndromes.

1.2.8 Ovine herpesvirus 1

OvHV-1 was not categorised in the last review update on viral taxonomy that has been published by (Davison, 2010). However, analysis of the thymidine kinase and VP23 locus sequence by (ŽIAK *et al.*, 2014) has shown that OvHV-1 lies within the *Macavirus* genus of the *Gammaherpesvirinae* subfamily.

Previously, OvHV-1 was proposed as the aetiological agent of Sheep Pulmonary Adenomatosis (SPA) which is a tumour of sheep (Martin *et al.*, 1979). Subsequently, Jaagsiekte sheep retrovirus (JSRV) was identified as the causative agent of SPA (Martin *et al.*, 1979). OvHV-1 has been experimentally inoculated into healthy lambs to study its pathogenic effects; although the pathological changes involved a focal cellular infiltration of lung

tissue at earlier stages of infection then widespread proliferative pneumonia at a later stage, no signs of SPA was seen (Scott *et al.*, 1984).

Interestingly, the results of a sero-surveillance of healthy sheep in Slovakia revealed a high percentage of infection (65-80 %) (Kopácek *et al.*, 2000). According to (Scott *et al.*, 1984), OvHV-1 can stay quiescently in sheep lung tissue then be reactivated at the time when SPA appears, suggesting the notion of reactivation due to stressful circumstances.

To date, no study has been conducted to quantify this virus in the UK. Also, there is a gap in the knowledge regarding its association with both MCF and SPA.

1.3 Malignant Catarrhal Fever

Malignant Catarrhal Fever (MCF) is a fatal disease of cattle and other ungulate animals including deer, bison, water buffalo, and pigs. Several related γ-herpesviruses cause MCF. They are harboured by their natural “reservoir” hosts without clinical disease and infect other “susceptible” hosts where they can cause fatal disease (Russell *et al.*, 2009).

The clinico-pathological signs of MCF are fever, ocular opacity and nasal discharge with arteritis, lymphoid proliferation, and mucosal necrosis of the digestive tract (Figure 1-6). The severity of the pathology depends on many factors including type of the causative agent and infected hosts (O’Toole & Li, 2014). A considerable amount of research has been conducted to understand MCF pathogenesis and to develop successful vaccine. To date, numerous aspects are still unknown. However, recent

advances in molecular approaches have provided some novel information about MCF.

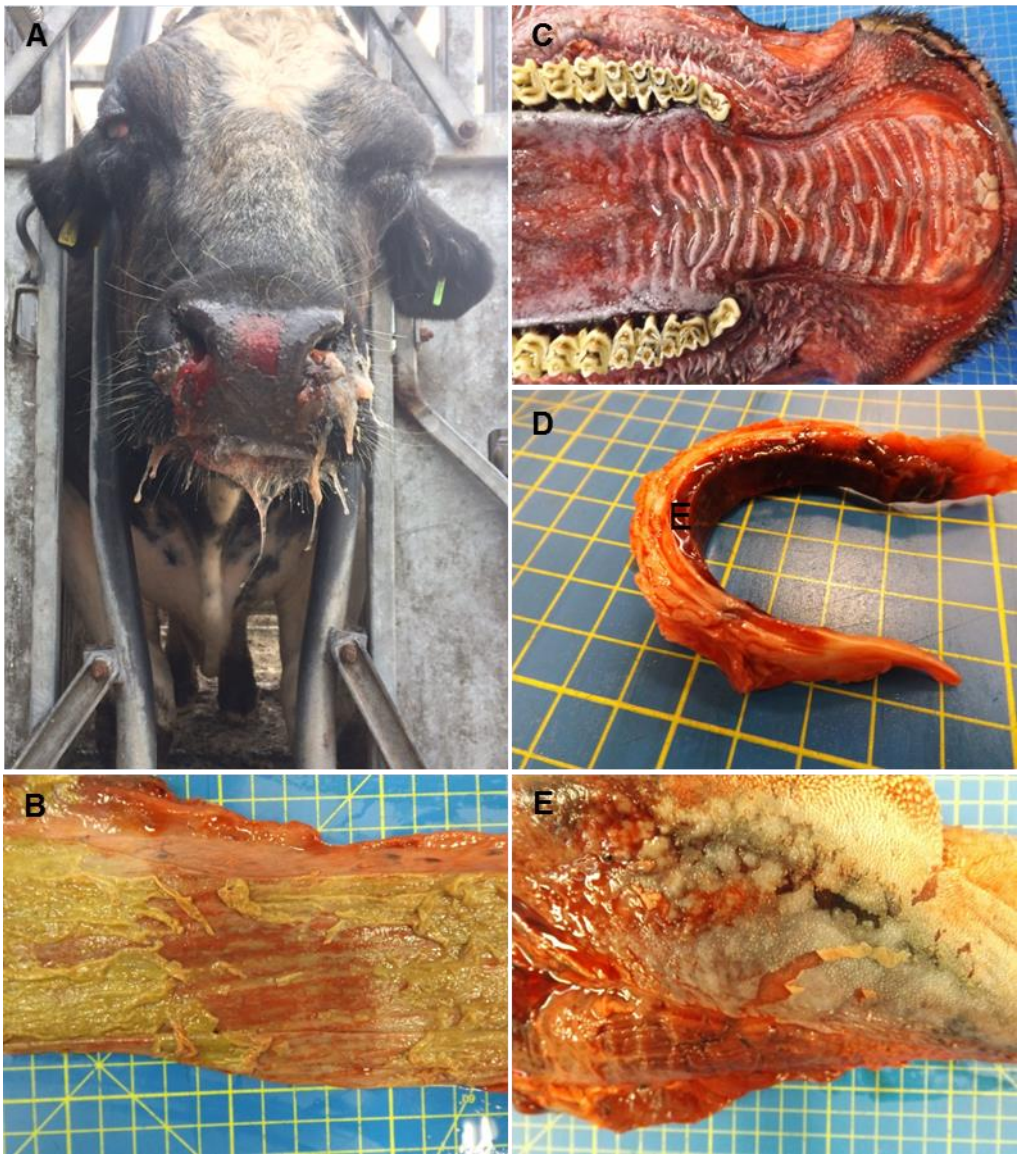

Figure 1-6. Gross pathognomonic haemorrhagic lesions of cow infected with MCF shows: (A) the classical head and eye signs with corneal opacity and mucopurulent nasal discharge, (B) oesophagus, (C) Upper palate showing involvement of buccal mucosa, (C) tracheal ring with sever haemorrhage, (D) tongue with sever haemorrhagic and erosive lesions.

1.3.1 Aetiology of MCF

Herpesviruses have co-evolved within particular hosts. Some herpesviruses are well adapted to their hosts; therefore, they exhibit no clinical signs, whereas infection of closely-related species can lead to severe clinical disease. All MCF-associated viruses are γ-herpesviruses within the macavirus genus. The aetiology of MCF is also depends on the geographical distribution of the reservoir hosts. For instance, MCF in cattle caused by alcelaphine herpesvirus 1 (AIHV-1) appears where its natural host, the wildebeest, is distributed in Eastern and Southern Africa. For this reason, this form is called wildebeest-associated MCF (WA-MCF) (Bedelian *et al.*, 2007). A common cause of MCF is OvHV-2 that is distributed globally wherever its natural host, sheep are reared with cattle or other MCF-susceptible hosts (Russell *et al.*, 2009). However, the number of aetiological agents known to cause MCF continues to increase. To date, there are at least ten MCF-associated viruses, six of them can cause disease naturally whilst causal associations are less clear for the remaining viruses (Table 1-2) (O'Toole & Li, 2014). MCF is a complex disease with a wide range of hosts (reservoir and susceptible) and a number of causative herpesviruses. Additionally, in some cases, more than one viral species might infect in one host.

Diagnosis of the MCF agents mostly relies on using of PCR to confirm the infection in the clinically-affected animals and C-ELISA for the prevalence of infection in the natural host species (OIE, 2004). This because the fact that OvHV-2 load increased systemically (including blood) during clinical MCF which may be detected by routine PCR. However, the viral load within the

reservoir species and latently infected hosts is low which may not always be detected by PCR. Nevertheless, serology is useful in reservoir species where infection is associated with antibody responses but not for clinical MCF cases, which do not always seroconvert. The CI- ELISA is also a useful tool in serology of multiple MCF viruses in reservoir species, as it recognises an epitope conserved in the gB glycoprotein of MCF viruses.

In the following sections, examples of the causative agents of MCF are discussed with focus on their relevance to MCF.

Table 1-2. List of MCF related herpesviruses in ruminants. Adopted from (O ’Toole & Li, 2014).

The virus	Reservoir host	Susceptible host
AIHV-1	Wildebeest	cattle
AIHV-2	Hartebeest	Barbary red deer
OvHV-2	Sheep	Cattle, bison, buffalo, goat deer, and pigs
CpHV-2	Goat	Buffalo, deer, and pig
White Tailed Deer- MCFV (WTD-MCFV)	Goat	Deer
Ibex- MCFV	Nubian ibex	Bongo
Hippotragine herpesvirus-1 (HipHV-1)	Roan antelope Scimitar-horned oryx	Not confirmed
Aoudad-MCFV	Aoudad	Not confirmed
Muskox-MCFV	Muskox	Not confirmed
Gemsbok-MCFV	Gemsbok	Not confirmed

1.3.1.1 Alcelaphine herpesvirus 1

AlHV-1 is harboured asymptomatically by blue and black wildebeest (*Connochaetes taurinus* and *Connochaetes gnou*, respectively). AlHV-1 can be transmitted horizontally and vertically so a high proportion of wildebeest are reported carriers from a young (Wambua *et al.*, 2016).

In horizontal transmission, infection occurs usually after 3 months of age due to maternal antibody (IgG) that provides protection during the early age. When calves become infected, they shed viral particles through nasal and ocular secretions and by six months old, infected animals shed less cell free virus unless they encounter stressful conditions (Russell *et al.*, 2009; Wambua *et al.*, 2016). Vertical transmission has also been demonstrated. This can occur via uterine transmission as about (50 %) of the parturient wildebeest were shown carry the viral DNA in their placental tissue (Lankester *et al.*, 2015).

AIHV-1 can be propagated *in vitro* by using T-lymphoblastoid cell lines known as large granular lymphocytes (LGLs). LGLs were originated from MCF-affected hosts. This has enabled researchers to understand the genome sequence of AIHV-1. AIHV-1 genome contains about 131,000 bp. This is flanked by terminal repeats of 1100 bp. The sequence contains at least 70 ORFs, of which ten genes are unique and are known as A1-A10. Eight of these unique genes are similar to those found in OvHV-2 (Figure1-8). Most of the non-unique ORFs (60) are conserved across homologous γ-herpesviruses (Russell *et al.*, 2009).

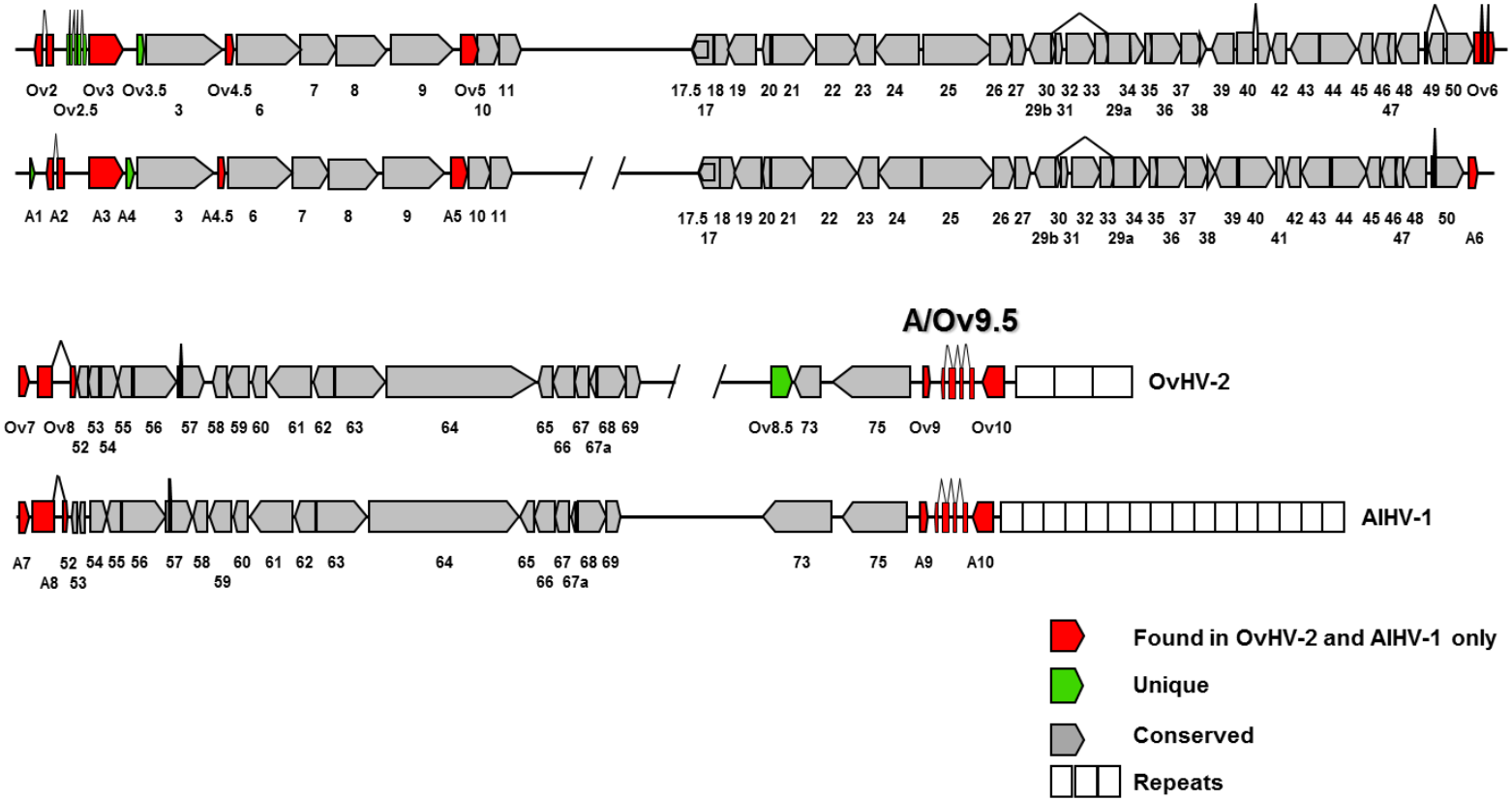

Figure 1-7. Schematic diagram shows the organisation of OvHV-2 and AIHV-1 genomes. The ORFs are seen as grey block arrows that refer to their position, and direction of translation with relevant ORF numbers. Adopted from (Hart *et al.*, 2007).

1.3.1.2 Ovine herpesvirus 2

OvHV-2 is the principal cause of MCF in several ruminant species (Hart *et al.*, 2007; Taus *et al.*, 2007). It is carried asymptomatically in sheep. Viral shedding occurs intermittently with higher shedding in adolescent sheep that may result in more transmission to susceptible species (Russell *et al.*, 2009).

There is no permissive cell line with which to propagate OvHV-2. This makes studying its biology and development of a suitable vaccine difficult. However, propagation of large granular lymphocytes (LGLs) that carry OvHV-2 or AIHV-1 originated from tissues of MCF-affected animals has helped to understand MCF pathogenesis (Russell *et al.*, 2009).

These T-lymphoblastoid cell lines have cytotoxic activity. The OvHV-2 genomic form and transcripts inside these cells are variable. The genomic DNA appears as linear and circular conformations inside the LGLs that originated from MCF-susceptible hosts (cattle and rabbit), indicating latent and lytic viral transcripts. In contrast, the peripheral blood mononuclear cells that of the reservoir host (sheep) contain a circular genomic DNA conformation with ORF73 transcription, indicating latency phase inside these cells (Thonur *et al.*, 2006). Efforts to detect the viral particles inside the cytoplasm of LGLs by using electron microscopy were efficient in case of AIHV-1 but not OvHV-2 (Cook & Splitter, 1988; Rosbottom *et al.*, 2002).

OvHV-2 genome contains 73 ORFs; most of these ORFs (62) are conserved homologues of other γ-herpesviruses (Figure 1-7) (Hart *et al.*, 2007).

Several OvHV-2 glycoproteins are encoded by ORFs that are homologous to AIHV-1 and other γ-HVs (Table 1-3). These glycoproteins play a fundamental role in OvHV-2 biology (Dry *et al.*, 2016). Some of these glycoproteins are conserved among all herpesviruses. For instance, gB and gH/gL are highly conserved and have a pivotal role in mediating fusion of host membrane (Hutt-Fletcher, 2007). Other conserved orthologous glycoproteins are involved in receptor binding such as gp70 and gH/gL in MuHV-4, gp180 (homologous to gp70) in BoHV-4, and gp150 in KSHV (Gillet *et al.*, 2015). All these glycoproteins bind to heparin receptor. Others are involved in cell tropism such as gp350/BLLF1 and gp42/BZLF2 of EBV (Hutt-Fletcher, 2007).

Antibodies against gB and gH/gL were shown to protect rabbits from OvHV-2-MCF (Cunha *et al.*, 2015). Recent data demonstrated that gB, gH, gL, and Ov8 are important glycoproteins in the fusion process of the cytoplasmic membrane of the infected cells (AlHajri *et al.*, 2017). The Ov7 gene of OvHV-2 is homologous to A7 gene in AIHV-1. The predicted product of this gene is likely an envelope glycoprotein and is analogous to BZLF2 protein of EBV. Thus, it is thought to be involved in the infection of B cell (Hart *et al.*, 2007).

OvHV-2 and AIHV-1 can also form a latent infection by expression of LANA protein. This protein is encoded by ORF73 in both viruses (Russell *et al.*, 2009; Taus *et al.*, 2015). Recently, it has been shown that LANA in AIHV-1 has a fundamental role in the lymphoproliferation and evading the virus from host immunity (Palmeira *et al.*, 2013; Sorel *et al.*, 2017).

OvHV-2 has a unique ORF, annotated as Ov2.5, that encodes a protein similar to ovine interleukin (IL)-10 to potentially modulate host immunity by stimulating mast cell proliferation and suppress the production of macrophage inflammatory chemokine (Jayawardane *et al.*, 2008).

Recently, eight microRNAs in the OvHV-2 genome have been suggested to be responsible for the regulation of expression the cell cycle inhibition (ORF20), viral reactivation (ORF50), and viral latency (ORF73) of OvHV-2; Although, some relationship to expression of ORF20 and ORF50, none of these microRNAs seems to be involved with ORF73, presumably other microRNAs could be involved in the latency (Riaz *et al.*, 2014).

Table 1-3. The ORFs encoding OvHV-2 glycoproteins. Adopted from (Hart *et al.*, 2007).

ORF	Amino acid length	AIHV-1 Identity (%)	HVS identity (%)	Glycoprotein
ORF8	863	76	44	gB
ORF22	750	63	27	gH
ORF27	293	51	28	Glycoprotein for cell to cell spreading
ORF39	408	80	44	gM
ORF47	151	45	28	gL
ORF53	102	51	35	gN
Ov7	121	60	NA	homologue of AlHV-1 A7
Ov8 (exon 2)	473	41	NA	homologue of AlHV-1 A8

1.3.1.3 Caprine herpesvirus 2

CpHV-2 is a γ-herpesvirus that was first recognised in goats by means of consensus PCR. Molecular surveys have shown that goats are a reservoir for this virus (Li *et al.*, 2001a). Sequence alignment analysis revealed that CpHV-2 is closely-related to OvHV-2 and AlHV-1 (Chmielewicz *et al.*, 2001).

As in sheep, CpHV-2 can be transmitted to healthy goats through direct contact wherever they kept together, which complicates the control strategy of MCF in the field (Li *et al.*, 2005a). Numerous studies have shown that CpHV-2 is also MCF-associated in various species of deer such captive sika deer (*Cervus nippon*) (Keel *et al.*, 2003), moose and roe deer (Vikøren *et al.*, 2006). Also, in water buffalo (Dettwiler *et al.*, 2011).

Although CpHV-2 and OvHV-2 are closely related to each other, they behave differently when they infect cattle or water buffalo as the latter appear to be more susceptible CpHV-2 -associated MCF (Stahel *et al.*, 2013).

1.3.1.4 Malignant Catarrhal Fever Virus-White-Tailed Deer

MCFV-WTD virus was firstly identified in white tailed deer suffering from signs of fatal MCF. The consensus PCR assay revealed a closely related genetic sequence to maccaviruses: OvHV-2, AIHV-1, and BoHV-6, with identity of (82, 71, 60)% respectively (Li *et al.*, 2000). This sequence was then further confirmed as a γ-herpesvirus by (Kleiboeker *et al.*, 2002). However, the reservoir host had not been identified in these studies until research by (Li *et al.*, 2013) that confirmed goat as a potential reservoir host for MCFV-WD that can cause disease in deer species.

1.3.2 Pathogenesis of MCF

The pathogenesis of MCF is characterised by profound consequences resulting in lymphoproliferation, vasculitis and epithelial inflammation (Russell *et al.*, 2009, 2012a). Herein, the pathogenesis of MCF in reservoir (sheep, goat) and susceptible (cattle, bison) hosts as well as rabbit as a laboratory animal model will be addressed.

1.3.2.1 Pathogenesis in Sheep

Sheep are asymptomatically infected with OvHV-2. All ages are predisposed to infection but the adolescent lambs appear to play an important role in viral transmission in which viral shedding through nasal secretions appears to be the usual route of transmission (O 'Toole & Li, 2014).

Experimental infection of sheep through nasal OvHV-2-aerosol nebulisation revealed lytic replication in the respiratory tract of infected sheep (Taus *et al.*, 2005). This was mainly in the turbinates, trachea, and lung tissues. This indicates the role of sheep as a reservoir host to transmit the virus into the environment (Cunha *et al.*, 2008). Detailed analysis revealed localisation of viral replication in alveolar epithelial cells at the early infection stage. This infected cell type was also found in the nasal secretions of naturally infected sheep during OvHV-2 shedding, indicating its role in OvHV-2 transmission (Taus *et al.*, 2010).

Although sheep are considered the natural host of OvHV-2, some studies have reported the occurrence of MCF in this species. In one report,

the respiratory and alimentary post-mortem pathognomonic signs included tracheal and pulmonary oedematous congestion, erosive lesions in the oral cavity and ulcerative congestion of the abomasal mucosa. Generalised organic and lymphatic tissue damage, involvement of widespread blood vascular necrosis with lymphocytes and macrophages infiltration was noticed as well (Yeruham *et al.*, 2004). In another UK study, a clinically infected, six-month old lamb suffered from clinical and pathological signs of MCF. Particularly, there was a generalised lymphocytoclastic arteritis. The molecular identification revealed OvHV-2 DNA (Gaudy *et al.*, 2012). Similar pathological changes were also demonstrated experimentally through nasal infection with a high OvHV-2 dose, resulting in pulmonary lymphocytic vasculitis and broncho-interstitial pneumonia (Li *et al.*, 2005b). Interestingly, the systematic distribution of vasculitis seems to depend on the mode of infection. For instance, in nasal viral nebulisation, vasculitis was restricted within lung tissue whilst in natural MCF cases, generalised vasculitis is usually recorded (O'Toole & Li, 2014).

A cutaneous form of MCF in sheep has also been reported, presenting as granulomatous mural folliculitis with multinucleated giant cells, lymphocytes, and eosinophil infiltration, accompanied by an increase in the level of viral DNA within these lesions (Slater *et al.*, 2016).

1.3.2.2 Pathogenesis in Goat

Goats are considered as a carrier and susceptible hosts for MCF-viruses (Fernández-Aguilar *et al.*, 2016; Jacobsen *et al.*, 2007). It can be infected with OvHV-2 and CpHV-2 (Vikøren *et al.*, 2006). Both are

transmitted in goats horizontally via the respiratory method. Similar to OvHV-2 transmission in sheep, vertical transmission has not been reported in goat (Li *et al.*, 2005a). Several studies have shown that goats also carry other MCF- viruses. For instance, three herpesvirus sequences were detected in wild ungulates species such as muskox (*Ovibos moschatus*), Nubian ibex (*Capra nubiana*), and gemsbok (*Oryx gazella*), these sequences have a high similarity to MCFV-WTD (81.5 %), CpHV-2 (89.3 %), and AlHV-1(85.1 %) respectively (Li *et al.*, 2003). Recently, a new partial glycoprotein B sequence of a novel herpesvirus has been identified in Pyrenean chamois (*Rupicapra p. pyrenaica*) with high similarity (96.6, 81.5) % to Rupicapra rupicapra gammaherpesvirus 1 and OvHV-2 respectively, and tentatively named "Rupicapra pyrenaica gammaherpesvirus-1 (RpHV-1)". It is suggested to be harboured naturally by deer (*Rupicapra p. pyrenaica*) (Fernández-Aguilar *et al.*, 2016).

The pathological lesions of MCF in goats have not been widely reported. The signs in infected goats appeared as clinical neurological observations with digestive and corneal involvement. Tissue damage was seen in several organs including kidney, spleen, lung, brain and liver with vascular lesions that appeared as lympho-histiocytic with fibrinoid necrosis especially in medium sized arteries (Jacobsen *et al.*, 2007). Goats are unusual in being reservoir and susceptible hosts.

1.3.2.3 Pathogenesis in Cattle

Cattle often succumb to MCF with fatal consequences (O'Toole *et al.*, 1997). The disease is characterised by severe clinical signs with variable

forms such as peracute, alimentary, neurological and cutaneous. The lesions may appeared in eye and head as corneal opacity and oculo-nasal discharge while the post mortem pathognomonic lesions appeared as systemic vasculitis with petechial haemorrhages in the respiratory and gastrointestinal tracts as well as urinary bladder (O'Toole & Li, 2014; Russell *et al.*, 2009). These histopathological lesions considered as the definitive diagnostic approach for MCF while laboratories have recruited the serological and molecular approaches as diagnostic tests (OIE, 2004).

Tissue damage is thought to occur because of immune deregulation that results is accumulation of lymphocytes, predominantly $CD8^+$, that have a natural killer phenotype. Interestingly, only a few of these aggregated cells contain viral genes while the vast majority of them do not. In some lesions, these cells are thought to be associated with vasculitis (Russell *et al.*, 2009).

Vasculitis in MCF is distributed systemically (Liggitt *et al.*, 1980). The lesions appear with numerous infiltrated mononuclear cells, including lymphocytes and lymphoblasts with lower proportion of macrophages, neutrophils and plasma cells. The mononuclear cells infiltrate mainly at the vascular adventitia with less in the medial and intimal layer. However, frequent perivascular lymphocyte infiltration was noticed at the tissue where the capillaries and small venules are more prevalent and sub-venular and pre-medial adventitial mononuclear localization tend to be found prominently in the mild arterial cases. However, the acute damage was noticed with massive accumulation of large mononuclear cells on the entire adventitia (Liggitt & DeMartini, 1980; Simon *et al.*, 2003; Taus *et al.*, 2006).

Recently, it has been reported that characterisation of vasculitis depends on the form of the disease. In the acute form, affected vessels appear with severe lymphocytic arteritis-periarteritis accompanied by necrosis of the tunica media whereas, in chronic cases where animals survived from the acute phase, vasculitis included persisting proliferative arteriopathy in the medium-calibre arteries (O'Toole & Li, 2014).

The current hypothesis in our study includes that OvHV-2 latency within infiltrating cells of vasculitis lesions possibly has a role in development of MCF.

1.3.2.4 Pathogenesis in Bison

Bison are highly sensitive to OvHV-2-associated MCF with a high mortality rate that might reach (100 %) during stressful circumstances. The clinical signs are similar to that seen in cattle but the onset of the disease is rapid, therefore it is difficult to notice as the bison are widely spread in the pasture and often just found dead (Collins *et al.*, 2000; Epp *et al.*, 2016). In some studies, it has been found that the infection rate correlates with the distance from sheep, the lowest rate was demonstrated as (0.43 %) at greater than 5 kilometres (Li *et al.*, 2008a). Experimental infection with a low OvHV-2 dose (5000 copies of DNA) leads to death even in seropositive bison (Gailbreath *et al.*, 2010).

The pathological lesions in natural infection showed variability; a remarkable change is lymphoid cell infiltration in the adventitial layer of the cerebral arteriole in the carotid rete, rumen papilla accompanied with necrosis of renal cortex. In some cases, the infection may become chronic in

which the vasculitis is characterised by an increase the thickness of the arteriole wall due to an extension of the intimal layer as a result of conversion its cell into a spindle shape; lymphoid cells appear in the adventitial layer to a lesser extent in the tunica media layer (Schultheiss *et al.*, 1998). The histological lesions of arteritis-phlebitis in bison is accompanied in least extent with fibrinoid necrosis in tunica medial, which in most cases appears as an acute endarteritis and/or endophlebitis that referred to grade 1 arteritis (Schultheiss *et al.*, 2000).

MCF in bison has been induced experimentally by intravenous inoculation of OvHV-2 and the histological changes were reported as an accumulation of lymphoid cells particularly in the adventitial layer of the rete mirabile artery (Liggitt *et al.*, 1980). Since then, MCF has been produced experimentally by intra-nasal infection (O'Toole *et al.*, 2007). In this case, pathological changes in lung tissue were seen as peribronchiolar pneumonia with alveolar fibrin accumulation.

MCF in bison is a disease of immune deregulation (Nelson *et al.*, 2010). The predominant infiltrating lymphocytes at these sites were identified as $CD8^+$/$perforin^+$/$WC1^-$ γδ T cells, which have an innate immunological regulatory role, not $CD8^+$ αβ T cells. The involvement of $CD8^+$ cells in the pathogenesis of vasculitis has been demonstrated in rabbits as well. On the other hand, recent experimental infection in bison revealed OvHV-2 capsid protein within perivascular fibroblast cells. Nevertheless, the role of OvHV-2 in the progression of vasculitis has never been shown (Nelson *et al.*, 2013).

OvHV-2 transcribed three viral genes (ORF25, ORF50, and ORF73) markers of lytic and latent cycles. These encoded proteins detected in lung at

a high level after 9-12 days post infection (DPI). However, expression of host immune response- related genes were found at a low level in both lung and LN. This was combined with increase the systemic viral load after (16-21) DPI (Cunha *et al.*, 2012).

1.3.2.5 Pathogenesis in rabbits

In rabbits, there is a similar host–OvHV-2 interaction to that seen in bison. Thus, there is lower expression of inflammatory response genes accompanied by high viral replication within the lung tissue and followed by systemic viral dissemination. As in infection of natural hosts, the severity of tissue damage correlates with the level of viral DNA and mRNA transcripts (Cunha *et al.*, 2013).

Lymphoid cell accumulation in rabbits was reported previously as T-cell infiltration not B-cell (Anderson *et al.*, 2007). However, in another study, infiltration of both T and B cells were detected (Li *et al.*, 2011a). In another pathological study, OvHV-2 capsid and tegument proteins that encoded by ORF43 and ORF63 respectively were localised in the appendix of experimentally infected rabbit. Histo-pathologically, epithelial and microfold cells (M-cells) were the exclusive target sites for viral replication, suggesting a new pathogenic mechanism taking part in the M-cells (Meier-Trummer *et al.*, 2009a).

1.3.3 MCF-diagnosis

The propagation of the OvHV-2 is not routinely successful unlike AIHV-1. MCF-like clinical signs are similar to from numerous enteric and vesicular syndromes such as: vesicular stomatitis, infectious bovine rhinotracheitis, bovine viral diarrhoea, mucosal disease, foot and mouth disease, epizootic haemorrhagic disease, and bluetongue (Holliman, 2005). Identifying the aetiological agents of MCF depends on developing reliable serological tests and genomic detection (Li *et al.*, 2011b). Currently, PCR technique has been used widely to detect DNA of the MCF-viruses in the clinically-affected animals while the C-ELISA has been recruited for diagnosis of the natural host species (OIE, 2004). Basically, PCR assay enables diagnosticians to identify clinical MCF associated with high viral load throughout the host organs (including blood). In contrast, reservoir species generally have latent infection, which is often associated with low viral load and therefore could not always be detected by routine PCR. A serological assay is useful to demonstrate infection in reservoir species where it is associated with antibody responses but not for clinical MCF cases, which do not always seroconvert. The Cl-ELISA is also a useful tool in serology of multiple MCF viruses in reservoir species, as it recognises an epitope conserved in the gB glycoprotein of MCF viruses.

There are numerous serological tests to monitor antibodies against MCF viruses. These assays are mostly based on using AIHV-1 as antigen due to the feasibility of propagation of this species *in vitro*. One of these assays is an ELISA test that based on using a monoclonal antibody that

recognise a conserved epitope, MAB15-A, of the AlHV-1 glycoprotein complex. This assay has very high specificity (91-100%) but limited sensitivity (Li *et al.*, 1994, 1995). This drawback was tackled by using a direct WC11-ELISA that uses AIHV1-cell lysate as an alternative antigen (Fraser *et al.*, 2006).

It has been shown that using PCR permits the detection MCF with high sensitivity and specificity. Since PCR and DNA processing has been developed, numerous epidemiological and evolutionary studies have been conducted that clarify different aspects of MCF. Both conventional and quantitative PCR makes disease diagnosis more efficient through detection of viral DNA (Li *et al.*, 2011b). It has been also used for other purposes such as identifying novel herpesvirus (Chmielewicz *et al.*, 2001) or differentiate different MCF viruses (Cunha *et al.*, 2009).

1.3.4 MCF-vaccine development approaches

To date, there is no effective control measure for MCF. The sole strategy is to separate the reservoir host from susceptible animals, but this is not always possible. In addition to cattle, other susceptible hosts such as bison and deer are reared in farms near sheep and OvHV-2 can be transmitted from a distance (Li *et al.*, 2008a; Russell *et al.*, 2009). Therefore, finding a successful vaccine would be useful to protect susceptible hosts.

Previously, two vaccine models using attenuated AIHV1, live or inactivated, were used in rabbit but these approaches did not prevent MCF (Patel & Edington, 1982; Rossiter, 1982). In another study, cattle immunised with AIHV-1 that had been isolated from an MCF case showed short term

protection when challenged with different strains of AIHV-1 (Mirangi, 1991). A promising approach has been achieved by (Haig *et al.*, 2008) using a cell-free, attenuated AIHV-1 (strain C500), with Freunds' adjuvant. Challenge 10 weeks after initial immunisation, reliably revealed protection against intra-nasal challenge with virulent AIHV-1. Protection was accompanied by a high titre of virus-neutralising antibodies in the nasal secretions of vaccinated cattle. Further evaluation was conducted by (Russell *et al.*, 2012b) to demonstrate the protective duration of vaccinated cattle by using the same vaccine but with licensed adjuvant and to examine the level of local and systematic antibody response. The results showed successful protection for three or six months, when the immunised cattle were challenged with intranasal virulent AIHV-1. Analysis of the initial anti-viral antibody revealed that vaccinated cattle had high titres of local and systematic antibodies. Because of this finding, it has been suggested that there is a pivotal role for localised mucosal defence in prevention initial viral entry. Recently, a field vaccination trail using a similar vaccine strategy of attenuated AIHV-1 resulted in reducing infection by 56 % in immunised cattle that were grazed closely with wildebeest (Lankester *et al.*, 2016).

Recent data demonstrated that antibodies to gB and gH/gL protected rabbits from OvHV-2 MCF (Cunha *et al.*, 2015).

1.4 Herpesvirus vaccine development approaches

Several studies have been conducted to produce effective vaccine against human herpesviruses, particularly cytomegalovirus (CMV) and HSV-1. However, viral latency and pathogenicity as well as vaccine

immunogenicity have hindered the efforts to develop efficient vaccines (Bialas & Permar, 2016). For instance, only a vaccine against human herpesvirus type 3 (HHV-3) has been adopted for clinical administration (McGregor *et al.*, 2013). A live-attenuated CMV vaccine was generated but was unsuccessful in CMV prevention. Recombinant attenuated CMV vaccine was used with Interleukin-12 co-administration that showed insufficient immune response (Bialas & Permar, 2016; Schleiss, 2016).

Subunit vaccination using homologous proteins from human CMV has proved effective in clinical trials. CMV-gB glycoprotein was reported as a safe and immunogenic subunit. It has been suggested that using of this subunit with a protein complex known as (gH/gL/UL128-UL130-UL131), most likely efficient in the CMV prevention (Bialas & Permar, 2016).

1.5 Viral vectored vaccines

Development of classical vaccines is based on using of killed or inactivated pathogens. These approaches have some drawbacks such as pathogen mutations and short-term protection. However, recent advancements in molecular and biological fields have improved the targeting of the immune response effectively (Marín-López & Ortego, 2016).

Viral vectored vaccine technology has been developed by using a viral vector to deliver and express an immunogenic protein. Recently, use of this technology has extended to human and animal diseases (Jorge & Dellagostin, 2017). Also, it is useful to overcome the limitations of using the conventional vaccines (Baron *et al.*, 2018). Numerous commercial viral vectors are available in the veterinary field (Marín-López & Ortego, 2016).

The attenuated poxvirus is an important vector in this new generation approach (Moss, 2013). It has many advantages including: efficient DNA recombination with strong genetic promoter as well as inducing of a high level of immune response (Verheust *et al.*, 2012). Therefore, it has been used in many applications (Kreijtz *et al.*, 2013).

1.5.1 Modified Vaccinia Virus Ankara (MVA)

Modified vaccinia Ankara (MVA) is an attenuated virus derived from vaccinia that was developed during the smallpox eradication programme. This was achieved by long-term passages (516) of vaccinia virus on primary chicken embryo fibroblasts (CEF) which caused genetic mutations (Verheust *et al.*, 2012). This technique relies on insertion of a gene of interest into MVA plasmid that contains homologous flanks to MVA virus which expressed under potential specific vaccinia virus promotor. Transferring of this plasmid into MVA-infected cells consequently leads to a homologous recombination and generation of a recombinant virus. This recombinant virus obtained in a cell lysate which then subjected to several rounds of plaque purification (Staib *et al.*, 2004).

This technology is available and has been used as vaccines/vaccination candidates in man and other animals with a known safety profile (Verheust *et al.*, 2012). MVA vaccines have been developed against numerous viral diseases such as: HSV-1 (Browne *et al.*, 1993; Forrester *et al.*, 1991), HIV (Wyatt *et al.*, 2008), Smallpox (von Sonnenburg *et al.*, 2014), blue tongue virus (Marín-López & Ortego, 2016), influenza virus (Florek *et al.*, 2017), and Ebola virus (Domi *et al.*, 2018). Also, it has been

adopted against parasitic disease (malaria), bacterial pathogens (tuberculosis) as well as in cancer therapy (Gilbert, 2013).

The MVA vector has been shown to cause a high level of cellular and humoral immune response (García-Arriaza *et al.*, 2010; Gilbert, 2013; Price *et al.*, 2013). It can be produced in a large-scale which extends its use in many prophylactic and therapeutic applications (Cottingham & Carroll, 2013). MVA system has high safety perspectives due to highly attenuation virus and the virus only replicates within cell's cytoplasm (Verheust *et al.*, 2012).

Recent advancement in the molecular approaches has promoted this technology. For instance, deleting the evasive genes leads to better immune response after vaccination (Ryerson & Shisler, 2018).

1.6 Aims of the study

Recently, our lab has shown that OvHV2 can persist in non-diseased cattle suggesting that other factors, possibly other virus infections could be involved in the pathogenesis of MCF. In the UK, numerous pathognomonic cases of MCF in bison, water buffalo, and deer have been reported as OvHV-2 negative (Amin, 2015).

Our hypothesis involves that as well as OvHV-2, other macavirus members, such as BoHV-6 and OvHV-1, or other herpesviruses might have a role to play in the pathogenesis of MCF. Therefore, our target is to investigate which herpesviruses are involved in MCF. For this purpose, two PCR formats were employed, PAN herpesvirus nested and q-PCR, as qualitative and quantitative approaches to examine these cases and assess the potential of other herpesviruses being involved in MCF.

The Latency Associated Nuclear Antigen (LANA) that is encoded by ORF73 of OvHV-2 has an essential role in maintaining the virus during latency but its role is not fully understood. Therefore, we aimed to express this protein *in vitro* in two approaches; firstly, by expressing a portion of oLANA to use it as antigen for production of polyclonal antibody to investigate OvHV-2 latency and its role in clinical disease. Secondly, express the whole length of oLANA to characterise its expression and validate the assay.

Furthermore, bison, water buffalo and deer have been reared recently in the UK. However, farmers are facing a serious issue due to the high susceptibility of these hosts to MCF and without an effective vaccine against

OvHV-2. Therefore, we aim to express OvHV2- glycoproteins (gB, gH, gL, and Ov7) in recombinant modified vaccinia Ankara virus to develop a suitable subunit vaccine.

Explaining the abovementioned aspects will give new insights in preventing MCF in reservoir host (sheep) and susceptible hosts (cattle, bison, water buffalo, goat, and deer).

2. Chapter two: Materials and methods

2.1 Animal tissue samples

Necropsy tissue specimens (n= 208) from several species were used in this study. Sheep (n= 14) as the natural reservoir of OvHV-2 and suspected Ovine Pulmonary Adenomatosis cases (n= 35) from the UK; cattle without clinical signs (n= 33: 15 from the UK and 18 from Switzerland) and with signs of characteristic MCF (n= 30), Bison without pathological signs (n= 29) and with evidence of MCF (n= 40) from the UK, Deer (n= 13), (only tissues preserved in RNAlater) and goats (n= 14) (pathological cases that had history of pneumonia) fixed in formalin from Switzerland. All these samples were kindly provided by Institute of Veterinary Pathology, Vetsuisse Faculty, University of Zurich, Switzerland and Moredun Research Institute, UK.

2.1.1 DNA extraction and processing

All DNA extraction and processing protocols, as described in the following sections, were conducted according to (Vinet & Zhedanov, 2005).

2.1.1.1 Nasal swab

The samples were mixed vigorously for 5 s then incubated for 1 h at 50 °C in water bath then a (1/ 25) v/v of PG-L2P purifier™ (DNA genotek, Canada) was added to the nasal material in a new 1.5 ml tube and mixed for 5 s then incubated in ice for 10 min followed by centrifugation at 15000x *g* for 5 min. The clear supernatant was transferred into new 1.5 ml tube and a (1/ 20) v/v of 5 M NaCl was added and 600 µl of 100 % ethanol was added and mixed gently by inversion 10 times. The DNA was then precipitated by standing the samples for 10 min and centrifuged at 15000x *g* for 2 min. The supernatant was removed without disturbing the pellet which then washed by adding 250 µl of 70 % ethanol then removed by centrifugation and pipetting. The DNA was dissolved by adding 100 µl of TE buffer (10 mM Tris. Cl,1 mM EDTA, pH= 8) with mixing gently (Bartlett & Stirling, 2003).

2.1.1.2 Formalin-fixed paraffin-embedded (FFPE) tissue sections

The paraffin-fixed samples were treated with 1 ml of xylene with vigorous mixing by vortex for 10 s followed by centrifugation at 15000x *g* for 5 min. The supernatant was discarded by pipetting then the pellet was washed six-times in 1 ml (100 %) ethanol with mixing using a vortex. The tubes were covered with stretched parafilm and pierced with several holes into the foil and incubated at 37 °C until complete evaporation of ethanol. The DNA was extracted by using the QIAamp® DNA FFPE tissue kit according to

manufacturer's recommendations as in the following protocol (section 2.1.1.3).

2.1.1.3 Blood and tissue specimens

Fresh tissues collected at necropsy were homogenized in phosphate-buffered saline (pH 7.4, (3 g of tissue/ 5 ml) then 1 ml homogenate was centrifuged at 12,000x *g* for 1 min and the pellet used for DNA extraction. Blood samples were collected into tubes containing Ethylenediaminetetraacetic acid (EDTA). DNA was extracted from homogenised tissues and blood using QIAamp DNA tissue and blood kit (Qiagen) according to the manufacturer's manual, the samples were firstly lysed by using proteinase k then the lysate transferred onto the DNeasy mini spin column and centrifuged to bind the DNA with the membrane of spin column then DNA was washed to remove contaminants and eluted by the supplied reagents.

2.1.2 DNA gel electrophoresis

The electrophoresis of the DNA was performed by using gels containing 0.8 % agarose in electrophoresis tanks (Bio-rad, UK). The agarose was prepared in 1x TAE buffer (40 mM Tris-base, 20 mM acetic acid, 1 mM EDTA). For DNA visualisation, SYBR® Safe DNA Gel Stain (1 X) was added (Invitrogen, UK), then the solution was poured without creating air bubbles into the plastic tray after sealing its ends with laboratory tape, the comb was then inserted before agarose-solidify completely so both, tape and

comb, were withdrawn gently and the casting gel tray was placed in the electrophoresis tank which then filled with sufficient 1 x TAE buffer. Each DNA sample was mixed with 1 x DNA sample loading buffer (Bioline, USA) before loading into each well alongside appropriate DNA molecular weight markers (1 kb or 100 bp ladder) (Cleaver Scientific, UK). The DNA was electrophoresed at 110 mA then visualised using a UV trans-illuminator ChemiDoc (Bio-rad, UK).

2.1.3 Amplicon purification

All PCR products were either purified directly at the end of the PCR run in which one volume diluted with 5 volumes of PB buffer (5 M guanidine hydrochloride, 30 % isopropanol, QIAquick PCR Purification Kit Protocol), according to the manual recommendations. The mixture was then applied to the spin column for DNA binding and spun at 13000 rpm for 1 min followed by washing with 750 µl of PE buffer (10 mM Tris-HCl pH 7.5, 80 % ethanol). The spin column was then placed in a new Eppendorf tube to elute the DNA with 50 µl of EB buffer (10 mM Tris·Cl, pH 8.5) and centrifuged at 13000 rpm for 1 min.

For PCR products purified from gels, the PureLink® Quick gel extraction Kit (Invitrogen), was used, following the manufacturer's manual that involved a similar basic workflow, except that the PCR product was electrophoresed as in (section 2.1.2) then excised from the gel and solubilised with L3 buffer (undescribed components) at 50 °C for 15 min then

washed with buffer W1 (undescribed components) then eluted with E5 buffer (10 mM Tris-HCl, pH 8.5).

2.1.4 DNA transformation and cloning

The PCR amplicons were firstly purified (see section 2.1.3) then cloned by means of 3' adenine-overhangs into the commercial vector (pCR2.0 TOPO), according to the manufacturer's recommendation (Invitrogen, UK). The reaction was performed by mixing 4 µl of fresh purified amplicons with 1 µl of the provided salt buffer (1.2 M NaCl, 0.06 M $MgCl_2$) and 1 µl of the supplied plasmid (10 ng/µl linearized plasmid, 100 µg/ml BSA, phenol red, 50 glycerol, 50 mM Tris, 0.1 % 100X triton, 1 mM DTT). The reaction was incubated at room temperature for 5 min then 2 µl of the mixture was delivered into one vial of chemically competent *Escherichia coli* (Mach1™ One Shot®, Invitrogen) and incubated for 30 min on ice. The bacterial mixture was then heat-shocked by at 42 °C in a water bath for 30 sec then incubated immediately on ice for 5 min followed by adding 250 µl of the provided S.O.C. medium (Invitrogen) (2 % tryptone, 0.5 % yeast extract, 10 mM NaCl, 2.5 mM KCl, 10 mM $MgCl_2$, 10 mM $MgSO_4$, and 20 mM glucose) into the transformed *E coli* which was then incubated at 37 °C with shaking at 200 rpm for 1 h.

2.1.5 Selection of transformed *Escherichia coli*

Transformed bacteria (50 µl) (see section 2.1.4), was streaked on a pre-warmed Luria-Bretani agar plate (LB 1 % w/v tryptone, 0.5 % w/v yeast

extract, 1 % w/v NaCl) supplemented with 50 µg/ml ampicillin (sigma, UK) and pre-spread with 50 µl of x-gal (40 µg/ml) stock (Promega, USA) which was then incubated for 24 h at 37 °C. The white- well separated colonies were sub-cultured in 5 ml LB broth containing 50 µg/ ml of ampicillin at 37 °C for overnight for further preparation as in section (2.1.6).

2.1.6 Preparation of recombinant plasmids DNA

The recombinant plasmids that had been transformed and amplified inside bacteria were harvested for insert confirmation by mini-preparation. Selected clones were prepared as required by maxi-preparation according to the manufacturing recommendation's (Qiagen).

All plasmids were prepared initially by minipreparation of the saturated growth culture that resulted from inoculating individual-single white colony into 5 ml LB broth (see 1.2.5). This was pelleted by centrifugation at 6000 x *g* for 15 min at 4 °C then the pelleted cells were re-suspended in 300 µl of the supplied resuspension buffer P1 (50 mM Tris.Cl, 10 mM EDTA, 100 µg/ml RNAse A) followed by adding similar amount of lysis buffer P2 (200 mM NaOH, 0.1 w/v SDS). After thoroughly mixing by inverting, the mixture was then left at RT for 5 min and neutralised by adding 350 µl of N3 neutralisation buffer (4.2 M Gu-HCl, 0.9 M potassium acetate, pH 4.8). The lysed bacterial protein was pelleted at 2000x *g* for 10 min at 4 °C. Then 800 µl of supernatant was transferred into the supplied columns (QIAprep 2.0 spin) which were then spun at 3000x *g* for 1 min, washed once with 500 µl of buffer PB (5 M guanidine hydrochloride, 30% isopropanol), spun at 3000 *g* for 30 sec then washed again by adding 750 µl of PE buffer (10 mM Tris-HCl

pH 7.5, 80% ethanol). The flow-through solution was discarded, and the residual washing buffer was removed completely from column's membrane by further centrifugation for 1 min. Finally, the DNA was eluted by placing the QIAprep column in a new Eppendorf tube and adding 50 µl of EB buffer (10 mM Tris.Cl, pH 8.5) at the centre of the QIAprep 2.0 spin column and letting stand for 1 min. Plasmid was finally recovered by centrifugation at 3000x *g* for 1 min and stored at 4 °C.

For confirmation of inserts, the *Eco*RI restriction enzyme (Promega, USA) was used to cut the 5'..G˅AATTC..3' sequence sites within (pCR2.0 TOPO) vector. According to the manufacturer's recommendation, the reaction was performed using a mixture of 16.3 µl of deionized water, 2 µl RE 10X buffer, 0.2 µl acetylated BSA, 1 µg/ µl DNA, and *Eco*RI (0.5 µl) and incubated at 37 °C for 2 h. The cut fragments were checked by gel electrophoresis, (see 2.1.2) before sending for sequence (see 2.6.8).

Amplification of plasmid DNA was achieved by maxi-preparation using column extraction (Qiagen). A purified sub-cultured single colony of *E. coli* that was carrying the plasmid of interest was used to inoculate 400 ml of LB broth containing the standard concentration of antibiotic, as described in (2.1.5). Following the manufacturer's manual, an overnight saturated culture was spun at 6000x *g* for 15 min at 4 °C. The pelleted cells were re-suspended by adding 10 ml of supplied P1 buffer (50 mM Tris.Cl, 10 mM EDTA, 100 µg/ml RNAse A), then lysed with 10 ml of P2 buffer (200 mM NaOH, 0.1 w/v SDS) and then incubated at RT for 5 min. The cell lysate was neutralised by adding 10 ml of P3 buffer (3 M potassium acetate, PH 5.5) and kept on ice for 5 min then centrifuged at 2000x *g* for 10 min at 4 °C. The

supernatant was transferred into (QIAgen tip 500) that had been equilibrated by adding 10 ml of QBT buffer (750 mM NaCl, 50 mM MOPS, 15 % isopropanol v/v, 0.15 % Triton X-100 v/v) and left to flow by gravity. When the plasmid was completely bound to the column's membrane, it was washed twice with 30 ml of QC buffer (1.0 M NaCl, 50 mM MOPS, 15 % isopropanol v/v). Finally, the plasmid DNA was recovered with 15 ml of QF buffer (1.25 M NaCl, 50 mM Tris-Cl, and 15 % isopropanol v/v) and then precipitated by adding 10 ml of molecular grade isopropanol (Sigma, UK). After centrifugation at 5000x *g* for 1 h at 4 °C, the DNA precipitates were washed with 5 ml of 70 % molecular grade ethanol (Sigma, UK) and centrifuged at 15000x *g* for 10 min. Pellets were then air dried and eluted in dH_2O.

To store bacterial clones, 850 µl of sub-confluent bacterial culture was mixed with 150 µl of sterile glycerol (100 %) and immediately snap frozen in dry ice and kept at -80 °C as a glycerol stock (Ferrer-Miralles *et al.*, 2015).

2.1.7 Deoxyribonucleic acid (DNA) measurement

All the DNA samples were measured according to the Invitrogen Qubit® flourometer recommendations. Basically, each DNA and Qubit® standards were placed into Qubit® assay tubes and diluted (1:200) using the Qubit® dsDNA BR reagent to 200 µl final volume. This was then incubated at RT for 2 min and measured by Qubit® 2.0 Fluorometer, Invitrogen. The DNA was either used directly or stored at -20 °C until further use.

2.1.8 DNA sequences

Selected plasmids were sequenced at Source Bioscience (Rochdale, UK) after being confirmed by restriction enzyme digestion by using appropriate primers. Data were aligned using Basic Local Alignment Search Tool (BLAST) at the National Centre for Biotechnology Information website's (http://www.ncbi.nlm.nih.gov/) to confirm the cloned targets.

2.2 Polymerase Chain Reaction (PCR)

2.2.1 PAN nested PCR

A nested consensus PCR of degenerate, dI-substituted primers of a highly conserved sequence was employed to detect the DNA polymerase (DPOL) gene. The reaction consists of two rounds of amplification which were performed in similar reaction conditions to include modified and unmodified primers, as has been used previously by (Ehlers *et al.*, 2007; Vandevanter *et al.*, 1996) (Table 2-1). In this protocol, the total reaction volume (25 µl) contained 12.5 µl of 2x Qiagen multiplex PCR master mixes including HotStart Taq DNA polymerase with 3 mM $Mg2^{+}$. In first round, 1 µM of each modified (3-DFA, 4-ILK, 8-KG1) and unmodified (1-DFA, 2-ILK, 7-KG1) primers was used and approximately 400 ng of genomic DNA was added. In the second round, a similar amount of primers, modified (6-TGV, 10-IYG) and unmodified (5-TGV, 9-IYG) and master mix were used but only 1 µl of the product from the first round was used for the second round. A similar temperature profile was used in both rounds as follows. Activation of

the Taq enzyme at 95 °C for 12 min then 45 cycles of 20 s at 95 °C, 30 s annealing at 46 °C, and 30 sec extension at 72 °C, followed by a final extension step at 72 °C for 10 min.

All PCR products were purified, cloned and the inserts were extracted by miniprep, checked by *Eco*RI restriction enzyme then sequenced according to the previous sections (2.1.4); all the sequences were assembled by using MEGA7 software (software, version 7.0.21) (Kumar *et al.*, 2016) and aligned at NCBI website to identify the detected herpesviruses.

Table 2-1

The primers used for PAN- nested PCR.

Modified		
Primer	Round	Sequence 5'→ 3'*
3-DFA	1	GAYTTYGCIAGYYTITAYCC
4-ILK	1	TCCTGGACAAGCAGCARIYSGCIMTIAA
8-KG1	1	GTCTTGCTCACCAGITCIACICCYTT
6-TGV	2	TGTAACTCGGTGTAYGGITTYACIGGIGT
10-IYG	2	CACAGAGTCCGTRTCICCRTAIAT
Unmodified		
1-DFA	1	GAYTTYGCNAGYYTNTAYCC
2-ILK	1	TCCTGGACAAGCAGCARNYSGCNMTNAA
7-KG1	1	GTCTTGCTCACCAGNTCNACNCCYTT
5-TGV	2	TGTAACTCGGTGTAYGGNTTYACNGGNGT
9-IYG	2	CACAGAGTCCGTRTCNCCRTADAT

Abbreviation: The codons include: I: inosine; Y: Pyrimidine: C or T; R: purine: A or G.

2.2.2 Real time PCR

2.2.2.1 Design of primers and probes

Conserved sequences within glycoprotein B gene were selected as a target for the Taqman q-PCR by means of GeneScript Bioinformatics software at (https://www.genscript.com/ssl-bin/app/primer). For OvHV-2, the genome copy number was estimated using OvHV-2-specific primers (ORF63-specific) (Stahel *et al.*, 2013), For BoHV-6, we adopted the published assay based on the gB gene sequence (Kubiś *et al.*, 2013) (Table 2-2). The possibility of non- specific reactions with other sequences was avoided by using an alignment search tool (BLAST) at the National Centre for Biotechnology Information website's (http://www.ncbi.nlm.nih.gov/). The 12s-ribosomal DNA internal genome was used to normalise the q-PCR data (Gatesy *et al.*, 1997). Specific primers and probes were delivered lyophilized then diluted to 100 pmol/µl by using a qPCR probe dilution buffer (10 mM Tris-HCl; PH 8; 1 mM EDTA) (eurofins, UK). Sets of primer stocks were further diluted to a working concentration of (20 pmol/µl) and for the probes (10 pmol/µl). All these stocks were kept at -20 °C in the dark (Basu, 2015).

Table 2-2. The taqman q-PCR primer sequences

Target	Primer	Sequence 5'→3'	Annealing temperature °C
OvHV-1	F	GTATGGCAGCCGTTAGTTCA	57.3
	R	AAGGCGTAGACGCTTCATCT	
	probe	**FAM**-CTCGCTTAGCGTCTACAAGCTGTTGC-**TAMRA**	
BoHV-6	F	ACCCCGTAAAAGTGATTTACCC	56.4
	R	GTAGTAGTCATGCATAGCTAGC	
	Probe	**FAM**-CAAAAGATCAGAGAGCAGCAAGAG-**TAMRA**	
OvHV-2	F	GAGAACAAGCGCTCCCTACTGA	56
	R	CGTCAAGCATCTTCATCTCCAG	
	Probe	**FAM**-AGTGACTCAGACGATACAGCACGCGACA-**TAMRA**	
Bison LHV	F	GGTTTGCTTCCCTGCTTAAA	60
	R	CTCCAAGTCTGCGAGCTGTA	
	Probe	**FAM**-CTTTCCAGCATGGTCCGCCC-**TAMRA**	
CpHV-2	F	TCAAGAGCAACAGGAACCAG	60
	R	CTATGCTGCTCACCACGTTT	
	Probe	**FAM**-AGGCTGCCAAAGGCGTCCAC-**TAMRA**	
12s-internal DNA	F	GCG GTG CTT TAT AYC CTT CTA GAG	60
	R	TTAGCAAGRATTGGTGAGGTTTATC	
	Probe	**VIC**-AGCCTGTTCTATAAYCGAT-**MGBNFQ**	

Abbreviation: FAM: 5' modification (6-Fluorescein amidite); **TAMRA**: 3' modification quencher; **VIC**: 5' modification: commercial fluorescent dye, **MGBNFQ**: 5' modification (minor grove binder nucleotide quencher); Y: (Pyrimidine) C or T.; R: (purine) A or G.

2.2.2.2 The q-PCR optimal conditions

The reaction mixtures were optimized to contain 7 µl of (2x) TaqMan® universal PCR master mix that consists of Gold® ultra-pure AmpliTaq DNA polymerase, Uracil-N glycosylase (UNG), dNTPs with dUTP, ROX™ passive reference dye and buffer master mix (applied biosystem, UK); the primers and probes were at concentration of (0.5 pmol/µl) in 20 µl total reaction volume. Initially, the optimal annealing temperature of primers and probes were determined by gradient protocols (DNA Engine Opticon 2, UK) in a range of (55-60) °C. The optimal cycling temperature profile in all q-PCR assays involved an initial 50 °C for 2 min followed by 13 min of 95 °C then 39 cycles of 95°C for 15 sec, finally, 1 min of the optimal annealing temperature as mentioned in (Table 2-2).

2.2.2.3 Production of reference plasmids for viral quantification

The constructed reference genes were produced by cloning PCR products as described in section (2.1.4). The concentration of the obtained plasmids was measured by using a Qubit fluorimeter as described in (2.1.7) and they were sequenced (2.1.8) for final confirmation. The starting concentrations were calculated according to the following formula (Dhanasekaran *et al.*, 2010; Godornes *et al.*, 2007):

[Number of copies/ µl= (DNA (g/ µl) x [6.022×10^{23}])/ (length x 650)]

Where 6.022x1023 is Avogadro's number; (length) is the number of the base pair (bp) in the reconstructed plasmid; 650 is the average weight of each base pair in Daltons. The calculation results were also checked by means of DNA copy number calculator software at (http://scienceprimer.com/copy-number-calculator-for-realtime-pcr) website. Serial tenfold dilutions were performed using nuclease-free water supplemented with yeast tRNA (25 mg/ml) (Invitrogen™ AM7119, UK). In order to preserve these plasmids from degradation, numerous aliquots (5 µl/ tube) were kept in -20 °C for further use.

Genome copy numbers were estimated using 100 ng genomic DNA and a Taqman PCR approach with primers specific for each virus. Normalisation to account for variability in DNA quality and contaminants was performed using primers specific for the ruminant 12s-ribosomal DNA internal genome. Therefore, the exact genome copy number and normalization was determined using limiting dilutions of reference plasmids as detailed in the result chapter in a background of high molecular weight (Biassoni & Raso, 2014).

2.2.2.4 Estimation of assays validity

The intra and inter assay variation were analysed by performing five runs for each reference plasmid in tenfold serial dilutions independently in duplicate starting from ($2x\ 10^7$) to ($2x\ 10^0$) copy/ 2 µl.

The assay specificity was determined by cross testing clinical diagnostic samples known to be positive for other herpesviruses. All the quantification statistics were analysed by means of graph pad prizm software

using T-test mann-whitney and Fisher's exact test. The assays were also validated according to MIQE guidelines to include: mean value, standard deviation, coefficients of variation (CV) of the Ct values, and the standard error of mean of means for each plasmid (Bustin *et al.*, 2009; Taylor *et al.*, 2010).

2.3 Cell line culture

Cells were thawed in a 37 °C water bath for about 1-3 min then added into 10 ml tissue culture media containing foetal calf serum. Cells were passaged after 2-4 days, when they reached about 90 % confluent. All cell lines except the LGL cell line (see 2.3.1) were split and harvested to new flasks using 0.25 % Trypsin-EDTA (Life technologies, UK) to detach monolayer cells. Cells near 90 % confluent were washed twice by PBS, harvested by adding 3 ml of trypsin and incubated at 37 °C for 3 min. The trypsinisation process was inhibited by adding 7 ml of tissue culture media containing 10 % foatel calf serum. Cells were then split to new flasks after counting by haemocytometer. About 1 x 10^6 cell/ ml were seeded into T175 cm^2 tissue culture flask (Corning, UK) and maintained as in sections (2.3.1, 2.3.2, and 2.3.3).

2.3.1 Large granulocyte lymphocyte (LGL)

The large granulocyte lymphocyte cell line known as (BJ2586) contains OvHV-2 and was propagated from infected rabbits *in vitro*; this line was kindly provided for this study by (George Russell, Moredun institute).

This cell line was maintained in Iscove's Modified Dulbecco's Medium (IMDM) (Sigma, USA) that contained 10 % foetal calf serum (Sigma, UK), penicillin (100 U/ml) / streptomycin (100 µg/ ml) (Sigma, UK), 1 % L-glutamine (Sigma, UK), and 350 IU/ ml of IL-2 (Chiron, UK) (Schock *et al.*, 1998). This cell line was grown in suspension at 37 °C and 5 % CO_2 as recommended by (Schock *et al.*, 1998).

2.3.2 Human embryonic kidney (HEK293)

HEK293 cells were maintained in Dulbecco's Modified Eagle's Medium (DMEM) (Sigma, UK) supplemented with 10 % fetal calf serum (Sigma, UK), penicillin (100 U/ml) / streptomycin (100 µg/ ml) (Sigma, UK) and 1% L-glutamine (Sigma, UK). The cells were cultured at 37 °C with 5 % CO_2.

2.3.3 Baby Hamster Kidney (BHK)

The BHK cell line was maintained in Minimum Essential Media (MEM) (Sigma, UK) that was supplemented with 10 % fetal calf serum (Sigma, UK), penicillin (100U/ ml)/ streptomycin (100 µg/ ml) (Sigma, UK) and 1 % L-glutamine (Sigma, UK). The cells were cultured at 37 °C with 5 % CO_2.

2.4 Cell line transfection

2.4.1 Calcium phosphate precipitation

The transfection of HEK293 cells with [pVR1255-ORF73 alongside GFP vector (pEGFP-N1)] as a control for transfection efficiency was performed by mixing 156.16 µl of 2 M $CaCl_2$ with 50 µg plasmid-DNA in Eppendorf tube. This was added gently in a drop wise fashion to 1280 µl of 2x HBS- buffered saline (274 mM NaCl, 10 mM KCl, 1.4 mM Na2HPO, 4·7 H_2O) and then incubated for 30 min at RT. This transfection solution was then delivered in drop wise fashion to 150 cm^2 tissue culture round dish containing 23 ml of complete medium seeded with 4x 10^6 of HEK293 (50-60 % confluent). After incubation for 24 h, the transfected cells were washed twice with PBS before being harvested, washed with a 500 µl of PBS and centrifuged at 4 °C for 5 min at 2500 rpm. The pellet was then treated as described in (2.5.2) (Wang & Mei, 2013).

2.4.2 Lipofectamine reagent

The transfection of BHK cells was prepared by diluting Lipofectamine-2000 reagent (5 µl) in 250 µl of Opti-MEM media. At the same time, a similar amount of Opti-MEM was added into each DNA vector [rMVA-(gB, gH, gL, and Ov7)] (0.625 µg/ well). These components were incubated for 5 min at RT then the DNA vector solution was mixed with diluted lipofectamine-2000 and then incubated for 30 min at RT. The procedures were continued as in (2.15.1).

2.5 Sodium- dodecyl sulphate polyacrylamide gel electrophoresis (SDS-PAGE)

2.5.1 Reagent for SDS-PAGE and western immunoblotting

Sample loading buffer (2 x) containing 62.5 mM Tris–HCl pH 6.8, 3 % (w/v) SDS, 5 % β– mercapto-ethanol, 10 % glycerol and 0.01 % bromophenol blue. **Running buffer** consisting (50 mM Tris, 192 mM glycine, 0.1 % (w/v) SDS pH 8.3. **Transfer buffer** 120 mM Tris, 192 mM glycine and 20 % (v/v) methanol. **Tris buffered saline-tween 20 (TBS-T)** containing 20 mM Tris-HCl, pH 7.5, 150 mM NaCl and 0.1 % (v/v) Tween 20. **Blocking buffer** containing 5 % (w/v) fat-free skimmed-milk (Marvel) in TBS-T.

2.5.2 Sample preparation

2.5.2.1 Cell line

The monolayer cell lines (section 2.3.2 and 2.3.3) were harvested from tissue culture flasks, 6- well or T175 (Corning, UK) by scraper then transferred into eppendorf tube, washed 2x by PBS and centrifuged at 2000 rpm at 4 °C for 5 min. The suspension cell line (section 2.3.1) was harvested by centrifugation at 1500 rpm at 4 °C for 10 min. Equal amount of sample loading buffer (about 20 µl) was added into the pelleted cells for protein extraction. The lysates were then boiled in heating block at 90 °C for 5 min then kept - 80 °C

2.5.2.2 Animal tissue

Whole protein lysates of sheep and cattle tissue previously tested for OvHV-2 by q-PCR assay was extracted by cutting frozen tissue into small pieces (100- 250 mg) followed by adding 500 µl of RIPA buffer (50 mM Tris, [pH 7.5], 150 mM NaCl, 1 % NP40 alternative (v/v), 0.5 % sodium deoxycholate (w/v), 0.1 % SDS) and 300 µl of a protease inhibitor cocktail (AEBSF 23 mM, EDTA 100 mM, Bestatin 2 mM, Pepstatin A 0.3 mM, E-64 0.3 mM) (Sigma, USA). The lysates were then sonicated at low output and 30% amplification for 20 sec and then spun at 14000x g at 4 °C for 10 min (Vibra-cell ultrasonic liquid processor, sonics vcx130). Finally, the supernatants were collected in aliquots and quantified by bicinchonic acid assay (PierceTM BCA protein assay kit, UK). The lysates were boiled and kept as in (section 2.4.2.1).

2.5.3 Gel preparation and running

The plastic plates (90 mm-wide x 83 mm-high x 1 mm-thick) (ATTO, AE6530 mPAGE, Japan) were thoroughly cleaned by methanol then dried and assembled according to the manufacturer instruction. The resolving gel stock (15 ml/ 2 gels) was prepared freshly with dH_2O at a concentration 12 % [(5 ml of 1.5 M Tris pH 8.8, 3.9 ml H_2O, 6 ml of 30 % acrylamide, 75 µl of 20 % SDS, 75 µl of 10 % (w/v) ammonium persulfate (APS), 25 µl tetramethylenediamine (TEMED)]. After pouring the resolving gel into the plastic plates, it was overlaid by adding 200 µl dH_2O then permitted to polymerize for 30 min. Then (5 ml/ 2 gels) of stacking gel [(0.62 ml of 0.5 M

Tris pH 6.8, 0.833 ml of 30 % acrylamide, 25 µl of 20 % SDS, 50 µl of 10 % (w/v) APS, 5 µl TEMD)] was added after removing the H_2O, to fill the space above the resolving gel; the comb was then inserted immediately without forming air bubbles. When the gel was completely polymerized, the comb was removed gently. Protein samples in SDS-PAGE sample buffer were loaded alongside with protein marker (Spectra™ Multicolour Broad Range Protein Ladder, thermos scientific, Lithuania). Electrophoresis was performed using a vertical gel apparatus (ATTO, Japan) at 220 V for 60 min at room temperature (Walker, 2012).

2.6 Comassie blue staining

SDS-PAGE gels were stained with Coomassie Brilliant blue (0.25 % w/v) plus 100 ml glacial acetic acid, 400 ml methanol in a total volume of 1000 ml H_2O, filtered through Whatman filter paper before use. The gels were immersed in the stain for 30 min on a shaker at RT and then de-stained by washing 5 times with de-stain buffer comprising 400 ml methanol, 100 ml concentrated acetic acid in a total volume of 1L H_2O. Finally, gels were imaged by white light transillumination using chemidoc documentation system (BioRad) (Walker, 2012).

2.7 Western immunoblotting

The wet transfer method was used to transfer the proteins from electrophoretic gel onto polyvinylidene fluoride (PVDF) membranes. The gel was washed three times for 10 min with transfer buffer and the protein then

transferred into PVDF membrane that had been soaked in 100 % methanol for 16 sec followed by 5 min in freshly prepared transfer buffer at RT.

The transfer apparatus was assembled by placing the gel and membrane in a sandwich of double filter papers and sponges that were saturated with transfer buffer. The PVDF membrane was always placed between the gel and the positive electrode in a vertical electrophoresis tank that was filled with cold transfer buffer and frozen cool block. The tank was kept cold during the electrophoresis by placing in an ice tray. The electro-blotting was performed at 200 V for 60 min. Then the PVDF membrane was blocked overnight at 4 °C in blocking buffer [5 % (w/v) skimmed-milk powder (Marvel, UK) in TBS-T].

Subsequently, the membrane was incubated with the required concentration of primary antibody diluted in blocking buffer for 2 h at RT with gentle shaking. Then the membrane was washed 5 times for 5 min with TBS-T [(20 mM Tris-HCl, pH 7.5, 150 mM NaCl, 0.1 % (v/v) Tween20)]. The membrane was then incubated with the secondary antibody labelled with horse raddish peroxidase, diluted appropriately (referred in the following relevant sections) for 1 h. The membrane was then washed a further 5 x for 5 min in TBS-T and protein bands were then developed by adding a freshly prepared substrate working solution (ECL) by mixing both substrate components 1:1 (0.1 mL/ cm^2) (Bio-Rad ECL substrate) and visualised by using chemidoc documentation system (Bio-Rad, UK) (Kurien & Scofield, 2015).

2.8 Indirect immunofluorescent assay

The HEK293 or BHK cells for IF staining were seeded onto coverslips (section 2.3.2 and 2.3.3). Initially, the cells were fixed for 15 min with 4 % paraformaldehyde prepared in PBS then washed 3X in buffer containing 1X PBS 0.1 % (v/v) Triton x-100 for 10 min at RT to induce cell membrane permeability. Then nonspecific binding sites were blocked by washing 3X in blocking buffer containing (1x PBS, 2 % donkey serum, 1 % Triton X-100). The slides were incubated with the primary antibody diluted 1:500 in blocking buffer. After 1 h, the slides were washed 3 X in washing buffer (1 X PBS-0.5 % tween-20) for 30 min to remove unbounded antibody followed by adding the secondary antibody (Alexa Fluor® 488 diluted at 1:200) for 1 h. The cells were washed 3 X in washing buffer then one drop of Prolong Gold® anti-fade reagent (Invitrogen, UK) were applied on each coverslip and incubated overnight in dark. The slides were examined under fluorescent microscopy (Carl Zeiss, Axio Imager 2) (Marchisio & Trusolino, 1999).

2.9 Immunohistological staining

Immuno-histological staining was undertaken at the Histology Laboratory, Institute of Veterinary Pathology, Vetsuisse Faculty, University of Zurich. The horseradish peroxidase (HRP) method was used. Sections (3-5 µm thick) were prepared from paraffin blocks and mounted on charged slides (Superfrost® Plus; Menzel-Gläser, Thermo Scientific). Sections were deparaffinised in xylene and graded alcohol (100 %, 95 %, 70 %) and underwent antigen retrieval by incubation in citrate buffer pH 6.0 (S2022;

Dako) in a pressure cooker at 98 °C for 20 min. Slides were transferred into TBS-Tween buffer (Dako 3006) and a Dako autostainer where they were incubated with the primary antibody diluted 1:500 in dilution buffer (S2022; Dako) for 12-15 h at 4 °C. After subsequent blocking of endogenous peroxidase activity with Dako REALTM peroxidase Blocking Solution (S2023; Dako) for 10 min at room temperature (RT), slides were incubated with the secondary antibody solution (EnVision + System HRP goat anti-rabbit; K4003; Dako) for 30 min at RT, and visualization with DAB (K3468; Dako) for 10 min at RT. Between each incubation step, slides were washed with TBS-Tween. After removal from the autostainer, sections were counterstained for 2 sec with haematoxylin, rinsed with tap water, subjected to graded alcohol (70 %, 95 %, 100 %) and xylene and cover slipped (Buchwalow & Böcker, 2010).

2.10 Heterologous expression of the recombinant protein

Recombinant GST-oLANA protein was expressed by growing a single colony in BL21 (DE3) bacteria in 10 ml of LB broth containing ampicillin (50 µg/ ml) at 37 °C combined with shaking at 200 rpm. Then a (1:10) dilution was used in volume fresh 9 ml LB broth with a similar concentration of ampicillin and incubated until the growth culture a density (OD_{959}) reached 0.6.

The expression of protein was induced by using β-d-1-thiogalactopyranoside (IPTG) (Sigma, USA) at a final concentration of 0.5 mM; the bacteria were subjected to additional incubation for 3 h then pelleted at 6000 rpm for 5 min. The pellet was re-suspended in 50 µl of SDS-PAGE

sample buffer and the cells were then disrupted by sonication on ice with low output and 30 % amplification for 15 sec. Proteins were analysed by SDS-PAGE followed by Comassie blue staining (see section 2.6). BL21 strain containing pGEX-3X vector without insert was used as a negative control (Samuelson, 2011).

2.11 GST-oLANA solubility

The expressed protein was examined for its solubility by using GST-Sepharose beads. GST-oLANA protein was produced by adding 1 % of primary culture to volume LB broth with ampicillin (50 µg/ ml). At the mid-log growth phase (OD_{595}=0.6), IPTG (0.1 mM) was added for a further 3 h incubation at 37 °C. Then 1.5 ml was pelleted by centrifugation at 3000 rpm for 5 min. The pellet was re-suspended in 300 µl of protease inhibitor cocktail that includes AEBSF (23 mM), EDTA (100 mM), bestatin (2 mM), pepstatin A (0.3 mM), E-64 (0.3 mM) (Sigma, USA). The protein was released by sonication on ice with low output and 30 % amplification for 15 sec. The mixture was spun at 6000 rpm for 5 min to form a pellet which was then kept on ice for analysis purpose while the supernatant was transferred to a new tube to be purified by anti-GST-Sepharose beads.

After equilibration of GST-Sepharose beads by washing three times with PBS, 50 µl of 50 % GST bead suspension was added to the supernatant and incubated for 5 min at RT. A 1 ml portion of PBS supplemented with 1 % triton X-100 was added to the solution and then spun at 6000 rpm for 30 sec in a microfuge. The supernatant was discarded, and the beads precipitate washed twice with PBS before being re-suspended in 50 µl of SDS-PAGE

sample buffer. The pellet from the original sample was thawed and re-suspended in 150 µl of SDS-PAGE sample buffer. Finally, samples analysed by SDS-PAGE to test whether the recombinant protein was expressed in soluble or insoluble form (Rosenberg, 2006).

2.12 Purification of GST-oLANA by inclusion protein preparation

An overnight culture was diluted at 1:10 into 10 ml fresh LB medium supplemented with ampicillin (50 µg/ml) (Sigma, USA) and incubated at 37 °C with shaking at 200 rpm until the culture reached a density (OD_{595}) of 0.6. At this point, IPTG was added to the culture at a final concentration of 0.5 mM to initiate protein expression. The incubation then continued for an additional 3 h at 37 °C with agitation at 200 rpm. The cells were harvested by centrifugation at 4000x *g* for 5 min and re-suspended to a final concentration of 10 % of 1 ml inclusion body prep buffer (100 mM NaCl, 1 mM EDTA, 50 mM Tris PH 8.0) supplemented with 1 mg/ ml of lysozyme (Sigma, USA) and incubated at RT for 20 min. The solution was then pelleted by centrifugation at 5000x *g* for 10 min, the pellet was snap frozen at -80 °C overnight and then thawed, re-suspended in 1 ml inclusion body prep buffer supplemented with 0.1 % w/v sodium deoxycholate and incubated for 10 min on ice with occasional mixing. $MgCL_2$ and DNaseI (sigma, USA) were added to a final concentration of 8 mM/ml and 10 µg/ml respectively followed by incubation at 4 °C with occasional mixing for 1 h.

Five aliquots were used in similar conditions to separate the insoluble target protein from soluble contaminants by centrifugation for 10 min at

(2000, 6000, 8000, 10000, 12000x *g*) respectively. A (1:1) dilution of 2x SDS-PAGE sample buffer was used for the supernatant while the insoluble fractions were suspended once in 1 ml inclusion body prep buffer supplemented with 1% v/v octylphenoxypolyethoxyethanol (nonidet-NP40) (Sigma, USA) then pelleted and washed with 1 ml inclusion body prep buffer and then protein samples were prepared by suspending the pellet in 200 µl of 2x SDS-PAGE sample buffer. Both supernatants and pellets were analysed by SDS-PAGE; subsequently, a large-scale inclusion body preparation was conducted using the same procedure with low speed centrifugation (2000 *g*) for 10 min to clarify the best inclusion body separation.

The concentration of GST-oLANA was estimated by SDS-PAGE (12 %) electrophoresis in comparison with serial dilutions of known concentrations of bovine serum albumin that were loaded in (200, 100, 50, 25, 12.5, 6.3, 3.1, 1.6 µg/ µl) as a standard calibrator for 10 µl of GST-oLANA of (one pellet re-suspended in 1 ml SDS- sample buffer) then stained by Comassie brilliant blue (see section 2.6) and analysed by Image Lab software (Ferrer-Miralles *et al.*, 2015).

2.13 Rabbit immunisation for antibody production

At the point when the GST-oLANA was confirmed to be immuno-reactive, it was purified (section 2.12) and used as an antigen to immunise rabbit (Pacific Immunology Antibody Production Corporation (USDA registration 93-R-283, USDA license 93-B-179, NIH/OLAW assurance A 4182-01) (1672 Main St. Ste., Ramona, CA 92065). The antigen was administered firstly with complete then incomplete Freund ’s adjuvant (CFA

and IFA) during the period of 19 October 2015-28 January 2016. At the end of the immunization programme, the antisera were collected and named (anti-oLANA).

2.14 Purification of rabbit anti-oLANA antibodies

2.14.1 Adsorption to acetone precipitated GST expressing bacteria

The initial purification of anti-oLANA was performed to remove cross-reacting and GST-specific antibodies. A suspension of BL21 bacteria containing merely the pGEX-3X vector induced by IPTG was lysed in 0.9 % NaCl (1g of bacteria/ 1 ml of saline). The mixture was incubated in ice for 5 min, then the appropriate amount of acetone was added (8 ml acetone/ 2 ml of suspension). The suspension mixed vigorously and incubated at 0 °C for 30 min with occasional mixing. The lysate was then spun at 10000 *g* for 10 min in a microfuge and the pellet re-suspended and incubated at 0 °C for 10 min. The mixture was cleared by centrifugation at 10000x *g* for 10 min and the pellet was spread in a clean filter paper until dry then collected in a secured container. The antisera were adsorbed using 1 % of the bacterial acetone powder at 4 °C with rotation for 30 min then centrifuged at 10000x *g* for 10 min (Rosenberg, 2006).

2.14.2 Affinity chromatography of rabbit IgG

The adsorbed serum was purified finally by affinity chromatography medium that contains recombinant protein G provided in MABTrapTM Kit (GE healthcare Bio-science, Sweden). Firstly, the HiTrap column and the antisera were equilibrated by using binding buffer (2.5 ml of concentrated binding buffer was added to 22.5 ml high quality water). The column was washed with 3 ml after removing of the preserving ethanol. The antisera were diluted (1:1) and applied into the column. Antibody was then eluted using elution buffer (0.5 ml of concentrated elution buffer and 4.5 ml high quality water). Each 600 µl of purified IgG was re-natured immediately by using 300 µl of neutralising buffer (20 % ethanol, 20% trometamol).

2.15 Generation of Modified Vaccinia Ankara recombinants expressing OvHV-2 glycoproteins

2.15.1 Propagation and titration of Vaccinia Ankara virus

BHK cells were seeded in 6- well plates (5x 10^5/ well) until they reached near confluence (see 2.3.3). Then ten-fold serial dilutions of modified vaccinia Ankara virus (10^{-4} to 10^{-8}) were used to inoculate BHKs (1 ml/ well). The cells were then incubated for 1 h at 37 °C with gentle swirling every 10 min. After that, viral inocula were removed and the cells were overlaid with 2 ml of complete MEM containing 2.5 % FCS, 0.5 % methylcellulose and incubated for 48 h until cytopathic effect appeared. Finally, the media was removed, and the cells were washed with PBS carefully then fixed with acetone-methanol (60-40) for 10 min followed by staining with 0.1 % crystal violet for 10 min.

2.15.2 Construction of rMVA-glycoproteins

Plasmid insertion vectors for insertion and expression of heterologous proteins in modified vaccinia Ankara and containing gB, gH, gL, and Ov7 of OvHV-2 were designed and synthesized by Thermofisher (Wyatt *et al.*, 2008). These glycoproteins are encoded by ORF8, ORF22, ORF47, and Ov7 respectively and they were named rMVA-(gB, gH, gL, and Ov7). As can be seen in (Figure 2-3), the MVA vectors have flanks homologous with vaccinia virus, facilitating insertion of the construct into the MVA genome and also contain GFP under the control of the P11 promotor which enable

identification and selection of recombinants. The glycoproteins expressed by the recombinant MVA vectors were also designed to contain particular epitope tag proteins by which they can be detected. Thus, the Flag tag was used in rMVA-gB and rMVA-gH vectors; the HA and V5 tags were used in rMVA-gL and rMVA-Ov7, respectively. These were under the control of the modified H5 promoter (mH5) (Wang *et al.*, 2010).

2.15.3 Generation of Modified Vaccinia Ankara Virus recombinants

The BHK cells were firstly seeded (5x 10^5/ well) in 6- well plate (see 2.3.3) then infected with vaccinia virus (0.5x 10^5 pfu/ ml) (see 2.15.1) and transfected as described in (2.4.2). Prior to the end of incubation, the virus inoculum was aspirated from the cell monolayer, washed twice with PBS and the mixtures of DNA/ lipofectamine were then added. The volume was made up to 1 ml with MEM media and incubated for 4 h at 37 °C in 5 % CO_2. After that, the media was replaced with 1 ml of MEM containing 2.5 FBS and incubated 48 h at 37 °C. The cells were harvested in 0.5 ml media, transferred into sterilized tubes and lysed by conducting three cycles of freezing in dry ice and thawing in a 37 °C water bath. In each cycle, the contents were mixed by vortexing and the lysates were finally stored at -80 °C.

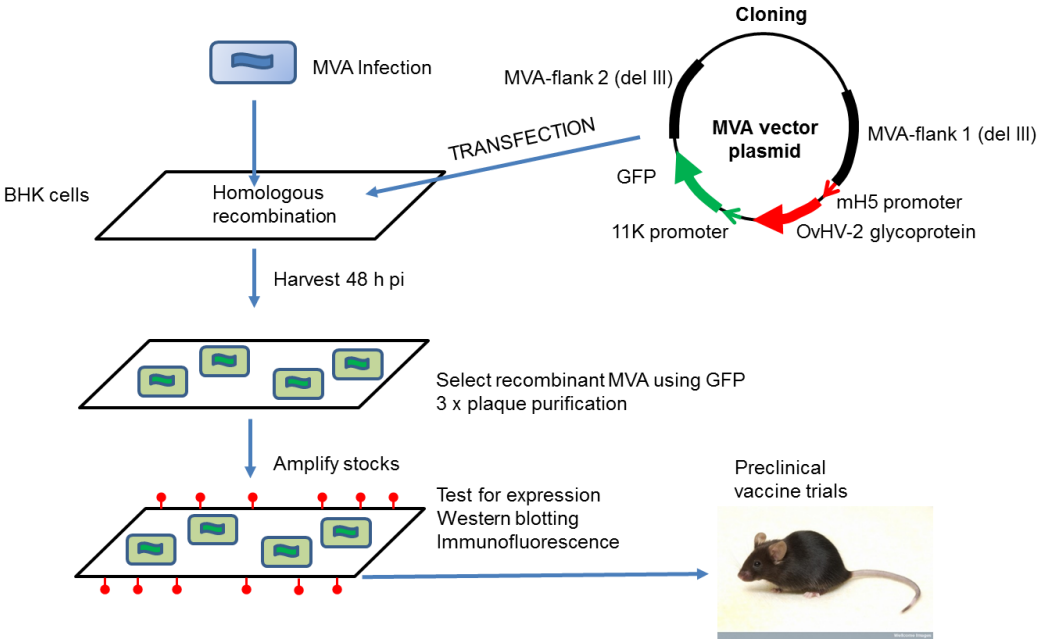

Figure 2-3. Schematic diagram shows the workflow of construction the Modified Vaccinia Ankara (MVA) recombinants expressing OvHV-2 glycoproteins.

2.15.4 Purification of rMVA by plaque selection

The generated recombinant viruses from (section 2.15.3) were purified by three rounds of plaque purification. This was performed by picking-up a separate GFP plaque of each recombinant MVA using a Gilson pipette tip and adding into 0.5 ml of MEM media. After 3 cycles of freezing and thawing, a portion was used to re-infect BHKs (Kremer *et al.*, 2012). Finally, each purified MVA was quantified by titration as described in section (2.15.1).

2.15.5 Large scale production of rMVAs

Each rMVA was used to infect BHK cells in T175 flasks as described in section (2.15.1) at a multiplicity of infection (MOI) of 5 PFU/ cell. After 24 h cells were collected, and virus released by homogenization, using a tight-fitting Dounce homogenizer. The virus stocks were then titrated as described in (2.15.1) and stored at -80 °C.

2.15.6 Immuno- precipitation of flag fusion protein

Immuno-precipitation using M2 affinity gel carrying an anti-flag mAb (Sigma, UK) was used to examine the expressed glycoprotein complexes. BHK cells (5x 10^5/ well) were cultured (see 2.3.3) for 24 h then infected with the recombinant MVAs (5 PFU/ cell) overnight, as in section (2.15.1). First, all the media was removed, then cells were washed carefully 3x with PBS and then lysed using TBS (50 mM Tris PH 8, 150 mM NaCl, 1 mM EDTA, 0.5 % NP40) with protease inhibitor (10 µl/ 1 ml). Anti-flag M2 affinity gel (40 µl)

was transferred into an Eppendorf tube and spun at 8000x *g* for 30 sec at 4 °C. The supernatant was then removed, and the packed gel was washed twice with 500 µl of TBS before adding cell lysate to the M2 gel. It was then incubated with agitation at 4 °C overnight. The resin-complex was spun at 8000 *g* for 30 sec at 4 °C to pellet the beads and washed 3 x with 500 µl of TBS. Finally, the flag- fusion complexes were eluted by adding 100 µl of glycine (0.1 M, HCl pH 3.5) for 5 min with low agitation then pelleted at 8000 *g* for 30 sec. The supernatant was transferred into fresh tube containing 10 µl of buffer (Tris HCl 0.5 M, 1.5 M NaCl, pH 7.4). The protein complex was analyzed further as described in (2.15.6).

2.15.7 De-glycosylation of recombinant glycoproteins

The immuno-precipitated complexes were cleaved by using Peptide: N-Glycosidase F (PNGase F), following the manufacturer's recommendation (BioLabs, UK). A 10 µg portion of glycoprotein complex was combined with 1 µl of (10 x) glycoprotein denaturation buffer (0.5 % SDS, 40 mM DTT) was made up to 10 µl with dH_2O and denatured by heating the mixture at 100 °C for 10 min. Then, 2 µl of 10 x Glyco-Buffer 2 (50 mM Sodium Phosphate, pH 7.5), 2 µl of 10 % NP-40 and 1 µl of PNGase F were added. The mixture was made up to 20 µl with dH_2O and incubated at 37 °C for 1 h. Cells were harvested (see 2.5.2.1) and tested by western immunoblotting as described in section (2.7).

2.15.8 Mouse immunization by the rMVAs

To test the immunogenicity of the MVA recombinants, viruses were used to inoculate mice via the intraperitoneal route. All work was performed under UK Home Office Licence 70/8599. Mice (BALB/c strain) were purchased from Charles River, aged 6 weeks and were immunized with 1x 10^4 PFU of virus by IP. Mice were boosted 3 weeks later and were euthanized, and blood collected for serum production 2 weeks after the boost.

3. Chapter three: The role of gamma-herpesviruses in the pathogenesis of Malignant Catarrhal Fever

3.1 Abstract

There is no permissive cell line to propagate most of the aetiological agents of MCF, which has hindered the understanding of disease pathogenesis. However, PCR has improved our understanding of aspects of MCF disease (Russell *et al.*, 2009). Previous studies in our laboratory have shown that cattle without MCF can carry OvHV-2, indicating other factors, possibly herpesviruses are involved in MCF (Amin, 2015). Therefore, the aim of this study was to identify other factors that possibly induce MCF apart from MCF viruses. In this study, a combination of two PCR assays (PAN herpesvirus endpoint and qPCR) as qualitative and quantitative approaches (see 2.2), were employed to examine sheep, goats, cattle without MCF and cattle with signs of MCF, bison, and water buffalo to identify which γ-herpesviruses may be involved in MCF. The results showed that although the related bovine herpesvirus 6 and ovine herpesvirus 1 are endemic commensals of cattle, they could afford cross-protection from infection with

OvHV-2 and development MCF. Combining these two PCR assays will help in the diagnosis of MCF in various hosts.

3.2 Results

3.2.1 PAN- herpes consensus nested PCR

Modified and unmodified primers of degenerate and deoxyinosine-substituted primers from a highly conserved sequence of the herpesvirus DNA polymerase (DPOL) gene were used in this approach as described in (2.2.1). Specific amplified fragments, 288 bp in length, were produced from this technique (Figure 3-1). These were cloned into *E coli* to produce plasmids for gene sequencing. These were then aligned using NCBI BLAST analyses to identify the detected species. DNA samples were tested from animals with or without MCF from multiple ruminant species. The results showed detection of six γ-herpesviruses including: OvHV-2, Bison LHV, CpHV-2, BoHV-6, Caprine LHV, and Reindeer γ-HV (Table 3-1). Although OvHV-2 was identified in all cattle with MCF (100 %), it was not found in any bison with MCF. However, Bison LHV, CpHV-2, and Reindeer γ-HV were identified in 8 of 25 cases. Two of three cases of water buffalo with MCF were positive for OvHV-2.

The detection of Bison LHV in water buffalo is interesting but is unlikely to be the cause of disease in this case.

The data obtained from testing deer samples highlight only four cases were positive. Notably, one case of semi-domesticated reindeer (*Rangifer*

tarandus) was co-infected with CpHV-2 and Reindeer γ-herpesvirus. Interestingly, BoHV-6 was detected in goat.

Caprine LHV was detected in one goat that had pathological signs of chronic granulomatous pneumonia according to the pathological report obtained from Institute of Veterinary Pathology, Vetsuisse Faculty, University of Zurich, Switzerland. Additionally, Reindeer γ-herpesvirus was identified in deer (*Rangifer tarandus*) and in one bison with MCF which is interesting. Therefore, to exclude contamination, this case was tested twice by PAN-nested PCR and exactly similar sequence was found.

The obtained DNA sequences from the currently diagnosed herpesviruses were further analysed to characterise the phylogenetic evolutionary relationship. The phylogenetic tree revealed that OvHV-2 and CpHV-2 were closely related to the previously identified MCF-viruses whereas reindeer gamma-HV, Bison LHV, BoHV-6, and Caprine LHV were demonstrated in another clade (Figure 3-2).

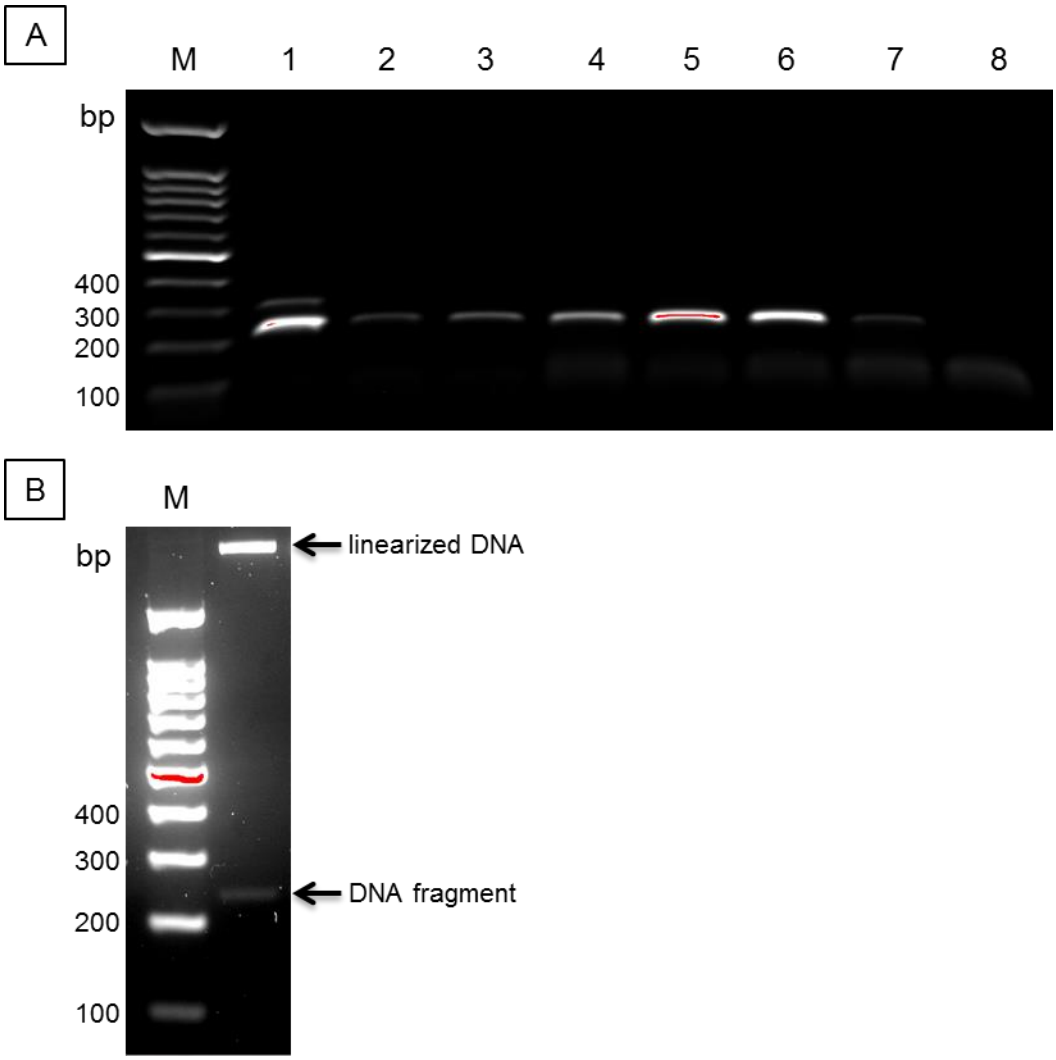

Figure 3-1. Gel electrophoresis (1.5 % agarose) image shows PCR products of DPOL consensus herpesvirus nested PCR. These were amplified by modified and non-modified primers, electrophoresed by the end of the second round before being cloned into *E coli*, lanes (1-7) are positive samples; lane 8 is control negative at which ddH_2O was used instead of template DNA. (B) The reconstructed plasmid with *Eco*RI enzyme for positive clone analysis. (M) is DNA marker (100 bp, Cleaver Scientific).

Table 3-1. The identified herpesviruses in tested animals (n= 54) by PAN-herpesvirus nested PCR and sequencing.

Identified virus	Cattle without MCF signs n(Lung, LN)= 8		Bison without MCF signs n (LN)= 2		Bison with MCF signs n (LN)= 25		Buffalo with MCF signs n (BC)= 3		Deer with MCF n (BC)= 13		Goat n (lung)= 3	
	Infected	%	Infected	%	Infected	%	Infected	%	Infected	%	Infected	%
OvHV2	8	100	0	0	0	0	2	66.6	0	0	0	0
Bison LHV	0	0	0	0	6	24	1	33.3	0	0	0	0
CpHV2	0	0	0	0	1	4	1	33.3	2	15.3	1	33.3
BoHV6	0	0	0	0	0	0	0	0	0	0	1	33.3
Caprine LHV	0	0	0	0	0	0	0	0	0	0	2	66.6
Reindeer ɣ-HV	0	0	0	0	1	4	0	0	2	15.3	0	0

Abbreviation: sample number (n), Mediastinal lymph node (LN), Buffy coat (BC).

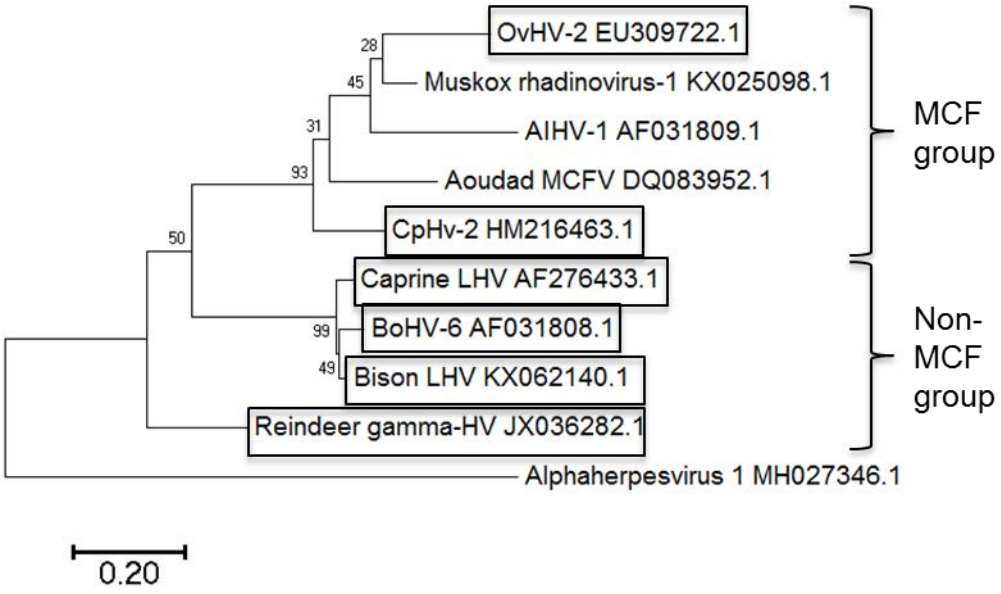

Figure 3-2. Maximum Likelihood phylogram based on nucleotide sequences of the DNA polymerase genes of the identified herpesviruses. Box shaded are the identified species. The bootstrap consensus tree was constructed from 1000 replicates to provide support for individual nodes by using MEGA7 software, version 7.0.21.

3.2.2 q-PCR assays

Five quantitative assays including: OvHV-1, BoHV6, OvHV2, Bison LHV, and CpHV2 were developed (as described in 2.2.2) and used to analyse the frequency and load of different ruminant gamma-herpesviruses in DNA samples. These were established by designing specific primers and probes (see 2.2.2.1) to produce reference plasmids for viral quantification (see 2.2.2.3) by optimal protocol (see 2.2.2.2). The quantification results were normalised by quantifying 12s- ribosomal DNA.

3.2.2.1 Assay specificity

There was no evidence for any cross reaction when the assays used to test samples that are known to be positive for only particular species. For instance, known EHV2-positive samples were negative. Another approach was used by testing clinical samples of cattle with MCF that were OvHV-2 positive. Additionally, combining the data from the PAN-consensus PCR provided further confirmation on q-PCR specificity, as some samples appeared to be infected with particular herpesviruses such as: CpHV2, OvHV2, Reindeer herpesvirus, and Bison LHV. All these lines of evidence provide confidence in the specificity of the developed assays.

3.2.2.2 Assay sensitivity

Repeatability (intra-assay variation) and reproducibility (inter-assay variation) of each developed q-PCR were estimated by five experiments in

which the Ct value of duplicates of each dilution of the standard plasmid was calculated. The validation of the sensitivity results for the OvHV-1 reference plasmid are listed in (Table 1 in the appendix) which revealed the lowest coefficient of variation for (2×10^3) copy number (0.03 %) which was in experiment (IV) and the highest (5.05 %) for (2×10^0) in the same experiment. The coefficients of determination (R^2) were calculated in all experiments of this reference as (0.983 ± 0.466).

The results obtained from the BoHV-6 reference plasmid are presented in (Table 2 of the appendix) which revealed a lowest coefficient of variation (0.004 %) that was calculated in (2×10^5) copy number of experiment (I) whilst the highest (5.31 %) for copy number (2×10^1) in the experiment (V). The coefficients of determination (R^2) were calculated in all experiments of this reference as (0.983 ± 0.375).

As can be seen from the (Table 3 of the appendix), in OvHV-2 standard reference, the lowest coefficient of variation (0) was reported in copy number (2×10^4) in the experiment (II) and the highest (3.51 %) for (2×10^2) copy number in experiment (V). The overall value of coefficient of determination (R^2) in this reference was 0.999 ± 0.13.

The lowest coefficient of variation in Bison LHV reference standard was (0.02 %) in experiment (V) of (2×10^0) copy numbers while the highest (2.84 %) in experiment (II) of (2×10^2) copy number (Table 4 in the appendix). The coefficient of determination (R^2) in this reference was (0.997 ± 0.2). In CpHV-2 standard plasmids, the lowest coefficient of variation was found in experiment number (IV) as (0.04 %) at (2×10^6) copy number whereas the highest (4.72 %) was determined in experiment number (III) of

(2×10^7) copy number (Table 5 in the appendix). The coefficient of determination (R^2) in this reference was (0.999± 0.1).

It is apparent that 12s- ribosomal DNA internal genomic control was amplified in all DNA samples, indicating that a similar DNA template quantity was used in the q-PCR assays. Therefore a normalisation strategy was adopted successfully to account for the errors in the assay quantification and reaction efficiency caused by DNA quality and contamination (Figure 3-3).

From these data, it was concluded that these assays were highly specific and sensitive.

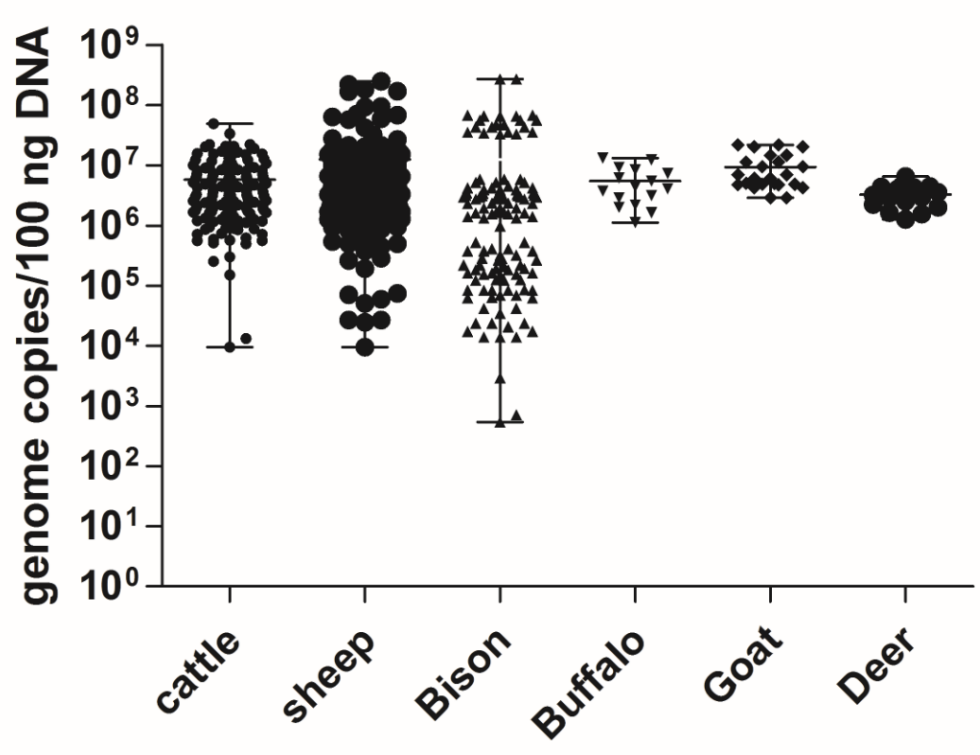

Figure 3-3. Logarithmic amplification of the internal 12s-ribosomal DNA\ 100 ng template of cattle, sheep, bison, buffalo, goat, and deer DNA were plotted in normal distribution by using Graph Pad prism (version 7, GraphPad Software Inc, CA, USA). The normalisation was conducted to account the variability of DNA quality and contamination.

3.2.3 Gamma-herpesvirus frequency and loads

In this study, different sample sources including: cattle without MCF (lung, LN), cattle with signs of MCF (lung, spleen, buffy coat), sheep (lung, LN), sheep with SPA (lung, blood), goats (lung), bison (blood, nasal swab), bison with MCF (lymphoid cells), buffalo with MCF (lung, LN), and deer (spleen, buffy coat, nasal swab) were tested for gammaherpesviruses by q-PCR. Our results show a complex pattern of infection and co-infection with several ruminant γ-herpesvirus species. However, MCF was only associated with a high viral load of OvHV-2 or CpHV-2.

3.2.3.1 OvHV-1

Of interest, OvHV-1 was detected in more than half of the healthy cattle but not in cattle with MCF. In fact, this finding is novel as OvHV-1 has only been detected previously in sheep. Although, OvHV-1 was found in high a proportion of cattle (54 %), it was not found in cattle with MCF ($P<0.01$); apparently it does not cause MCF (Table 3-2).

Testing sheep samples revealed that OvHV-1 was endemic in this species. There was higher infection rate (71 %) in comparison with sheep that suffered from SPA (53 %). Interestingly, goats were negative for this viral species. The data obtained from testing healthy bison revealed that (11 %) were infected with OvHV-1. Nevertheless, bison, buffalo and deer with MCF were negative.

Viral DNA loads were variable among those positive samples as the higher median viral load (589 copies/ 100 ng DNA) was found in sheep that

infected with SPA whilst the lower (9 copies/ 100ng DNA) was detected in cattle without MCF.

3.2.3.2 BoHV-6

The same samples were also tested for BoHV-6. This virus was detected in 30 % cattle without MCF and 11 % of those with signs of MCF. These percentages were not significantly differ (P>0.01). Importantly, BoHV-6 was found in goats with high frequency (50 %) with peak load of 4395 copies/ 100 ng DNA. This level of viral load was not found in cattle. This is the first time that this species was detected in goats. Another interesting finding is that BoHV-6 appeared to be enzootic in bison as well with an infection rate of 22 %. However, BoHV-6 was not detected in numerous hosts such as sheep (with or without SPA) and deer. It was not seen in bison and buffalo with MCF, suggesting the possibility of cross protection against OvHV-2 as in OvHV-1 in these species.

BoHV-6 quantification in cattle with MCF was detected in a median viral load (27 copies/ 100 ng DNA). This was lower than the median viral load in healthy cattle (44 copies/ 100 ng DNA). Overall, the highest median load (125 copies/ 100 ng DNA) was seen in healthy bison (Table 3-2).

The results of OvHV-1 and BoHV-6 genomic loads revealed that they are commensals in cattle. In this aspect, both viruses were prevalent in cattle without MCF (lung and LN) organs as shown in (Figure 3-4). Quantification of OvHV-1 revealed maximum values of 36 and 136 copies/ 100 ng DNA in lung and LN respectively, while BoHV-6 had slightly higher viral loads (412 and 660 copies/ 100 ng DNA in lung and LN respectively). Only a few samples of

cattle with MCF (3 out of 27), mainly lymphoid cells, were found positive for BoHV-6 but with a relatively low median viral load (26 copies/ 100 ng DNA). In the analysis of sheep samples, OvHV-1 was detected in lung with a maximum load of 1611 copies/ 100ng DNA which is higher than the load in the lungs of healthy cattle, while in LN tissue, it was 66 copies/ 100 ng DNA.

3.2.3.3 OvHV-2

OvHV-2 was detected in all cattle with MCF and in 50 % of buffalo with MCF whereas goats, healthy bison, bison with MCF, and deer were not infected.

The obtained data revealed that cattle with MCF infected with high OvHV-2 viral loads as the value was reached (7.6×10^9 copies/ 100 ng DNA) whilst the value in buffalo was found as (3×10^5 copies/ 100 ng DNA) (Table 3-2).

3.2.3.4 Bison LHV

Bison LHV was found in healthy bison and bison with MCF. It was detected in a lower proportion (11 %) in the latter as compared with healthy bison (44 %). The median viral loads (13 copies/ 100 ng DNA in healthy bison and 23 copies/ 100 ng DNA in bison with MCF) were relatively low. In one case, a buffalo with MCF was diagnosed with this viral species (134 copies/ 100 ng DNA), implying that it can cross host (Table 3-2).

3.2.3.5 CpHV-2

Surprisingly, only one case of 14 goat samples was found positive for CpHV-2 (20 copies / 100 ng DNA). A high proportion of healthy bison (78 %) carried CpHV-2. A lower proportion of bison with MCF (48 %) were infected with this virus. Viral loads in both cases were relatively low (63 copies/ 100 ng DNA in bison with MCF versus 36 copies/ 100 ng DNA in healthy bison).

Several deer were found positive with a very low median viral load (4 copies/ 100 ng DNA). Additionally, one case of a buffalo with MCF was found to be infected with CpHV-2 and with a very high viral load (1.2×10^7 copies/ 100 ng DNA) which indicates its role in causing MCF (Table 3-2).

3.2.3.6 Gamma-herpesviruses co-infection

The results showed numerous multiple infections in both healthy and MCF cases by using pan-herpesvirus nested PCR and q-PCR. In healthy cattle, four cases were found positive for OvHV-1 and BoHV-6. In cattle with MCF, only three cases were detected positive for BoHV-6 and OvHV-2. In buffalo with MCF, there was one case of co-infection including OvHV-2, CpHV-2, and Bison LHV. In healthy bison, four positive cases were detected for Bison LHV and CpHV-2. One of these cases was also infected with OvHV-1 while another case was found positive for BoHV-6 as well. In bison with MCF, three cases of co-infections were found positive for Bison LHV and CpHV-2. In deer samples, there was one case of co-infection detected by pan-herpesvirus nested PCR for CpHV-2 and Reindeer gamma-herpesvirus.

Table 3-2. Results of q-PCR assays frequency and viral DNA load quantifications in the tested animals.

Host	Tested	Viral species																			
		Infection%	OvHV-1			Infection%	BoHV-6			Infection%	OvHV-2			Infection %	Bison LHV			Infection %	CpHV-2		
			Min	Max	Med		Min	Max	Med		Min	Max	Med		Min	Max	Med		Min	Max	Med
Healthy cattle	33	54.5	3	80	9	30.3	9	536	44	-	-	-	-	-	-	-	-	-	-	-	-
Cattle/ MCF	27	0	0	0	0	11.1	7	31	27	100	154	7.6×10^{9}	1.1×10^{5}	-	-	-	-	-	-	-	-
Sheep	14	71.4	4	1611	18	0	0	0	0	-	-	-	-	-	-	-	-	-	-	-	-
Sheep/ SPA	41	53.6	4	13749	589	0	0	0	0	-	-	-	-	-	-	-	-	-	-	-	-
Goat	14	0	0	0	0	50	7	4395	30	0	0	0	0	-	-	-	-	7.1		20	
Bison	9	11.1		20		22.2	100	149	125	0	0	0	0	44	3	214	13	78	16	92	36
Bison/ MCF	45	0	0	0	0	0	0	0	0	0	0	0	0	11.1	2	146	23	48.8	3	299	63
Buffalo/ MCF	6	0	0	0	0	0	0	0	0	50	114	3×10^{5}	1×10^{4}	16.6		134		16.6		1.2×10^{7}	
Deer	13	0	0	0	0	0	0	0	0	0	0	0	0	-	-	-	-	15.8	3	5	4

Abbreviation: minimum (min), maximum (max), median (med)/ 100 ng genomic DNA, not tested (-), only one positive sample was diagnosed (empty box).

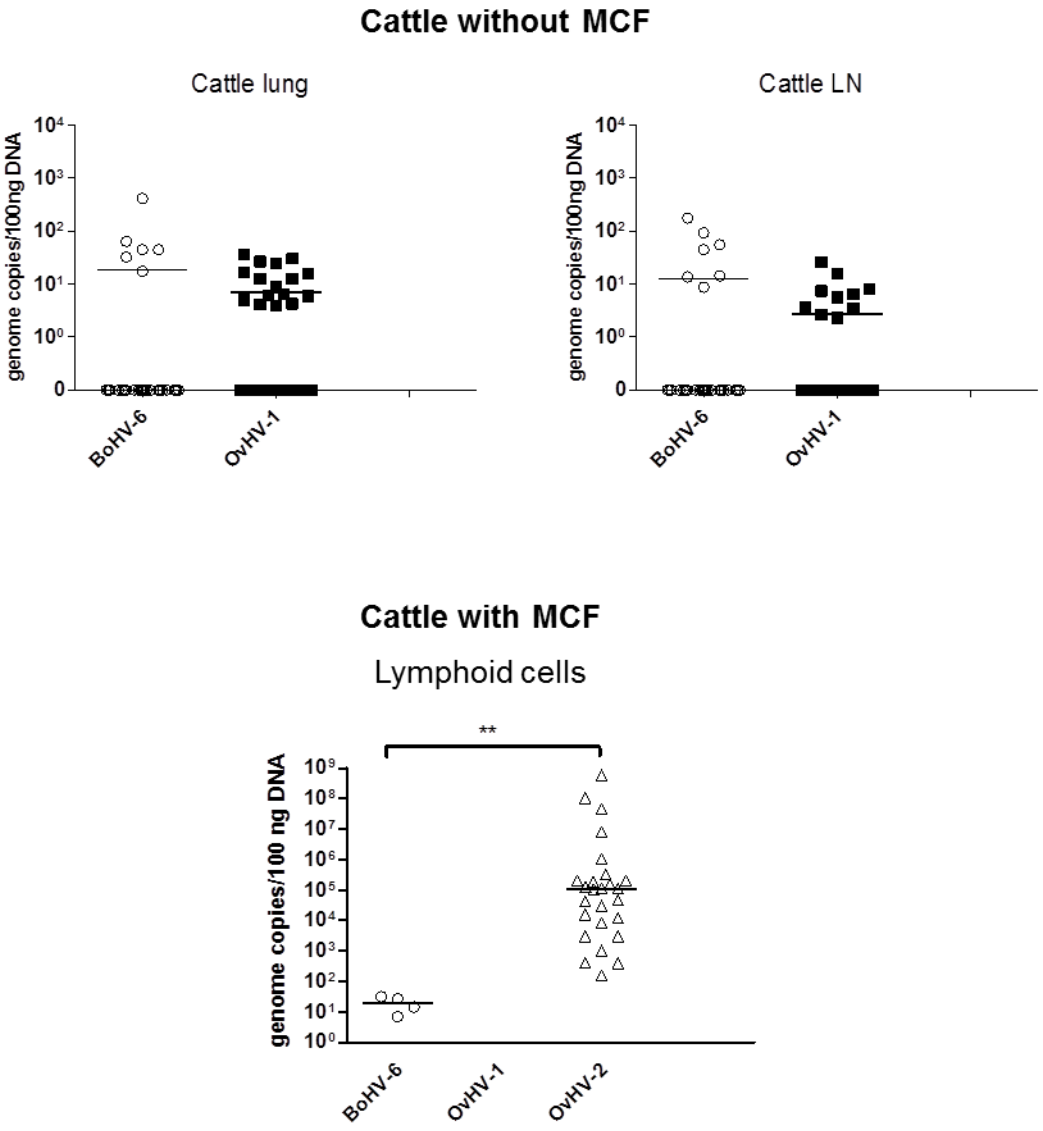

Figure 3-4. BoHV-6, OvHV-1 and OvHV-2 loads DNA (copies/ 100 ng DNA) in lung and LN of healthy cattle and lymphoid cells of cattle with MCF. Analysed by T-test mann-whitney (Graph Pad prism version 7, Inc, CA, USA).

3.3 Discussion

Studies in our laboratory have revealed that OvHV-2 can be harboured in cattle without MCF signs. Therefore, we suggested that possibly other factors involved in MCF apart from MCF viruses. The hypothesis of this study was whether the presence of alternative gamma-herpesviruses involved with OvHV-2 in causing MCF or co-infections with OvHV-2 could induce MCF. The generated data showed a complicated scenario, arising from infection and co-infection by γ-herpesviruses with infection of multiple ruminant hosts by some species. Importantly, the results suggested that quiescent infection with ruminant ɣ-herpesviruses other than OvHV-2 provides protection for cattle against OvHV-2 infection and prevent MCF. For instance, although OvHV-1 was enzootic in cattle without MCF, it was not found in cattle with MCF. This suggests that OvHV-1 infection may in some way protect against the development of MCF in cattle. Assessment of the role of these viral species revealed that, in line with previous work, MCF is associated with high viral load of OvHV-2 and CpHV-2.

The PAN-herpesvirus nested PCR was based on using consensus degenerate primers to amplify highly conserved coding motifs of herpes viral DNA polymerase. The sequence of this gene is highly conserved among the herpesvirus species. This assay was established by (Vandevanter *et al.*, 1996). For more sensitivity and wider range of herpesvirus diagnosis, the assay was then modified by (Ehlers *et al.*, 1999b) through combining of the degenerate and deoxyinosin- substituted primers. This later assay was adopted in the current study (see Table 2-1). The specificity of using these

primers in generating species-specific products has been determined by the researchers who developed this approach. It has been successfully employed by others to demonstrate not only known herpesviruses but also newly recognised members with a high sensitivity and specificity (Chmielewicz *et al.*, 2003; Ehlers *et al.*, 2007; Fernández-Aguilar *et al.*, 2016). This technique was therefore adopted in the current study and resulted in detecting six herpesvirus species (OvHV-2, Bison LHV, CpHV-2, BoHV-6, Caprine LHV, and Reindeer γ herpesvirus). In contrast, this assay is perhaps not suitable for conducting epidemiological surveillance because it is labour-intensive and relatively expensive.

The involvement of other ruminant gammaherpesviruses apart from known MCF viruses is poorly understood with no reports in their occurrence in bison, water buffalo, and deer. These hosts have been reported to be highly susceptible to MCF without producing infectious particles (Cunha *et al.*, 2012; Taus *et al.*, 2014).

Taqman q-PCR assays were developed and used in this study to detect and quantify OvHV-1, BoHV-6, OvHV-2, Bison LHV, and CpHV2. This technique has been employed to perform numerous epidemiological and pathological studies due to its advantages of highly sensitivity, reliability, and speed (Cunha *et al.*, 2009; Elia *et al.*, 2008; Hughes *et al.*, 2010; Kim *et al.*, 2003; Traul *et al.*, 2005).

OvHV-1 and BoHV-6 are highly related but both were detected to a greater or lesser extent in sheep (not enzootic for BoHV-6) and cattle without MCF. The finding of OvHV-1 in healthy cattle is novel as it has only been reported in sheep previously (Kopácek *et al.*, 2000; Scott *et al.*, 1984).

Importantly, OvHV-1 was not detected in cattle with MCF while BoHV-6 was diagnosed in some MCF cases with lower viral load than in cattle without MCF. This suggests particularly OvHV-1 infection may in some way prevent triggering of MCF in cattle and perhaps afford cross-protection among these viruses. They all belong to the macavirus genus, share a high degree of sequence homology and may therefore be antigenically cross-reactive. However, all these rumminant herpesviruses are split into MCF and non-MCF viruses depending on their genetic discrepances. The phylogenetic relationship between these viruses based on DNA polymerase gene sequence showed this attitude (Figure 3-2). This finding will help to provide new insight into preventing MCF.

OvHV-1 has been associated with SPA in sheep (Martin *et al.*, 1979). We used our q-PCR assay to quantify this viral species in sheep that suffered from SPA to demonstrate the role of OvHV-1 in this disease. The obtained results showed that some SPA cases are still negative for OvHV-1 while quantification of the positive ones revealed massive elevation of the viral copy number (Table 3-2). This indicates that OvHV-1 is not the causative agent of SPA, while the high viral copies in the identified cases might be the result of the OvHV-1 lytic replication due to the stressful conditions of adenomatosis or effects of SPA on immunity.

The obtained BoHV-6 quantification data fits with the previous reports of its prevalence in healthy cattle (Kubiś *et al.*, 2013). However, other studies demonstrated that BoHV-6 could be involved in unresponsive endometritis of dairy cattle (Banks *et al.*, 2008; Cobb *et al.*, 2006). Recently, BoHV-6 has been also detected in some buffalo cases that suffered from

lymphoproliferation. Interestingly, these cases were not present for bovine leukemia virus (BLV). However, the pathological role of BoHV-6 has not been confirmed yet (de Oliveira *et al.*, 2015). In another study, viral meta-genomics analysis was used to address the aetiological agents associated with Bovine Respiratory Disease (BRD) and non-suppurative encephalitis in cattle; interestingly, BoHV-6 was proposed to be one of the viruses that was responsible in causing these syndromes (Ng *et al.*, 2015).

Another novel finding was identifying of BoHV-6 in goats suffering from chronic penumonia. This suggests a role for this host in viral transmission and explains how this virus may spread to cattle. This might be due to the direct contact between goats and cattle, which may occur in Switzerland where these samples came from. The most obvious conclusion from this analysis is that viral loads of both viruses are increased in lungs of diseased sheep and goats that probably resulted from a local immune defect in the infected animals.

The current data demonstrates that as in sheep, goats seem to be another reservior host for MCF viruses (CpHV-2); this agrees with previous studies that suggest a potential role of goats as reservoir for MCFV-WTD that leads to MCF in white- tailed deer (*Odocoileus virginianus*) (Li *et al.*, 2013). Finding BoHV-6 in goats (50 % of samples) and (30 % of cattle samples) was unexpected and could be explained by the fact that the nomenclature of BoHV-6 was established on the basis of its first identification in cattle therefore this name is tentatively referenced. This raises the question as to whether goats are the natural or merely accidental host for this viral species. There is strong evidence for the role of goats as a reservior host for other

herpesviruses. We established the q-PCR for quantification of CpHV-2. One case MCF in deer was also diagnosed positive for CpHV-2. It can be concluded that the evolutionary relationship of these ruminants make them suitable hosts for the closely related herpesviruses.

BoHV-6, CpHV-2, OvHv-1, and Bison LHV were identified in healthy bison whereas bison with MCF were infected with only CpHV-2. Interestingly, CpHV-2 and OvHV-2 were quantified in high viral load in one case of water buffalo with MCF. In another case, a buffalo was diagnosed with Bison LHV raising the question of which is the natural host for this viral species. Little is known about this viral species. This study is the first to quantifiy bison LHV and further work is required to investigate its pathological role in more ruminants.

Cattle are relatively resistant to MCF, probably as they have been farmed with sheep for long time. Sheep are the natural host for OvHV-2 and MCF appears as sporadic cases in cattle with occasional outbreaks. Previously, OvHV-2 was detected in a longitudinal study in healthy cattle (Powers *et al.*, 2005). A recent study in our laboratory has shown similar findings (Amin, 2015).

In this study, an OvHV-2 q-PCR assay was used to test MCF cases to demonstrate the prevalence and relationship with other gammaherpesviruses. Importantly, all the pathological MCF cases were diagnosed with very high viral loads of OvHV-2 (except bison with MCF), wherease other viral species were either not found or had low viral loads.

It has been shown that bison are highly sensitive to OvHV-2 (O'Toole *et al.*, 2002; O'Toole & Li, 2014). Our analysis of bison showed that some

had MCF symptoms but were not present for OvHV-2. In these cases, the bison may have not had MCF or the presence of low viral loads of Bison LHV or CpHV-2 within this highly sensitive host could still be a factor in causing the immune-dysregulation and MCF development. Reindeer gamma herpesvirus was identified in deer but due to time limitation and small number of deer samples to test, q-PCR assay was not developed to quantify this viral species.

Our results revealed that more than half of the healthy cattle were positive for OvHV-1. However, cattle with MCF were not found infected. BoHV-6 was detected in 30 % of healthy cattle and in 11 % of cattle with MCF. In contrast, BoHV-6 was not detected in bison and buffalo with MCF. This data suggested that OvHV-1 possibly has a role in preventing MCF due to the antigenic similarity (Figure 3-5).

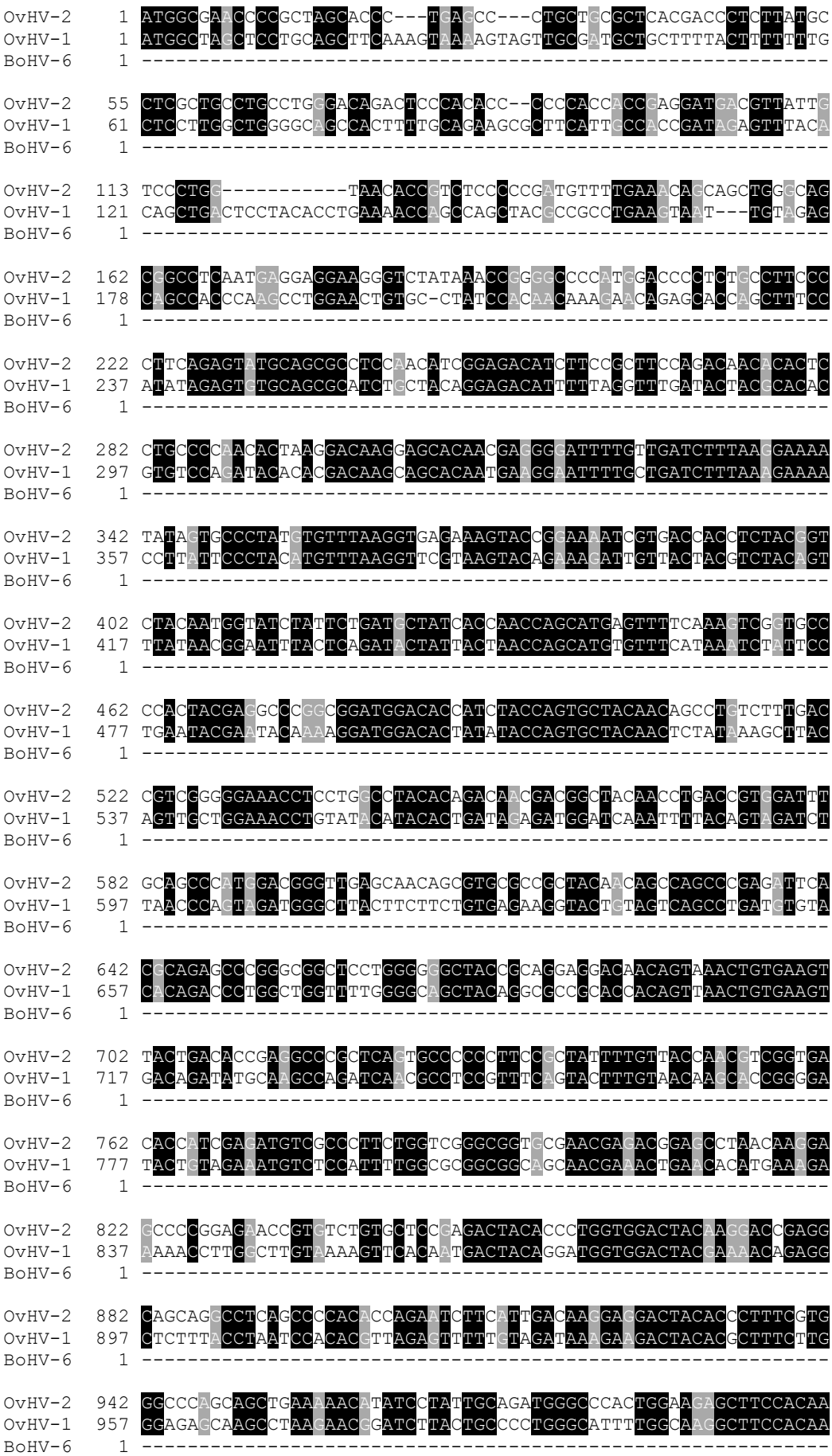
OvHV-2 1 ATGGCGAACCCGCTAGCACCC---TGAGCC---CTGCTGCGCTCACGACCCTCTTATGC
OvHV-1 1 ATGGCTAGCTCCTGCAGCTTCAAAGTAAAAGTAGTTGCGATGCTGCTTTTACTTTTTTG
BoHV-6 1 --
OvHV-2 55 CTCGCTGCCTGCCTGGGACAGACTCCCACACC--CCCCACCACCGAGGATGACGTTATTG
OvHV-1 61 CTCCTTGGCTGGGGCAGCCACTTTTGCAGAAGCGCTTCATTGCCACCGATACAGTTTACA
BoHV-6 1 --
OvHV-2 113 TCCCTGG-----------TAACACCGTCTCCCCCGATGTTTTGAAACACCAGCTGGGCAG
OvHV-1 121 CAGCTGACTCCTACACCTGAAAACCAGCCAGCTACGCCGCCTGAACTAAT---TGTAGAG
BoHV-6 1 --
OvHV-2 162 CGGCCTCAATGAGGAGGAAGGGTCTATAAACCGGGGCCCCATGGACCCCTCTGCCTTCCC
OvHV-1 178 CAGCCACCCAAGCCTGGAACTGTGC-CTATCCACAACAAAGAACAGAGCACCAGCTTTCC
BoHV-6 1 --
OvHV-2 222 CTTCAGAGTATGCAGCGCCTCCAACATCGGAGACATCTTCCGCTTCCAGACAACACACTC
OvHV-1 237 ATATAGAGTGTGCAGCGCATCTGCTACAGGAGACATTTTAGGTTTGATACTACGCACAC
BoHV-6 1 --
OvHV-2 282 CTGCCCCAACACTAAGGACAAGGAGCACAACGAGGGGATTTTGTTGATCTTTAAGGAAAA
OvHV-1 297 GTGTCCAGATACACACGACAAGCAGCACAATGAAGGAATTTTGCTGATCTTTAAAGAAAA
BoHV-6 1 --
OvHV-2 342 TATAGTGCCCTATGTGTTTAAGGTGAGAAAGTACCGGAAAATCGTGACCACCTCTACGGT
OvHV-1 357 CCTTATTCCCTACATGTTTAAGGTTCGTAAGTACAGAAAGATTGTTACTACGTCTACAGT
BoHV-6 1 --
OvHV-2 402 CTACAATGGTATCTATTCTGATGCTATCACCAACCAGCATGAGTTTTCAAAGTCGGTGCC
OvHV-1 417 TTATAACGGAATTTACTCAGATACTATTACTAACCAGCATGTGTTTCATAAATCTATTCC
BoHV-6 1 --
OvHV-2 462 CCACTACGAGGCCCGGCGGATGGACACCATCTACCAGTGCTACAACAGCCTGTCTTTGAC
OvHV-1 477 TGAATACGAATACAAAAGGATGGACACTATATACCAGTGCTACAAGTCTATAAAGCTTAC
BoHV-6 1 --
OvHV-2 522 CGTCGGGGGAAACCTCCTGGCCTACACAGACAACGACGGCTACAACCTGACCGTGGATTT
OvHV-1 537 AGTTGCTGGAAACCTGTATACATACACTGATAGAGATGGATCAAATTTTACAGTAGATCT
BoHV-6 1 --
OvHV-2 582 GCAGCCCATGGACGGGTTGAGCAACAGCGTGCGCCGCTACAACAGCCAGCCCGAGATTCA
OvHV-1 597 TAACCCAGTAGATGGGCTTACTTCTTCTGTGAGAAGGTACTGTAGTCAGCCTGATGTGTA
BoHV-6 1 --
OvHV-2 642 CGCAGAGCCCGGGCGGCTCCTGGGGGGCTACCGCAGGAGGACAACAGTAAACTGTGAAGT
OvHV-1 657 CACAGACCCTGGCTGGTTTTGGGGCAGCTACAGGCGCCGCACCACAGTTAACTGTGAAGT
BoHV-6 1 --
OvHV-2 702 TACTGACACCGAGGCCCGCTCAGTGCCCCCCTTCCGCTATTTTGTTACCAACGTCGGTGA
OvHV-1 717 GACAGATATGCAAGCCAGATCAACGCCTCCGTTTCAGTACTTTGTAACAACCACCGGGGA
BoHV-6 1 --
OvHV-2 762 CACCATCGAGATGTCGCCCTTCTGGTCGGGCGGTGCGAACGAGACGGACCCTAACAAGGA
OvHV-1 777 TACTGTAGAAATGTCTCCATTTTGGCGCGGCGGCAGCAACGAAACTGAACCACATGAAAGA
BoHV-6 1 --
OvHV-2 822 GCCCCGGAGAACCGTCTCTGTGCTCCGAGACTACACCCTGGTGGACTACAAGGACCGAGG
OvHV-1 837 AAAACCTTGGCTTGTAAAGTTCACAATGACTACAGGATGGTGGACTACGAAAACAGAGG
BoHV-6 1 --
OvHV-2 882 CAGCAGGCCTCAGCCCCACACCAGAATCTTCATTGACAAGGAGGACTACACCCTTTCGTG
OvHV-1 897 CTCTTTACCTAATCCACACGTTAGAGTTTTTGTAGATAAAGAAGACTACAGCGTTTCTTG
BoHV-6 1 --
OvHV-2 942 GGCCCAGCAGCTGAAAAACATATCCTATTGCAGATGGGCCCACTGGAAGAGCTTCCACAA
OvHV-1 957 GGAGAGCAAGCCTAAGAACCGATCTTACTGCCCCTGGGCATTTTGGCAAGCGTTCCACAA
BoHV-6 1 --


OvHV-2 1002 TGCAATCAAAACTGAGCATGAGAACAGCTACCATTTTGTGGCCAATGATATCACCGCGTC
OvHV-1 1017 CGGCATTCAAACTAAGCACAACTCCACGTATCACTTTGTAGCTAATGAAATTACAGCTTC
BoHV-6 1 ----------
OvHV-2 1062 CTTCTTCACCCCAACACAGAAGCTCAGGATGTCACCAAAACCCACACATGCCTGAATAG
OvHV-1 1077 ATTTTCTAGGCCACATAGTCAGTATACAGATTTTGATAAGAAGTTTCCTTGCTTAAAAGA
BoHV-6 1 ----------
OvHV-2 1122 CCTGATAGAAAGCGACATGACCAGCAGGTTGGAGAAGGTGAATGGGACCCACGTGACGAA
OvHV-1 1137 AAACATTGAACCTGAAATGAACTTAAAGCTGCAAAAAGTTAATGGCACCCACCAAAAGTC
BoHV-6 1 ----------
OvHV-2 1182 CGGCAGCCGCCAGTACTATCTAACCAACGGGGGGCTGCTGCTGGTGTGGCAGCCCCTGGT
OvHV-1 1197 TGGACAAGTTGAATACTACAAAACTGACGGAGGCCTTATCTTAGTATGGCAGCCGTTAGT
BoHV-6 1 ----------
OvHV-2 1242 CCAACAGAAGCTACTGAACGCCCAGGACTTGCTGGAGGCCGTGGCTTCCAAACACAACGT
OvHV-1 1257 TCAGCAACAGCTTGTAGACGCTAAGCGAGAGCTAGATGAAGCGTCTACGCCTTCACCA--
BoHV-6 1 ----------
OvHV-2 1302 GACCAGGTCGGCCAGGAGCCGCCGGCAGCGCCGGGCTGTCAGCAGCATCCTCATAGATGA
OvHV-1 1315 -----------------------GTGCGGAAGCGAGCTCGCAGACAGCTACCTGAAGA
BoHV-6 1 ----------
OvHV-2 1362 TGATGTTTACACTGCTGAGTCTGCGCTCCTCCTGACCCAGATCCAGTTTGGCCTACGACAT
OvHV-1 1350 AGAAGTGTACACGAAAGAGAACGCAGCTTTGCTAGCTCAAATTCAGTACGCTTATGACAG
BoHV-6 1 ----------
OvHV-2 1422 GCTGCGCAGCCAAATCAATACTGTGCTCGAGGAGCTGTCCGGGGCCTGGTGTCGGGAGCA
OvHV-1 1410 CCTGCGCACTCAAATTAACAACGTGCTAGAAGAGCTGTCTCGGGGCATGGTGCAGAGAGCA
BoHV-6 1 ----------
OvHV-2 1482 GCACAGGGCCTCCCTCATGTGGAACGAGCTGAGTAAGATCAACCCTACCAGCGTGATGAG
OvHV-1 1470 GCAGCGAGCCACTCTAATGTGGAACGAGCTCAGTAAGATTAATCCTACCAGTGTTATGAC
BoHV-6 1 ----------AAC
OvHV-2 1542 CTCTATCTACGGGCCGCCAGTCTCTGCCAAGCGAATCGGGGACGTGATCTCCGTCTCGCA
OvHV-1 1530 TTCTATCTATGGAAAGCCAGTTTCAGCTAAAAGGCTAGGCGACGCAATTTCAGTATCTCA
BoHV-6 4 TTCCATTTACGGAAAACCCGTTTCAGCTAAAAGGTTAGGCGACGCTATCTCAGTGTCCCA
OvHV-2 1602 CTGCGTAGTGGTGGACCAGCAGAGCGTGTCCCTGCACAGGAGCATGCGCGCTCCCCGGGCG
OvHV-1 1590 GTGCGTCGTAGTTGACCAGGGCAGTGTTTCGCTGCATAAAAGCATGAGAAAGAGT-----
BoHV-6 64 GTGCGTCGTAGTTGACCAGAGCAGCGTTTCTTTGCACAAAAGTATGAGGCAGAGC-----
OvHV-2 1662 AGACCACGCACACGAGTGCTACTCTAGGCCTCCCGTCACCTTCAAGTTTATCAATGACAG
OvHV-1 1645 ----GACAGCGACGGCTGCTATTCAAGGCCGCTTGTGACGTTCAAGTTTATAAACGACAC
BoHV-6 119 ----GCCGGCGACGGCTGTTACTCAAGACCGCTAGTCACATTTAAGTTTTTAAATGACAC
OvHV-2 1722 CCACCTGTACAAGGGCCAGTTGGGGGTGAACAATGAAATCCTGCTCACCACAACCGCCCT
OvHV-1 1701 AAACATATACAGGGGCCAGTTGGGAGTGAGCAACGAAATACTGCTAACTACTAGCGCGGT
BoHV-6 175 AAACGTCTATAGGGGCCAGTTGGGAGTCAGCAATGAAATATTGCTGACCACCAGCGCGGT
OvHV-2 1782 GGAGGTGTGCCACGAGAACACCGAGCATTATTTCCAGGGGGGTAACAACATGTACTTTTA
OvHV-1 1761 AGAAACTTGCCACGATGGCGCTGAGCACTACTTTCAAGGTGGAGAGTACATGTACAAATA
BoHV-6 235 GGAAGCCTGTCATGATGGCGCCGAGCACTACTTTCAGGGAGGAGCGCACATGTACAAGTA
OvHV-2 1842 CAAAAACTACAGGCACGTAAAGACTATACCCGTGAGCGCTGTCGCTACCCTAGACACCTT
OvHV-1 1821 CAAAAACTACGAGCATGTACAGACTATTCCTCTCAGTGCAGTAGCTACTTTAGATACCTT
BoHV-6 295 CAAAAACTACGAACACACTGAAACTATTCCTCTCAGCGCAGTGTCCACCTTAAACACCTT
OvHV-2 1902 TATCGTGCTGAACCTGACCCTGGTGGAGAACATTGACTTTCAGGTCATAGAGCTGTACTC
OvHV-1 1881 TATAGTTTTAAACCTAACATTGCTTGAAAATATTGATTTCCACGTCATTGAGCTCTACTC
BoHV-6 355 TATAGTCCTCAACTTGACTTTGCTCGAAAACATTGACTTCCATGTAATAGAGCTTTACTC
OvHV-2 1962 CAGGGAGGAGAAGCGCATGAGCACGGTTTTTGACATCGAGACCATGTTCAGGGAGTACAA
OvHV-1 1941 TAGAGAAGAAAAGCGACTAAGCAGCGTGTTTGACATAGAAACTATGTTTAGAGAGTACAA

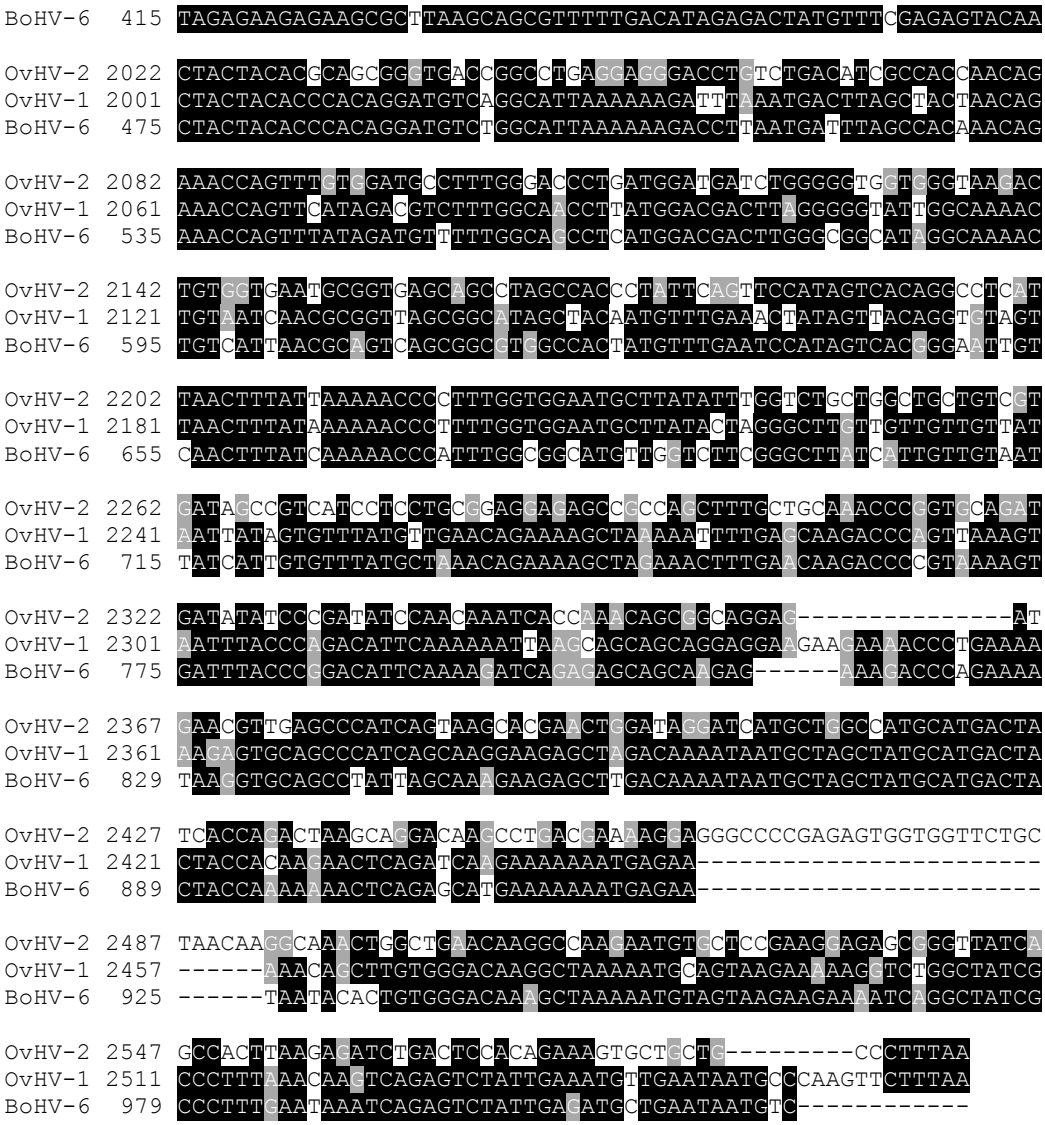

Figure 3-5. Sequence alignment of the nucleotides that encode for glycoprotein B of OvHV-2 (AF385442.1), OvHV-1 (sequence obtained from Moredun Research Institute), and BoHV-6 (AF327832.1) shows the genetic similarity. This was conducted by using “Clustal Omega” programme and is displayed using the “BOXSHADE” programme. The identical nucleotides are depicted in black, whilst similar are depicted in grey. Dashes are relevant to gaps in the sequence.

3.4 Conclusion

The quiescent infection with ruminant γ-HV other than OvHV-2 may cross-protect cattle from OvHV-2 infection and perhaps MCF. This may be explained by the genetic similarity of the identified viruses that presumably share antigenic similarity. This has been reported in three herpesvirus groups including: bubaline herpesvirus 1 (BuHV1) and BoHV5, between the strains of CvHV1 with ElkHV, as well as in CpHV1 and CvHV2 that are both closely related to BoHV-1 (das Neves *et al.*, 2010). Moreover, limited antigenic cross-reactivity has been shown in OvHV-2 and AIHV-1 (Taus *et al.*, 2015).

4. Chapter four: Pathological description of the OvHV-2-Latency Associated Nuclear Antigen (oLANA) in sheep, cattle without MCF, and cattle with MCF

4.1 Abstract

The pathogenesis of MCF is characterised by complicated consequences resulting in lymphoproliferation and vasculitis (Russell *et al.*, 2009). However, there is still a gap in explaining the key events regarding how the host immune system is deregulated during MCF; particularly, the role of lymphoid cytotoxicity. The LANA protein of OvHV-2 encoded by the open reading frame 73 is homologous to LANA proteins of other γ-herpesviruses and so is likely a key factor in OvHV2- latency. In KSHV, LANA is expressed in both latent and lytic cycles and has been found to play a fundamental role in establishing and maintaining latency (Verma *et al.*, 2007).

The aim of the present study was to gain more insight into the pathogenesis of MCF through the investigation of LANA expression, using a novel OvHV-2 LANA (oLANA)-specific antibody (see section 2.14). An anti-oLANA rabbit polyclonal antibody was produced and tested by western immunoblotting on tissue lysates of cattle and sheep positive for OvHV-2 by PCR, alongside lysates of a rabbit LGL cell line that carries OvHV-2. The

expressed oLANA protein was recognised by the generated PAb. Additionally, full-length oLANA was expressed *in vitro* for further validation of the results. Finally, the antibody was used to demonstrate oLANA *in situ* in cells of OvHV-2-infected sheep, cattle without MCF, and cattle with MCF, using immunohistochemistry (IHC).

The results demonstrated abundant OvHV-2- LANA in epithelial and endothelial cells as well as leukocytes, regardless of the infected species or the presence of disease. This finding could open new areas for the diagnosis and pathogenesis of MCF- latency.

4.2 Results

4.2.1 Production of anti-oLANA rabbit polyclonal antibody

4.2.1.1 Construction of the pGEX-3X-ORF73 portion

A portion of the ORF73 gene that encodes for the OvHV-2 LANA protein (C terminal) was amplified by conventional PCR (Figure 4-1). This domain is conserved among most gamma-herpesviruses (see section 1.1.4.1.2) and (Figure 1-4). The primers were designed manually to include *Eco*RI restriction sites at the 5' end as following: forward 5' ATGAATTCAATGGAAGCCCCTTCTAGCG 3' and reverse 5' GCGAATTCTGTTAACCGCTCCTGCCTG 3'. The total amplification reaction volume was 20 µL containing 90 ng of ORF73 template [C75 cosmid clone (Hart *et al.*, 2007)], 0.2 µM of each primer, 150 µM dNTPs, 2 µl of 10X buffer for KOD XL DNA polymerase, 0.5 U of KOD XL DNA polymerase. The

cycling parameters were 30 cycles of 94 °C for 30 sec, 52 °C for 5 sec and 74 °C for 60 sec, and final extension of 74 °C for 10 min. The amplified product (366 bp) was electrophoresed (see 2.1.2) and purified by using gel extraction kit (see 2.1.3), then digested with EcoR1 restriction endonuclease enzyme (see 2.1.6) and purified by QIAgene purification kit (see 2.1.3). The fragment was cloned into pGEX-3X vector that contains glutathione s-transferase at the C-terminus by means of *Eco*RI site recombination of restriction enzyme as described in section (2.1.6). After linearizing the vector (5 µg) with *Eco*RI restriction endonuclease enzyme, it was treated with 1 U of calf intestinal alkaline phosphatase (CIAP) (Invitrogen) according to the recommending of the supplier. The fragments were purified and then ligated using 45 ng PCR DNA, 304 ng vector, 1 U of T4 ligase with 4 µl of 1X T4 ligation buffer and H2O to a final volume of 20 µl. The reaction was then incubated overnight at 4 °C. The ligation mix was used to transform One-shot® Top10 competent *E. coli* cells as described in section (2.1.4), cultured as in (2.1.5), and prepared as in (2.1.6). The positive clone from a single ampicillin resistant colony was confirmed by *Bam*HI restriction digest for orientation (Figure 4-1). DNA from pGEX-3X-ORF73 with the fragment in the correct orientation was transformed into BL21 *E. coli* for protein expression by electroporation. This was achieved by adding 5 µl of pGEX-3X-ORF73 in an ice-cold electroporation cuvette and 45 µl of thawed BL21 competent cells. The mixture was then shocked electrically at 2.5kv, 25mA, and 800v, incubated for 2 min on ice then cultured and prepared as in sections (2.1.5 and 2.1.6) respectively. In parallel, pGEX-3X vector without insert was transformed as a negative control.

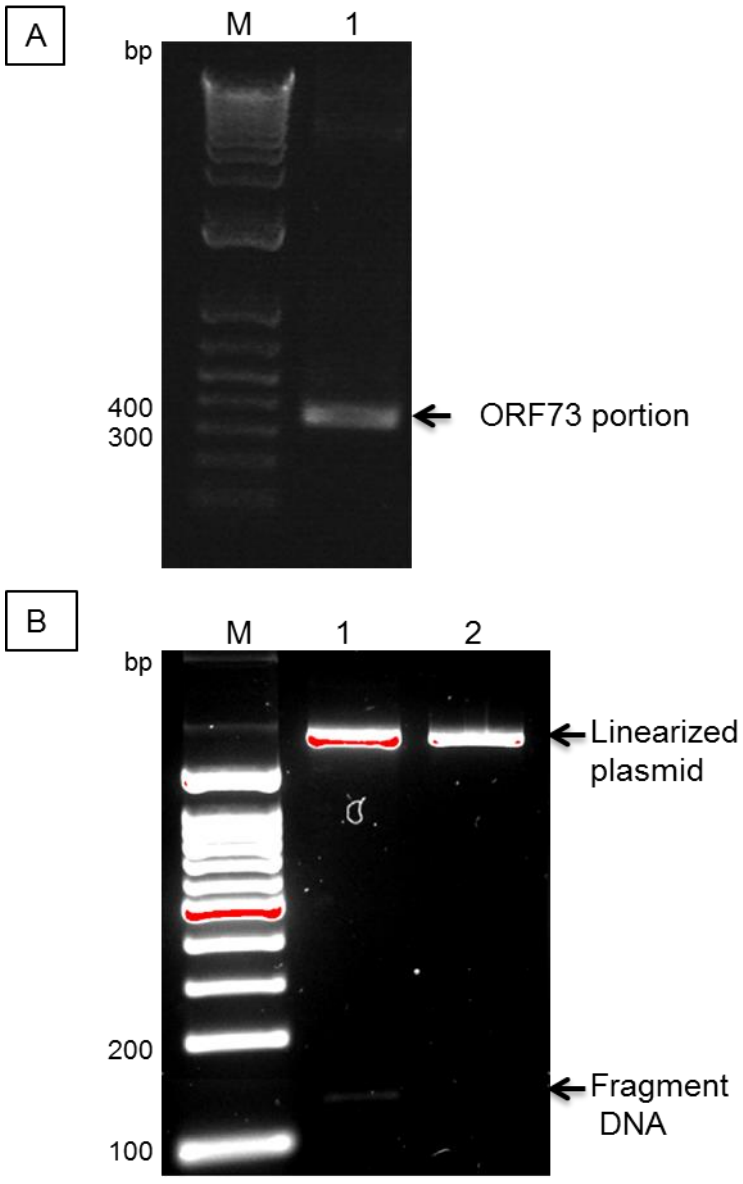

Figure 4-1. Gel electrophoresis (1 % agarose) images show (A-1) amplicon from ORF73 of 348 bp. (B) *Bam*HI restriction of pGEX-3X clones; 1: the correct orientation with 178bp fragment; 2: is one clone without insert as a control negative.

4.2.1.2 Heterologous expression of oLANA-antigen

A bacterial clone that carried pGEX-3X-oLANA (or control containing no insert) was tested for its ability to express the GST- oLANA fusion protein using β-d-1-thiogalactopyranoside (IPTG) induction. The GST-oLANA fusion protein was expressed as expected at a molecular weight of 39 kDa after IPTG induction (Figure 4-2). This band was not found in the non-induced preparation and the negative control. To demonstrate the solubility of the expressed protein, affinity chromatography was undertaken by harvesting the protein from bacteria induced with IPTG. The protein was released by sonication and then pelleted by centrifugation at 6,000 rpm for 5 min. The pellet was kept in ice for further analysis whilst supernatant was analysed after binding to GST beads. The supernatant and pellet were analysed by 12 % SDS-PAGE. No soluble fusion protein was seen, and no fusion protein was found in the supernatant that was processed with the GST beads. However, the pellet of the cell lysate revealed that GST-oLANA is highly insoluble, probably due to intracellular aggregation as inclusion bodies (Figure 4-2). Thereafter, the expressed protein was purified by cell disruption and inclusion body preparation. To exclude that the centrifugation speed would affect the purity of these inclusion bodies, optimal separation of the insoluble protein from the soluble contaminants was carried out by a series of spinning forces, from lower to higher centrifugation force: (2,000, 6,000, 8,000, 10,000, 12,000) *g* for 10 min. Subsequently, both supernatant and pellet were analysed by 12 % SDS-PAGE. As can be seen in (Figure 4-3), the protein aggregates were stable at all centrifugation conditions. Thus, a

lower centrifugation speed (2,000 x*g*) for 10 min was used as a standard speed for this purpose. GST-oLANA protein was then produced and purified on a large scale by inclusion body preparation. The concentration of the protein produced was estimated using standard concentrations of BSA protein electrophoresed alongside with GST-oLANA in SDS-PAGE gels which were then stained with the Coomassie blue stain. These dilutions were used as a standard calibrator. The concentration of GST-oLANA was estimated at 128 µg/ µl (Figure 4-4).

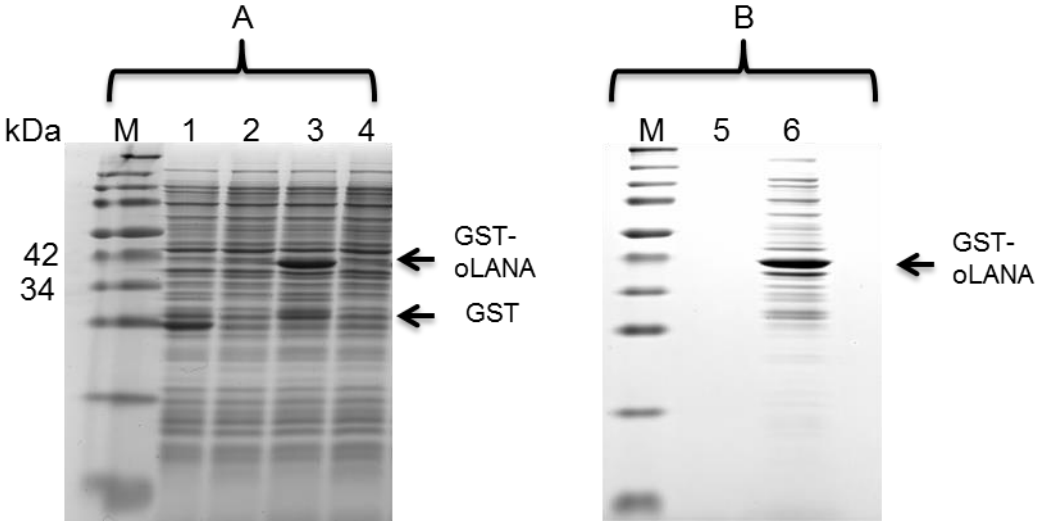

Figure 4-2. Images of Coomassie stained SDS-PAGE (12 %) gels showing analysis of the expressed GST-oLANA fusion protein; M: is the molecular weight marker (Spectra™ Multicolour Broad Range Protein Ladder, Thermoscientific). (A) Expression of GST-oLANA; 1: pGEX-3X vector treated with IPTG in which GST is expressed at a molecular weight of 24 kDa; 2: pGEX-3X only without IPTG treatment; 3: pGEX-3X-ORF73 treated with IPTG in which the fusion protein is expressed at 39 kDa; 4: pGEX-3X-ORF73 portion without treatment. (B) Solubility analysis of the expressed GST-oLANA fusion protein; 5: supernatant of the expressed protein processed with GST chromatography 6: pelleted lysate of the expressed fusion protein.

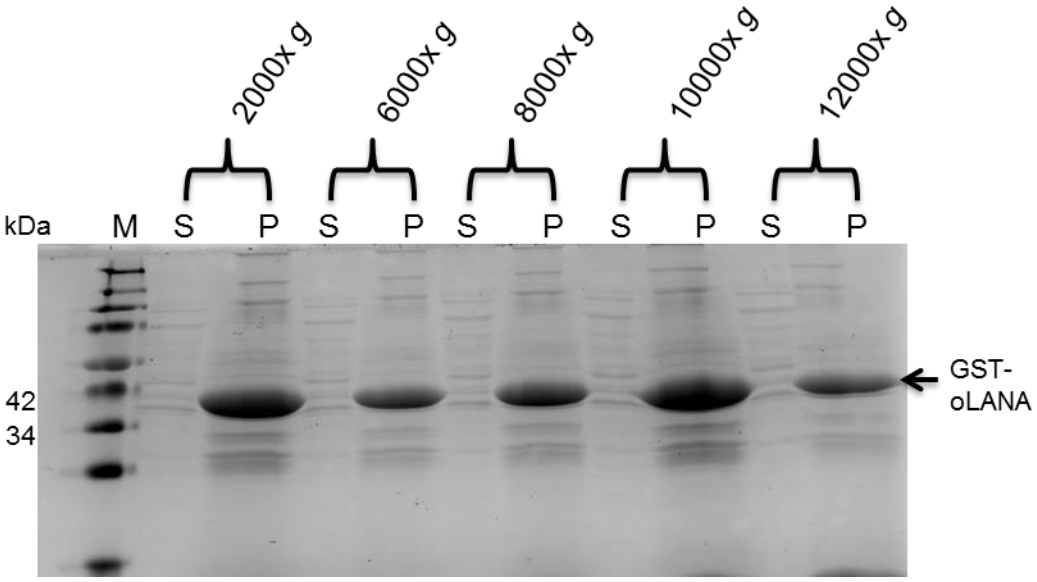

Figure 4-3. Image of SDS-PAGE gel (12 %) stained with Coomassie blue shows analysis of the expressed GST-fusion protein after centrifugation at the indicated forces; S: supernatant; P: pellet lysates; M: molecular weight marker (Spectra™ Multicolour Broad Range Protein Ladder, Thermoscientific.

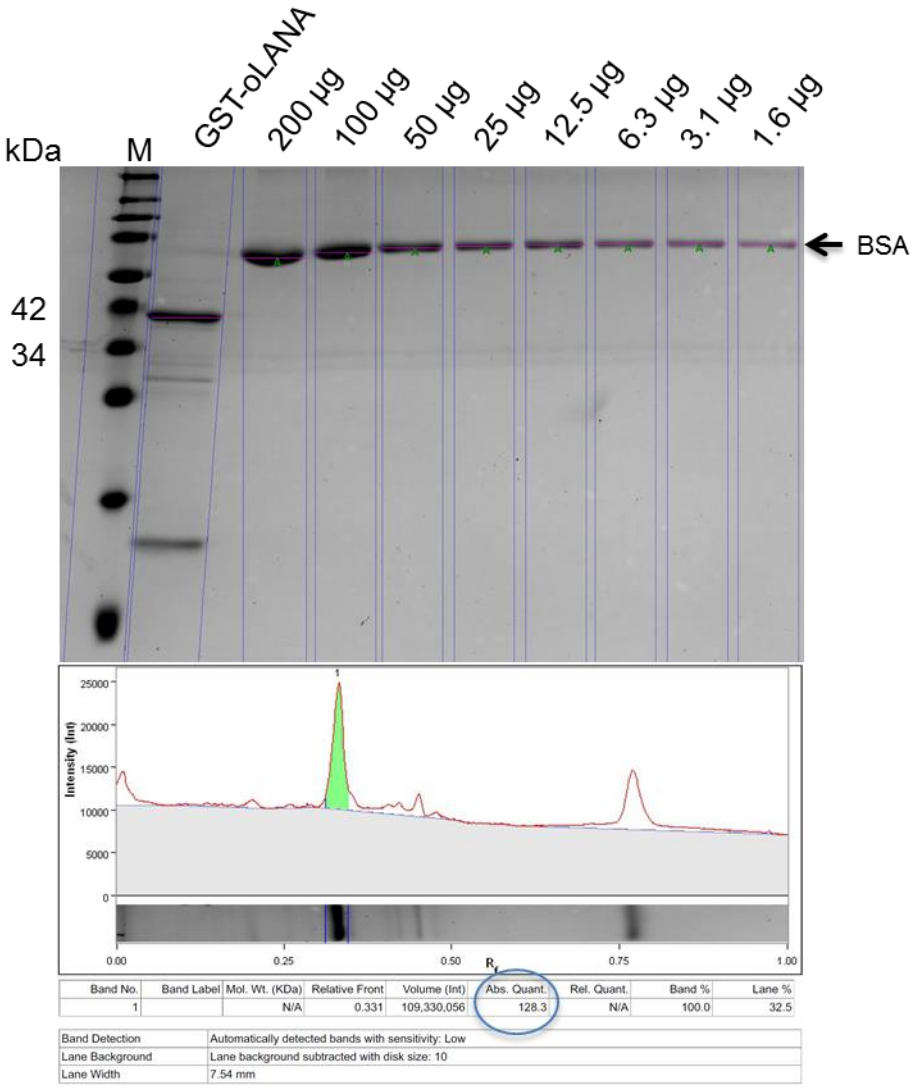

Figure 4-4. Estimation of GSToLANA concentration. Proteins were analysed by SDS-PAGE (12 %) followed by Coomassie blue staining. GST-oLANA was run alongside known concentrations of Bovine Serum Albumin (BSA) as a standard; M: molecular weight marker (Spectra™ Multicolour Broad Range Protein Ladder, Thermoscientific); oLANA concentration was estimated using the ImageLab software (BioRad).

4.2.1.3 Production of anti-oLANA rabbit polyclonal antibody

The expressed inclusion proteins were used as antigen for the generation of a polyclonal antibody (Ab) after they had been tested for their immune reactivity against sera from OvHV-2-infected sheep and cattle that had been confirmed positive by PCR (Amin, 2015). Using western immunoblotting analysis, the GST-oLANA inclusion bodies were electrophoresed using SDS-PAGE then blotted onto a PVDF membrane and probed with the sera, followed by HRP labelled rabbit anti-cow or anti-sheep antibodies (Abcam, UK). The GST-oLANA protein was recognised by both sera and bands of the expected size (39 kDa) observed with breakdown products, while the respective bands were not obtained from the supernatants. This finding confirms that GST-oLANA is insoluble. The GST-oLANA fusion protein was then used as antigen to immunise two rabbits at a commercial provider (Pacific Immunology Antibody Production Corporation, Ramona, USA) and the generated polyclonal antibody (PAb) purified by bacterial-acetone precipitation (2.3.10.1) and affinity chromatography (2.3.10.2) then tested for its immune reactivity against GST-oLANA by western immunoblotting (Figure 4-5).

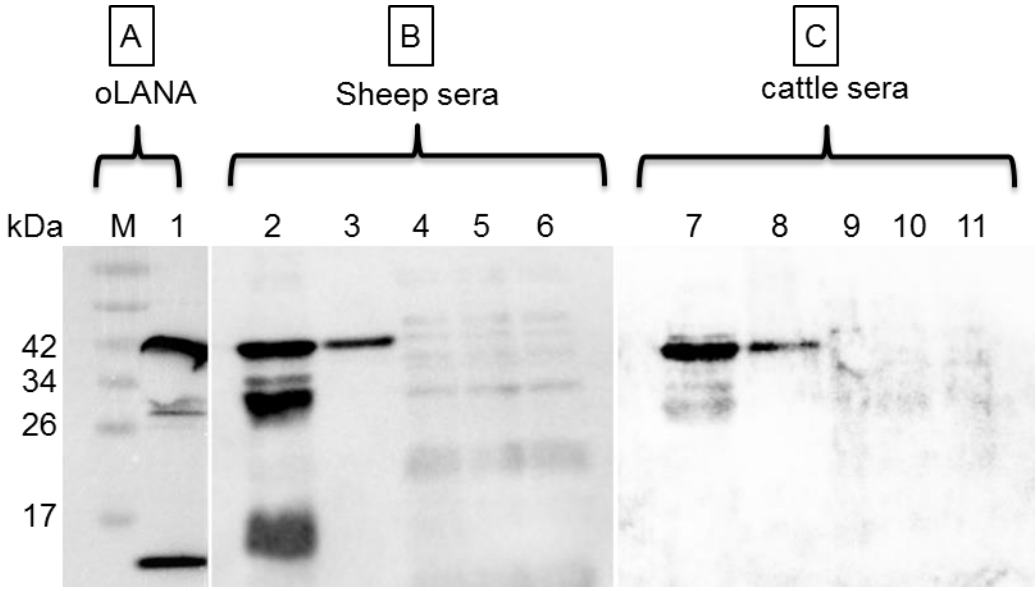

Figure 4-5. Western immunoblotting analysis image shows the immune recognition of GST-oLANA fusion protein. (A) Is GST-oLANA reacted with the rabbit oLANA polyclonal antibody (1:5000) and probed with goat anti-rabbit IgG (1:5000) (Vector Laboratories, USA). (B) Is GST-oLANA recognised by OvHV-2-sheep sera (1:2000) and probed with rabbit anti-sheep (1:2000) (Abcam, UK). (C) is GST-oLANA recognised by OvHV-2-cattle sera (1:2000) and probed with rabbit anti-cow (1:2000) (Abcam, UK); M: is molecular weight marker (Spectra™ Multicolour Broad Range Protein Ladder, Thermoscientific); 1, 2, 7 are GST-oLANA fusion protein; 3, 8 are GST-oLANA previously isolated from SDS-gel; 4, 9 are supernatants; 5, 10 are protein lysate extracted from bacteria carrying pGEX-3X only treated with IPTG; 6, 11 are protein lysate extracted from bacteria carrying pGEX-3X without IPTG treatment.

4.2.1.4 Western immunoblotting analysis of oLANA

The anti-oLANA PAb was then used to characterise oLANA in OvHV-2-infected cells. These showed clear bands with the OvHV-2-positive samples, whereas no band was found in the negative animals. To confirm the specificity of the assay, a mouse tissue lysate was used as a negative control; this showed no reaction (Figure 4-6). Similar in sheep and cattle, usually 36 kDa was detected but one or two with two bands including a 13 kDa. Subsequently, OvHV-2 infected rabbit large granulocyte lymphocytes (cell line-BJ2586) were also analysed by western immunoblotting. These revealed a similar band at 36 kDa, with a second, smaller band at 17 kDa (Figure 4-7). Additionally, the LGL lysates were probed with goat anti-rabbit-HRP conjugate alone as a negative control.

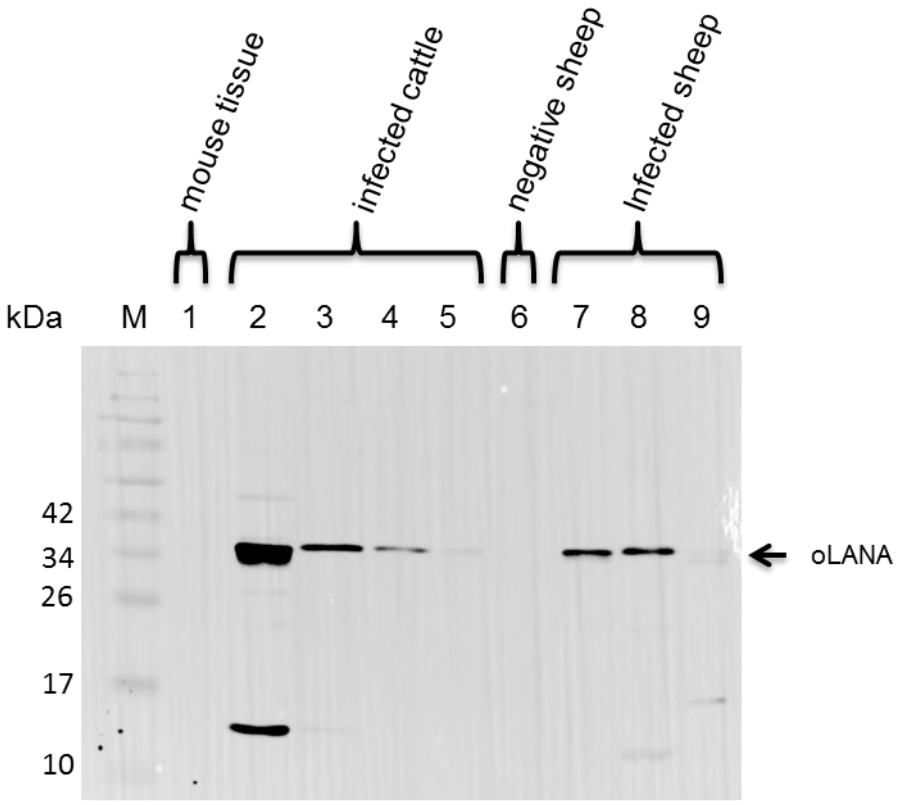

Figure 4-6. Western immunoblotting analysis image shows the immune reactivity of oLANA in tissue lysates with anti-oLANA polyclonal antibody; M: is molecular marker (Spectra™ Multicolour Broad Range Protein Ladder, Thermoscientific); 1: is mouse tissue lysate a control negative that shows no reaction; 2-5: are OvHV-2-positive cattle tissue lysates; 6 is OvHV2-negative sheep tissue lysate; 7-9: are OvHV-2-positive sheep tissue lysate; oLANA polyclonal antibody was used in (1:5000) and probed with goat anti-rabbit IgG (1:5000) (Vector Laboratories, USA).

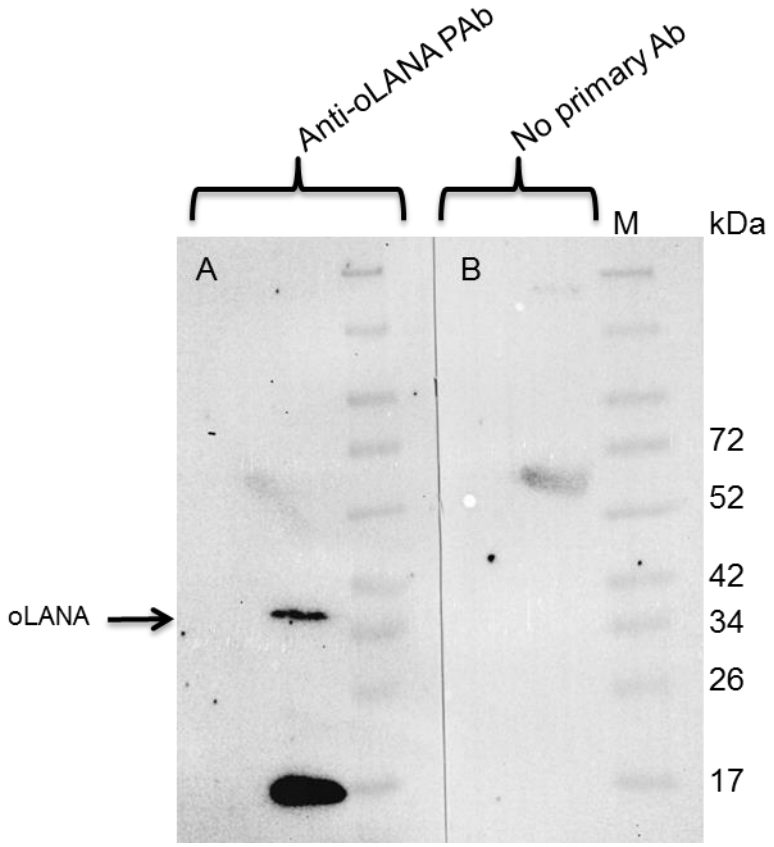

Figure 4-7. Western immunoblotting analysis image shows the immune reactivity of oLANA in rabbit large granulocyte lymphocytes infected cell line (BJ2586). (A) Is the membrane incubated with anti-oLANA polyclonal antibody at (1:5000) and probed with goat anti-rabbit IgG (1:5000) (Vector Laboratories, USA). (B) Is the similar protein lysate treated with only secondary antibody as another control strategy; M: is molecular marker (Spectra™ Multicolour Broad Range Protein Ladder, Thermoscientific).

4.2.2 Expression of oLANA in mammalian cells

To definitively confirm the molecular weight of oLANA, it was expressed in human embryonic kidney (HEK293) cells by inserting the entire ORF73 into the pVR-1255 mammalian expression vector. The construct was used to transfect HEK293 cells using the calcium chloride method (described in 2.4.3). oLANA was detected using the PAb in western immunoblotting and immune fluorescent assays.

4.2.2.1 Construction of the pVR-ORF73

Initially, the entire ORF73 was amplified by conventional PCR (Figure 4-8) by means of KOD XL DNA polymerase kit (Novagen, USA). The primers were designed manually to include *Not*I restriction site at the forward primer 5’ ATGCGGCCGCCGCCGCCACCATGGTGCTTTTACGAAGTGG 3’ and *Bcl*I restriction site at the reverse 5’ TAGCTGATCATTAATGGTGCTTTTACGAAGTGG 3’., These were designed so the fragment could be inserted between the *Not*I and *Bam*HI sites of pVR1255 in the correct orientation. *Bcl*I was chosen as there is a *Bam*HI site in the coding sequence of ORF73. *Bcl*I-cut DNA has a compatible overhang with *Bam*HI-cut DNA but the resulting join cannot be cut with either enzyme. The total amplification reaction volume was 20 µL containing 90 ng of ORF73 template [(C75 cosmid clone (Hart *et al.*, 2007)], 0.2 µM of each primer, 150 µM dNTPs, 2 µl of 10X buffer, and 0.5 U of KOD XL DNA polymerase. The thermal cycles were 30 cycles of 94 °C for 30 sec, 55 °C for 5 sec and 74 °C for 60 sec, and final extension of 74 °C for 10 min. The purified amplicon was

cut using Bcl1 and Not1 (NEB, UK) in a total volume of 20 µl containing 2 µl NEB 3.1 buffer, 170 ng of purified amplicon, 1 µl of Bcl1. This was incubated for 1 h at 50 °C then Not1 (1 µl) was added with further incubation for 1 h at 37 °C. Similar reaction conditions were used to linearize the mammalian expression vector (pVR1255) with *Bam*HI and *Not*I, using 1 µg plasmid. The vector was treated then with 1 U of calf intestinal alkaline phosphatase (CIAP) (Invitrogen, UK) to prevent re-ligation of blunt ends, then purified by a PCR purification kit before being ligated in a total reaction volume (20 µl) containing 300 ng of the vector and 50 ng insert, 1U of T4 ligase, 4 µl of 1x T4 ligation buffer and then incubated at 4 °C overnight. The ligation mixes were transformed into Mach1 *E. coli* chemically competent cells (Invitrogen, UK) and cultured in LB medium supplemented with Kanamycin (30 µg/ ml) as in section (2.1.4). Single colonies were sub-cultured overnight in LB broth supplemented with Kanamycin meanwhile plasmids DNA were prepared as in section (2.1.6). DNA sequencing was carried out for final confirmation, using forward 5’ AATAGCTGACAGACTAACAGACTG 3’ and reverse 5’ GAGTGAGCTGATACCGCTC 3’ primers of the pVR-1255 vector. Presence of ORF73 insert was obtained by sequencing but with some gaps possibly due to the multiple tandem repeats within the central domain that lead to sequence limitation.

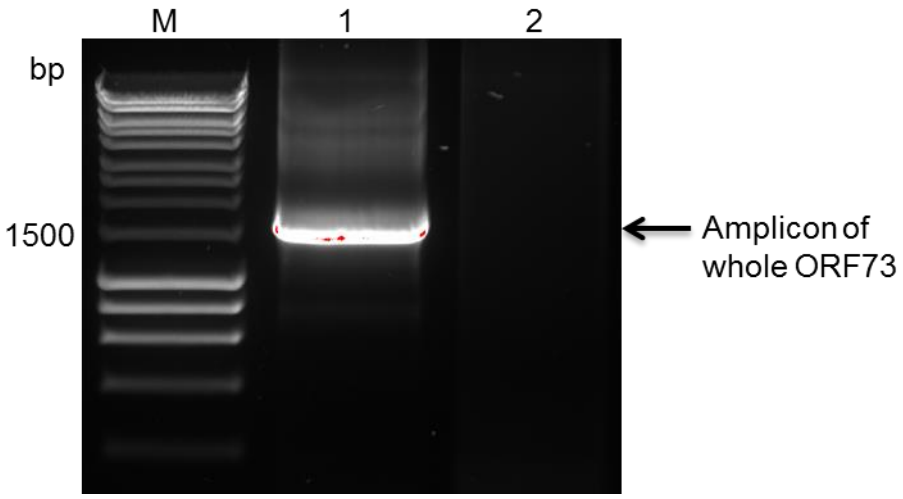

Figure 4-8. Amplicon of whole ORF73 were analysed by gel electrophoresis (1 % agarose). The amplication of ORF73 was conducted by using primers including the restriction enzyme site *Bam*HI and *Not*I (lane 1), lane (2) including H_2O as template for control negative.

4.2.2.2 Transfection and expression of oLANA in HEK293 cells

The expression of oLANA protein was carried out by transfection of HEK293 with calcium phosphate. The expressed protein was analysed by western immunoblotting with anti-oLANA PAb to confirm the apparent molecular weight of transfected oLANA. The result showed a specific band at (36 kDa), corresponding to size obtained from OvHV-2-positive tissue samples and the infected LGL cell (Figure 4-9). This result confirms the native expression of oLANA. Incubation of the membrane with the pre-immune rabbit serum (negative control) yielded no reaction. Thus, it is confirmed that oLANA is expressed at a molecular weight lower than the expected one and that the produced anti-oLANA PAb is highly specific to oLANA.

An immunofluorescence and IHC assays were also carried out to localise oLANA within HEK293 cells. The results showed detection of the expressed oLANA antigen which validates the specificity of the generated anti-oLANA PAb (Figure 4-10 and 4-11).

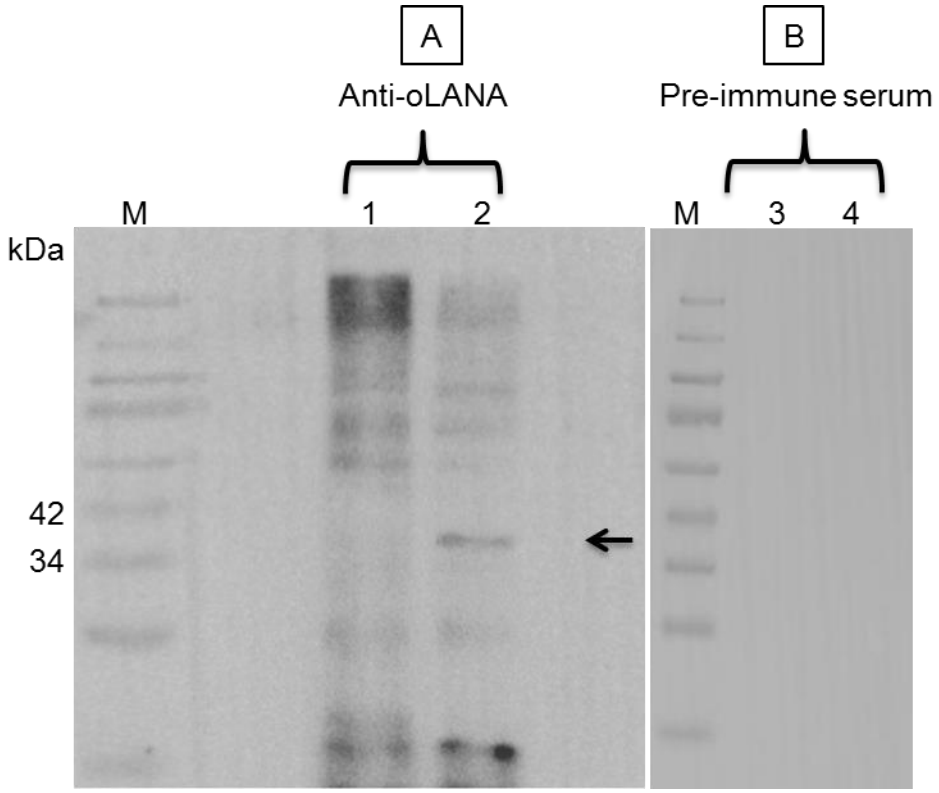

Figure 4-9. Western immunoblotting analysis (12 %) image shows the immune reactivity of the expressed oLANA by using anti-oLANA poyclonal antibody (1:2000) which recognised by goat anti-rabbit IgG labelled with HRB in dilution factor (1:5000) from (Vector Laboratories, USA). (A1) is the protein lysate of HEK193 cells transfected with only the pVR1255 vector as a control negative; (A2) is the protein lysate of HEK293 cells transfected with pVR1255-ORF73 that encoded for LANA expression. (B) is similar to (A) but incubated with the pre-immune serum of the immunised rabbit as another negative control that shows no reaction.

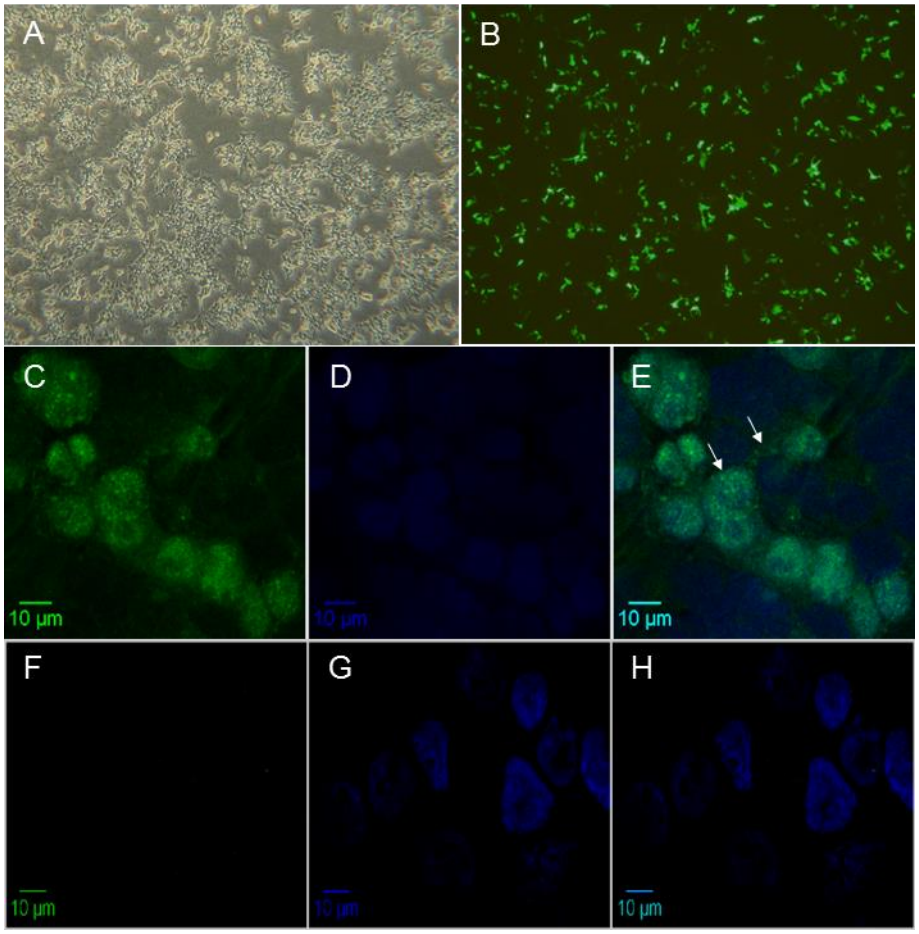

Figure 4-10. Localisation of oLANA within HEK293 cells by IF. (A) Cells grown to 90% confluence (10X). (B-H) Fluorescence images. (B) Cells transfected with pEGFP-N1. The green fluorescence signal confirms GFP expression and thereby demonstrates the transfection efficiency. (C-E) HEK293 cells transfected with the pVR1255-ORF73 vector for oLANA expression, incubated with rabbit anti-oLANA PAb and stained with anti-rabbit-FITC488 and DAPI as nuclear counterstain. Cells exhibit predominantly nuclear punctate signals and occasional cytoplasmic protein expression (arrows). (C) staining for oLANA. (D) DAPI staining of nuclei. (E) merged. (F-H) HEK293 cells transfected with pVR1255 vector, incubated with rabbit anti-oLANA PAb and stained with anti-rabbit-FITC488 and DAPI as nuclear counterstain (negative control) which revealed no specific reaction.

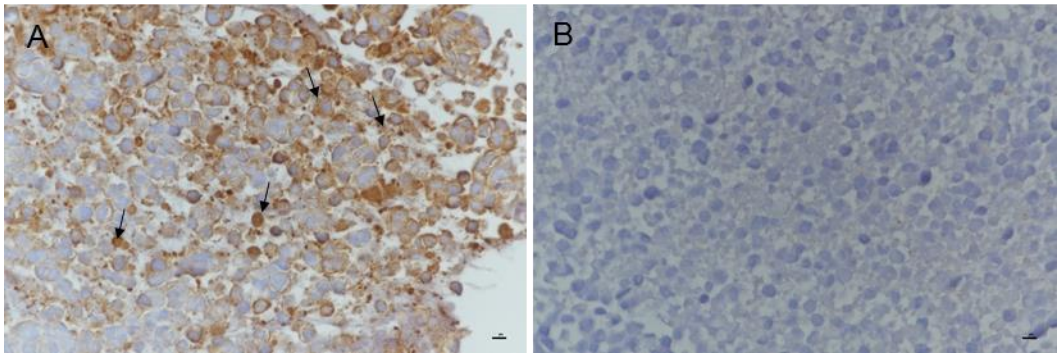

Figure 4-11. Immunohistochemistry staining images for oLANA antigen expression within HEK293 cells. (A) HEK293 cells transfected with the pVR1255-ORF73 vector for oLANA expression (arrows), incubated with rabbit anti-oLANA PAb (1:500), stained with (EnVision + System HRP Rabbit; K4003; Dako) and visualization with DAB (K3468; Dako). (B) HEK293 cells transfected with the pVR1255-ORF73 vector then incubated with pre-immune serum and processed as in (B).

4.2.3 *In situ* demonstration of oLANA expression in tissues by immunohistochemistry (IHC)

4.2.3.1 Identification of oLANA expression in tissues of OvHV-2 infected sheep

Sheep are the natural hosts for OvHV-2. Therefore, the following tissues were examined: lung, tongue, nasopharynx, mediastinal lymph node, spleen, thymus, and placenta that had previously been tested for OvHV-2 by PCR, *in situ* hybridisation (ISH), and IHC in our laboratory (Amin, 2015). Tissue specimens originated from healthy, slaughtered sheep of variable age and were subjected to IHC for the detection of oLANA, using the new PAb. Expression of oLANA was represented by a nuclear and/or cytoplasmic reaction in a wide range of cell types.

Lung and mediastinal lymph node: These were examined in a 7-months-old, healthy, slaughtered sheep (13L-2594A) and had been tested OvHV-2 positive before by PCR, ISH and IHC (Amin, 2015) (Figure 4-12 to 4-14).

In the lung, expression of oLANA was evident as nuclear and/or cytoplasmic reaction in alveolar lining cells (morphology consistent with type II pneumocytes and/or alveolar macrophages) as well as lymphocytes and macrophages/ dendritic cells in the bronchus-associated lymphoid tissue (BALT) (Figure 4-12). Detection of oLANA in lung tissue of another healthy sheep (13L-4220E) revealed similar reaction with involvement of the bronchial epithelial cells, bronchiolar glands and BALT (Figure 4-13).

Expression of oLANA was also detected in the mediastinal lymph node of the same animal (13L-2594A) as strong nuclear and/or cytoplasmic reaction. Predominantly, the reaction was noticed inside and outside lymphatic follicles (B zone). Morphologically, macrophages and lymphocytes were identified as positive cells (Figure 4-14).

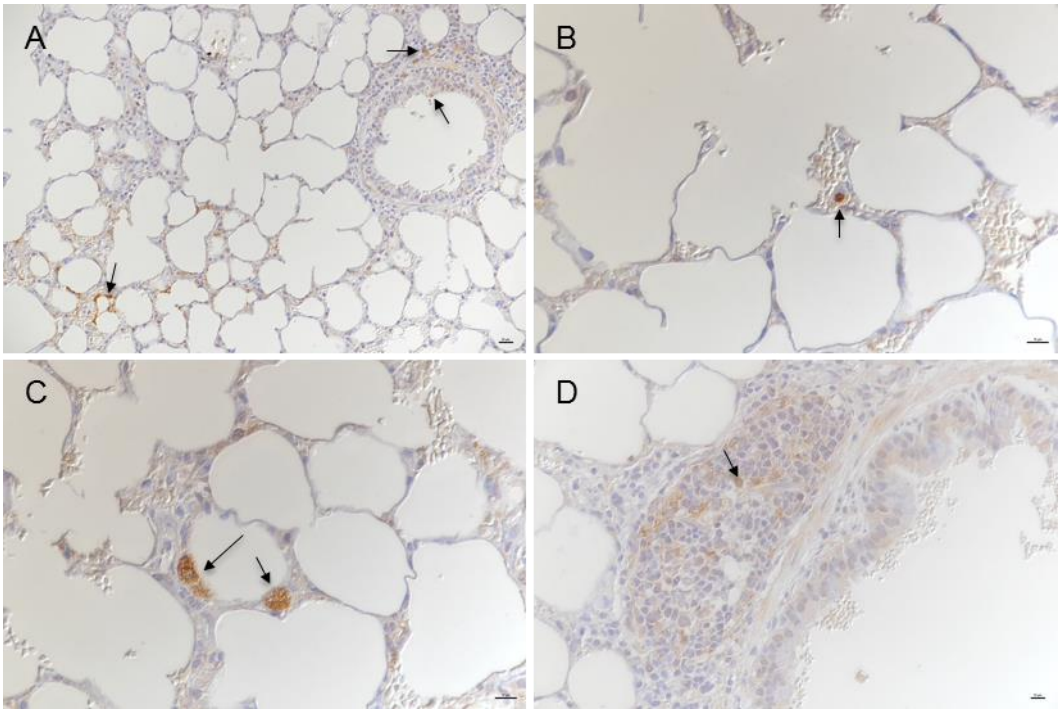

Figure 4-12. Immunohistochemistry staining images for oLANA antigen expression in the lung of a 7-month-old healthy sheep previously tested positive for OvHV-2 by PCR, ISH and IHC (Amin, 2015) (13L-2594A). (A) oLANA is expressed in a wide range of cell types (arrows), scale bar= 20 µm. (B) Higher magnification of A, showing nuclear oLANA expression in an interstitial cell (arrow), scale bar= 10 µm. (C) oLANA is seen as nuclear and/or cytoplasmic reaction in cells with the morphology of a type II pneumocyte (long arrow) and an alveolar macrophage (short arrow), scale bar= 10 µm. (D) oLANA expression in lymphocytes (and macrophages/dendritic cells) in the BALT (arrow), scale bar= 10 µm. Visualized with DAB and counterstained with haematoxylin.

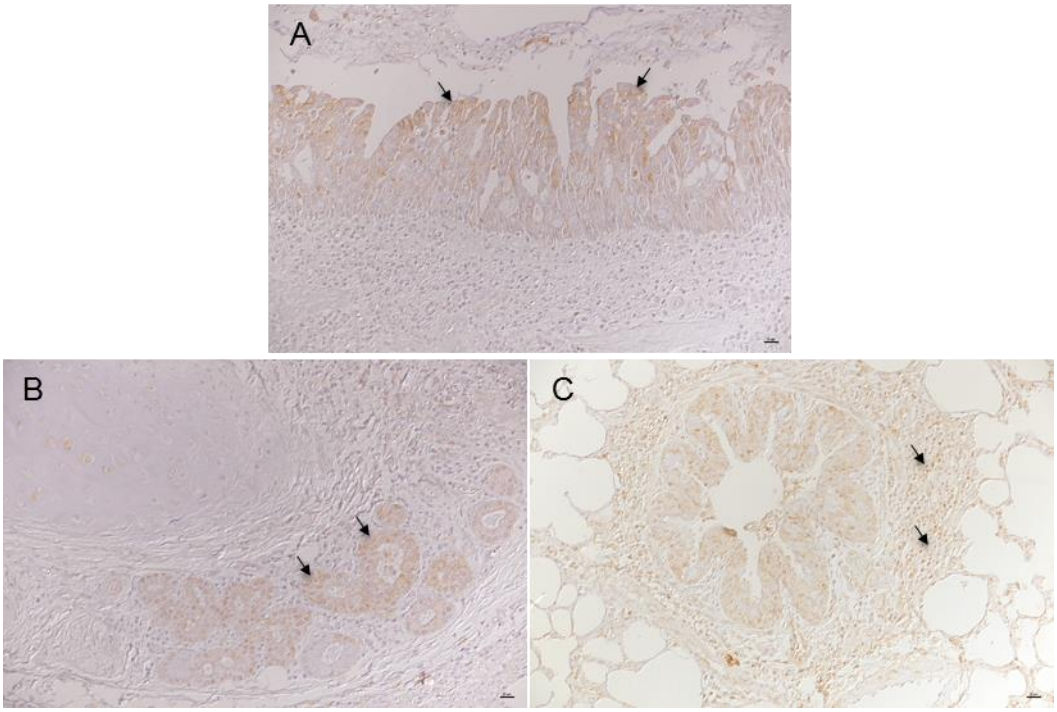

Figure 4-13. Immunohistochemistry staining images for oLANA antigen expression in the lung of a 10-month- old healthy sheep previously tested positive for OvHV-2 by PCR, ISH and IHC (Amin, 2015) (13L-4220D). (A) Depicts a cytoplasmic oLANA expression in the bronchial respiratory epithelial cells (arrows), scale bar= 20 µm. (B) Higher magnification of A, showing cytoplasmic oLANA expression in the bronchial glands (arrows), scale bar= 20 µm. (C) oLANA is seen as nuclear and/or cytoplasmic reaction in BALT lymphocytes, scale bar= 20 µm. Visualized with DAB and counterstained with haematoxylin.

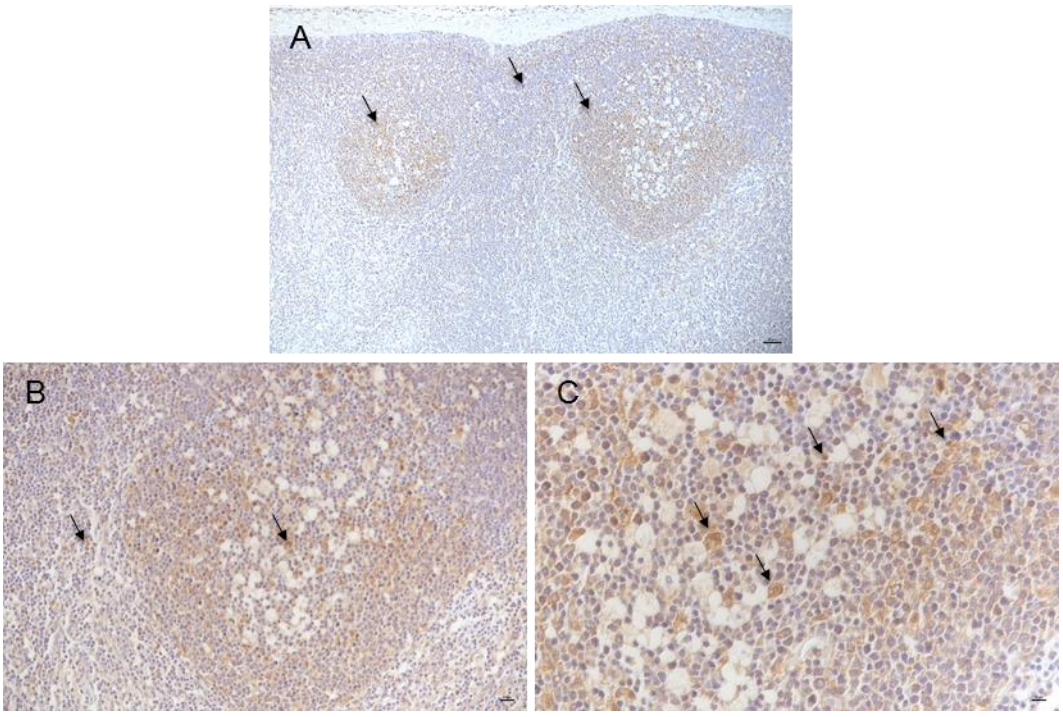

Figure 4-14. Immunohistochemistry staining images for oLANA antigen expression in the mediastinal lymph node a 7-month-old, healthy sheep previously tested positive for OvHV-2 by PCR, ISH and IHC (Amin, 2015) (13L-2594A). (A) Shows oLANA expression in likely to be lymphocytes inside and outside follicles (arrows), scale bar = 50 µm. (B) Higher magnification of A, showing nuclear oLANA expression in probably lymphocytes (arrows), scale bar = 20 µm. (C) Higher magnification of B, showing oLANA expression in likely lymphocytes (arrows) and macrophages/dendritic cells (both nuclear and cytoplasmic reaction) in the a follicle, scale bar = 10 µm. Visualized with DAB and counterstained with haematoxylin.

Tongue and spleen: These were tested in another healthy, slaughtered 10-month-old sheep (13L-4220E) previously tested OvHV-2-positive by PCR (Amin, 2015) (Figure 4-15).

In the tongue, oLANA was expressed in the covering epithelium, with weak cytoplasmic expression in the stratum basale and moderate expression in the stratum spinosum. The protein was also expressed in the cytoplasm of the lingual striated muscle cells and in scattered ductal and acinar epithelial cells in the salivary gland. In addition, sub-epithelial lymphocytes, venous endothelial cells and arterial smooth muscle cells were also found to be positive. Occasional stromal fibroblasts also exhibited a weak cytoplasmic reaction (Figure 4-15).

In spleen of the same animal (13L-4220E), oLANA was expressed in the nucleus of a percentage of lymphocytes within follicles and red pulp. A cytoplasmic reaction of oLANA was exhibited in occasional cells within follicles. Morphologically, follicular dendritic cells and macrophages seem to be positive for oLANA.

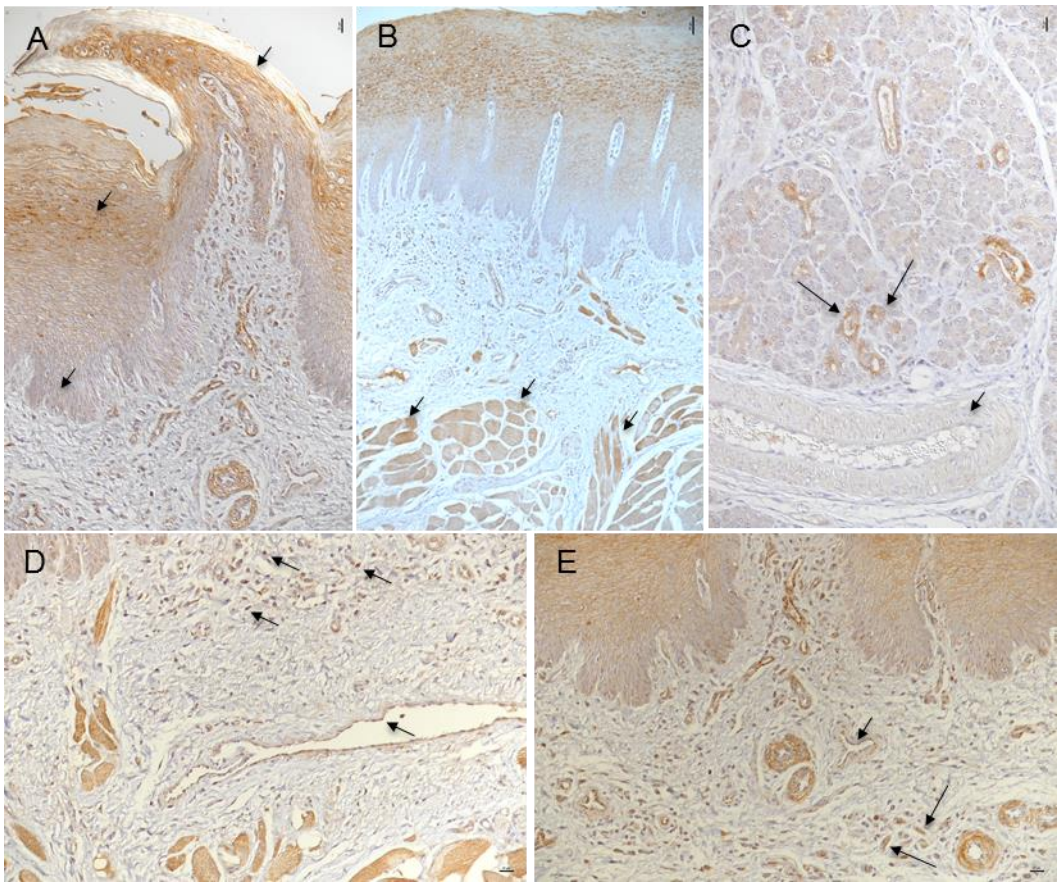

Figure 4-15. Immunohistochemistry staining images for oLANA antigen expression in the tongue of a 10-month-old, healthy sheep previously tested positive for OvHV-2 by PCR, ISH and IHC (Amin, 2015) (13L-4220E). (A) Strong cytoplasmic oLANA expression in the lingual epithelium, with weak expression in the stratum basale and moderate expression in the stratum spinosum (arrows), scale bar = 20 µm. (B) depicts oLANA antigen in striated muscle cells (arrows), scale bar= 50µm. (C) shows oLANA expression in salivary gland as a cytoplasmic reaction within glandular epithelial cells (long arrows); occasional smooth muscle cells within vascular tunica media of local large artery exhibited nuclear and/or cytoplasmic reaction (short arrow), scale bar= 20µm. (D) shows oLANA antigen with strong cytoplasmic expression in percentage of sub-epithelial lymphocytes (black arrows) and venous endothelium (arrows), scale bar = 20µm. (E) demonstrates cytoplasmic oLANA expression in numerous fibroblasts (long arrows); vascular endothelial cells and arterial smooth muscle cells within tunica are seen infected (short arrow), scale bar= 20 µm. Visualized with DAB and counterstained with hematoxylin.

Lung, spleen, thymus, and placenta: These were tested in a sheep foetus (stillborn) and from an OvHV-2-infected sheep (S13-1453), both tested positive for OvHV-2 by PCR and ISH (Amin, 2015) (Figure 4-16).

In the lung, oLANA was found to be expressed by respiratory epithelial cells and scattered mononuclear cells with macrophage morphology in the parenchyma as well as in arterial smooth muscle cells (Figure 4-16). In the spleen, oLANA expression observed in scattered mononuclear cells in red pulp, and in the thymus, it was found in disseminated macrophages in cortex and medulla and in dendritic cells in the medulla (Figure 4-16, D-F).

In the placenta, oLANA was expressed mainly by smooth muscle cells in the media of arteries. Stromal fibroblasts also exhibited weak staining for oLANA (Figure 4-17).

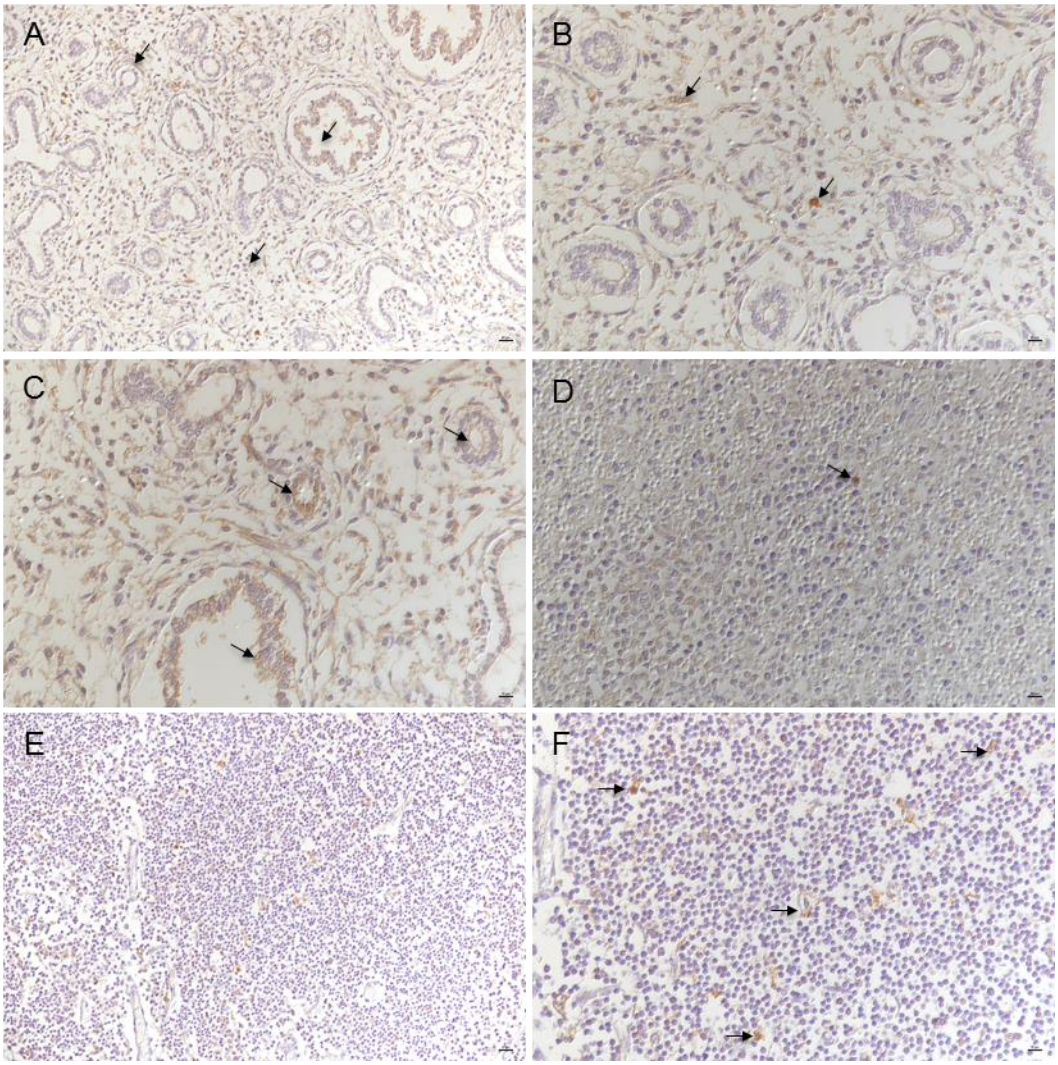

Figure 4.16. Immunohistochemistry staining images for oLANA antigen expression in the lung (A-C), spleen (D), thymus (E-F) of a stillborn sheep foetus suffered from atelectasis (crown rump length= 17.5 cm) previously tested positive for OvHV-2 by PCR, ISH and IHC (Amin, 2015) (S13-1453). (A) Expression of oLANA is seen in the respiratory epithelium (arrow) and in association with alveoli, scale bar = 20 µm. (B) Higher magnification of A, showing oLANA expression in scattered mononuclear cells in the interstitium (arrows), scale bar= 10 µm. (C) Higher magnification of B shows cytoplasmic reaction of oLANA in respiratory epithelial cells and vascular smooth muscle cells (arrows), scale bar= 10 µm. (D) In the spleen, occasional mononuclear cells in the red pulp are found to express oLANA (arrow), scale bar= 10 µm. (E) In the thymus, a moderate number of disseminated cells in cortex and medulla are found to express oLANA, scale bar= 20 µm. (F) Higher magnification of E, showing oLANA expression in likely medullary macrophages and dendritic cells (arrows), scale bar= 10 µm. Visualized with DAB and counterstained with haematoxylin.

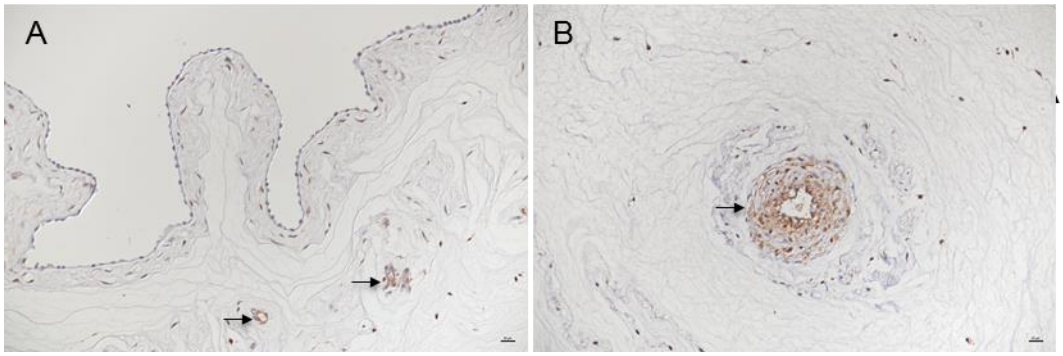

Figure 4.17. Immunohistochemistry staining images for oLANA antigen expression in the placenta of a stillborn sheep foetus suffered from atelectasis (crown rump length=17.5 cm) previously tested positive for OvHV-2 by PCR, ISH and IHC (Amin, 2015) (S13-1453). (A) Shows arterial smooth muscle cells revealed oLANA expression (arrows), a proportion of stromal fibroblasts also exhibits a weak reaction, scale bar= 20 µm. (B) Expression of oLANA is restricted to vessel walls, where is mainly seen in the cytoplasm of smooth muscle cells of the arterial tunica media (arrow), scale bar= 20 µm. Visualized with DAB and counterstained with haematoxylin.

4.2.3.2 Identification of oLANA expression in OvHV2-infected cattle without MCF

In a previous study, a number of cattle was identified as OvHV-2-infected, but did not suffer from MCF; infection had been confirmed by PCR and RNA-ISH (Amin, 2015). Tissues from selected animals were also tested for oLANA expression. As in sheep, these cattle may be latently infected for OvHV-2. Similarly, oLANA expression was represented by a nuclear and/or cytoplasmic reaction in a wide range of cell types (Figure 4-18 to 4-25).

Nasopharynx, tongue, lung, mediastinal lymph node, spleen, and thymus: These from a 7-week-old OvHV-2-positive calf (S13-1419) that had died with a severe ulcerative abomasitis (not related to MCF) were examined for oLANA expression (Figure 4-18). In the nasopharynx, oLANA was abundantly expressed with variable intensity in the cytoplasm of squamous epithelial cells. Endothelial cells also exhibited weak oLANA expression. In the turbinate or nasal skin, a similar reaction pattern was found; there was weak to moderate cytoplasmic staining of the squamous epithelium and the epithelium of hair follicles. Moreover, oLANA was expressed in glandular epithelial cells of the sebaceous glands. The sub-epithelial connective tissue with embedded artery and striated muscle bundles revealed weak cytoplasmic oLANA expression in striated muscle cells and arterial smooth muscle cells as well as endothelial cells with involvement of occasional intravascular leukocytes. Importantly, expression of oLANA was demonstrated in the salivary gland, both within the acinar and ductal epithelium (Figure 4-18).

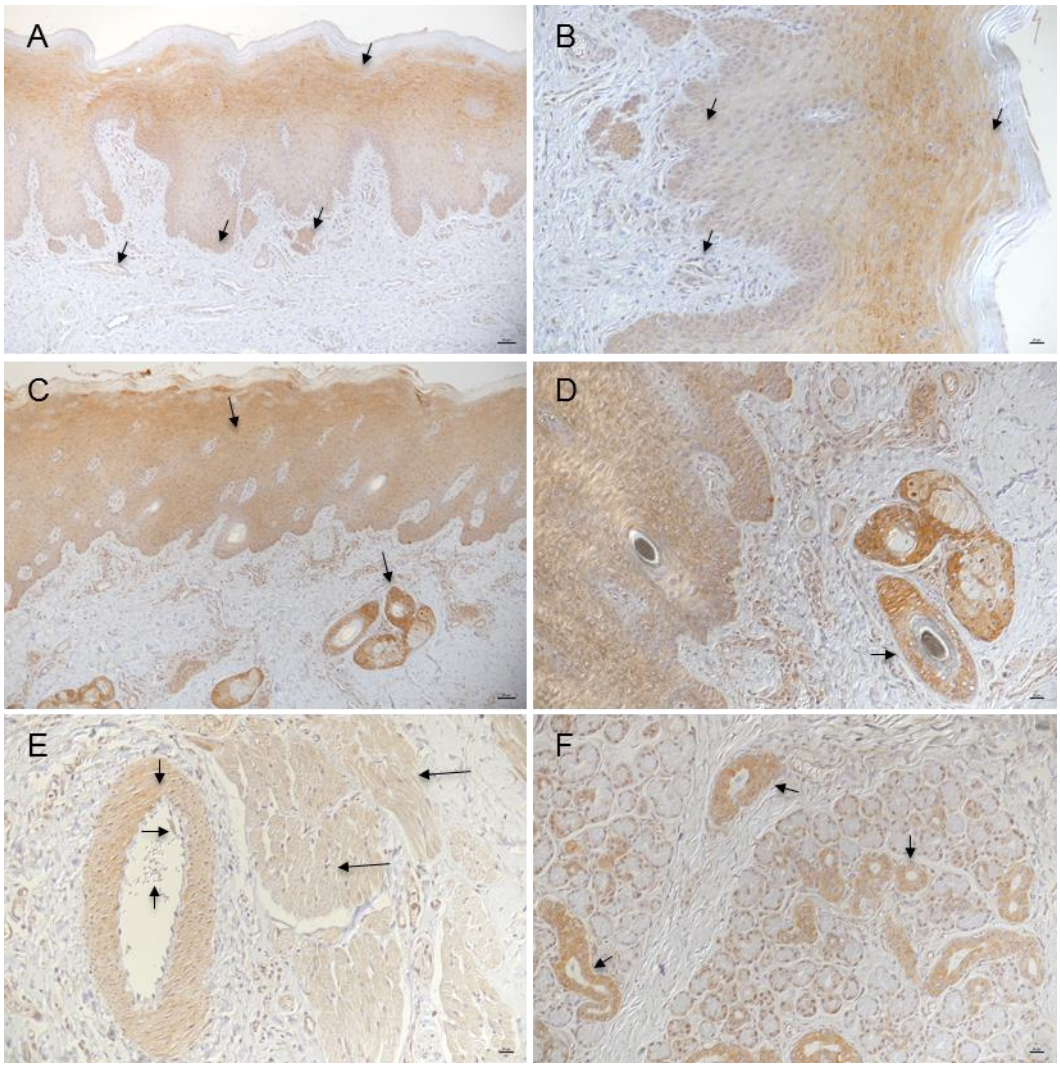

Figure 4-18. Immunohistochemistry staining images for oLANA antigen expression in the nasopharynx of a 7 week- old, cattle without MCF suffered from severe ulcerative abomasitis, previously tested positive for OvHV-2 by PCR, ISH and IHC (Amin, 2015) (S13-1419). (A) The squamous epithelium exhibits variably intense cytoplasmic expression of oLANA (arrows), scale bar= 50 µm. (B) Higher magnification of A, showing weak oLANA expression in the basal layers and moderate staining in the upper layers of the squamous epithelium, scale bar= 20 µm. (C) Shows again the oLANA expression in the squamous epithelium of the epidermis, and in the follicular epithelium (black arrows), scale bar= 50 µm. (D) Higher magnification of C, confirming oLANA expression in epithelial cells in the hair follicles (arrow) and in epithelial cells in the sebaceous glands, scale bar= 20 µm. (E) Sub-epithelial connective tissue with embedded artery and striated muscle bundles, showing weak cytoplasmic oLANA expression in striated muscle cells (long arrows) and arterial smooth muscle cells as well as endothelial cells, and in occasional positive intravascular leukocytes (short arrows), scale bar= 20µm. (F) Expression of oLANA is also seen in the salivary gland, both within the acinar and ductal epithelium (arrows), scale bar= 20 µm. Visualized with DAB and counterstained with haematoxylin.

In the tongue, oLANA expression was mainly seen in squamous epithelial cells while the reaction was weakly expressed in the presumably endothelium of sub-epithelial vessels or smooth muscle cells (Figure 4-19).

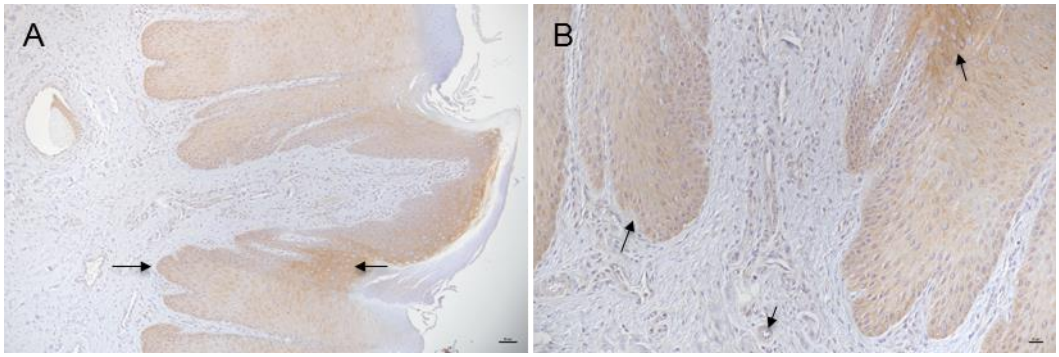

Figure 4-19. Immunohistochemistry staining images for oLANA antigen expression in the tongue of a 7 week- old, calf without MCF suffered from severe ulcerative abomasitis, previously tested positive for OvHV-2 by PCR, ISH and IHC (Amin, 2015) (S13-1419). (A) shows variable intensity of cytoplasmic oLANA reaction squamous epithelium (arrows), scale bar = 50µm. (B) Higher magnification of A demonstrate weak to moderate expression of oLANA in the stratum spinosum and weakly reaction in the stratum basale; the endothelium of sub-epithelial vessels are also seen positive with weak expression (arrow), scale bar= 20 µm. Visualized with DAB and counterstained with haematoxylin.

The lung showed weak cytoplasmic oLANA expression in bronchiolar epithelial cells and arterial smooth muscle cells. Morphologically, scattered positive cells consistent with (alveolar) macrophages were found in alveoli and interstitium (Figure 4-20).

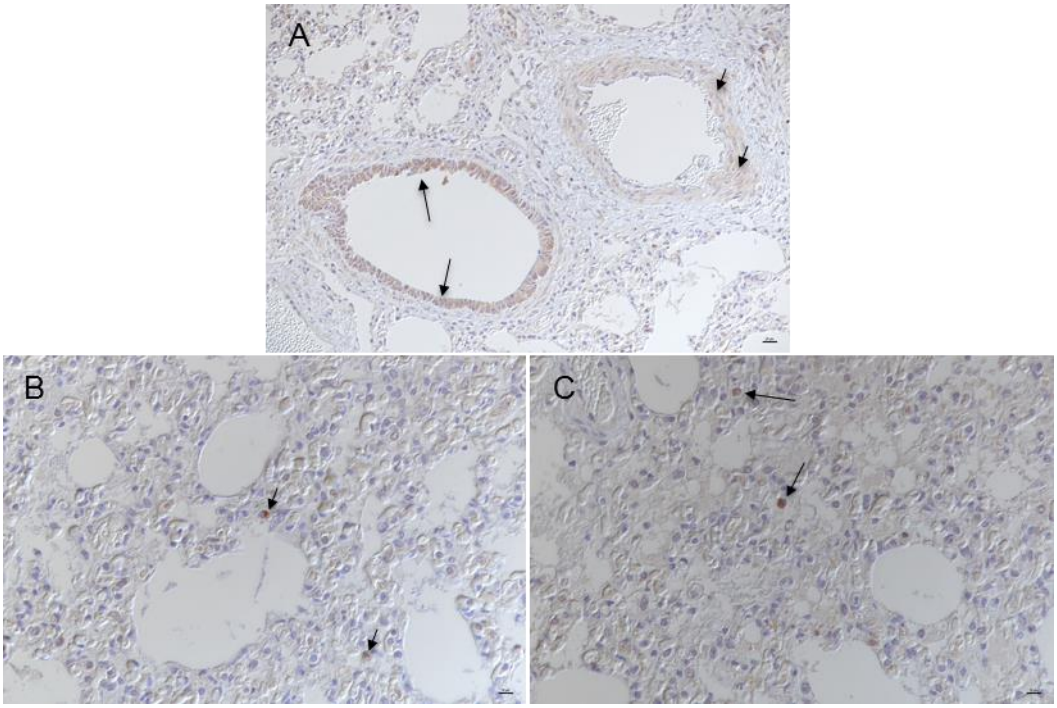

Figure 4-20. Immunohistochemistry staining images for oLANA antigen expression in the lung of a 7 week- old, cattle without MCF suffered from severe ulcerative abomasitis, previously tested positive for OvHV-2 by PCR, ISH and IHC (Amin, 2015) (S13-1419). (A) There is weak cytoplasmic oLANA expression in bronchialar epithelial cells (long arrows) and arterial smooth muscle cells (short arrows), scale bar= 20 µm. (B) Scattered cells in the pulmonary interstitium are also positive (arrows), scale bar= 10 µm. (C) There are also scattered cells with the morphology of likely alveolar macrophages that express oLANA (arrows), scale bar = 10 µm. Visualized with DAB and counterstained with haematoxylin.

In the mediastinal lymph node, numerous cells consistent with macrophages and follicular dendritic cells were observed in which cytoplasmic oLANA was detected. However, nuclear expression of oLANA was noticed in proportion of lymphocytes within the lymphatic follicle (Figure 4-21, A). In the spleen, oLANA was exhibited, with variable intensity of cytoplasmic reaction, in macrophages that localised in red and white pulp, whereas the reaction was nuclear reaction in occasional lymphocytes (Figure 4-21, B). In the thymus, oLANA was represented in likely numerous tingible body macrophages in which a cytoplasmic reaction was detected (Figure 4-21, C).

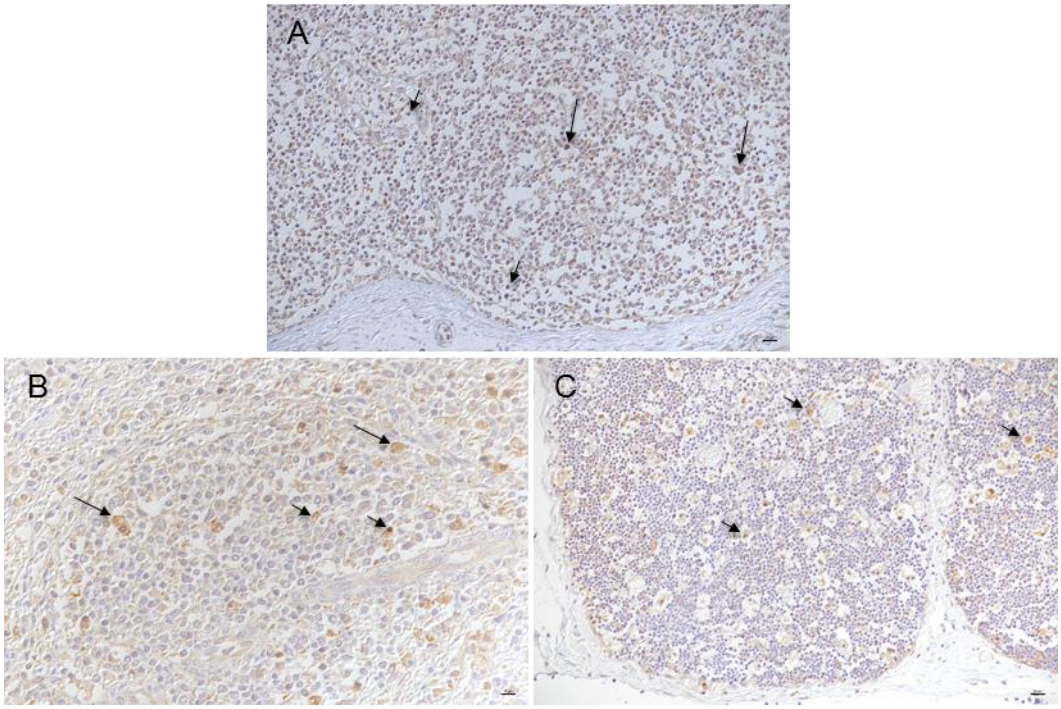

Figure 4-21. Immunohistochemistry staining images for oLANA antigen expression in the mediastinal lymph node (A), spleen (B), and thymus (C) of a 7 week- old, cattle without MCF suffered from severe ulcerative abomasitis, previously tested positive for OvHV-2 by PCR, ISH and IHC (Amin, 2015) (S13-1419). (A) In the mediastinal lymph node, cytoplasmic oLANA expression is seen in cells likely consistent with macrophages and follicular dendritic cells (long arrows) while a nuclear reaction is noticed in probably lymphocytes within the follicle (short arrows), scale bar = 20 µm. (B) In the spleen, macrophages (long arrows) in red and white pulp exhibit a cytoplasmic reaction, whereas occasional lymphocytes seem to exhibit a nuclear reaction (short arrows), scale bar = 10 µm. (C) In the thymus, cytoplasmic oLANA expression is seen in cells consistent with tingible body macrophages (arrows), scale bar = 20 µm. Visualized with DAB and counterstained with haematoxylin.

Lung, mediastinal lymph node, spleen, thymus, and placenta were examined from a 7-month-old foetus (S13-1483-8) of a cow that had been tested positive for OHV2 by PCR and ISH (Amin, 2015) (Figure 4-22 to 4-25).

The lung exhibited oLANA expression in bronchiolar respiratory epithelium. Expression of oLANA was detected in a proportion of positive cells consistent with macrophages (Figure 4-22).

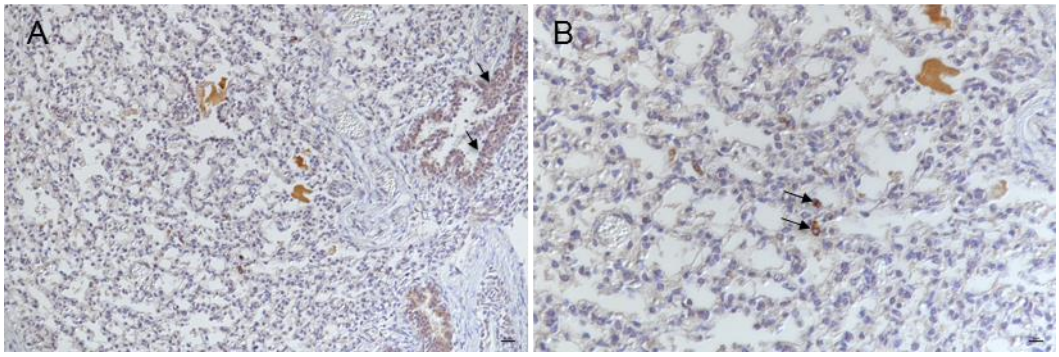

Figure 4-22. Immunohistochemistry staining images for oLANA antigen expression in lung of a 7 week- old, cattle without MCF suffered from foetal atelectasis, previously tested positive for OvHV-2 by PCR, ISH and IHC (Amin, 2015) (S13-1483-8). (A) Shows cytoplasmic oLANA expression in bronchiolar respiratory epithelium (arrows), scale bar = 20 µm. (B) Higher magnification of A depicts individual positive cells likely consistent with macrophages, scale bar = 10 µm. Visualized with DAB and counterstained with haematoxylin.

In the mediastinal lymph node analysis, expression of oLANA was demonstrated in probably numerous lymphocytes, macrophages and/or follicular dendritic cells within a lymphatic follicle. The adipose tissue surrounding the lymph node revealed cytoplasmic oLANA expression in arterial smooth muscle cells and endothelial cells (Figure 4-23).

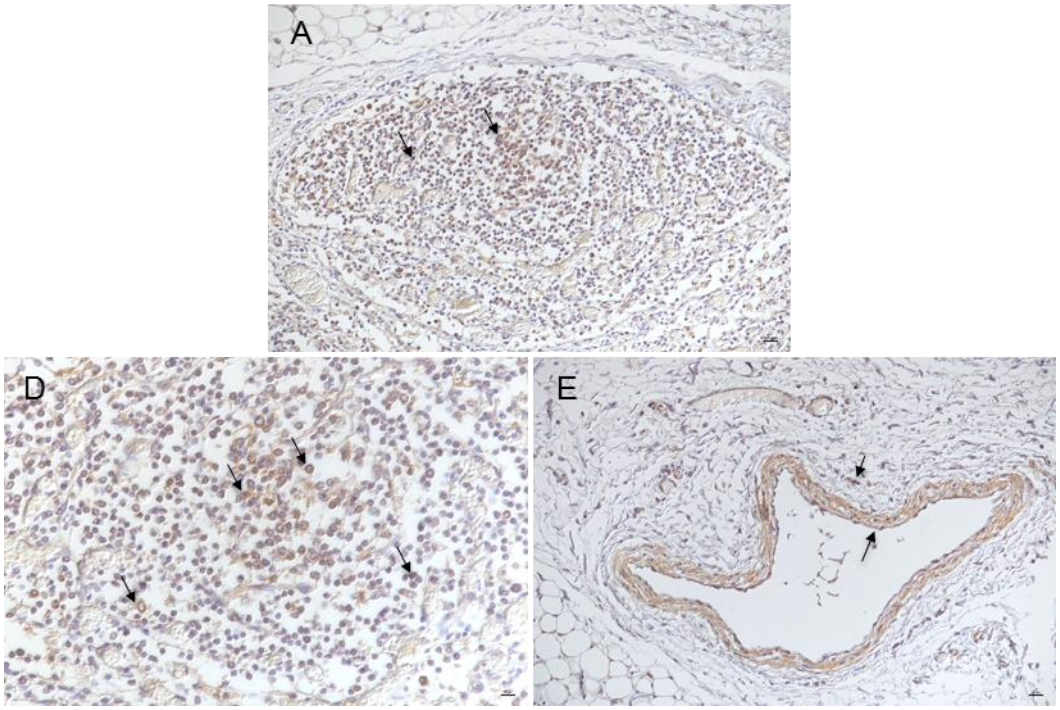

Figure 4-23. Immunohistochemistry staining images for oLANA antigen expression in mediastinal lymph node of a 7 week- old, cattle without MCF, suffered from foetal atelectasis, previously tested positive for OvHV-2 by PCR, ISH and IHC (Amin, 2015) (S13-1483-8). (A) Expression of oLANA is seen in numerous lymphocytes within a lymphatic follicle (arrows), scale bar= 20 µm. (D) Higher magnification of C, demonstrating oLANA expression in probably numerous lymphocytes, macrophages and/or follicular dendritic cells (arrows) in a follicle, scale bar = 10 µm. (E) The adipose tissue surrounding the lymph node shows cytoplasmic oLANA expression in arterial smooth muscle cells and endothelial cells (arrows), scale bar= 20 µm. Visualized with DAB and counterstained with haematoxylin.

In the spleen, a proportion of positive cells in red pulp exhibited oLANA expression while there were occasional macrophages and/or dendritic cells exhibit oLANA expression within thymus tissue (Figure 4-24).

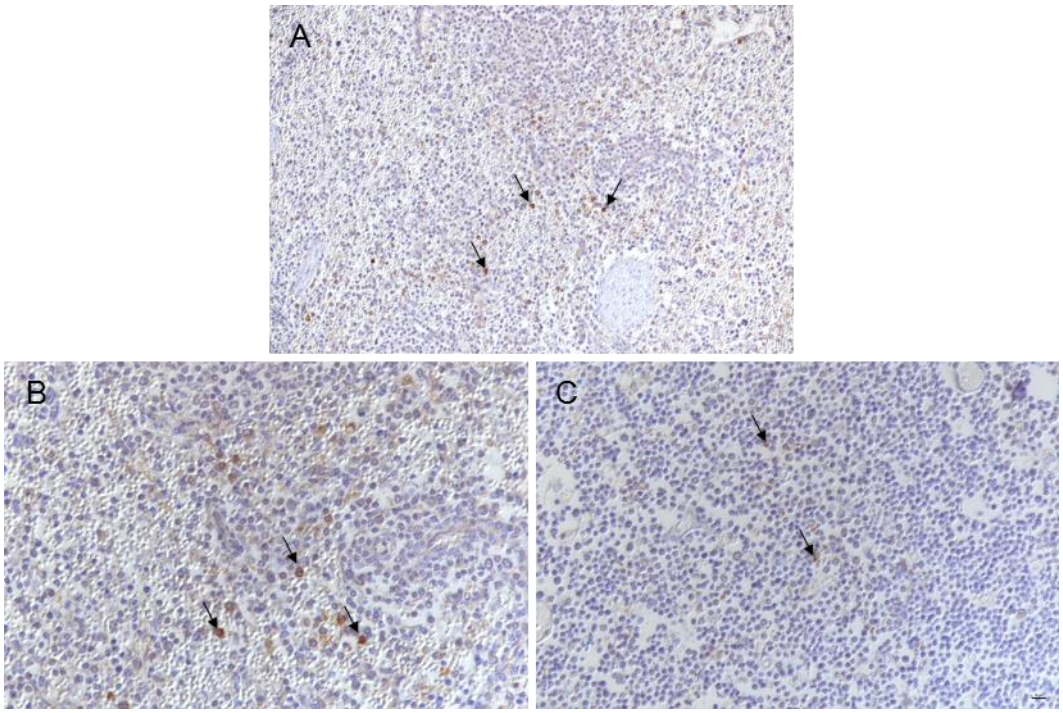

Figure 4-24. Immunohistochemistry staining images for oLANA antigen expression in spleen (A-B) and thymus (C), of a 8 month- old cattle without MCF, previously tested positive for OvHV-2 by PCR, ISH and IHC (Amin, 2015) (S13-1483-8). (A) In the spleen, a proportion of cells in red pulp shows oLANA expression (arrows), scale bar = 20 µm. (B) Higher magnification of A, showing oLANA expression in likely numerous lymphocytes (arrows), scale bar = 10 µm. (C) In the thymus, probably individual macrophages and/or dendritic cells exhibit oLANA expression (arrows), scale bar = 10 µm. Visualized with DAB and counterstained with haematoxylin.

In the placenta, oLANA was demonstrated as a strong reaction within vascular smooth muscle cells and epithelium. Moreover, stromal fibroblasts and trophoblasts were found infected (Figure 4-25).

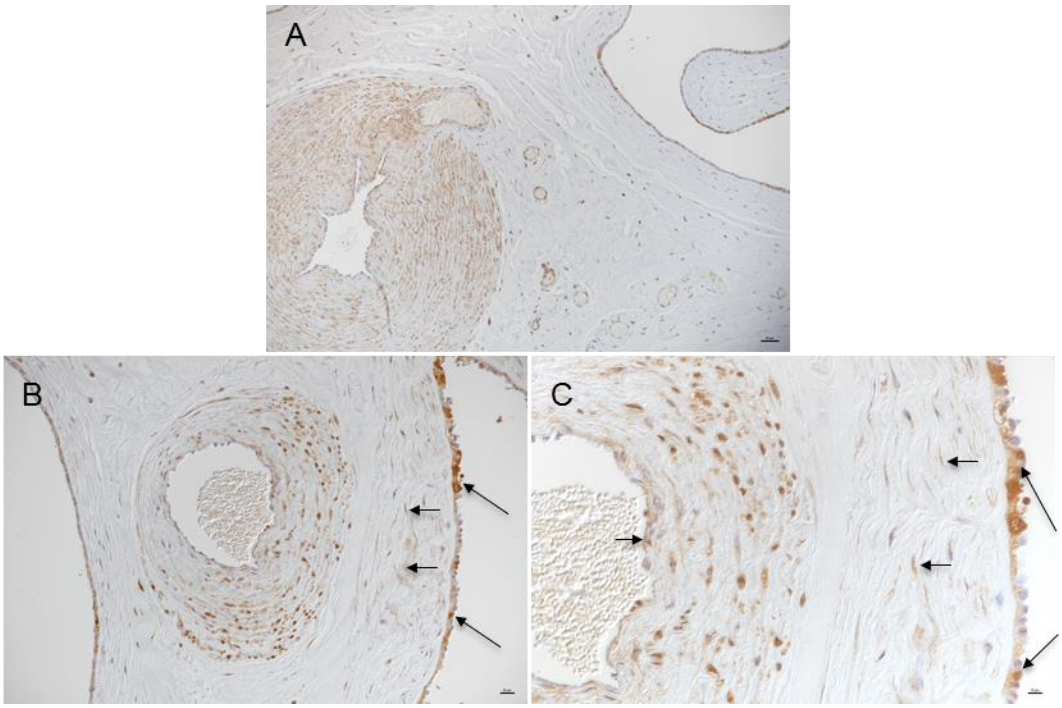

Figure 4-25. Immunohistochemistry staining images for oLANA antigen expression in placenta of an 8 month- old cattle without MCF, previously tested positive for OvHV-2 positive by PCR, ISH and IHC (Amin, 2015) (S13-1483-8). (A) The placenta exhibits strong staining for oLANA in vascular smooth muscle cells and epithelium, scale bar = 50 µm. (B) Higher magnification of A, showing oLANA expression in smooth muscle cells of an arterial wall (short arrows), stromal fibroblasts and trophoblasts (long arrows), scale bar = 20 µm. (C) Higher magnification of B, depicting the same positive cells. In the artery, there is also weak staining in endothelial cells (short arrow), scale bar= 10 µm. Visualized with DAB and counterstained with haematoxylin.

4.2.3.3 Immune-histological description of oLANA in buffalo with MCF

The rete mirabile, showing the pathognomonic vasculitis, and the retropharyngeal lymph node was examined from a 2-year-old water buffalo with confirmed MCF (S11-1232-8) (Figure 4-26).

In the rete mirabile, oLANA was expressed by infiltrating cells within arterial walls and in the adventitia, in the smooth muscle cells of the tunica media and, less intensely, in endothelial cells as well as a few intravascular leukocytes (Figure 4-26).

The retropharyngeal lymph node from another buffalo with confirmed MCF (S12-0124) was tested as a representative of the lymphatic tissues. Here, oLANA expression was mainly evident in macrophages/ follicular dendritic cells. Moreover, there were scattered positive lymphocytes outside lymphatic follicles. Similar to the arteries in the rete mirabile, arteries in the adipose tissue surrounding the retropharyngeal lymph node also exhibited a strong oLANA expression in the smooth muscle layer and exhibited the protein also in endothelial cells (Figure 4-27). The pre-immune serum was used to replace the primary antibody and served in the IHC staining protocol, as a negative control. No reaction was detected (Figure 4-27 E).

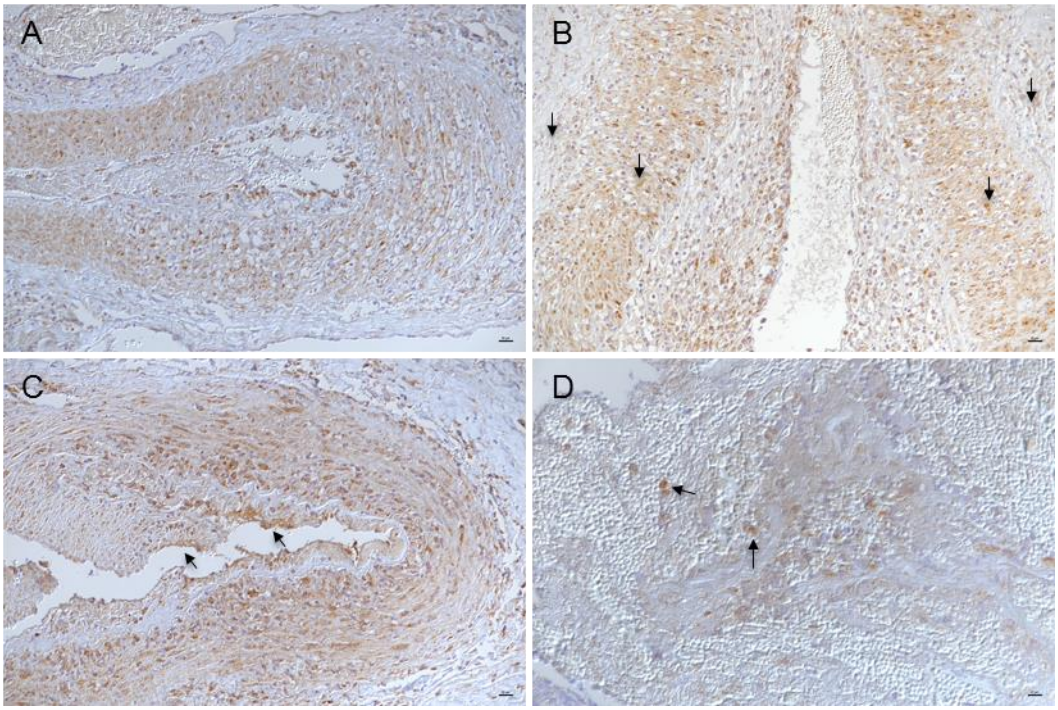

Figure 4.26. Immunohistochemistry staining images for oLANA antigen expression in the rete mirabile artery of a 2 year- old water buffalo with MCF (S11-1232-8). (A) Rete mirabile with marked mononuclear arteritis and periarteritis typical for MCF. (A) Expression of oLANA is widespread, within arterial smooth muscle cells and infiltrating leukocyte, scale bar = 20 µm. (B) Higher magnification of A, highlighting the expression of oLANA in adventitial and medial infiltrating cells and medial smooth muscle cells (arrows), scale bar = 20 µm. (C) Artery with oLANA expression also in endothelial cells (arrows), scale bar = 20 µm. (D) Arterial lumen, showing oLANA expression by a proportion of likely intravascular leukocytes (arrows), scale bar = 10 µm. Visualized with DAB and counterstained with haematoxylin.

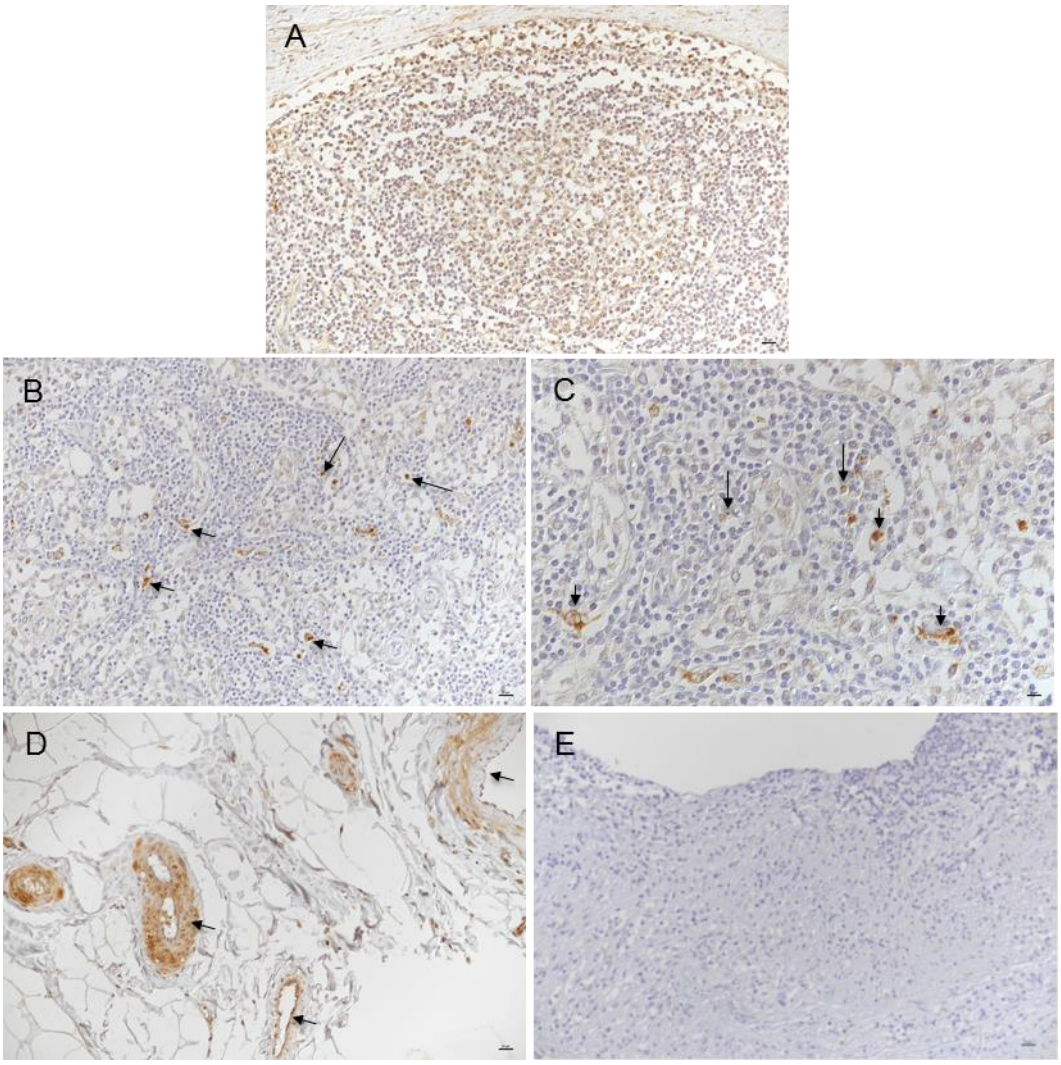

Figure 4.27. Immunohistochemistry staining images for oLANA antigen expression in retropharyngeal lymph node of an adult buffalo with MCF (S12-0124). (A) Expression of oLANA within a lymphatic follicle, scale bar= 20 µm. (B) oLANA expression is mainly evident in macrophages/ follicular dendritic cells (short arrows) as well as scattered lymphocytes (long arrows) outside follicles, scale bar= 20 µm. (C) Expression of oLANA in likely several macrophages (short arrows) and lymphocytes (long arrows) within medullary sinuses, scale bar= 10 µm. (D) In the adipose tissue surrounding the lymph node, there is strong oLANA expression in arterial smooth muscle cells and endothelial cells (arrows), scale bar = 20 µm. (E) Section incubated with the rabbit pre-immune serum instead of the primary antibody, as a negative control, showing no reaction, scale bar= 20 µm. Visualized with DAB and counterstained with haematoxylin.

4.3 Discussion

4.3.1 Expression of oLANA *in vitro*

In this study, a specific anti-oLANA PAb has been produced to assess the expression of oLANA in infected animals. A portion of ORF73 within the C terminal domain was expressed in bacteria and used to immunise rabbits for antisera generation. The C terminal domain of OFR73 is highly conserved (reviewed in section 1.1.4.1.2) and therefore chosen to produce the anti-oLANA PAb. The GST-oLANA protein was expressed at a molecular weight of 39 kDa after IPTG induction. This fusion protein was found highly insoluble when expressed by this method (Samuelson, 2011) (Figure 4-2).

In western immunoblotting analysis, The GST-oLANA was recognised by sera from OvHV-2- infected sheep and cattle. Therefore, it was used as an antigen for rabbit anti-oLANA PAb generation. Also, the anti-oLANA PAb was found to recognise the expressed GST-oLANA. When tissue lysates of OvHV-2-infected sheep and cattle were examined, oLANA appeared as a band of approximately 36 kDa and an occasional additional smaller band of approximately 13 kDa. This molecular weight was lower than expected from the 495 amino acids (Figure 4-28). Possibly, this resulted from the presence of numerous acidic tandem repeats that are localised within the central domain of oLANA (Verma *et al.*, 2007). These repeats could lead to faster migration of oLANA in SDS-PAGE gels during electrophoresis as a result of the negative charge. Presence of this central tandem repeats was also demonstrated in KSHV to evade host immunity by preventing the MHC class I peptide presentation (Kwun *et al.*, 2011).

The C terminal domain of oLANA protein (GenBank accession no. AAL05844) contains a putative internal ATG start codon (Figure 4-28). This internal domain was expressed in this study to produce the anti-oLANA. This possibly represents the detected 13 kDa band in the expressed oLANA within positive tissue lysate, LGL cells, and *in vitro* expressed oLANA. The comparison of oLANA protein from different OvHV-2 strains (personal communication) showed a high degree of polymorphism (Figure 4-29). Presumably, this genetic variability has an implication on the expression level of oLANA or its function that may affect the pathogenicity of OvHV-2 (Taus *et al.*, 2007).

```
1   MVLLRSGTSTDGDEDGRGRRPGPKKRPVTEGKGEGPGGEEEGPGGEGEGPGGEVEGPGGE
61  GEGPGGEVEGPGGEGEGPGGEVEGPGGEVEGPGGEGEGPGEEVEGPGGEGEGPEGE
121 GEGPGGEGEGPGGEGEGPGGEVEGPGGEGEGPGGEVEGPGGEGEGPEGEGEGPGGEGEGP
181 GGEEEGPGGEEEGPGGEEEGPGGEGEGPGGEGEGPVGEGEGPGGEGEGPGGEEEGPGGEE
241 EGPGGEGEGPEGEGEGPGGEGEGPGGGGPGGEEEEEEEEGEEEEEEEEEEEEEEEEEEEE
301 EEEEEEEEEEEEEEEEEEEEEEEEEEEGEGEGPGGEGEGPGGEGEGPGGEGEGPGGEGE
361 EGEEPEDPMEGPSSGPPVRGRRKRPPKHQPETDRAKRKKLAPIWDPTLKEATYSLHLNCT
421 SKDPVVRVSRSVRALNPNAPHSNIFFTGGMYTFVIYGNDKEAVESLFQFLLQDAMNNPQA
481 GAVNISTGPLTPSLPFNQQ
```

Figure 4-28. The putative amino acid sequence of oLANA, GenBank accession no. AAL05844, shows numerous tandem repeats. The glutamic acid repeats are highlighted in red and the internal domain in green.

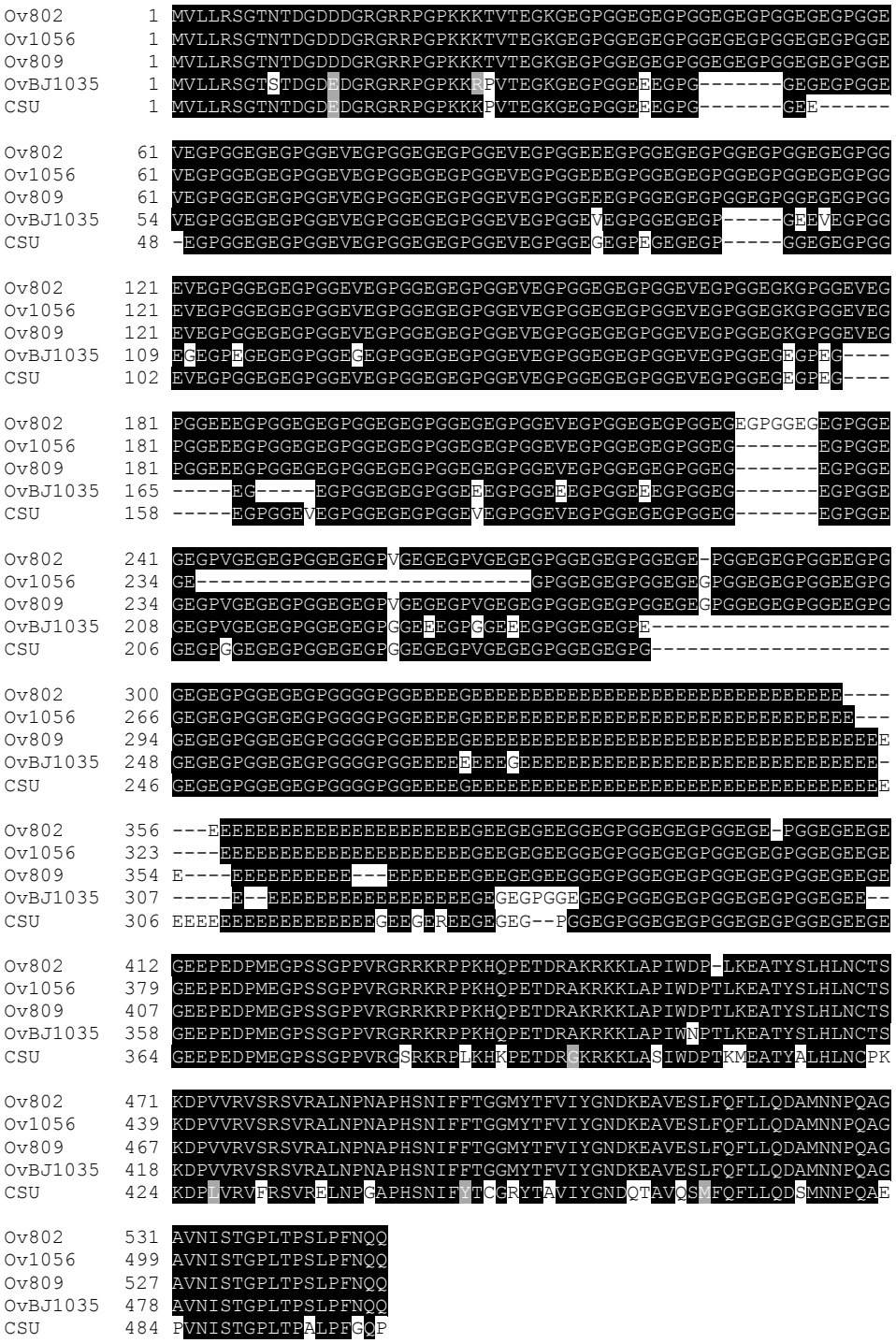

Figure 4-29. Sequence alignment of oLANA amino acids in different OvHV-2 strains shows the genetic polymorphism. This was conducted by using “Clustal Omega” programme and is displayed using the “BOXSHADE” programme. The identical residues are depicted in black, whilst similar residues are depicted in grey. Dashes are relevant to gaps in the sequence.

4.3.2 Expression of oLANA *in vivo*

OvHV-2 is a cell-associated virus and has not yet been propagated *in vitro*. Therefore, the latent phase of OvHV-2 infection is poorly understood (Russell *et al.*, 2009). Identifying oLANA as a possible marker of latently infected cells is important to understand MCF. The aim of this study was to define the key events in MCF latency and pathology. Expression of oLANA was demonstrated in OvHV-2-infected sheep, OvHV-2-infected cattle without MCF and ruminants with confirmed MCF using the novel anti-oLANA PAb that was produced in this study.

The results showed abundant oLANA expression in epithelial cells in the oral cavity and respiratory tract, in arterial smooth muscle cells, vascular endothelial cells and leukocytes (i.e. lymphocytes as well as macrophages and dendritic cells), regardless of infected species and disease. Also, although oLANA is mainly known as a nuclear protein (Verma *et al.*, 2007), here we showed that a cytoplasmic isoform exists in most positive cell types. This finding was also observed in the transfected cells used to demonstrate where oLANA is expressed in an infected cell. The detection of latently infected cells by demonstration of OvHV-2-LANA is informative, as they likely have a role in viral persistence in the host. Latent infection of epithelial cells could also enable OvHV-2 to spread into the environment, whereas latently infected endothelial cells could be a source for viral systemic spread.

In infected cattle without MCF, oLANA was detected in B cells and macrophages/dendritic cells in lymphatic tissues. In cattle with MCF, oLANA was found in infiltrating leukocytes in the arteritis and periarteritis in the rete

mirabile. A recent study confirmed that the infiltrating cells are mainly T cells and macrophages (Saura *et al.*, 2018). Both were found to express oLANA, and so did the endothelial cells. Arteritis in the rete mirabile is considered as pathognomonic for MCF (O 'Toole & Li, 2014).

Nuclear expression of LANA is a characteristic feature and well-known in other γ-herpesviruses such as KSHV where it tethers viral DNA to the host cell chromosome (Rahayu *et al.*, 2016). However, oLANA was also observed in the cytoplasm (Figure 4-12). To date, a high level of cytoplasmic LANA expression was noticed during the lytic phase of KSHV reactivation (Zhang *et al.*, 2016). This cytoplasmic form blocks cGAS-STING–dependent induction of interferon in host cells and causes suppression of the innate immune response while inducing viral reactivation.

Recently, an additional pathway of cytoplasmic-LANA in KSHV has been found that inhibits innate immunity via suppression of IF-β and NF-kB as well as inducing KSHV-reactivation. This occurs by interfering with cGAS-STING and production of IF-β and Rad50-Mre11-CARD9 (MRN complex) (Mariggiò *et al.*, 2017). The cytoplasmic-LANA in KSHV is encoded by the C terminal domain of ORF73 which is highly conserved as in OvHV-2 (reviewed in section 1.1.4.1.2). This mechanism could be similar in the pathogenesis of OvHV-2; it implies that OvHV-2 potentially modulates host cells to survive via oLANA expression.

4.3.3 Detection of oLANA in the natural host (sheep)

Sheep are well-adapted to OvHV-2 and do not develop any clinical signs after infection (O 'Toole & Li, 2014). Tissues from infected sheep that

had previously been found positive by PCR and ISH (Amin, 2015) were examined for oLANA expression. The results showed abundant expression in epithelial and endothelial cells, likely macrophages/ dendritic cells, and lymphocytes. Importantly, viral gene expression in vascular endothelial cells might play a pivotal role in viral systemic spread in sheep. Also, in this species, oLANA expression was found to be both nuclear and cytoplasmic (Figure 4-12).

In the respiratory tissue, oLANA was demonstrated as nuclear and/or cytoplasmic reaction in alveolar lining cells (morphological consistent with type II pneumocytes and/or alveolar macrophages). Moreover, likely lymphocytes and macrophages/ dendritic cells in the BALT (Figure 4-12) as well as bronchial epithelial cells and bronchiolar glands were found positive for oLANA expression (Figure 4-13). These immune cells could be modulated by OvHV-2 because the virus encodes for a similar to ovine IL-10 to deactivate the function of macrophages (Jayawardane *et al.*, 2008).

Detection of infected alveolar epithelial cells (predominantly with cytoplasmic reaction of oLANA) could support the notion that cytoplasmic oLANA could be evidence of OvHV-2 reactivation as in KSHV by modulating this cell type via the cGAS-STING and MRN complex pathway (Mariggiò *et al.*, 2017). OvHV-2 reactivation within respiratory epithelial cells may reflect the way by which OvHV-2 spreads. This corroborates the previous finding by (Li *et al.*, 2004) of OvHV-2 replication in the sheep nasal cavity as well as in lung tissue of experimentally infected sheep (Taus *et al.*, 2005). The airway epithelium supports lytic OvHV-2 infection (Taus *et al.*, 2010). However, the results of the present study also indicate oLANA as a possible marker for

latency within the respiratory epithelium; viral reactivation does also occur in infected sheep. Thereby, the airways could mediate viral spread at any time post infection. Indeed, nasal secretions were found as the principle mode of transmission between the reservoir hosts and susceptible host (Li *et al.*, 2001b).

Detection of oLANA in the lower airway (lung) presented as a predominant cytoplasmic expression within the bronchiolar epithelial layer while the reaction was nuclear in numerous cells within the alveolar wall and interstitium. This suggests a dynamic role possibly led by shifting the oLANA expression within these tissues in comparison with the upper airway enabling OvHV-2 maintenance and/or its release because of the efficient viral-host interaction. The modulation of host cells by OvHV-2- was suggested by (Riaz *et al.*, 2014) as transcriptional modulation controlled by encoding of viral microRNAs. These microRNAs contain predicted interaction codons with ORF73 (latency associated), ORF50 (reactivation), and ORF20 (cell cycle inhibition) to control OvHV-2 biology (lytic and latent cycles). This also agrees with our observations, but further work is needed to understand the relation between cytoplasmic or nuclear expression of oLANA and encoding of these microRNAs.

Finding oLANA expression within respiratory tissue is logical because OvHV-2 initially replicates in the lung (Li *et al.*, 2008b). Here, transcription of a lytic gene (ORF25) was initially detected in the sheep respiratory tract, particularly within turbinate tissue, whilst there was no expression in other tissues (Cunha *et al.*, 2008). OvHV-2 gene expression including: replication (ORF25), reactivation (ORF50), and latency (ORF73), correlated with the

severity of MCF-lesions in experimentally infected rabbits (Cunha *et al.*, 2013). Therefore, finding evidence of oLANA expression in these tissues may support the notion of the efficient adaptation of OvHV-2 to sheep.

In the tongue, oLANA was also expressed by the covering epithelium, with cytoplasmic expression in the stratum basale and stratum spinosum. Moreover, similar reaction was demonstrated in scattered ductal and acinar epithelial cells in the salivary gland. Importantly, the sub-epithelial lymphocytes, venous endothelial cells and arterial smooth muscle cells were also found to be positive (Figure 4-15). This could also contribute to OvHV-2 spread via salivary secretions. Another route possibly occurs via direct contact in newly-born lambs when they come into nose-to-nose contact with their mothers and are infected by released virus from salivary glands.

The obtained data from testing the lymphatic tissues such as lymph node, spleen, and thymus described oLANA as strong nuclear and/or cytoplasmic reaction. Morphologically, macrophages, follicular dendritic cells, and lymphocytes appeared positive (Figures 4-14). Establishment of OvHV-2 infection in these cell types had previously been confirmed by (Amin, 2015). Eventually, macrophages have phagocytic activity and thus OvHV-2 is likely to be engulfed by this cell type and consequently dysregulated. Generally, targeting of these cell types by OvHV-2 was confirmed by (Meier-Trummer *et al.*, 2010). Macrophages and splenic dendritic cells are also latently-infected by MHV-68 in mice (Flano *et al.*, 2000). Detection of oLANA in numerous antigen presenting cells (macrophages and/ or dendritic cells) is important because these cells are responsible for potential sentinel immunity (Hussell

et al., 2014). However, harbouring latent infection could cause dysregulation of these cell types as in KSHV (Thakker *et al.*, 2015).

We observed oLANA expression in the placenta, predominantly by smooth muscle cells in the media of arteries as well as stromal fibroblasts (Figure 4-17). A previous study in our laboratory by (Amin, 2015) showed OvHV-2 transcription in the placenta, mainly in placental epithelium and stromal fibroblasts. This was detected by PCR (with low copy number) but not RNA-ISH or IHC.

Together with these data, the expression of oLANA suggests that OvHV-2 may be vertically transmitted and may even lead to persistent infection and immune tolerance in the offspring in sheep. Vertical transmission of OvHV-2 has been reported in cattle (Headley *et al.*, 2015); similarly, it has been demonstrated for AlHV1 in wildebeest (Li *et al.*, 2011b), and CvHV2 in reindeer (das Neves *et al.*, 2009a, c). However, no confirmation has yet been achieved for OvHV-2 in sheep (O'Toole & Li, 2014) and CpHV-2 in goat (Li *et al.*, 2005a).

4.3.4 Detection of oLANA in cattle without MCF

Cattle are sensitive to MCF. However, it has been shown that a high proportion of cattle without MCF carry OvHV-2 (Amin, 2015). These confirmed positive animals were examined here to detect oLANA expression in cattle without MCF.

Interestingly, OvHV-2 positive cattle without MCF exhibited oLANA expression, again both cytoplasmic and nuclear, in various cell types, i.e. epithelial cells, endothelial cells, and vascular smooth muscle cells.

In the nasopharynx, oLANA was predominantly expressed with cytoplasmic reaction in squamous epithelial cells as well as glandular epithelial cells of the sebaceous glands. A similar reaction was also revealed within the sub-epithelial connective tissue as the striated muscle cells and arterial smooth muscle cells as well as endothelial cells with involvement of occasional intravascular leukocytes were found positive. Importantly, expression of oLANA was also demonstrated in the salivary gland, both within the acinar and ductal epithelium (Figure 4-18). These sites are considered as portals for entrance of OvHV-2 (O 'Toole & Li, 2014). MCF was induced by nasal aerosol infection with OvHV-2 in numerous susceptible hosts such as cattle (Taus *et al.*, 2006) and pigs (Li *et al.*, 2012), and it was shown to occur in bison even when sheep were some distance away (Li *et al.*, 2008a).

The lung exhibited oLANA expression in bronchiolar and alveolar respiratory epithelium. Morphologically, scattered positive cells consistent with (alveolar) macrophages were found in alveoli and interstitium (Figure 4-20). The lung tropism of OvHV-2 infection in bison has been determined by (Cunha *et al.*, 2012) as OvHV-2 transcribed three viral genes (ORF25, ORF50, and ORF73) that encodes for lytic and latent cycles. These encoded proteins were detected in lung at a high level after 9-12 days post infection (DPI). However, expression of the host immune response- related genes was found at a low level in both lung and LN. This was combined with increase the systemic viral load after (16-21) DPI.

It can be suggested that oLANA expression is highly regulated to enable OvHV-2 to disseminate systematically inside host organs via

migration of the infected macrophages that carry OvHV-2 into local lymph nodes.

In the tongue, abundant cytoplasmic oLANA was detected in the epithelium and salivary gland. Additionally, the endothelial cells and smooth muscle cells of sub-epithelial vessels were also found positive (Figure 4-15). As stated above, this cytoplasmic form of oLANA could occur during viral reactivation for the systemic spread.

Examination of the mediastinal lymph nodes from infected cattle revealed oLANA staining in numerous macrophages and presumably follicular dendritic cells with a cytoplasmic reaction that localised in the lymphatic follicles. Occasional lymphocytes also exhibited nuclear oLANA staining. In other lymphatic tissues, i.e. spleen and thymus, oLANA staining was seen in the same cell types including macrophages, follicular dendritic cells, and tingible body macrophages (in the thymus). This fits with previous reports by (O 'Toole & Li, 2014; Russell *et al.*, 2009) including infection of lymphoid cells by OvHV-2. Our finding suggests a possible modulation of these cell types by OvHV-2 to evade host immunity.

The role of oLANA in lymphoid tissues seems to be fundamental. For instance, in cattle with MCF, transcriptional analysis was conducted for host tissue (lymphoid tissues) and OvHV-2 during the early and late infection periods. This showed a low level of IL-2 transcripts that correlated with elevated ORF73 (oLANA transcript) (Meier-Trummer *et al.*, 2009b). Thus, oLANA may negatively regulate lymphocyte activation by IL-2. This could further support the previous concept of circumventing host defence in these

cell types during the latent cycle (Kwun *et al.*, 2011; Sorel *et al.*, 2017; Thakker *et al.*, 2015; Zaldumbide *et al.*, 2007).

It was interesting to see oLANA expression in the vasculature (endothelial cells and smooth muscle cells) and the epithelium in the placenta (Figure 4-25). This provides further evidence of vertical transmission of OvHV-2 as possible in naturally infected cattle and supports previous findings, where viral lytic gene expression was seen in the placenta of cattle (Headley *et al.*, 2015). Finding oLANA expression within the placental epithelium implies the possibility of OvHV-2 dissemination.

In this study, finding oLANA expression within vascular endothelial cells is important to find possible explanations for the way in which OvHV-2 circulated and trigger MCF. Possibly, infected endothelial cells induce vascular inflammatory responses. This consequently causes infiltration and recruitment of leukocytes from the blood within tunica adventitia via vasa vasorum as well as the remodelling processes (cytokines and chemokines stimulation) at the later stages (Davis *et al.*, 2003). Other herpesviruses such as KSHV, HSV,HCMV, and EBV have a tropism to the endothelial cell and likely remodel this cell type (Brunson *et al.*, 2016; Hong *et al.*, 2004; Sinzger, 2008). This mechanism likely induces the fatal vasculitis of MCF.

4.3.5 Detection of oLANA in cattle with MCF

The expression of oLANA in MCF lesions was examined, choosing the rete mirabile showing the typical arteritis and periarteritis.

A severe vasculitis with fibrinoid necrosis and thickening of the vascular intima was seen with substantial mononuclear infiltration within the

tunica adventitia and tunica intima. The pathological changes have been reported in numerous susceptible hosts such as rabbit, bison, cattle, and water buffalo (O 'Toole & Li, 2014).

In the present study, oLANA was detected as a strong nuclear and/or cytoplasmic reaction within infiltrating cells. It was also found in endothelial cells and medial smooth muscle cells. Positive intravascular leukocytes were also observed, which confirm systemic viral infection during disease. Critically, there are oLANA positive endothelial cells in the rete mirabile associated with vasculitis. The rete mirabile is critical for the supply of blood to the brains of ungulates so this novel observation may explain sudden death in MCF.

In previous experimental studies inducing MCF in bison, cells infiltrating the vascular walls were found to be predominantly $CD8^+$/$perforin^+$ γδ T cells (Nelson *et al.*, 2010). It may be these cells express oLANA. Whether this is the case is currently being investigated in a separate study undertaken at the Institute of Veterinary Pathology, Vetsuisse Faculty, University of Zurich. Preliminary results have shown oLANA expression within infiltrating cells in acute and chronic vascular lesions. Besides an infiltration by macrophages and fewer T cells within the tunica adventitia, activation of the endothelial cells was seen in affected arteries. Cells expressing oLANA were endothelial cells, smooth muscle cells as well as infiltrating macrophages and lymphocytes as confirmed by specific immuno-histology. Both types of leukocytes were observed to be proliferating. These findings suggest that MCF-vasculitis is macrophage-driven rather than lymphoproliferative and that the vasculitis is virus driven (Saura *et al.*, 2018).

Macrophages play a fundamental role in host innate immunity. However, detection of oLANA as a marker for latency within morphologically detected macrophages could explain the dysregulation of this cell type as a sentinel cells within vasculatures. This possibly led to evade the innate immunity and enables OvHV-2 to survive. Also, macrophages considered a long-living cell in the tissue. Therefore, dysregulation of this cell type could be fundamental in MCF pathogenesis. Dysregulation of the macrophages by KSHV has been observed by (Bhaskaran *et al.*, 2017) and deactivation of the dendritic cells as evasive mechanism was demonstrated in AIHV-1 (Myster *et al.*, 2015).

In experimentally induced MCF in bison, it was shown that an OvHV-2 protein (ORF25) was expressed in infiltrating fibroblasts. However, this was not found in the vascular endothelium, smooth muscle cells or leukocytes (Nelson *et al.*, 2013).

The localisation of OvHV-2 within the vasculature may have an impact on triggering MCF. It appears to drive infiltration of lymphocytes and vasculitis.

4.3.6 Comparison of oLANA expression in sheep, cattle without MCF, and cattle with MCF

The expression of oLANA was demonstrated in non-lymphatic and lymphatic tissues. Generally, infected cell types were similar regardless of the species and, in cattle, whether the animals were suffering from MCF or not.

In both infected sheep and cattle, oLANA expression was seen in the respiratory tract and oral mucosal epithelium. This could indicate OvHV-2 reactivation/ replication resulting in virus spread. However, the protein was also expressed in the vasculature (endothelium) and in lymphatic tissues. Predominantly, macrophages and lymphocytes (B subtype) were found positive for oLANA. This suggests a successful strategy by which OvHV-2 can be spread systemically. The vascular endothelium has a permeability function, and this could help for the systemic spread of OvHV-2 via infected cells. This could also cause initial inflammation to evoke the immune response via the expressed cytokines and chemokines by endothelial cells of the adventitial vasa vasorum and ultimately leading to fatal vasculitis. These key events were similarly found in KSHV (Ballon *et al.*, 2015).

In cattle with MCF, oLANA was expressed more intensely, and particularly in infiltrating leukocytes in the typical vascular lesions and in cells in the vessel walls and the endothelium. Critically, there are infected endothelial cells in the rete mirabile associated with vasculitis. In this instance, presence of oLANA in the vasculature likely plays a pivotal role in developing MCF as both types of leukocytes (macrophages and lymphocytes) can carry OvHV-2. However, both cell types play different fundamental roles in MCF pathogenesis. The inflammatory infiltrates within the vascular lesions have been demonstrated as abundant T-lymphocytes ($CD8^+$ that have a natural killer phenotype), B- cells ($CD79a^+$), and macrophages (O'Toole & Li, 2014). Interestingly, only small numbers of these lymphocytes have been shown carry OvHV-2 (Russell *et al.*, 2009; Schock & Reid, 1996).

4.3.7 Conclusion

The survival of OvHV-2 in the adapted and susceptible hosts most likely occurs by numerous strategies. It may remain entirely latent following primary infection as an episome inside cells. Demonstration of oLANA antigen within the epithelial cells might be supportive for the environmental spread. Detection of positive vascular endothelial cells and smooth muscle cells possibly help OvHV-2 to disseminate systemically and ultimately MCF-triggering. Presenting of oLANA expression within likely macrophages and follicular dendritic cells could imply the dysregulation of antigen presentation and recognition of OvHV-2. This could allow OvHV-2 to survive efficiently inside the hosts. Finding oLANA expression within the placenta may be an evidence for the vertical transmission during the sub-clinical infection. These strategies likely represent key events in OvHV-2 pathogenesis.

5. Chapter five: Generation of Recombinant Modified Vaccinia Ankara expressing OvHV-2 glycoproteins (rMVA-glycoproteins)

5.1 Abstract

Recently, highly MCF-susceptible hosts including bison, water buffalo and deer have been farmed in the UK. However, they are facing serious issues of developing clinical MCF. Therefore, an effective vaccine is urgently needed to prevent the disease. Nevertheless, since OvHV-2 has not yet been propagated *in vitro*, neither live-attenuated nor killed vaccines have been effectively produced (Russell *et al.*, 2009). Therefore, attempts towards developing a preventive vaccine mostly depend on producing virus glycoprotein subunits. For instance, effective candidates including gB and gH/gL heterodimer complex were found to prevent MCF in rabbits (Cunha *et al.*, 2015). The aim of this study was to express the OvHV-2- glycoproteins including gB, gH, gL, and Ov7 in modified vaccinia Ankara virus (MVA) to develop a suitable subunit vaccine. The gB and gH/gL glycoproteins have an important role OvHV-2 biology by inducing membrane-fusion while Ov7 is homologous to A7 gene in AIHV-1 and analogous to BZLF2 protein of EBV that interact with gp42 and involved in membrane fusion and B cell infection

(Hart *et al.*, 2007; Hutt-Fletcher, 2007). We hypothesised that Ov7 possibly interact with gH/gL complex as a heterotrimer. The results demonstrate modification and production of rMVA virus that carried OvHV-2-glycoproteins. As expected, gH and gL interacted as a heterodimer and were glycosylated in Baby Hamster Kidney fibroblast (BHK) cells via post translational modification. However, the Ov7 glycoprotein did not interact as a heterotrimer with this complex. Production of these rMVA-glycoproteins could help in prevention of MCF.

5.2 Results

5.2.1 Recombination of rMVA-glycoproteins

The MVAs plasmids were designed to carry ORF8, ORF22, ORF47, and Ov7 that encode gB, gH, gL, and Ov7 glycoproteins respectively. All the targeted genes were expressed under the MVA H5 promoter and fused with tags: FLAG (for gB and gH), HA (for gL), V5 (for Ov7) genes to enable a suitable selection, purification, characterisation and large-scale production of each rMVA-glycoprotein (see 2.15.1 to 2.15.7).

The recombination was performed using BHK cells via MVA inoculation and transfection with MVA-plasmid insertion vectors. The resulting recombinants appeared as green fluorophore signals under fluorescent microscopy (Figures 5-1, 5-2, 5-3, and 5-4). These recombinants were harvested and purified by three cycles of plaque isolation and inoculation of the single separated fluorescent plaque. Cytopathic effect

within BHK cells appeared as cell-rounding with fluorescent plaque (Figure 5-5).

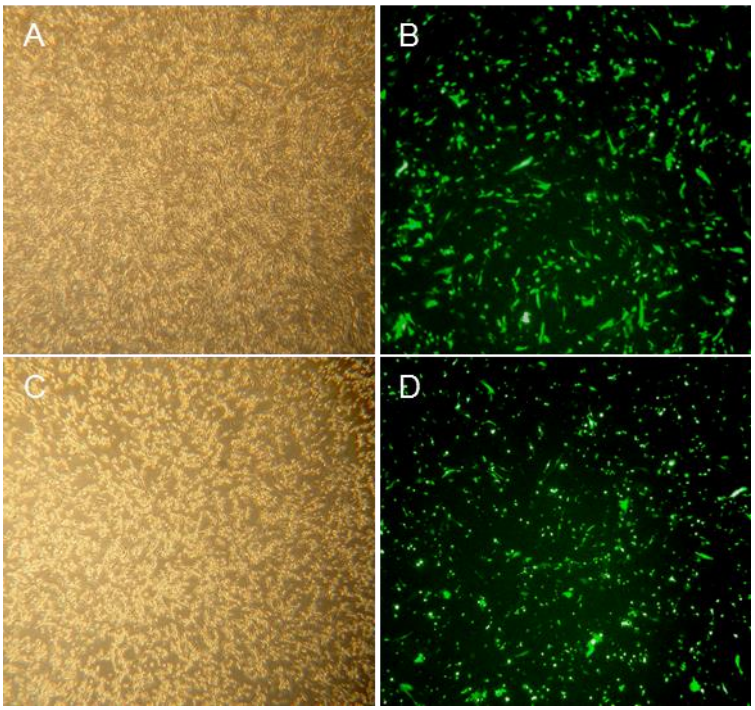

Figure 5-1. MVA-gB recombination. (A and B) are BHK cells infected with 0.5 x 10^5 PFU of vaccinia virus followed by transfection with MVA-gB plasmid (0.62 µg/ well) then incubated for 24h post inoculation. (C and D) are the same cells after 48 h post inoculation. All imaged under fluorescent microscope at 4X magnification.

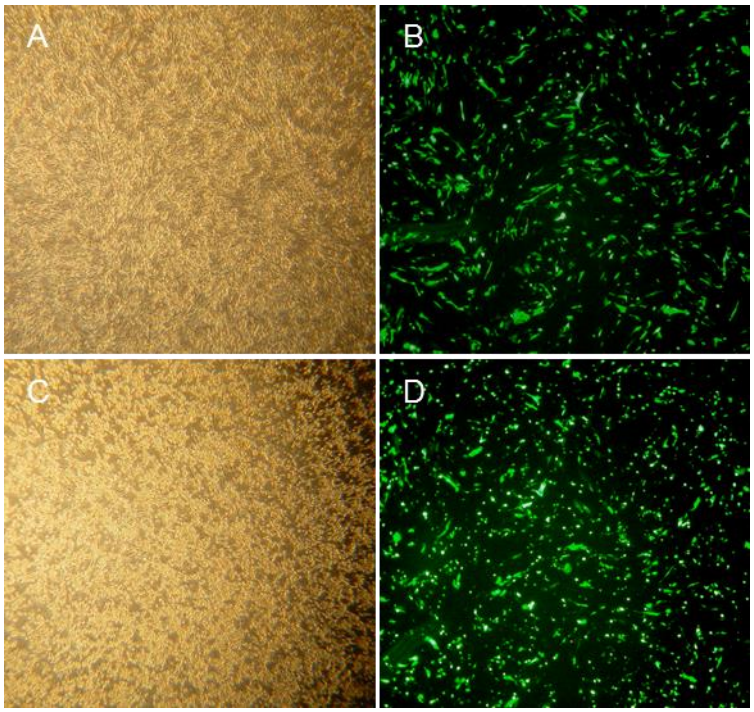

Figure 5-2. MVA-gH recombination. (A and B) are BHK cells infected with 0.5 x 10^5 PFU of vaccinia virus followed by transfection with MVA-gH plasmid (0.62 µg/ well) then incubated for 24h post inoculation. (C and D) are the same cells after 48 h post inoculation. All imaged under fluorescent microscope at 4X magnification.

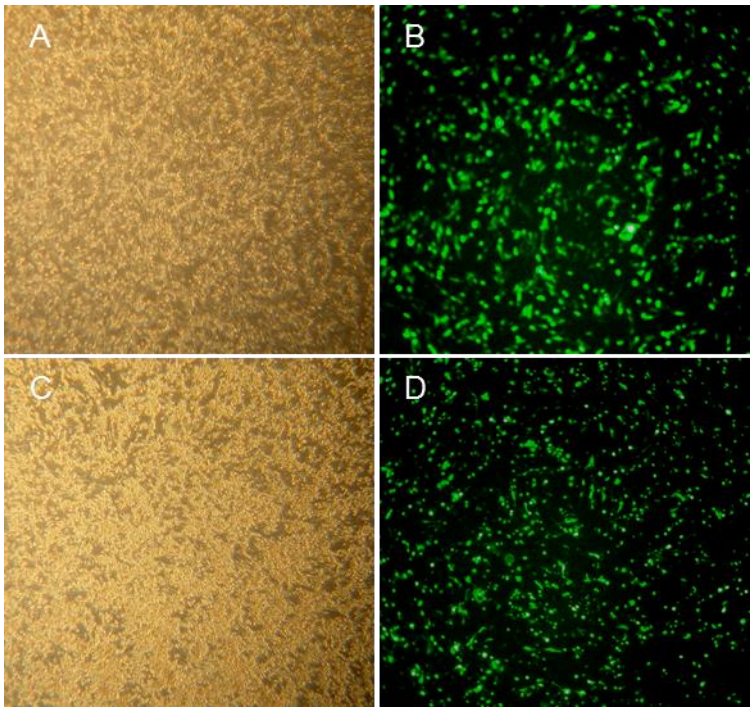

Figure 5-3. MVA-gL recombination. (A and B) are BHK cells infected with 0.5 x 10^5 PFU of vaccinia virus followed by transfection with MVA-gL plasmid (0.62 µg/ well) then incubated for 24h post inoculation. (C and D) are the same cells after 48 h post inoculation. All imaged under fluorescent microscope at 4X magnification.

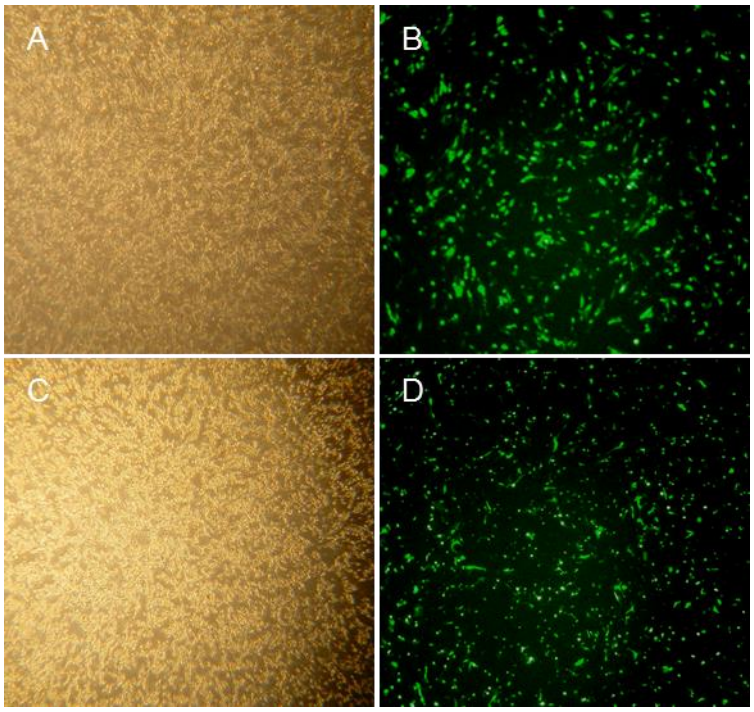

Figure 5-4. MVA-Ov7 recombination. (A and B) are BHK cells infected with 0.5 x 10^5 PFU of vaccinia virus followed by transfection with MVA-Ov7 plasmid (0.62 µg/ well) then incubated for 24h post inoculation. (C and D) are the same cells after 48 h post inoculation. All imaged under fluorescent microscope at 4X magnification.

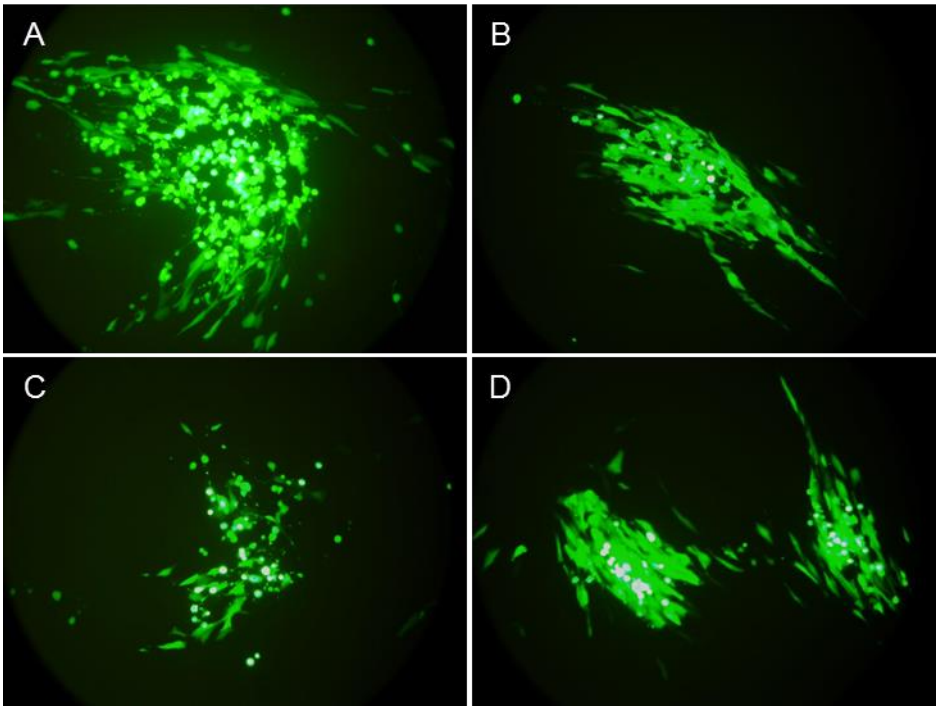

Figure 5-5. Final plaque purification of the rMVA-glycoproteins in BHK cells after 3-rounds of inoculation and purification. (A) Is rMVA-gB. (B) Is rMVA-gH. (C) Is rMVA-gL. (D) Is rMVA-Ov7. All are imaged under fluorescent microscopy at 60X magnification.

5.2.2 Expression of rMVA-glycoproteins

BHK cells were inoculated with each rMVA-glycoproteins at (0.5 x 10^5 pfu/ ml)/ well as described in section (2.15.3). Thereafter, the expressed proteins were identified and characterised via detection of the expressed TAG-fusion proteins by western immunoblotting and live immunofluorescent assays.

5.2.2.1 Detection of rMVA-glycoproteins by western immunoblotting

The whole cell-lysate of BHK cells infected with each rMVA-glycoprotein were analysed by immune blotting using MAbs for the corresponding glycoproteins as described in section (2.6.5.1).

The whole cell-extract that had been infected with rMVA-gB was analysed with anti-FLAG-HRP. The gB protein was detected as three bands with molecular weight approximately 130, 92, and 55 kDa. In the rMVA-gH infected cells, the expressed protein was detected as two bands of 95 and 57 kDa. However, the rMVA-gL expressed protein was detected by anti-HA-HRP with a molecular weight of 33 kDa. Detection of the expressed recombinant protein in rMVA-Ov7 infected BHK cells was demonstrated by using anti-V5-HRP and showed a molecular weight of approximately 30 kDa (Figure 5-6).

In other viruses, gH and gL form a heterodimer. It was also possible that, like EBV, Ov7 could associate with gH/gL in a heterotrimeric complex. The combined expression of gH/gL and gH/gL/Ov7 (mixed inoculation of these rMVA-glycoproteins) was initially characterised by western

immunoblotting. The predicted product of Ov7 gene is likely a glycoprotein and this is analogous to BZLF2 protein of EBV that interacts with gb42 to induce fusion membrane and B cell infection (Hart *et al.*, 2007).

After mixing rMVA-gH/gL, gH expression was detected as a single band at 94 kDa. A gH protein band of a similar molecular weight was seen in rMVA-(gH/gL/Ov7) mixed infection by using anti-FLAG to detect gH while detection of the gL in rMVA-(gH/gL) and rMVA-(gH/gL/Ov7) revealed a similar size of 28 kDa. This was slightly lower than the previously detected band. The expressed Ov7 protein from this mixture revealed detection of band at 32 kDa. However, two bands at higher molecular weight (134, 89) kDa were additionally demonstrated from this mixture by using anti-V5 (Figure 5-7).

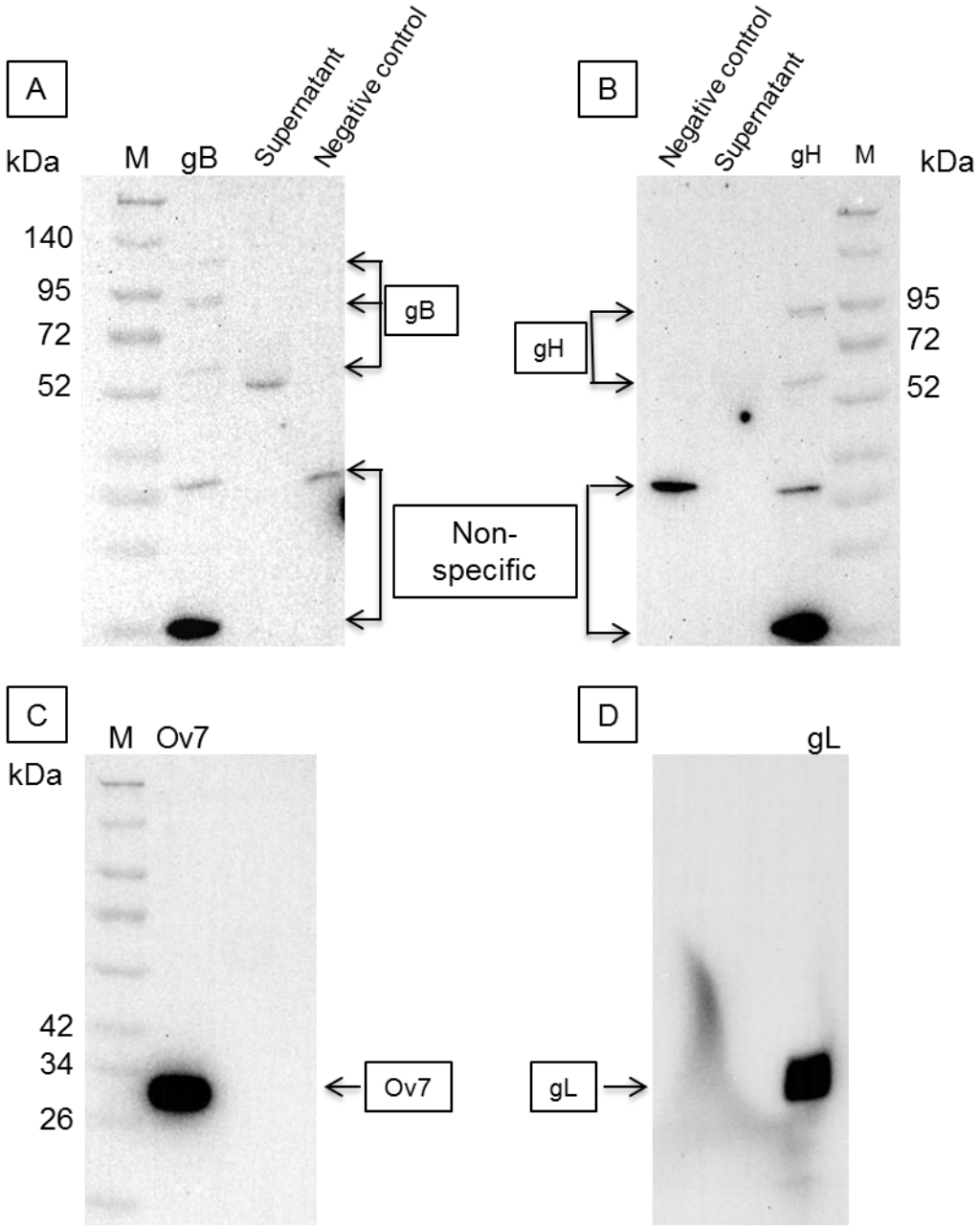

Figure 5-6. Western immunoblotting analysis (12 %) images show the immune reactivity of the expressed rMVA-glycoproteins. (A) Is detection of the expressed gB, subjected to anti-FLAG primary antibody and probed with anti-mouse secondary antibody labelled with HRP. (B) Is detection of the expressed gH, subjected to anti-FLAG primary antibody and probed with anti-mouse secondary antibody labelled with HRP. (C) Is detection of the expressed Ov7, subjected to anti-V5 primary antibody and probed with anti-mouse secondary antibody labelled with HRP. (D) Is detection of gL, subjected to anti-HA primary antibody and probed with anti-rat secondary antibody probed with HRP.

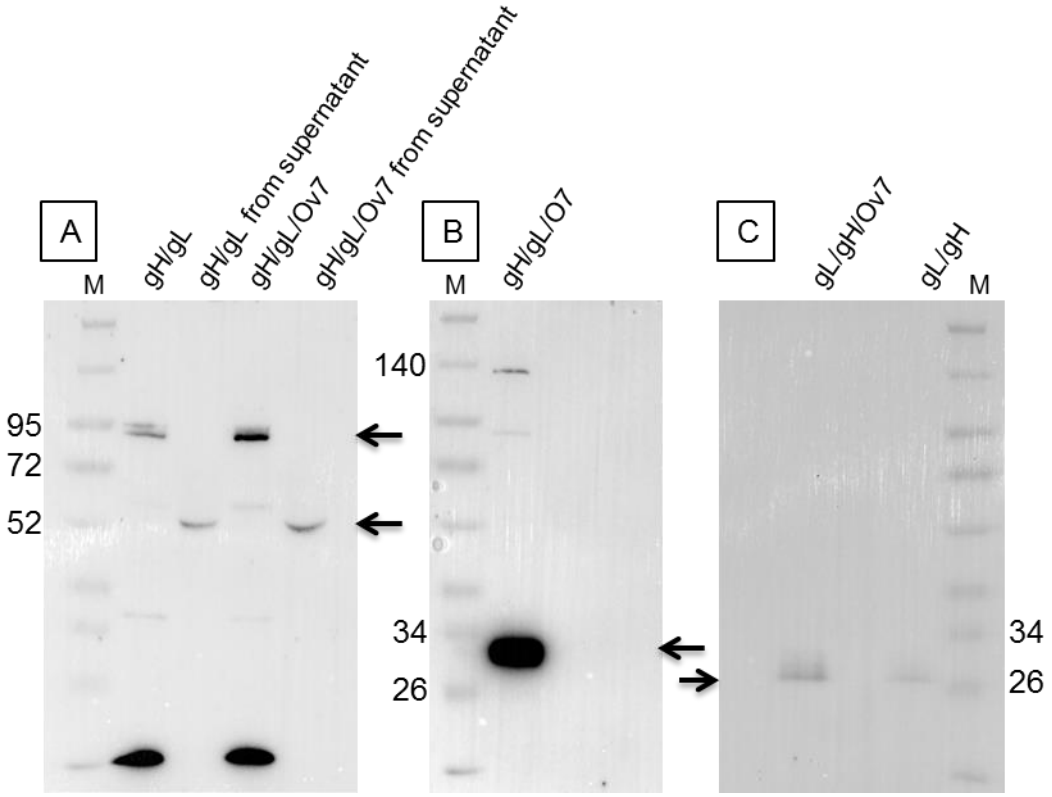

Figure 5-7. Western immunoblotting analysis (12 %) image shows the immune reactivity of the expressed rMVA-glycoproteins (mixed infection) in BHK cells. (A) Is detection of the expressed gH after co-infection with either rMVA-(gH/gL) or rMVA-(gH/gL/Ov7) and subjected to primary anti-flag and secondary anti-mouse labelled with HRP. (B) Is detection of the expressed Ov7 after co-infection with rMVA-(gH/gL/Ov7) and subjected to primary anti-V5 and secondary anti-mouse. (C) Is detection of the expressed gL after co-infection with either rMVA-(gH/gL) or rMVA-(gH/gL/Ov7) and subjected to anti-HA primary antibody and anti-rat secondary antibody labelled with HRP.

5.2.2.2 Detection of rMVA-glycoproteins by live immunofluorescent assay

Live IF assay was performed for cellular localisation of the expressed rMVA-glycoproteins. This was achieved by detecting the corresponding rMVA-glycoprotein fusion-TAGs using FITC-conjugated specific monoclonal antibodies (see 2.15.2). The BHK cells for IF staining were seeded onto coverslips and infected with rMVA-gB, rMVA-gH/gL, and rMVA-gH/gL/Ov7 (5 PFU/ cell) (see 2.15.1). Initially, the cells were washed twice with PBS containing 0.2 % BSA, 0.2 % Sodium Azide (Sigma, UK). Then, the appropriate amount of the relevant primary antibodies supplied from (Sigma, UK); anti-Flag (1:1000) and anti-V5 (1:2000) were both of mouse-origin while the anti-HA (1:2000) of rat origin were diluted in PBSAA (PBS, 0.2 % BSA, 0.2 % sodium azide) and then added. The slides were incubated for 10 min at RT. Cells were then washed very carefully 3 x with PBSAA before adding the relevant secondary (anti-rat, 1:500, anti-mouse, 1:200) labelled with FITC (Sigma, UK). Finally, cells were washed gently 3 x with PBSAA, fixed with 4 % paraformaldehyde in PBS and treated with anti-fade DAPI stain and examined as in section (2.8).

The staining with anti-FLAG-FITC conjugate showed that rMVA-gB in BHK infected cells was detected predominantly at the cell surface. This cell-surface localisation was also found in the mixed inoculation with rMVA-(gH/gL) when gL protein detected by anti-HA-FITC conjugate (Figure 5-8).

The gH protein in rMVA-(gH/gL) and rMVA-(gH/gL/Ov7) detected using anti-FLAG-FITC conjugate appeared also on the cell surface (Figure 5-

9). In the latter mixed inoculation, gL and Ov7 were also detected by anti-HA-FITC and anti-V5-FITC conjugates respectively (Figure 5-10).

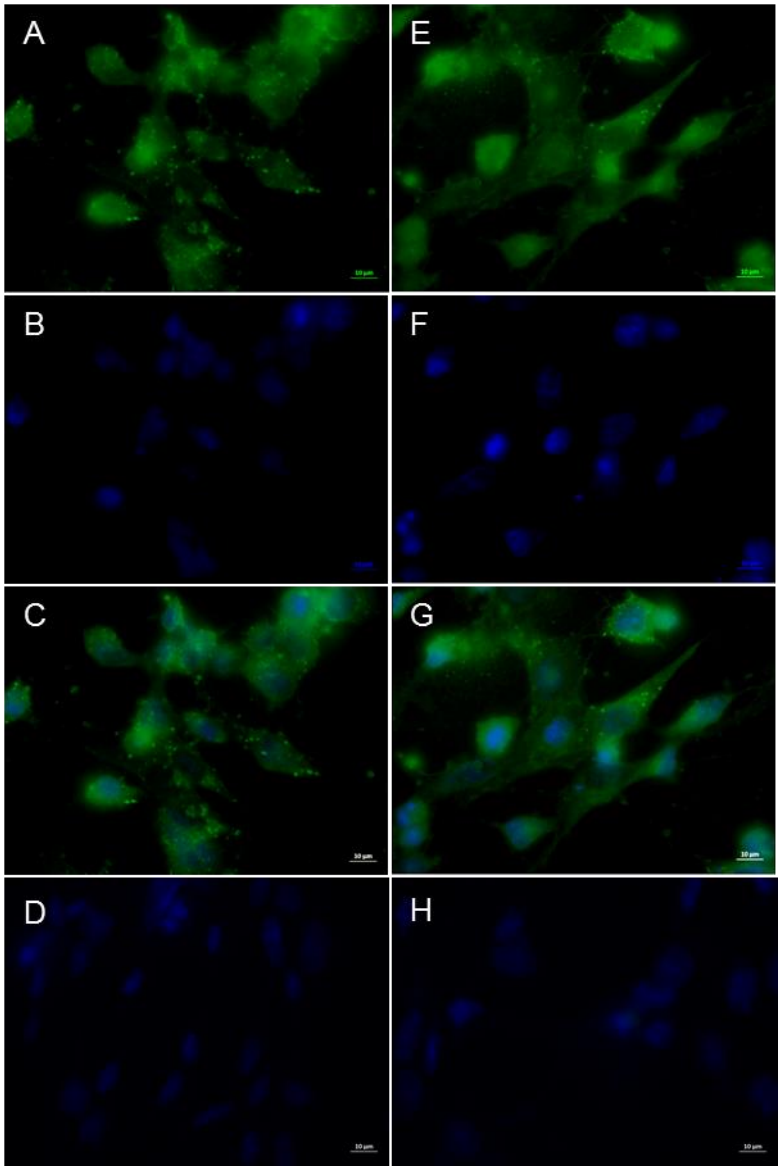

Figure 5-8. Live Indirect immunofluorescent analysis of the produced rMVA-glycoproteins (MVA-gB, MVA-gH/gL) in BHK cells inoculated with 5 PFU/ cell and incubated for 24 h. (A) Is rMVA-gB subjected to anti-FLAG primary antibody then anti-mouse secondary antibody labelled with FITC stain. (B) Is similar cells stained with DAPI. (C) Is merged image of A and B. (D) Is the negative control in which non-infected cells were stained. (E) Is detection of gL in the mix of rMVA-(gH/gL) stained with anti-HA primary antibody then anti-rat secondary antibody labelled with FITC. (F) Is similar cells stained with DAPI. (G) Is merged of E and F. (H) Is the negative control in which non-infected cells were stained.

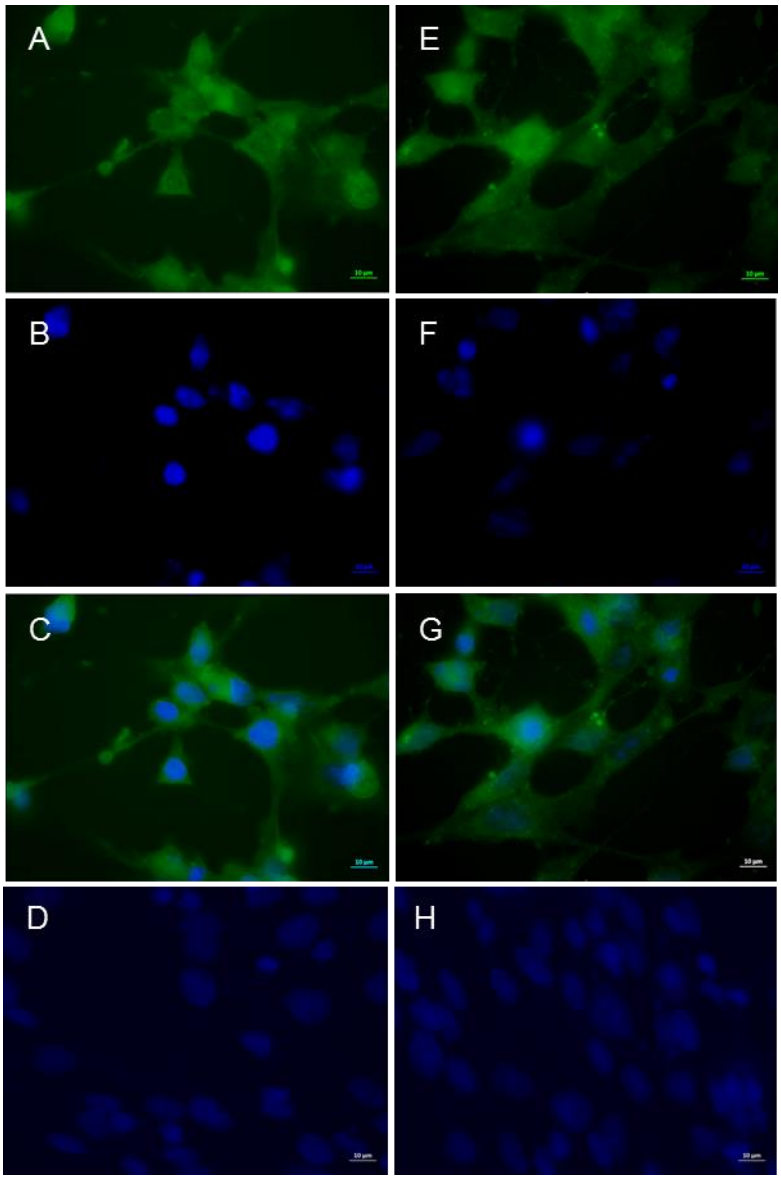

Figure 5-9. Live Indirect immunofluorescent analysis of the produced rMVA-glycoproteins (MVA-gH/gL, MVA-gH/gL/Ov7) in BHK cells inoculated with 5 PFU/ cell and incubated for 24 h. (A) Is detection of gH in the mix of rMVA-(gH/gL) stained with anti-FLAG primary antibody then anti-mouse secondary antibody labelled with FITC stain. (B) Is similar cells stained with DAPI. (C) Is merged image of A and B. (D) Is the negative control in which non-infected cells were stained. (E) Is detection of gH in the mix of rMVA-(gH/gL/Ov7) stained with anti-FLAG primary antibody then anti-mouse secondary antibody labelled with FITC. (F) Is similar cells stained with DAPI. (G) Is merged image of E and F. (H) Is the control negative in which non-infected cells were stained.

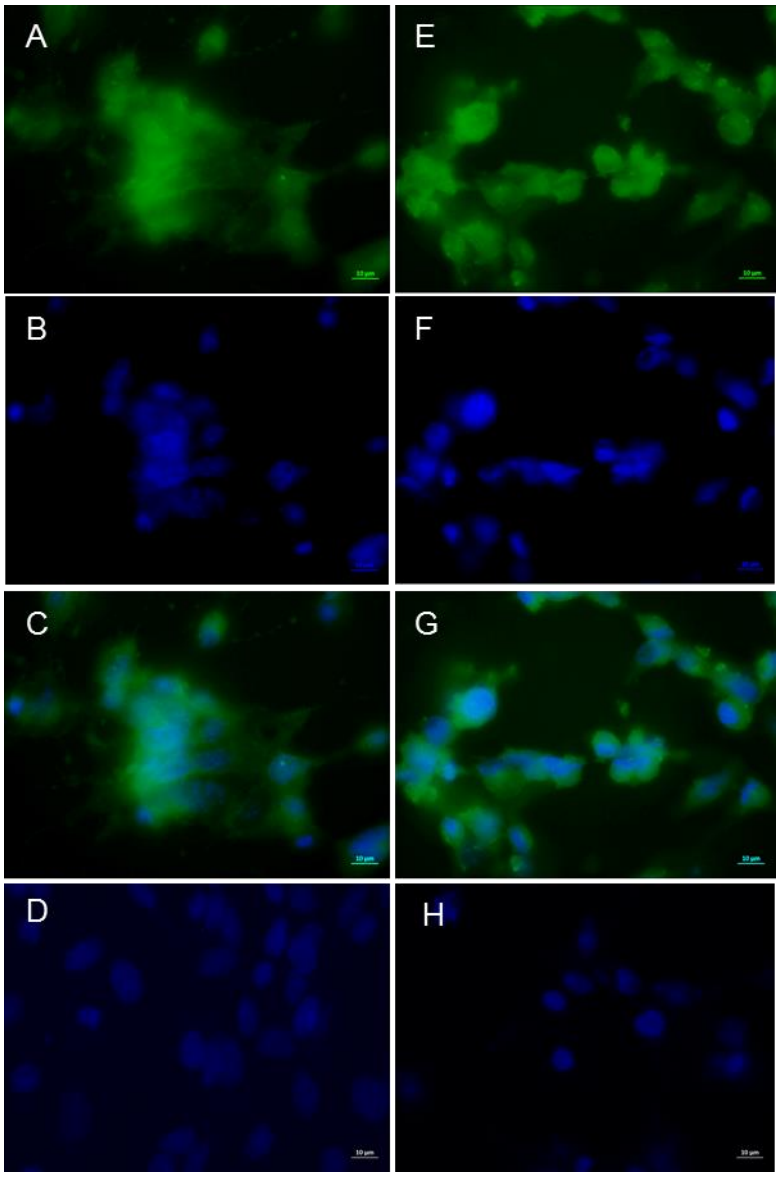

Figure 5-10. Live Indirect immunofluorescent analysis of the produced rMVA-glycoproteins (MVA-gH/gL/Ov7) in BHK cells inoculated with 5 PFU/ cell and incubated for 24 h. (A) Is detection of gL in the mix of rMVA-(gH/gL/Ov7) stained with anti-HA primary antibody then anti-rat secondary antibody labelled with FITC stain. (B) Is similar cells stained with DAPI. (C) Is merged image of A and B. (D) Is the negative control in which non-infected cells were stained. (E) Is detection of Ov7 in the mix of rMVA-(gH/gL/Ov7) stained with anti-V5 primary antibody then anti-mouse secondary antibody labelled with FITC. (F) Is similar cells stained with DAPI. (G) Is merged image of E and F. (H) Is the negative control in which non-infected cells were stained.

5.2.3 Characterisation of the expressed rMVA-glycoproteins

The combined expression of gH/gL and gH/gL/Ov7 were characterised for interaction in complexes by immunoprecipitation and de-glycosylation. Whole cell lysates were extracted following combined viral inoculation and then subjected to immunoprecipitation by Mab M2 affinity gel that pulls down FLAG tagged proteins. The immuno-precipitated gH-FLAG protein from these complexes was probed with anti-FLAG-HRP conjugate (PA1-984B) to detect gH protein. In rMVA-(gH/gL), a 94 kDa band corresponding to this protein was detected, indicating that gH/gL was expressed as heterodimer. The detected gL protein (originated from gH/gL/Ov7) revealed exactly the same size at 28 kDa (Figure 5-11C). However, the expressed Ov7-V5 was not detected following the pulldown lysate using anti-V5-HRP conjugate. This indicates that Ov7 was not part of a heterotrimer in gH/gL complex.

The gH protein from the gH/gL and gH/gL/Ov7 complexes was cleaved by using N-glycosidase F enzyme (PNGase F). The cleaved gH protein was detected at 74 kDa, indicating that this protein is processed post-transitionally inside BHK cells by addition of 21 kDa of glycan groups (Figure 5-11).

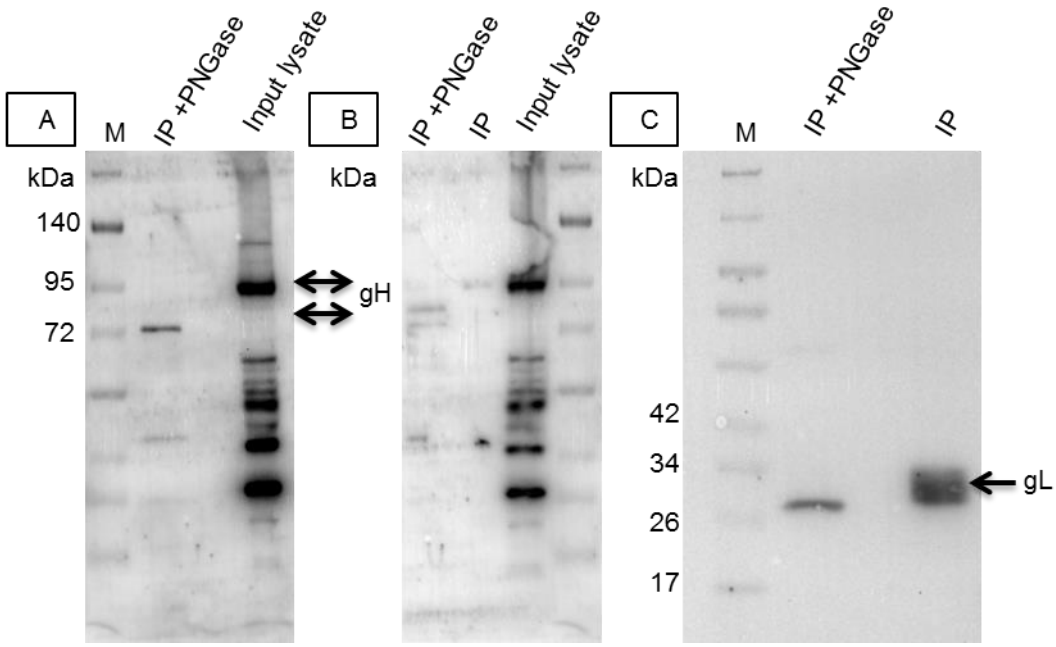

Figure 5-11. Western immunoblotting analysis (12 %) image shows immunoprecipitation of the expressed rMVA-glycoproteins with M2 beads carrying an anti-flag mAb followed by PNGase treatment for the de-glycosylation. (A-B) are detection of the de-glycosylated gH using anti-FLAG-HRP conjugate after co-infection of BHK cell line with rMVA-(gH/gL) and rMVA-(gH/gL/Ov7) respectively. (C) Is detection of gL using anti-HA-HRP conjugate after co-infection of BHK cell line with rMVA-(gH/gL/Ov7).

5.3 Discussion

5.3.1 Construction of MVA recombinants

In this study, MVA virus was modified to encode OvHV-2 glycoproteins (gB, gH, gL, and Ov7) as the question was how MCF genes can be exploited for vaccine purpose. The obtained results also showed that among these glycoproteins, gH and gL were produced inside BHK cells as a heterodimer whereas Ov7 did not interact with this complex as heterotrimer. This was revealed by immunoprecipitation and de-glycosylation (described in section 5.2.3 and Figure 5-11).

The plasmid MVA-cassettes were designed to contain GFP-TAG-glycoproteins. Homologous sequences to vaccinia virus were also included in both sides for efficient recombination. One direct repeat was located in one side followed by vaccinia P11 promoter to drive GFP expression and prevent its sequence deletion during rMVA passages. This also provides a visible marker of the rMVA during the purification or expression of these glycoproteins. These constructs were designed similar to (Wyatt *et al.*, 2008) (see 2.15.2).

All the inserted targeted genes (ORF8, ORF22, ORF47, and Ov7) were expressed under the control of the modified H5 promoter (mH5). This native sequence promoter is potentially important for the genetic stability of rMVAs even after multiple passages (Wang *et al.*, 2010). These genes were also fused and tagged with FLAG protein in gB and gH, HA in gL, and V5 in Ov7. This was necessary for selection, purification, and characterisation of the produced glycoproteins.

Recently, numerous applications have been developed using MVA for many vaccine candidates such as HIV (Wyatt *et al.*, 2008), ebola virus (Domi *et al.*, 2018), and influenza virus (Barbieri *et al.*, 2018). This because of high clinical safety as well as inducing a potential immune response arising from stimulation of dendritic cells and activation of T cell responses (Verheust *et al.*, 2012).

5.3.2 MVA-glycoproteins production

The expression of the rMVA-glycoproteins was evaluated by infecting BHK cells with the generated rMVAs (either individually or by mixing gH/gL or gH/gL/Ov7). The cell lysates were then probed by western immunoblotting and IF assays. As expected, all the recombinant MVAs demonstrated stable modification. This was observed from expression of the GFP protein after three cycles of cells inoculation and during the passages (Figure 5-5). These glycoproteins are fundamental in OvHV-2 biology (AlHajri *et al.*, 2017; Cunha *et al.*, 2015; Russell *et al.*, 2009). Therefore, gB, gH, gL, and Ov7 glycoproteins were expressed in the MVA system as logical candidates that could provide potential immune responses to prevent MCF in susceptible hosts.

In most herpesviruses, there are orthologous glycoproteins that have an important role in host- cell entry (Eisenberg *et al.*, 2012). Although the biological role of OvHV-2-glycoproteins is poorly characterised, numerous studies have shown that gB, gH, and gL are important vaccine candidates to prevent MCF in rabbit model (Cunha *et al.*, 2015). Additionally, as in most herpesviruses, these glycoproteins are likely responsible for variable cell-

tropism (Sathiyamoorthy *et al.*, 2017). This could explain our observation of OvHV-2 targeting numerous cell types (as showed in 4.2.3), including epithelial and endothelial cells as well as leukocytes.

Recently, it has been shown that gB, gH, gL, and Ov8 of OvHV-2 are essential to induce fusion of the membrane of the infected cells (AlHajri *et al.*, 2017). This pathway was also shown in KSHV by glycoproteins gB, gH, and gL (Pertel, 2002). As well as in herpes simplex virus infection via recruitment of gB, gH,gL, and gD (Spear *et al.*, 2006).

The predicted molecular weight of these glycoproteins using bioinformatics software analysis (https://www.bioinformatics.org/sms/prot_mw.html), revealed that gB protein (GenBank accession no. ABB22229) of 863 amino acids should have a molecular mass of 97.5 kDa. A similar molecular weight was predicted for gH (GenBank accession no. ABB22240) (750 amino acids; 85.68 kDa) while the predicted size of gL (GenBank accession no. YP_438170) (151 amino acids) was predicted to be 50.1 kDa molecular weight. Finally, Ov7 (GenBank accession no. YP_438174) (121 amino acids), was predicted to be 14.25 kDa.

Western immunoblotting analysis showed that rMVA-gB with the FLAG tag was detected as three bands at molecular weights of 130, 92, and 55 kDa (Figure 5-6). These bands most likely corresponded to whole gB length but could reflect cleavage of the recombinant protein and indicating a post translational processing inside BHK cells. Additionally, there was a smaller size band at 52 kDa detected in the supernatant of the same infected cells. This was possibly breakdown product.

These results are comparable to those previously generated by (Cunha *et al.*, 2015) as two bands at (102 and 90) kDa were detected from transfected Chinese Hamster Ovary (CHO) cells.

The OvHV-2-gB (encoded by ORF8), is homologous to that in AlHV-1 (Hart *et al.*, 2007). A1HV-1gB was previously shown to have a similar molecular weight, approximately ~100 kDa with additional two bands (50 and 20) kDa that resulted from cleavage process (Dry *et al.*, 2016).

The glycoprotein B in both viruses share antigenic and serological cross-reactivity (Dry *et al.*, 2016). Therefore, here, production of OvHV-2-gB could be valuable candidate to neutralise both viral species.

In rMVA-gH, two bands were detected at 95 and 57 kDa. This was slightly higher than expected, but these bands possibly represent the cleavage of the whole protein. However, rMVA-gL expression, a lower molecular weight at 33 kDa than expected was observed representing gL protein that fused with HA tag (Figure 5-6). The expressed rMVA-Ov7 protein was detected at 30 kDa which was higher than expected. These results agreed with those obtained by (Cunha *et al.*, 2015) as a single band corresponding to OvHV-2-gH protein was observed at 90 kDa whereas the gL protein was not detected from the individual transfection until was co-expressed with gH protein which revealed the size of gL protein as 35 kDa. The gB was expressed at 102 kDa with a smaller band representing the cleavage protein. Combining of gB and gH/gL vaccines were found protective to all the challenged animal while using of either gB or gH/gL revealed prevention of MCF at 83 % (Cunha *et al.*, 2015). In numerous herpesviruses,

gL is required for processing (folding and transport) of gH, and both are expressed as a heterodimer (Eisenberg *et al.*, 2012; Peng *et al.*, 2010).

5.3.3 Glycoproteins interaction

The obtained data demonstrated expression of the rMVA-glycoproteins as a monomer. The aim was to examine whether OvHV-2-glycoproteins as in other herpesviruses could possibly co-exist as multimers when combined. These glycoproteins were initially co-infected and analysed by western immunoblotting and IF assays then further studied by IP analysis. The results revealed that gH/gL were expressed as heterodimer but not heterotrimer with Ov7 (see 5.2.3). The interaction of gB with gH/gL complex as a trimer for the entry stoichiometry has not been studied here due to lack of required techniques.

Finding of gH/gL complex has been shown in many herpesviruses such as EBV (Hutt-Fletcher, 2007). However, this complex could co-exist as trimer or even pentamer when combined with other glycoproteins. These glycoprotein combinations are known as entry complexes, which allow the virus to infect wide range of cell types. For instance, EBV is able to target epithelial cells via gH/gL complex but it can also invade B cells through gHgL/gp42 complex (Sathiyamoorthy *et al.*, 2017).

The combined expression was analysed by western immunoblotting and IF assays. The results exhibited detection of the expressed protein at the expected molecular weights and predominantly localised within the cell membrane (see 5.2.2.1, 5.2.2.2, and 5.2.3).

For further confirmation, these complexes were additionally analysed by immunoprecipitation using M2 affinity gel pulldown and then western immunoblotting. Anti-FLAG antibody was found to be eluted from M2 gel. Therefore, alternative Mabs (PA1-984B, Sigma) was used to detect the epitope-FLAG-tag sequence (DYKDDDDK) (see 5.2.3) and (Figure 5-11).

The expected molecular weight of gH at 94 kDa was detected from the eluted gH/gL combinations confirming the heterodimer expression of gH/gL. This finding reflects that of (Cunha *et al.*, 2015) who also found that both glycoproteins are expressed as a complex and the presence of gL is important for efficient processing and transporting of gH inside cells. However, in this study, Ov7 was not detected from the gH/gL/Ov7 mixture, indicating that Ov7 was not part of a heterotrimer with gH/gL (Figure 5-11). This could explain our previous finding of how OvHV-2 infects the epithelial, endothelial cells and leukocytes. The gH/gL complex was shown to be important for entry into these cells in other herpesviruses (human herpesviruses) (Sathiyamoorthy *et al.*, 2017). However, further analysis should be conducted to define which glycoprotein components enable OvHV-2 to infect B cells or other cell types.

5.3.4 De-glycosylation of gH/gL complex

The eluted gH/gL complex was de-glycosylated using N-glycosidase F enzyme (PNGase F). The deglycosylated gH protein was detected at 74 kDa, indicating the post-transitional modification of gH protein inside BHK cells. This occurs by addition of 21 kDa of glycan group (Figure 5-11). Addition of

this glycan group could better define the activity of the gH/gL complex and virus biology.

Prediction of the N-glycosylation sites within the gH protein (GenBank accession no. ABB22240) using bioinformatics analysis software (https://www.hiv.lanl.gov/cgi-bin/GLYCOSITE/glycosite_main.cgi) revealed 9 N-glycosylation sites (Figure 5-12).

```
        10         20         30         40         50         60         70         80         90        100
         |          |          |          |          |          |          |          |          |          |
MPSVPHAPLL WISHNPPAPG GLLLCFFTIL SLWNNATGQR RPTISEHYAP SSALVITLDG TFYSAQFRWE DIEKIIRRPI IQDLWKWSKT EQPLKTTYET
       110        120        130        140        150        160        170        180        190        200
         |          |          |          |          |          |          |          |          |          |
YKDIYKFPGK SIKVQDGHQI GMCQPYNTTR QVDFWKGITT ATVGDRYDGD LSIFKNQLRQ ELFFYISNVF PPSHETHGAF YPVRRHMIYT SLSLDNGRYQ
       210        220        230        240        250        260        270        280        290        300
         |          |          |          |          |          |          |          |          |          |
LAGVATINYV SLVVAYQVSS VVTHSATIIF GDRLKLPSMR GSVSRGEISL VYNNAEELLL LTSNTDYAYF SQNLFPKNWS EVFTMITTNT ADQLAVLLQT
       310        320        330        340        350        360        370        380        390        400
         |          |          |          |          |          |          |          |          |          |
SMVDMARKDR CRNIHINSQF LTTYLAVLSL YYKIGMEMRY RSDFPVSLQC ILPKLYETDV CLDMVHRCYV DQYTRGFVTN GLHRLSAAIL AATPFYPEQG
       410        420        430        440        450        460        470        480        490        500
         |          |          |          |          |          |          |          |          |          |
LEVTPDWFLQ NLYYVDSKSD LQDKGMHGIS LILMDIYSRY VERFTLTNDD RKALFMVYNA LRGRKPTNST MSDKYTSLTY CYTTSMCSAA ELAWGIEFWG
       510        520        530        540        550        560        570        580        590        600
         |          |          |          |          |          |          |          |          |          |
HESTHNVYHS FSPCFMSLRF DYSLERLNIE GSHDVNLTKS QLSNGVSAMY SLLRSDTSNW AIQYLPIKTC ITDASKVKMI VPFVDTTFVI AVGAAAKGVT
       610        620        630        640        650        660        670        680        690        700
         |          |          |          |          |          |          |          |          |          |
YDVSETFLKS KMVVTVVNNS NCNEAYVSRE ALKIPVVYNM SYPKLTCQLC DSAVVSYDEY DGLQTLVYIS NHRVQQDVFA PDSLFFDFDN MHTHYLLLMN
       710        720        730        740        750        760        770        780        790        800
         |          |          |          |          |          |          |          |          |          |
NGTLFEIRGL YTNRAMNAII FILFAVAAIA GSFIVYKIVM YNLSKKESLK
```

Figure 5-12. Predicted amino acids sequence of gH protein. Red letters indicate the N-glycosylation sites.

5.4 Conclusions

The technology for producing recombinant MVA expressing foreign proteins is available with a well-known safety profile. The produced rMVA-glycoproteins (gB, gH/gL) are likely to be valuable in OvHV-2 biology. These candidates were found as an effective candidates to prevent MCF in rabbits (Cunha *et al.*, 2015). These glycoproteins have a fundamental role in the cell

entry. Using of multiple glycoproteins perhaps provide potential antigenic response. The expressed oLANA protein could also be used as another vaccine candidate against the latent infection. These vaccine candidates could help in MCF prevention in the highly susceptible hosts.

6. Chapter six: General discussion and recommendations

6.1 Triggering of MCF

MCF pathogenesis is poorly defined. The lack of a permissive cell line to propagate OvHV-2 has hindered the understanding of MCF. Nevertheless, numerous studies have been conducted by employing PCR and since this technique has improved, much has been discovered about MCF (Russell *et al.*, 2009). Recently, our laboratory has shown that OvHV-2 can be harboured in cattle without obvious signs of MCF. Therefore, it has been suggested that other factors or herpesviruses could be involved in triggering MCF (Amin, 2015).

The main hypothesis of this study was whether the presence of alternative γ-herpesviruses could interact with OvHV-2 in causing MCF or co-infections with OvHV-2 could induce MCF. Possibly, other factor involved to induce MCF apart from MCF-viruses.

Therefore, the first aim was to investigate the γ-herpesviruses in both asymptomatic and diseased hosts by using two PCR formats as qualitative and quantitative approaches: PAN-herpesvirus consensus and Real time PCR. The second aim was to describe which cell type supports latent OvHV-

2 infection in sheep, cattle without MCF, and cattle with MCF using an anti-oLANA PAb. The third aim was to produce OvHV-2-glycoproteins in MVA as logical vaccine candidates.

The results showed for the first time that (see Table 3-2), although the related ovine herpesvirus 1 is an endemic commensal of cattle, it may afford cross-protection from infection with OvHV-2 and development of MCF. It has been suggested that most animal herpesviruses have co-evolved with their corresponding hosts and these have some phylogenetic evolutionary relationship (Li *et al.*, 2005c). This phylogenetic relationship could provide some antigenic similarity. This was shown in three cervid herpesviruses including: Elk herpesvirus (ElkHV), cervid herpesvirus-1 (CerHV-1), and rangiferine herpesvirus (RanHV) as the encoding genes for gB, gC, and gD exhibited a closely relationship (Deregt *et al.*, 2005). More evidence was also found in a neutralisation study conducted by (Taus *et al.*, 2015) that revealed two potential antigenic members (AIHV-I/ AIHV-2) and (OvHV-2/CpHV-2) in which the neutralising antibody cross reactivity is only found within MCF virus subgroup but not between subgroups. This is likely based on the phylogenetic relationship between macaviruses that clustered into two groups, MCF and non-MCF virus group as stated in section (3.2.1). However, no clear sequence distinction within the MCF virus clade has so far been made, mainly due to a lack of extensive sequence data for the antigens of most MCF viruses.

Glycoprotein B is a highly conserved immunogenic protein. Alignment analysis of the genes that encode for this protein in OvHV-2, OvHV-1, and

BoHV-6 showed significant similarity as depicted in (Figure 3-5). This might explain the antigenic relationship between these viruses. However, these viruses discriminated genetically into MCF and non-MCF members as showed in (Figure 3-2).

It was assumed that MCF was possibly triggered by infiltrating cytotoxic T lymphocytes (Russell *et al.*, 2009). It has been hypothesised that detection of oLANA in asymptomatic and diseased animals will further define this hypothesis. The obtained data showed for the first time that, in cattle without MCF, oLANA is present likely in macrophages and B cells in lymph nodes. In cattle with MCF, virus can be seen predominantly in activated T cells, but more importantly endothelial cells as possibly induced by local inflammation that resulted from cytokines and chemokines. There are infected endothelial cells in the rete mirabile associated with vasculitis. The rete mirabile is critical for the supply of blood to the brains of ungulates, possibly explaining the sudden death in MCF.

The obtained data also showed that oLANA was detected in a wide range of cell types. This may explain the way by which OvHV-2 can survive. As in most herpesviruses, the virus genome can persists as an episome (Kelley-Clarke *et al.*, 2009). If the viral load increases for some reason, it may target T lymphocytes and inducing MCF. Finally, vascular endothelial cells also seem to be supportive for OVHV-2 infection. This might allow a continuous OvHV-2-influx into the blood circulation which consequently could lead to triggering MCF.

Use of this toolkit will be useful in the diagnosis of latent OvHV-2 infection in different hosts.

6.2 OvHV-2 vaccine candidates

OvHV-2 has not yet been propagated *in vitro* efficiently. Therefore, no effective vaccine has been produced (Russell *et al.*, 2009). In this study, OvHV-2 glycoproteins (gB, gH, gL, and Ov7) were produced in vaccinia virus as a vaccine candidate. These glycoproteins have been shown as efficient antigens (Cunha *et al.*, 2015). As in most herpesviruses, these glycoproteins are important in virus biology especially in binding to the host cell and fusion (Adler *et al.*, 2017). Conducting challenge immunisation trial will be useful to evaluate these vaccine candidates. Vaccine trials in small animals (rabbits or hamster) could be helpful because both are susceptible to MCF. We propose to vaccinate these animals with the recombinant MVAs then challenge with OvHV-2. However, the intravenous challenge with infected cells that carry OvHV-2 does not mimic a natural challenge and this route of infection may not be protected against by any vaccine, but OvHV-2 cannot be propagated therefore challenge virus is not available except when collected from sheep nasal secretions. In addition, cost and time limitations should be considered.

Appendix: Detailed results of repeatability (intra-assay variation) and reproducibility (inter-assay variation) precisions of the developed q-PCR assays.

Table 1. OvHV-1 standard plasmid shows the repeatability (intra-assay variation) and reproducibility (inter-assay variation) precisions.

Copy number	Intra-assay variation															Inter-assay variation			
	Experiment																		
	I			II			III			IV			V						
	Mean *cq*	SD	CV (%)	Mean *cq*	SD	CV (%)	Mean *cq*	SD	CV (%)	Mean *cq*	SD	CV (%)	Mean *cq*	SD	CV (%)	Mean of Means (cq)	SD	CV (%)	SE ±
2×10^7	20.46	0.07	0.3	19.91	0.94	4.72	20.2	0.07	0.3	20.81	0.19	0.91	20.46	0.07	0.34	20.36	0.33	1.62	0.15
2×10^6	22.26	0.72	3.23	21.62	0.29	1.34	22.64	0.15	0.66	19.16	0.41	2.13	22.26	0.72	3.23	21.5	1.4	6.51	0.62
2×10^5	23.87	0.41	1.71	24.89	0.38	1.52	24.27	0.33	1.35	23.29	0.22	0.94	23.87	0.41	1.71	24.03	0.59	2.45	0.26
2×10^4	25.66	0.18	0.7	27.17	0.12	0.4	26.4	0.11	0.41	25.42	0.06	0.23	25.66	0.18	0.7	26.06	0.72	2.76	0.32
2×10^3	28.74	0.16	0.5	31.84	0.13	0.4	29.93	0.01	0.03	28.89	0.36	1.24	28.74	0.16	0.55	29.62	1.33	4.49	0.59
2×10^2	32.93	0.14	0.4	35.47	0.27	0.76	33.76	0.39	1.15	32.68	0.31	0.94	32.93	0.14	0.42	33.55	1.14	3.39	0.51
2×10^1	35.71	0.21	0.58	38.4	1.66	4.32	38.69	1.15	2.9	35.41	1.12	3.16	35.71	0.21	0.58	36.78	1.61	4.37	0.72
2×10^0	39.71	0.33	0.83	39.01	0.98	2.51	37.2	1.88	5.05	37.24	1.67	4.48	39.71	0.33	0.83	38.5	1.26	3.27	0.56

Abbreviation: *cq*: quantification cycle; SD: standard deviation; CV (%): coefficient of variation percentage; SE: standard error.

Table 2. BoHV-6 standard plasmid shows the repeatability (intra-assay variation) and reproducibility (inter-assay variation) precisions.

Copy number	Intra-assay variation															Inter-assay variation			
	Experiment																		
	I			II			III			IV			V						
	Mean *cq*	SD	CV (%)	Mean *cq*	SD	CV (%)	Mean *cq*	SD	CV (%)	Mean *cq*	SD	CV (%)	Mean *cq*	SD	CV (%)	Mean of Means (cq)	SD	CV (%)	SE ±
2×10^7	18.55	0.37	1.99	18.85	0.45	2.38	18.32	0.62	3.38	18.13	0.42	2.31	17.84	0.22	1.23	18.33	0.38	2.07	0.17
2×10^6	20.76	0.04	0.19	19.95	0.57	2.85	19.37	0.61	3.14	19.37	0.6	3.09	19.68	0.16	0.8	19.82	0.57	2.87	0.25
2×10^5	22.09	0.1	0.004	21.91	0.24	1.09	21.34	0.37	1.73	20.9	0.36	1.72	20.68	0.55	2.65	21.38	0.61	1.26	0.27
2×10^4	25.98	0.04	0.15	25.8	0.23	0.89	25.35	0.24	0.94	24.6	0.12	0.48	24.84	0.03	0.12	25.31	0.59	2.33	0.26
2×10^3	29.44	0.28	0.95	29.35	0.31	1.05	28.88	0.27	0.93	27.69	0.14	0.5	28.03	0.09	0.32	28.67	0.78	2.72	0.35
2×10^2	31.86	0.33	1.03	33.41	0.48	1.43	32.9	0.49	1.48	30.71	0.89	2.89	31.2	0.44	1.41	32.01	1.13	3.53	0.5
2×10^1	36.67	0.33	0.89	36.92	0.52	1.4	36.32	0.55	1.51	32.19	1.71	5.31	35.27	0.41	1.16	35.47	1.94	5.46	0.86
2×10^0	39.16	0.09	0.22	38.49	1.34	3.48	37.33	0.89	2.38	38.22	1.19	3.11	39.17	0.36	0.9	38.47	0.76	1.97	0.34

Abbreviation: cq: quantification cycle; SD: standard deviation; CV (%): coefficient of variation percentage; SE: standard error.

Table 3. OvHV-2 standard plasmid shows the repeatability (intra-assay variation) and reproducibility (inter-assay variation) precisions.

Copy number	Intra-assay variation															Inter-assay variation			
	Experiment																		
	I			II			III			IV			V						
	Mean *cq*	SD	CV (%)	Mean *cq*	SD	CV (%)	Mean *cq*	SD	CV (%)	Mean *cq*	SD	CV (%)	Mean *cq*	SD	CV (%)	Mean of Means (cq)	SD	CV (%)	SE ±
2×10^7	13.41	0.07	0.52	13.45	0.35	2.6	13.05	0.18	1.37	13.26	0.03	0.22	13.79	0.14	1.01	13.39	0.27	2.01	0.12
2×10^6	16.24	0.36	2.21	16.12	0.22	1.36	16.53	0.15	0.9	16.44	0.16	0.97	16.68	0.08	0.47	16.4	0.22	1.34	0.1
2×10^5	19.14	0.38	1.98	19.05	0.16	0.83	19.46	0.32	1.64	19.21	0.36	1.87	19.77	0.4	2.02	19.32	0.29	1.5	0.13
2×10^4	21.67	0.09	0.41	22.06	0	0	22.22	0.04	0.18	22.29	0.45	2.01	22.5	0.09	0.4	22.14	0.31	1.4	0.13
2×10^3	24.73	0.3	1.21	25.18	0.26	1.03	25.52	0.03	0.11	25.33	0.12	0.47	25.68	0.14	0.54	25.28	0.36	1.42	0.16
2×10^2	28.03	0.19	0.67	27.87	0.18	0.64	28.58	0.21	0.73	28.34	0.007	0.02	28.41	0.16	3.51	28.24	0.28	0.99	0.12
2×10^1	30.39	0.36	1.18	30.58	0.08	0.26	30.87	0.3	0.97	30.53	0.3	0.98	30.86	0.18	0.58	30.64	0.21	0.68	0.09
2×10^0	33.33	0.33	0.99	33.87	0.05	0.14	34.46	0.23	0.66	34.34	0.53	1.54	34.08	0.1	0.29	34.01	0.44	1.29	0.19

Abbreviation: cq: quantification cycle; SD: standard deviation; CV (%): coefficient of variation percentage; SE: standard error.

Table 4. Bison LHV standard plasmid shows the repeatability (intra-assay variation) and reproducibility (inter-assay variation) precisions.

Copy number	Intra-assay variation															Inter-assay variation			
	Experiment																		
	I			II			III			IV			V						
	Mean *cq*	SD	CV (%)	Mean *cq*	SD	CV (%)	Mean *cq*	SD	CV (%)	Mean *cq*	SD	CV (%)	Mean *cq*	SD	CV (%)	Mean of Means (cq)	SD	CV (%)	SE ±
2×10^7	13.82	0.04	0.28	13.37	0.27	2.01	13.63	0.12	0.88	13.37	0.01	0.07	13.76	0.31	2.25	13.59	0.21	1.54	0.9
2×10^6	16.65	0.02	0.12	16.68	0.09	0.53	16.22	0.007	0.04	17.06	0.09	0.52	16.87	0.09	0.53	16.69	0.31	1.85	0.13
2×10^5	19.51	0.35	1.79	19.87	0.02	0.1	19.66	0.04	0.2	19.78	0.18	0.91	19.89	0.08	0.4	19.74	0.15	0.75	0.07
2×10^4	22.64	0.16	0.7	22.28	0.05	0.22	22.84	0.33	1.44	23.2	0.38	1.63	23.19	0.18	0.77	22.83	0.38	1.66	0.17
2×10^3	25.93	0.16	0.61	25.58	0.29	1.13	25.72	0.17	0.66	25.86	0.35	1.35	25.73	0.13	0.5	25.76	0.13	0.5	0.06
2×10^2	28.81	0.3	1.04	28.14	0.8	2.84	28.37	0.33	1.16	28.4	0.17	0.59	28.75	0.2	0.69	28.49	0.28	0.98	0.12
2×10^1	32.05	0.11	0.34	31.23	0.54	1.72	31.69	0.36	1.13	30.73	0.55	1.78	31.59	0.06	0.18	31.45	0.5	1.58	0.22
2×10^0	34.27	0.57	1.66	35.6	0.26	0.73	35.52	0.41	1.15	36.6	0.14	0.38	36.98	0.01	0.02	35.79	1.05	2.93	0.47

Abbreviation: cq: quantification cycle; SD: standard deviation; CV (%): coefficient of variation percentage; SE: standard error.

Table 5. CpHV-2 standard plasmid shows the repeatability (intra-assay variation) and reproducibility (inter-assay variation) precisions.

Copy number	Intra-assay variation															Inter-assay variation			
	Experiment																		
	I			II			III			IV			V						
	Mean *cq*	SD	CV (%)	Mean *cq*	SD	CV (%)	Mean *cq*	SD	CV (%)	Mean *cq*	SD	CV (%)	Mean *cq*	SD	CV (%)	Mean of Means (cq)	SD	CV (%)	SE ±
2×10^7	10.52	0.21	1.99	10.61	0.03	0.28	10.59	0.5	4.72	10.18	0.15	1.47	10.54	0.43	4.07	10.48	0.17	1.32	0.07
2×10^6	14.02	0.02	0.14	14.37	0.33	2.29	14.26	0.08	0.56	14.76	0.007	0.04	14.26	0.08	0.56	14.33	0.27	1.88	0.12
2×10^5	17.59	0.12	0.68	17.25	0.32	1.85	17.53	0.36	2.05	17.58	0.29	1.64	17.53	0.36	2.05	17.49	0.14	0.8	0.06
2×10^4	20.57	0.35	1.7	21.22	0.27	1.27	20.58	0.04	0.19	20.64	0.29	1.4	20.58	0.04	0.19	20.71	0.28	1.35	0.12
2×10^3	23.91	0.17	0.71	24.69	0.12	0.48	24.29	0.32	1.31	24.47	0.61	2.49	23.29	0.32	1.37	24.13	0.54	2.23	0.24
2×10^2	27.57	0.47	1.7	27.91	0.09	0.32	27.81	0.09	0.32	27.44	0.16	0.58	27.81	0.09	0.32	27.7	0.19	0.68	0.08
2×10^1	30.22	0.41	1.35	30.28	0.12	0.39	30.03	0.16	0.53	30.77	0.64	2.07	30.03	0.16	0.53	30.26	0.3	0.99	0.13
2×10^0	10.52	0.21	1.99	10.61	0.03	0.28	10.59	0.5	4.72	10.18	0.15	1.47	10.54	0.43	4.07	10.48	0.17	1.32	0.07

Abbreviation: cq: quantification cycle; SD: standard deviation; CV (%): coefficient of variation percentage; SE: standard error.

References

Adler, B., Sattler, C. & Adler, H. (2017). Herpesviruses and Their Host Cells: A Successful Liaison. *Trends Microbiol* **25**, 229–241. Elsevier Ltd.

AlHajri, S. M., Cunha, C. W., Nicola, A. V, Aguilar, H. C., Li, H. & Taus, N. S. (2017). Ovine Herpesvirus 2 Glycoproteins B, H, and L Are Sufficient for, and Viral Glycoprotein Ov8 Can Enhance, Cell-Cell Membrane Fusion. *J Virol* **91**, e02454-16 (R. M. Sandri-Goldin, Ed.).

Amin. **(2015).** *Infection of the Ovine herpesvirus 2 in the Reservoir Host , Sheep , and the Susceptible Host , Cattle*. PhD thesis, University of Liverpool.

Anderson, I. E., Buxton, D., Campbell, I., Russell, G., Davis, W. C., Hamilton, M. J. & Haig, D. M. (2007). Immunohistochemical Study of Experimental Malignant Catarrhal Fever in Rabbits. *J Comp Pathol* **136**, 156–166.

Angelova, M., Ferris, M., Swan, K. F., McFerrin, H. E., Pridjian, G., Morris, C. A. & Sullivan, D. E. (2014). Kaposi's sarcoma-associated herpesvirus G-protein coupled receptor activates the canonical Wnt/β-catenin signaling pathway. *Virol J* **11**, 218.

Anziliero, D., Santos, C. M. B., Brum, M. C. S., Weiblen, R., Chowdhury, S. I. & Flores, E. F. (2011). A recombinant bovine herpesvirus 5 defective in thymidine kinase and glycoprotein E is immunogenic for calves and confers protection upon homologous challenge and BoHV-1 challenge. *Vet Microbiol* **154**, 14–22. Elsevier B.V.

Ballon, G., Akar, G. & Cesarman, E. (2015). Systemic Expression of Kaposi Sarcoma Herpesvirus (KSHV) Vflip in Endothelial Cells Leads to a Profound Proinflammatory Phenotype and Myeloid Lineage Remodeling In Vivo. *PLOS Pathog* **11**, e1004581 (D. P. Dittmer, Ed.).

Banks, M., Ibata, G., Murphy, A. M., Frossard, J. P., Crawshaw, T. R. & Twomey, D. F. (2008). Bovine lymphotropic herpesvirus and non-responsive post-partum metritis in dairy herds in the UK. *Vet J* **176**, 248–250.

Barahona, H. H., Melendez, L. V, King, N. W., Daniel, M. D., Fraser, C. E.

O. & Preville, A. C. (1973). Herpesvirus aotus Type 2: A New Viral Agent from Owl Monkeys (Aotus trioirgatus) **127**, 171–178.

Baranowski, E., Keil, G., Lyaku, J., Rijsewijk, F. A. M., Oirschot, J. T. Van, Pastoret, P. & Thiry, E. (1996). Structural and functional analysis of bovine herpesvirus 1 minor glycoproteins **53**, 91–101.

Barbieri, A., Panigada, M., Soprana, E., Di Mario, G., Gubinelli, F., Bernasconi, V., Recagni, M., Donatelli, I., Castrucci, M. R. & Siccardi, A. G. (2018). Strategies to obtain multiple recombinant modified vaccinia Ankara vectors. Applications to influenza vaccines. *J Virol Methods* **251**, 7–14. Elsevier.

Baron, M. D., Iqbal, M. & Nair, V. (2018). Recent advances in viral vectors in veterinary vaccinology. *Curr Opin Virol* **29**, 1–7. The Authors.

Bartlett, J. M. S. & Stirling, D. (2003). *PCR Protocols*. *Methods Mol Biol*. New Jersey: Humana Press.

Basu, C. (2015). *PCR Primer Design*. *Methods Mol Biol* (C. Basu, Ed.). New York, NY: Springer New York.

Bedelian, C., Nkedianye, D. & Herrero, M. (2007). Maasai perception of the impact and incidence of malignant catarrhal fever (MCF) in southern Kenya. *Prev Vet Med* **78**, 296–316.

Bhaskaran, N., Ghosh, S. K., Yu, X., Qin, S., Weinberg, A., Pandiyan, P. & Ye, F. (2017). Kaposi's sarcoma-associated herpesvirus infection promotes differentiation and polarization of monocytes into tumor-associated macrophages. *Cell Cycle* **16**, 1611–1621. Taylor & Francis.

Bialas, K. M. & Permar, S. R. (2016). The March towards a Vaccine for Congenital CMV: Rationale and Models. *PLOS Pathog* **12**, e1005355 (K. R. Spindler, Ed.).

Biassoni, R. & Raso, A. (2014). *Quantitative Real-Time PCR*. Methods in Molecular Biology (R. Biassoni & A. Raso, Eds.). New York, NY: Springer New York.

Bilge-Dağalp, S., Güngör, E., Demir, A., Pinar-Muz, D., Vilmaz, V., Oguzoglu, T. C., Ataseven, V. S. & Alkan, F. (2010). The investigation of the presence of bovine herpesvirus type 4 (BoHV-4) in cows with metritis in a dairy herd. *Ankara Üniversitasi Vet Fakültesi Derg* **57**, 87–

91.

Biswas, S., Bandyopadhyay, S., Dimri, U. & H. Patra, P. (2013). Bovine herpesvirus-1 (BHV-1) – a re-emerging concern in livestock: a revisit to its biology, epidemiology, diagnosis, and prophylaxis. *Vet Q* **33**, 68–81.

de Boer, M., Zheng, T., Buddle, B. & McDougall, S. (2014). Detection of bovine herpesvirus type 4 antibodies and bovine lymphotropic herpesvirus in New Zealand dairy cows. *N Z Vet J* **62**, 351–355. Taylor & Francis.

Borah, S., Verma, S. C. & Robertson, E. S. (2004). ORF73 of herpesvirus saimiri, a viral homolog of Kaposi's sarcoma-associated herpesvirus, modulates the two cellular tumor suppressor proteins p53 and pRb. *J Virol* **78**, 10336–47.

Bouvard, V., Baan, R., Straif, K., Grosse, Y., Secretan, B., Ghissassi, F. El, Benbrahim-Tallaa, L., Guha, N., Freeman, C. & other authors. (2009). A review of human carcinogens—Part B: biological agents. *Lancet Oncol* **10**, 321–322.

Britton, P. & Jones, C. (2014). Central nervous system herpesvirus infections. *Paediatr Child Heal (United Kingdom)* **24**, 248–254. Elsevier Ltd.

Browne, H., Baxter, V. & Minson, T. (1993). Analysis of protective immune responses to the glycoprotein H-glycoprotein L complex of herpes simplex virus type 1. *J Gen Virol* **74**, 2813–2817.

Brunson, J. L., Khoretonenko, M. V & Stokes, K. Y. (2016). Herpesviruses. In *Vasc Responses to Pathog*, pp. 123–136. Elsevier.

Buchwalow, I. B. & Böcker, W. (2010). *Immunohistochemistry: Basics and Methods*. *Media*. Berlin, Heidelberg: Springer Berlin Heidelberg.

Bustin, S. A., Benes, V., Garson, J. A., Hellemans, J., Huggett, J., Kubista, M., Mueller, R., Nolan, T., Pfaffl, M. W. & other authors. (2009). The MIQE Guidelines: Minimum Information for Publication of Quantitative Real-Time PCR Experiments. *Clin Chem* **55**, 611–622.

Cai, Q., Xiao, B., Si, H., Cervini, A., Gao, J., Lu, J., Upadhyay, S. K., Verma, S. C. & Robertson, E. S. (2012). Kaposi's sarcoma herpesvirus upregulates Aurora A expression to promote p53 phosphorylation and

ubiquitylation. *PLoS Pathog* **8**.

Camero, M., Bellacicco, A. L., Tarsitano, E., Decaro, N., Martella, V., Tempesta, M. & Buonavoglia, C. (2007). Intravaginal administration of an inactivated vaccine prevents lesions induced by caprine herpesvirus-1 in goats. *Vaccine* **25**, 1658–1661.

Camero, M., Larocca, V., Lovero, A., Losurdo, M., Cirone, F., Marinaro, M., Buonavoglia, C. & Tempesta, M. (2015). Caprine herpesvirus type 1 infection in goat: Not just a problem for females. *Small Rumin Res* **128**, 59–62. Elsevier B.V.

Campos, F. S., Franco, A. C., Hübner, S. O., Oliveira, M. T., Silva, A. D., Esteves, P. A., Roehe, P. M. & Rijsewijk, F. A. M. (2009). High prevalence of co-infections with bovine herpesvirus 1 and 5 found in cattle in southern Brazil. *Vet Microbiol* **139**, 67–73.

Campos, F. S., Dezen, D., Antunes, D. A., Santos, H. F., Arantes, T. S., Cenci, A., Gomes, F., Lima, F. E. S., Brito, W. M. E. D. & other authors. **(2011).** Efficacy of an inactivated, recombinant bovine herpesvirus type 5 (BoHV-5) vaccine. *Vet Microbiol* **148**, 18–26. Elsevier B.V.

Campos, F. S., Franco, A. C., Oliveira, M. T., Firpo, R., Strelczuk, G., Fontoura, F. E., Kulmann, M. I. R., Maidana, S., Romera, S. A. & other authors. **(2014).** Detection of bovine herpesvirus 2 and bovine herpesvirus 4 DNA in trigeminal ganglia of naturally infected cattle by polymerase chain reaction. *Vet Microbiol* **171**, 182–188.

Cardoso, T. C., Gomes, D. E., Ferrari, H. F., Silva-Frade, C., Rosa, A. C. G., Andrade, A. L. & Luvizotto, M. C. R. (2010). A novel in situ polymerase chain reaction hybridisation assay for the direct detection of bovine herpesvirus type 5 in formalin-fixed, paraffin-embedded tissues. *J Virol Methods* **163**, 509–512.

Cardoso, T. C., Silva-Frade, C., Táparo, C. V., Okamura, L. H. & Flores, E. F. (2013). Validation of a reference control for an SYBR-Green fluorescence assay-based real-time PCR for detection of bovine herpesvirus 5 in experimentally exposed bovine embryos. *Mol Cell Probes* **27**, 237–242. Elsevier Ltd.

Chastant-Maillard, S. (2015). Impact of bovine herpesvirus 4 (BoHV-4) on reproduction. *Transbound Emerg Dis* **62**, 245–251.

Chmielewicz, B., Goltz, M. & Ehlers, B. (2001). Detection and multigenic characterization of a novel gammaherpesvirus in goats. *Virus Res* **75**, 87–94.

Chmielewicz, B., Goltz, M., Lahrmann, K.-H. & Ehlers, B. (2003). Approaching virus safety in xenotransplantation: a search for unrecognized herpesviruses in pigs. *Xenotransplantation* **10**, 349–356.

Christensen, L. S., Madsen, K. G., Nylin, B. & Rønsholt, L. (1996). A contribution to the systematization of bovine herpesvirus 1 based on genomic mapping by restriction fragment pattern analysis. *Virus Res* **46**, 177–182.

Cobb, S. P., Banks, M., Russell, C. & Thorne, M. (2006). Bovine lymphotrophic herpesvirus in a UK dairy herd. *Vet Rec* **158**, 807–808.

Cohen, S., Au, S. & Panté, N. (2011). How viruses access the nucleus. *Biochim Biophys Acta - Mol Cell Res* **1813**, 1634–1645. Elsevier B.V.

Collins, J. K., Bruns, C., Vermedahl, T. L., Schiebel, A. L., Jessen, M. T., Schultheiss, P. C., Anderson, G. M., Dinsmore, R. P., Callan, R. J. & DeMartini, J. C. (2000). Malignant Catarrhal Fever: Polymerase Chain Reaction Survey for Ovine Herpesvirus 2 and Other Persistent Herpesvirus and Retrovirus Infections of Dairy Cattle and Bison. *J Vet Diagnostic Investig* **12**, 406–411.

Cook, C. G. & Splitter, G. A. (1988). Lytic Function of Bovine Lymphokine-Activated Killer Cells from a Normal and a Malignant Catarrhal Fever Virus-Infected Animal. *Vet Immunol Immunopathol* **19**, 105–118.

Costa, E. A., Vasconcelos, A. C., Bomfim, M. R. Q., Amorim, H. B., Lima, G. B. L., Coelho, F. M. & Resende, M. (2011). Neurological disorder in cattle associated with bovine herpesvirus 4. *Arq Bras Med Vet e Zootec* **63**, 828–835.

Cottingham, M. G. & Carroll, M. W. (2013). Recombinant MVA vaccines: dispelling the myths. *Vaccine* **31**, 4247–4251. Elsevier Ltd.

Cunha, C. W., Traul, D. L., Taus, N. S., Oaks, J. L., O'Toole, D., Davitt, C. M. & Li, H. (2008). Detection of ovine herpesvirus 2 major

capsid gene transcripts as an indicator of virus replication in shedding sheep and clinically affected animals. *Virus Res* **132**, 69–75.

Cunha, C. W., Otto, L., Taus, N. S., Knowles, D. P. & Li, H. (2009). Development of a multiplex real-time PCR for detection and differentiation of malignant catarrhal fever viruses in clinical samples. *J Clin Microbiol* **47**, 2586–2589.

Cunha, C. W., Gailbreath, K. L., O'Toole, D., Knowles, D. P., Schneider, D. a., White, S. N., Taus, N. S., Davies, C. J., Davis, W. C. & Li, H. (2012). Ovine herpesvirus 2 infection in American bison: virus and host dynamics in the development of sheep-associated malignant catarrhal fever. *Vet Microbiol* **159**, 307–319. Elsevier B.V.

Cunha, C. W., O'Toole, D., Taus, N. S., Knowles, D. P. & Li, H. (2013). Are rabbits a suitable model to study sheep-associated malignant catarrhal fever in susceptible hosts? *Vet Microbiol* **163**, 358–363.

Cunha, C. W., Knowles, D. P., Taus, N. S., O'Toole, D., Nicola, A. V., Aguilar, H. C. & Li, H. (2015). Antibodies to ovine herpesvirus 2 glycoproteins decrease virus infectivity and prevent malignant catarrhal fever in rabbits. *Vet Microbiol* **175**, 349–355. Elsevier B.V.

Czopowicz, M., Kaba, J., Szalus-Jordanow, O., Nowicki, M., Witkowski, L. & Frymus, T. (2010). Serological evidence of lack of contact with caprine herpesvirus type 1 and bluetongue virus in goat population in Poland. *Pol J Vet Sci* **13**, 709–711.

Davis, C., Fischer, J., Ley, K. & Sarembock, I. J. (2003). The role of inflammation in vascular injury and repair. *J Thromb Haemost* **1**, 1699–1709.

Davison, A. J. (2010). Herpesvirus systematics. *Vet Microbiol* **143**, 52–69. Elsevier B.V.

De-Giuli, L., Magnino, S., Vigo, P. G., Labalestra, I. & Fabbi, M. (2002). Development of a polymerase chain reaction and restriction typing assay for the diagnosis of bovine herpesvirus 1, bovine herpesvirus 2, and bovine herpesvirus 4 infections. *J Vet Diagn Invest* **14**, 353–6.

Delhon, G., Moraes, M. P., Lu, Z., Afonso, C. L., Flores, E. F., Weiblen, R., Kutish, G. F. & Rock, D. L. (2003). Genome of bovine herpesvirus

5. *J Virol* **77**, 10339–10347.

Deng, H., Young, A. & Sun, R. (2000). Auto-activation of the rta gene of human herpesvirus-8 / Kaposi ' s sarcoma-associated herpesvirus. *J Gen Virol* 3043–3048.

Deregt, D., Gilbert, S. A., Campbell, I., Burton, K. M., Reid, H. W., Van Drunen Littel-Van Den Hurk, S., Penniket, C. & Baxi, M. K. (2005). Phylogeny and antigenic relationships of three cervid herpesviruses. *Virus Res* **114**, 140–148.

Dettwiler, M., Stahel, A., Krüger, S., Gerspach, C., Braun, U., Engels, M. & Hilbe, M. (2011). A possible case of caprine-associated malignant catarrhal fever in a domestic water buffalo (Bubalus bubalis) in Switzerland. *BMC Vet Res* **7**, 78.

Dhanasekaran, S., Doherty, T. M. & Kenneth, J. (2010). Comparison of different standards for real-time PCR-based absolute quantification. *J Immunol Methods* **354**, 34–39. Elsevier B.V.

Diallo, I. S., Corney, B. G. & Rodwell, B. J. (2011). Detection and differentiation of bovine herpesvirus 1 and 5 using a multiplex real-time polymerase chain reaction. *J Virol Methods* **175**, 46–52. Elsevier B.V.

Domi, A., Feldmann, F., Basu, R., McCurley, N., Shifflett, K., Emanuel, J., Hellerstein, M. S., Guirakhoo, F., Orlandi, C. & other authors. **(2018).** A Single Dose of Modified Vaccinia Ankara expressing Ebola Virus Like Particles Protects Nonhuman Primates from Lethal Ebola Virus Challenge. *Sci Rep* **8**, 864.

Donofrio, G., Flammini, C. F., Scatozza, F. & Cavirani, S. (2000). Detection of bovine herpesvirus 4 (BoHV-4) DNA in the cell fraction of milk of dairy cattle with history of BoHV-4 infection. *J Clin Microbiol* **38**, 4668–4671.

Donofrio, G. & Van Santen, V. L. (2001). A bovine macrophage cell line supports bovine herpesvirus-4 persistent infection. *J Gen Virol* **82**, 1181–1185.

Donofrio, G., Cavirani, S., Simone, T. & Van Santen, V. L. (2002). Potential of bovine herpesvirus 4 as a gene delivery vector. *J Virol Methods* **101**, 49–61.

Donofrio, G., Herath, S., Sartori, C., Cavirani, S., Flammini, C. F. & Sheldon, I. M. (2007). Bovine herpesvirus 4 is tropic for bovine endometrial cells and modulates endocrine function. *Reproduction* **134**, 183–197.

van Drunen Littel-van den Hurk, S. (2006). Rationale and perspectives on the success of vaccination against bovine herpesvirus-1. *Vet Microbiol* **113**, 275–82.

Dry, I., Todd, H., Deane, D., Percival, A., Mclean, K., Inglis, N. F., Manson, E. D. T., Haig, D. M., Nayuni, S. & other authors. **(2016).** Alcelaphine herpesvirus 1 glycoprotein B: recombinant expression and antibody recognition. *Arch Virol* **161**, 613–619.

Dubuisson, J., Bublot, M., Wellemans, G., Pastoret, P. P. & Thiry, E. (1991). Bovine herpesvirus 4 isolates: a comparison of three major glycoproteins. *Vet Microbiol* **29**, 251–259.

Dummer, L. A., Araujo, I. L., Campos, F. S., da Rosa, M. C., Finger, P. F., de Oliveira, P. D., Conceição, F. R., Fischer, G., Roehe, P. M. & Leite, F. P. L. (2016). Development of an Indirect ELISA for Serological Diagnosis of Bovine herpesvirus 5. *PLoS One* **11**, e0149134.

Egyed, L., Kluge, J. P. & Bartha, A. (1997). Histological studies of bovine herpesvirus type 4 infection in non-ruminant species. *Vet Microbiol* **57**, 283–289.

Egyed, L. (1998). Replication of bovine herpesvirus type 4 in human cells in vitro. *J Clin Microbiol* **36**, 2109–2111.

Ehlers, B., Goltz, M., Ejercito, M. P., Dasika, G. K. & Letchworth, G. J. (1999a). Bovine herpesvirus type 2 is closely related to the primate alphaherpesviruses. *Virus Genes* **19**, 197–203.

Ehlers, B., Borchers, K., Grund, C., Fro¨lich, K., Ludwig, H. & Buhk, H.-J. (1999b). Detection of New DNA Polymerase Genes of Known and Potentially Novel Herpesviruses by PCR with Degenerate and Deoxyinosine-Substituted Primers. *Virus Genes* **18**, 211–220.

Ehlers, B., Küchler, J., Yasmum, N., Dural, G., Voigt, S., Schmidt-Chanasit, J., Jäkel, T., Matuschka, F.-R., Richter, D. & other authors. **(2007).** Identification of novel rodent herpesviruses, including the first

gammaherpesvirus of Mus musculus. *J Virol* **81**, 8091–8100.

Eisenberg, R. J., Atanasiu, D., Cairns, T. M., Gallagher, J. R., Krummenacher, C. & Cohen, G. H. (2012). Herpes Virus Fusion and Entry: A Story with Many Characters. *Viruses* **4**, 800–832.

Elia, G., Tarsitano, E., Camero, M., Bellacicco, A. L., Buonavoglia, D., Campolo, M., Decaro, N., Thiry, J. & Tempesta, M. (2008). Development of a real-time PCR for the detection and quantitation of caprine herpesvirus 1 in goats. *J Virol Methods* **148**, 155–160.

Engels, M. & Ackermann, M. (1996). Pathogenesis of ruminant herpesvirus infections. *Vet Microbiol* **53**, 3–15.

Engels, M., Palatini, M., Metzler, A. E., Probst, U., Kihm, U. & Ackermann, M. (1992). Interactions of bovine and caprine herpesviruses with the natural and the foreign hosts. *Vet Microbiol* **33**, 69–78.

Epp, T., Waldner, C. & Woodbury, M. (2016). An observational study of mortality on bison farms in Saskatchewan with special emphasis on malignant catarrhal fever. *Can Vet J* **57**, 37–45.

Fabian, K., Makrai, L., Sachse, K., Szeredi, L. & Egyed, L. (2008). An investigation of the aetiological role of bovine herpesvirus 4 in bovine endometritis. *Vet J* **177**, 289–292.

Fan, Q., Yao, L., Ding, M., Wang, D.-J., Chen, H.-C. & Liu, Z.-F. (2012). Development of latex agglutination test for rapid detection of antibodies against Bovine herpesvirus 1 and Bovine herpesvirus 5 in cattle. *J Vet diagnostic Investig* **24**, 1162–5.

Favier, P. A., Marin, M. S., Morán, P. E., Odeón, A. C., Verna, A. E. & Pérez, S. E. (2014). Latency of bovine herpesvirus type 5 (BoHV-5) in tonsils and peripheral blood leukocytes. *Vet J* **202**, 134–40. Elsevier Ltd.

Fernández-Aguilar, X., Esperón, F., Cabezón, O., Velarde, R., Mentaberre, G., Delicado, V., Muñoz, M. J., Serrano, E., Lavín, S. & López-Olvera, J. R. (2016). Identification of a gammaherpesvirus belonging to the malignant catarrhal fever group of viruses in Pyrenean chamois (Rupicapra p. pyrenaica). *Arch Virol* **161**, 3249–3253.

Ferrer-Miralles, N., Saccardo, P., Corchero, J. L., Xu, Z. & García-

Fruitós, E. (2015). General Introduction: Recombinant Protein Production and Purification of Insoluble Proteins. In Methods in Molecular Biology, pp. 1–24. Edited by E. García-Fruitós. New York, NY: Springer New York.

Flano, E., Husain, S. M., Sample, J. T., Woodland, D. L. & Blackman, M. a. **(2000).** Latent Murine -Herpesvirus Infection Is Established in Activated B Cells, Dendritic Cells, and Macrophages. *J Immunol* **165**, 1074–1081.

Florek, N. W., Kamlangdee, A., Mutschler, J. P., Kingstad-Bakke, B., Schultz-Darken, N., Broman, K. W., Osorio, J. E. & Friedrich, T. C. (2017). A modified vaccinia Ankara vaccine vector expressing a mosaic H5 hemagglutinin reduces viral shedding in rhesus macaques. *PLoS One* **12**, e0181738 (S. Pöhlmann, Ed.).

Forrester, A. J., Sullivan, V., Simmons, A., Blacklaws, B. A., Smith, G. L., Nash, A. A. & Minson, A. C. (1991). Induction of protective immunity with antibody to herpes simplex virus type 1 glycoprotein H (gH) and analysis of the immune response to gH expressed in recombinant vaccinia virus. *J Gen Virol* **72**, 369–375.

Franceschi, V., Capocefalo, A., Jacca, S., Rosamilia, A., Cavirani, S., Xu, F., Qiao, W. & Donofrio, G. (2015). BoHV-4 immediate early 1 gene is a dispensable gene and its product is not a bone marrow stromal cell antigen 2 counteracting factor. *BMC Vet Res* **11**, 224. BMC Veterinary Research.

Fraser, S. J., Nettleton, P. F., Dutia, B. M., Haig, D. M. & Russell, G. C. (2006). Development of an enzyme-linked immunosorbent assay for the detection of antibodies against malignant catarrhal fever viruses in cattle serum. *Vet Microbiol* **116**, 21–28.

Fulton, R. W., d'Offay, J. M., Dubovi, E. J. & Eberle, R. (2016). Bovine herpesvirus-1: Genetic diversity of field strains from cattle with respiratory disease, genital, fetal disease and systemic neonatal disease and their relationship to vaccine strains. *Virus Res* **223**, 115–121. Elsevier B.V.

Gagnon, C. A., Allam, O., Drolet, R. & Tremblay, D. (2008). Cross-Canada

Disease Report Rapport des maladies diagnostiquées au Canada. *Can Vet J* **49**, 2006–2008.

Gailbreath, K. L., O'Toole, D., Taus, N. S., Knowles, D. P., Oaks, J. L. & Li, H. (2010). Experimental nebulization of American bison (Bison bison) with low doses of ovine herpesvirus 2 from sheep nasal secretions. *Vet Microbiol* **143**, 389–393. Elsevier B.V.

García-Arriaza, J., Nájera, J. L., Gómez, C. E., Sorzano, C. O. S. & Esteban, M. (2010). Immunogenic Profiling in Mice of a HIV/AIDS Vaccine Candidate (MVA-B) Expressing Four HIV-1 Antigens and Potentiation by Specific Gene Deletions. *PLoS One* **5**, e12395 (M. Lesniak, Ed.).

Garigliany, M.-M., Bayrou, C., Cassart, D., Jolly, S. & Desmecht, D. (2013). Bovine lymphotropic herpesvirus detected in Belgium. *Vet Rec* **172**, 535.2-536.

Gatesy, J., Amato, G., Vrba, E., Schaller, G. & DeSalle, R. (1997). A cladistic analysis of mitochondrial ribosomal DNA from the Bovidae. *Mol Phylogenet Evol* **7**, 303–319.

Gaudy, J., Willoughby, K., Lamm, C., Karavanis, E. & Logue, D. N. (2012). Possible natural MCF-like disease in a domestic lamb in Scotland. *Vet Rec* **171**, 563.1-563.

Gilbert, S. C. (2013). Clinical development of Modified Vaccinia virus Ankara vaccines. *Vaccine* **31**, 4241–4246. Elsevier Ltd.

Gillet, L., Frederico, B. & Stevenson, P. G. (2015). Host entry by gamma-herpesviruses — lessons from animal viruses? *Curr Opin Virol* **15**, 34–40. Elsevier B.V.

Godornes, C., Leader, B. T., Molini, B. J., Centurion-Lara, A. & Lukehart, S. A. (2007). Quantitation of rabbit cytokine mRNA by real-time RT-PCR. *Cytokine* **38**, 1–7.

Griffin, B. D., Verweij, M. C. & Wiertz, E. J. H. J. (2010). Herpesviruses and immunity: The art of evasion. *Vet Microbiol* **143**, 89–100. Elsevier B.V.

Haig, D. M., Grant, D., Deane, D., Campbell, I., Thomson, J., Jepson, C., Buxton, D. & Russell, G. C. (2008). An immunisation strategy for the protection of cattle against alcelaphine herpesvirus-1-induced malignant

catarrhal fever. *Vaccine* **26**, 4461–4468.

Hart, J., Ackermann, M., Jayawardane, G., Russell, G., Haig, D. M., Reid, H. & Stewart, J. P. (2007). Complete sequence and analysis of the ovine herpesvirus 2 genome. *J Gen Virol* **88**, 28–39.

He, Z., Liu, Y., Liang, D., Wang, Z., Robertson, E. S. & Lan, K. (2010). Cellular corepressor TLE2 inhibits replication-and-transcription-activator-mediated transactivation and lytic reactivation of Kaposi's sarcoma-associated herpesvirus. *J Virol* **84**, 2047–62.

Headley, S. A., Pimentel, L. A., Oliveira, V. H. S., Toma, H. S., Alfieri, A. F., Carvalho, A. M., dos Santos, M. D. & Alfieri, A. A. (2015). Transplacental Transmission of Ovine Herpesvirus 2 in Cattle with Sheep-associated Malignant Catarrhal Fever. *J Comp Pathol* **153**, 206–211. Elsevier Ltd.

Holliman, A. (2005). Differential diagnosis of diseases causing oral lesions in cattle. *In Pract* **27**, 2–13.

Hong, Y.-K., Foreman, K., Shin, J. W., Hirakawa, S., Curry, C. L., Sage, D. R., Libermann, T., Dezube, B. J., Fingeroth, J. D. & Detmar, M. (2004). Lymphatic reprogramming of blood vascular endothelium by Kaposi sarcoma–associated herpesvirus. *Nat Genet* **36**, 683–685.

Hughes, D. J., Kipar, A., Sample, J. T. & Stewart, J. P. (2010). Pathogenesis of a model gammaherpesvirus in a natural host. *J Virol* **84**, 3949–3961.

Hussell, T., Bell, T. J. & Fujimori, T. (2014). *Macrophages: Biology and Role in the Pathology of Diseases*. *Macrophages Biol Role Pathol Dis* (S. K. Biswas & A. Mantovani, Eds.). New York, NY: Springer New York.

Hutt-Fletcher, L. M. (2007). Epstein-Barr Virus Entry. *J Virol* **81**, 7825–7832.

Imai, K., Ishihara, R., Jayawardane, G. W., Nishimori, K. & Nishimori, T. (2002). Development of a shuttle polymerase chain reaction for the detection of bovine herpesvirus 2. *J Vet Med Sci* **64**, 953–6.

Imai, K., Ishihara, R. & Nishimori, T. (2005). First demonstration of bovine herpesvirus 2 infection among cattle by neutralization test in Japan. *J Vet Med Sci* **67**, 317–20.

Iman, M. B. (2012). Isolation of bovine herpesvirus-2 (BHV-2) from a case of

pseudo-lumpy skin disease in Egypt. *J Am Sci* **8**, 122–127.

Jacca, S., Rolih, V., Quaglino, E., Franceschi, V., Tebaldi, G., Bolli, E., Rosamilia, A., Ottonello, S., Cavallo, F. & Donofrio, G. (2016). Bovine herpesvirus 4-based vector delivering a hybrid rat/human HER-2 oncoantigen efficiently protects mice from autochthonous Her-2 + mammary cancer. *Oncoimmunology* **5**, e1082705.

Jacobsen, B., Thies, K., von Altrock, A., Förster, C., König, M. & Baumgärtner, W. (2007). Malignant catarrhal fever-like lesions associated with ovine herpesvirus-2 infection in three goats. *Vet Microbiol* **124**, 353–357.

Jayawardane, G., Russell, G. C., Thomson, J., Deane, D., Cox, H., Gatherer, D., Ackermann, M., Haig, D. M. & Stewart, J. P. (2008). A captured viral interleukin 10 gene with cellular exon structure. *J Gen Virol* **89**, 2447–2455.

Jha, H., Banerjee, S. & Robertson, E. (2016). The Role of Gammaherpesviruses in Cancer Pathogenesis. *Pathogens* **5**, 18.

Jia, J., Delhon, G., Tulman, E. R., Diel, D. G., Osorio, F. a., Wen, X., Kutish, G. F. & Rock, D. L. (2014). Novel gammaherpesvirus functions encoded by bovine herpesvirus 6 (bovine lymphotropic virus). *J Gen Virol* **95**, 1790–1798.

Jin, L., Löhr, C. V., Vanarsdall, A. L., Baker, R. J., Moerdyk-Schauwecker, M., Levine, C., Gerlach, R. F., Cohen, S. A., Alvarado, D. E. & Rohrmann, G. F. (2008). Characterization of a novel alphaherpesvirus associated with fatal infections of domestic rabbits. *Virology* **378**, 13–20.

Jones, C., Geiser, V., Henderson, G., Jiang, Y., Meyer, F., Perez, S. & Zhang, Y. (2006). Functional analysis of bovine herpesvirus 1 (BHV-1) genes expressed during latency. *Vet Microbiol* **113**, 199–210.

Jones, C. & Chowdhury, S. (2007). A review of the biology of bovine herpesvirus type 1 (BHV-1), its role as a cofactor in the bovine respiratory disease complex and development of improved vaccines. *Anim Heal Res Rev* **8**, 187–205.

Jones, C., da Silva, L. F. & Sinani, D. (2011). Regulation of the latency-

reactivation cycle by products encoded by the bovine herpesvirus 1 (BHV-1) latency-related gene. *J Neurovirol* **17**, 535–45.

Jorge, S. & Dellagostin, O. A. (2017). The development of veterinary vaccines: a review of traditional methods and modern biotechnology approaches. *Biotechnol Res Innov* **1**, 6–13. Sociedade Brasileira de Biotecnologia.

Kálmán, D. & Egyed, L. (2005). PCR detection of bovine herpesviruses from nonbovine ruminants in Hungary. *J Wildl Dis* **41**, 482–488.

Kautto, A. H., Alenius, S., Mossing, T., Becher, P., Belák, S. & Larska, M. (2012). Pestivirus and alphaherpesvirus infections in Swedish reindeer (Rangifer tarandus tarandus L.). *Vet Microbiol* **156**, 64–71.

Keel, M. K., Patterson, J. G., Noon, T. H., Bradley, G. a & Collins, J. K. (2003). Caprine herpesvirus-2 in association with naturally occurring malignant catarrhal fever in captive sika deer (Cervus nippon). *J Vet Diagn Invest* **15**, 179–83.

Kelley-Clarke, B., Ballestas, M. E., Komatsu, T. & Kaye, K. M. (2007). Kaposi's sarcoma herpesvirus C-terminal LANA concentrates at pericentromeric and peri-telomeric regions of a subset of mitotic chromosomes. *Virology* **357**, 149–157.

Kelley-Clarke, B., De Leon-Vazquez, E., Slain, K., Barbera, A. J. & Kaye, K. M. (2009). Role of Kaposi's sarcoma-associated herpesvirus C-terminal LANA chromosome binding in episome persistence. *J Virol* **83**, 4326–4337.

Kelly, L. A., Mezulis, S., Yates, C., Wass, M. & Sternberg, M. (2015). The Phyre2 web portal for protein modelling, prediction, and analysis. *Nat Protoc* **10**, 845–858. Nature Publishing Group.

Keuser, V., Gogev, S., Schynts, F. & Thiry, E. (2002). Demonstration of generalized infection with caprine herpesvirus 1 diagnosed in an aborted caprine fetus by PCR. *Vet Res Commun* **26**, 221–226.

Keuser, V., Schynts, F., Georgin, J. & Thiry, E. (2004a). Isolation of caprine herpesvirus type in Spain. *Vet Rec* **154**, 395–399.

Keuser, V., Schynts, F., Detry, B., Robert, B., Vanderplasschen, A., Pastoret, P., Thiry, E. & Collard, A. (2004b). Improved Antigenic

Methods for Differential Diagnosis of Bovine , Caprine , and Cervine Alphaherpesviruses Related to Bovine Herpesvirus 1. *J Clin Microbiol* **42**, 1228–1235.

Kim, O., Li, H. & Crawford, T. B. (2003). Demonstration of sheep-associated malignant catarrhal fever virions in sheep nasal secretions. *Virus Res* **98**, 117–122.

Kimura, H. (2018). *Human Herpesviruses*. Advances in Experimental Medicine and Biology (Y. Kawaguchi, Y. Mori & H. Kimura, Eds.). Singapore: Springer Singapore.

Kleiboeker, S. B., Miller, M. A., Schommer, S. K., Ramos-Vara, J. A., Boucher, M. & Turnquist, S. E. (2002). Detection and multigenic characterization of a herpesvirus associated with malignant catarrhal fever in white-tailed deer (Odocoileus virginianus) from Missouri. *J Clin Microbiol* **40**, 1311–8.

Kopácek, J., Rejholcová, O., Koptidesová, D., Ciampor, F., Rijsewijk, F. M., Reid, H. W., Pastorek, J. & Zelník, V. (2000). Characterization of RKZ isolate of ovine herpesvirus 1. *Acta Virol* **44**, 335–42.

Kreijtz, J. H. C. M., Gilbert, S. C. & Sutter, G. (2013). Poxvirus vectors. *Vaccine* **31**, 4217–4219.

Kremer, M., Volz, A., Kreijtz, J. H. C. M., Fux, R., Lehmann, M. H. & Sutter, G. (2012). Easy and Efficient Protocols for Working with Recombinant Vaccinia Virus MVA. In *Life Sci*, pp. 59–92.

Kubiś, P., Materniak, M. & Kuźmak, J. (2013). Comparison of nested PCR and qPCR for the detection and quantitation of BoHV6 DNA. *J Virol Methods* **194**, 94–101.

Kumar, S., Stecher, G. & Tamura, K. (2016). MEGA7: Molecular Evolutionary Genetics Analysis version 7.0 for bigger datasets. *Mol Biol Evol* **33**, msw054.

Kurien, B. & Scofield, R. (2015). *Western Blotting*. *Methods*, Methods in Molecular Biology (B. T. Kurien & R. H. Scofield, Eds.). New York, NY: Springer New York.

Kwun, H. J., da Silva, S. R., Qin, H., Ferris, R. L., Tan, R., Chang, Y. & Moore, P. S. (2011). The central repeat domain 1 of Kaposi's sarcoma-

associated herpesvirus (KSHV) latency associated-nuclear antigen 1 (LANA1) prevents cis MHC class I peptide presentation. *Virology* **412**, 357–365. Elsevier Inc.

Lan, K., Kuppers, D. A., Verma, S. C. & Robertson, E. S. (2004). Kaposi's Sarcoma-Associated Herpesvirus-Encoded Latency-Associated Nuclear Antigen Inhibits Lytic Replication by Targeting Rta: a Potential Mechanism for Virus-Mediated Control of Latency. *J Virol* **78**, 6585–6594.

Lankester, F., Russell, G. C., Lugelo, A., Ndabigaye, A., Mnyambwa, N., Keyyu, J., Kazwala, R., Grant, D., Percival, A. & other authors. **(2016).** A field vaccine trial in Tanzania demonstrates partial protection against malignant catarrhal fever in cattle. *Vaccine* **34**, 831–838. Elsevier Ltd.

Lankester, F., Lugelo, A., Mnyambwa, N., Ndabigaye, A., Keyyu, J., Kazwala, R., Grant, D. M., Relf, V., Haig, D. M. & other authors. **(2015).** Alcelaphine herpesvirus-1 (malignant catarrhal fever virus) in wildebeest placenta: Genetic variation of ORF50 and A9.5 alleles. *PLoS One* **10**, 1–14.

Li, H., Shen, D. T., Knowles, D. P., Gorham, J. R. & Crawford, T. B. (1994). Competitive inhibition enzyme-linked immunosorbent assay for antibody in sheep and other ruminants to a conserved epitope of malignant catarrhal fever virus. *J Clin Microbiol* **32**, 1674–1679.

Li, H., Keller, J., Knowles, D. P. & Crawford, T. B. (2001a). Recognition of another member of the malignant catarrhal fever virus group: An endemic gammaherpesvirus in domestic goats. *J Gen Virol* **82**, 227–232.

Li, H., Dyer, N., Keller, J. & Crawford, T. B. (2000). Newly recognized herpesvirus causing malignant catarrhal fever in white-tailed deer (Odocoileus virginianus). *J Clin Microbiol* **38**, 1313–1318.

Li, H., Shen, D. T., Toole, D. O. & Knowles, D. P. (1995). Investigation of sheep-associated malignant catarrhal fever virus infection in ruminants by PCR and competitive inhibition enzyme-linked immunosorbent assay . Investigation of Sheep-Associated Malignant Catarrhal Fever Virus Infection in Ruminants by PCR. *J Clin Microbiol* **33**, 2048–2053.

Li, H., Hua, Y., Snowder, G. & Crawford, T. B. (2001b). Levels of ovine herpesvirus 2 DNA in nasal secretions and blood of sheep: Implications for transmission. *Vet Microbiol* **79**, 301–310.

Li, H., Gailbreath, K., Bender, L. C., West, K., Keller, J. & Crawford, T. B. (2003). Evidence of Three New Members of Malignant Catarrhal Fever Virus Group in Muskox (Ovibos moschatus), Nubian ibex (Capra nubiana), and Gemsbok (Oryx gazella). *J Wildl Dis* **39**, 875–880.

Li, H., Taus, N. S., Lewis, G. S., Kim, O., Traul, D. L. & Crawford, T. B. (2004). Shedding of ovine herpesvirus 2 in sheep nasal secretions: The predominant mode for transmission. *J Clin Microbiol* **42**, 5558–5564.

Li, H., Keller, J., Knowles, D. P., Taus, N. S., Oaks, J. L. & Crawford, T. B. (2005a). Transmission of caprine herpesvirus 2 in domestic goats. *Vet Microbiol* **107**, 23–29.

Li, H., O'Toole, D., Kim, O., Oaks, J. L. & Crawford, T. B. (2005b). Malignant catarrhal fever-like disease in sheep after intranasal inoculation with ovine herpesvirus-2. *J Vet Diagn Invest* **17**, 171–175.

Li, H., Gailbreath, K., Flach, E. J., Taus, N. S., Cooley, J., Keller, J., Russell, G. C., Knowles, D. P., Haig, D. M. & other authors. **(2005c).** A novel subgroup of rhadinoviruses in ruminants. *J Gen Virol* **86**, 3021–6.

Li, H., Karney, G., O'Toole, D. & Crawford, T. B. (2008a). Long distance spread of malignant catarrhal fever virus from feedlot lambs to ranch bison. *Can Vet J* **49**, 183–185.

Li, H., Cunha, C. W., Davies, C. J., Gailbreath, K. L., Knowles, D. P., Oaks, J. L. & Taus, N. S. (2008b). Ovine herpesvirus 2 replicates initially in the lung of experimentally infected sheep. *J Gen Virol* **89**, 1699–1708.

Li, H., Cunha, C. W., Gailbreath, K. L., O'Toole, D., White, S. N., Vanderplasschen, A., Dewals, B., Knowles, D. P. & Taus, N. S. (2011a). Characterization of ovine herpesvirus 2-induced malignant catarrhal fever in rabbits. *Vet Microbiol* **150**, 270–277.

Li, H., Cunha, C. W. & Taus, N. S. (2011b). Malignant catarrhal fever: Understanding molecular diagnostics in context of epidemiology. *Int J*

Mol Sci **12**, 6881–6893.

Li, H., Brooking, A., Cunha, C. W., Highland, M. a., O'Toole, D., Knowles, D. P. & Taus, N. S. (2012). Experimental induction of malignant catarrhal fever in pigs with ovine herpesvirus 2 by intranasal nebulization. *Vet Microbiol* **159**, 485–489. Elsevier B.V.

Li, H., Cunha, C. W., Abbitt, B., deMaar, T. W., Lenz, S. D., Hayes, J. R. & Taus, N. S. (2013). Goats are a potential reservoir for the herpesvirus (MCFV-WTD), causing malignant catarrhal fever in deer. *J Zoo Wildl Med* **44**, 484–486.

Liggitt, H. D., Mcchesney, A. E. & Demartini, J. C. (1980). Experimental transmission of Bovine Malignant Catarrhal Fever to a bison (Bison bison). *J Wildl Dis* **16**, 299–304.

Liggitt, H. D. & DeMartini, J. C. (1980). The pathomorphology of malignant catarrhal fever. II. Multisystemic epithelial lesions. *Vet Pathol* **17**, 73–83.

Lillehaug, A., Vikøren, T., Larsen, I.-L., Åkerstedt, J., Tharaldsen, J. & Handeland, K. (2003). Antibodies to ruminant alpha-herpesviruses and pestiviruses in Norwegian cervids. *J Wildl Dis* **39**, 779–786.

Liu, W., Dong, D., Yang, Z., Zou, D., Chen, Z., Yuan, J. & Huang, L. (2015). Polymerase Spiral Reaction (PSR): A novel isothermal nucleic acid amplification method. *Sci Rep* **5**, 12723. Nature Publishing Group.

Mahan, S. M., Sobecki, B., Johnson, J., Oien, N. L., Meinert, T. R., Verhelle, S., Mattern, S. J., Bowersock, T. L. & Leyh, R. D. (2016). Efficacy of intranasal vaccination with a multivalent vaccine containing temperature-sensitive modified-live bovine herpesvirus type 1 for protection of seronegative and seropositive calves against respiratory disease. *J Am Vet Med Assoc* **248**, 1280–1286.

Maidana, S. S., Morano, C. D., Cianfrini, D., Campos, F. S., Roehe, P. M., Siedler, B., De Stefano, G., Mauroy, A., Thiry, E. & Romera, S. A. (2013). Multiplex PCR followed by restriction length polymorphism analysis for the subtyping of bovine herpesvirus 5 isolates. *BMC Vet Res* **9**, 111.

Malla, J. A., Chakravarti, S., Gupta, V., Chander, V., Sharma, G. K., Qureshi, S., Mishra, A., Gupta, V. K. & Nandi, S. (2018). Novel

Polymerase Spiral Reaction (PSR) for rapid visual detection of Bovine Herpesvirus 1 genomic DNA from aborted bovine fetus and semen. *Gene* **644**, 107–112. Elsevier.

Marchisio, P. C. & Trusolino, L. (1999). Immunofluorescence of Cultured Cells. In *Adhes Protein Protoc*, pp. 85–92. New Jersey: Humana Press.

Mariggiò, G., Koch, S., Zhang, G., Weidner-Glunde, M., Rückert, J., Kati, S., Santag, S. & Schulz, T. F. (2017). Kaposi Sarcoma Herpesvirus (KSHV) Latency-Associated Nuclear Antigen (LANA) recruits components of the MRN (Mre11-Rad50-NBS1) repair complex to modulate an innate immune signaling pathway and viral latency. *PLoS Pathog* **13**, 1–19.

Marín-López, A. & Ortego, J. (2016). Generation of Recombinant Modified Vaccinia Virus Ankara Encoding VP2, NS1, and VP7 Proteins of Bluetongue Virus, pp. 137–150.

Marinaro, M., Bellacicco, A. L., Camero, M., Tarsitano, E., Tempesta, M., Cassone, A. & Buonavoglia, C. (2009). Caprine herpesvirus-1-specific IgG subclasses in naturally and experimentally infected goats. *Vet Microbiol* **138**, 266–272.

Martin, W. B., Angus, K. W., Robinson, G. W. & Scott, F. M. M. (1979). The herpesvirus of sheep pulmonary adenomatosis. *Comp Immun Microbiol infect Dis* **2**, 313–325.

McCoy, M. H., Montgomery, D. L., Bratanich, A. C., Cavender, J., Scharko, P. B. & Vickers, M. L. (2007). Serologic and reproductive findings after a herpesvirus-1 abortion storm in goats. *J Am Vet Med Assoc* **231**, 1236–1239.

McGregor, A., Choi, K. Y., Schachtele, S. & Lokensgard, J. (2013). Human Herpesviruses and Animal Models. In *Anim Model Study Hum Dis*, pp. 905–925. Elsevier.

Meier-Trummer, C. S., Tobler, K., Hilbe, M., Stewart, J. P., Hart, J., Campbell, I., Haig, D. M., Glauser, D. L., Ehrensperger, F. & Ackermann, M. (2009a). Ovine herpesvirus 2 structural proteins in epithelial cells and M-cells of the appendix in rabbits with malignant catarrhal fever. *Vet Microbiol* **137**, 235–242.

Meier-Trummer, C. S., Rehrauer, H., Franchini, M., Patrignani, A., Wagner, U. & Ackermann, M. (2009b). Malignant catarrhal fever of cattle is associated with low abundance of IL-2 transcript and a predominantly latent profile of ovine herpesvirus 2 gene expression. *PLoS One* **4**.

Meier-Trummer, C. S., Ryf, B. & Ackermann, M. (2010). Identification of peripheral blood mononuclear cells targeted by Ovine herpesvirus-2 in sheep. *Vet Microbiol* **141**, 199–207. Elsevier B.V.

Minarovits, J., Gonczol, E. & Valyi-Nagy, T. (2007). *Latency Strategies of Herpesviruses* (J. Minarovits, E. Gonczol & T. Valyi-Nagy, Eds.). Boston, MA: Springer US.

Mirangi, P. K. (1991). Attemps to immunize cattle against virulent African malignant catarrhal fever virus (alcelephine herpesvirus-1) with a herpesvirus isolated from American cattle. *Vet Microbiol* **28**, 129–139.

Modrow, S., Falke, D., Truyen, U. & Schätzl, H. (2013). *Molecular Virology*. *Mol Virol*. Berlin, Heidelberg: Springer Berlin Heidelberg.

Moss, B. (2013). Reflections on the early development of poxvirus vectors. *Vaccine* **31**, 4220–4222. Elsevier Ltd.

Münz, C. (2016). Epstein Barr virus — a tumor virus that needs cytotoxic lymphocytes to persist asymptomatically. *Curr Opin Virol* **20**, 34–39.

Muylkens, B., Thiry, J., Kirten, P., Schynts, F. & Thiry, E. (2007). Bovine herpesvirus 1 infection and infectious bovine rhinotracheitis. *Vet Res* **38**, 181–209.

Myster, F., Palmeira, L., Sorel, O., Bouillenne, F., DePauw, E., Schwartz-Cornil, I., Vanderplasschen, A. & Dewals, B. G. (2015). Viral Semaphorin Inhibits Dendritic Cell Phagocytosis and Migration but Is Not Essential for Gammaherpesvirus-Induced Lymphoproliferation in Malignant Catarrhal Fever. *J Virol* **89**, 3630–3647 (L. Hutt-Fletcher, Ed.).

Nelson, D. D., Davis, W. C., Brown, W. C., Li, H., O'Toole, D. & Oaks, J. L. (2010). CD8+/perforin+/WC1− γδ T cells, not CD8+ αβ T cells, infiltrate vasculitis lesions of American bison (Bison bison) with experimental sheep-associated malignant catarrhal fever. *Vet Immunol Immunopathol* **136**, 284–291.

Nelson, D. D., Taus, N. S., Schneider, D. a., Cunha, C. W., Davis, W. C., Brown, W. C., Li, H., O'Toole, D. & Oaks, J. L. (2013). Fibroblasts express OvHV-2 capsid protein in vasculitis lesions of American bison (Bison bison) with experimental sheep-associated malignant catarrhal fever. *Vet Microbiol* **166**, 486–492. Elsevier B.V.

das Neves, C. G., Mørk, T., Thiry, J., Godfroid, J., Rimstad, E., Thiry, E. & Tryland, M. (2009a). Cervid herpesvirus 2 experimentally reactivated in reindeer can produce generalized viremia and abortion. *Virus Res* **145**, 321–328.

das Neves, C. G., Rimstad, E. & Tryland, M. (2009b). Cervid herpesvirus 2 causes respiratory and fetal infections in semidomesticated reindeer. *J Clin Microbiol* **47**, 1309–1313.

das Neves, C. G., Mork, T., Godfroid, J., Sorensen, K. K., Breines, E., Hareide, E., Thiry, J., Rimstad, E., Thiry, E. & Tryland, M. (2009c). Experimental Infection of Reindeer with Cervid Herpesvirus 2. *Clin Vaccine Immunol* **16**, 1758–1765.

das Neves, C. G., Thiry, J., Skjerve, E., Yoccoz, N. G., Rimstad, E., Thiry, E. & Tryland, M. (2009d). Alphaherpesvirus infections in semidomesticated reindeer: A cross-sectional serological study. *Vet Microbiol* **139**, 262–269.

das Neves, C. G., Roth, S., Rimstad, E., Thiry, E. & Tryland, M. (2010). Cervid herpesvirus 2 infection in reindeer: A review. *Vet Microbiol* **143**, 70–80. Elsevier B.V.

das Neves, C. G., Roger, M., Yoccoz, N. G., Rimstad, E. & Tryland, M. (2009e). Evaluation of three commercial bovine ELISA kits for detection of antibodies against Alphaherpesviruses in reindeer (Rangifer tarandus tarandus). *Acta Vet Scand* **51**, 9.

Ng, T. F. F., Kondov, N. O., Deng, X., Van Eenennaam, A., Neibergs, H. L. & Delwart, E. (2015). A metagenomics and case-control study to identify viruses associated with bovine respiratory disease. *J Virol* **89**, 5340–9.

O'Toole, D., Li, H., Miller, D., Williams, W. R. & Crawford, T. B. (1997). Chronic and recovered cases of sheep-associated malignant catarrhal fever in cattle. *Vet Rec* **140**, 519–524.

O'Toole, D., Li, H., Sourk, C., Montgomery, D. L. & Crawford, T. B. (2002). Malignant catarrhal fever in a bison (Bison bison) feedlot, 1993-2000. *J Vet Diagn Invest* **14**, 183–93.

O'Toole, D., Taus, N. S., Montgomery, D. L., Oaks, J. L., Crawford, T. B. & Li, H. (2007). Intra-nasal inoculation of American bison (Bison bison) with ovine herpesvirus-2 (OvHV-2) reliably reproduces malignant catarrhal fever. *Vet Pathol* **44**, 655–662.

O 'Toole, D. & Li, H. (2014). The Pathology of Malignant Catarrhal Fever, With an Emphasis on Ovine Herpesvirus 2. *Vet Pathol* **51**, 437–452.

OIE. **(2004).** Malignant Catarrhal Fever. *Man Diagnostic Tests Vaccines Terr Anim fifth ed,France PP 570-579*.

de Oliveira, C. H. S., de Oliveira, F. G., Gasparini, M. R., Galinari, G. C. F., Lima, G. K., Fonseca, A. A., Barbosa, J. D., Barbosa-Stancioli, E. F., Leite, R. C. & dos Reis, J. K. P. (2015). Bovine herpesvirus 6 in buffaloes (Bubalus bulalis) from the Amazon region, Brazil. *Trop Anim Health Prod* **47**, 465–468.

Oliveira, M. T., Campos, F. S., Dias, M. M., Velho, F. A., Freneau, G. E., Brito, W. M. E. D., Rijsewijk, F. A. M., Franco, A. C. & Roehe, P. M. (2011). Detection of bovine herpesvirus 1 and 5 in semen from Brazilian bulls. *Theriogenology* **75**, 1139–1145. Elsevier Inc.

Owen, D. J., Crump, C. M. & Graham, S. C. (2015). Tegument assembly and secondary envelopment of alphaherpesviruses. *Viruses* **7**, 5084–5114.

Palmeira, L., Sorel, O., Van Campe, W., Boudry, C., Roels, S., Myster, F., Reschner, A., Coulie, P. G., Kerkhofs, P. & other authors. **(2013).** An essential role for γ-herpesvirus latency-associated nuclear antigen homolog in an acute lymphoproliferative disease of cattle. *Proc Natl Acad Sci U S A* **110**, E1933-42.

Patel, J. R. & Edington, N. (1982). The effect of antibody and complement on the expression of herpesvirus of bovine malignant catarrhal fever in cultured rabbit lymphocytes. *Vet Microbiol* **7**, 325–333.

Peng, L., Ryazantsev, S., Sun, R. & Zhou, Z. H. (2010). Three-Dimensional Visualization of Gammaherpesvirus Life Cycle in Host Cells by Electron

Tomography. *Structure* **18**, 47–58.

Pertel, P. E. (2002). Human Herpesvirus 8 Glycoprotein B (gB), gH, and gL Can Mediate Cell Fusion. *J Virol* **76**, 4390–4400.

Peshev, R. & Christova, L. (2013). Bovine Herpes virus 4 (BHV4) infection induced by stress in imported cows. *Rev Med Vet (Toulouse)* **164**, 112–119.

Piper, K. L., Fitzgerald, C. J., Ficorilli, N. & Studdert, M. J. (2008). Isolation of caprine herpesvirus 1 from a major outbreak of infectious pustular vulvovaginitis in goats. *Aust Vet J* **86**, 136–138.

Powers, J. G., VanMetre, D. C., Collins, J. K., Dinsmore, R. P., Carman, J., Patterson, G., Brahmbhatt, D. & Callan, R. J. (2005). Evaluation of ovine herpesvirus type 2 infections, as detected by competitive inhibition ELISA and polymerase chain reaction assay, in dairy cattle without clinical signs of malignant catarrhal fever. *J Am Vet Med Assoc* **227**, 606–611.

Price, P. J. R., Torres-Domínguez, L. E., Brandmüller, C., Sutter, G. & Lehmann, M. H. (2013). Modified Vaccinia virus Ankara: Innate immune activation and induction of cellular signalling. *Vaccine* **31**, 4231–4234. Elsevier Ltd.

Purushothaman, P., Dabral, P., Gupta, N., Sarkar, R. & Verma, S. C. (2016). KSHV Genome Replication and Maintenance. *Front Microbiol* **7**, 1–14.

Raaperi, K., Orro, T. & Viltrop, A. (2014). Epidemiology and control of bovine herpesvirus 1 infection in Europe. *Vet J* **201**, 249–256.

Rahayu, R., Ohsaki, E., Omori, H. & Ueda, K. (2016). Localization of latency-associated nuclear antigen (LANA) on mitotic chromosomes. *Virology* **496**, 51–58. Elsevier.

Riaz, A., Dry, I., Levy, C. S., Hopkins, J., Grey, F., Shaw, D. J. & Dalziel, R. G. (2014). Ovine herpesvirus-2-encoded microRNAs target virus genes involved in virus latency. *J Gen Virol* **95**, 472–80.

Rodríguez, M., Barrera, M., Sánchez, O., Rodríguez, E. C., Martínez, N., Parra, N. C. & Toledo, J. R. (2012). First report of bovine herpesvirus 5 in bull semen. *Arch Virol* **157**, 1775–1778.

Roperto, F., Pratelli, A., Guarino, G., Ambrosio, V., Tempesta, M., Galati, P., Iovane, G. & Buonavoglia, C. (2000). Natural caprine herpesvirus 1 (CpHV-1) infection in kids. *J Comp Pathol* **122**, 298–302.

Rosbottom, J., Dalziel, R. G., Reid, H. W. & Stewart, J. P. (2002). Ovine herpesvirus 2 lytic cycle replication and capsid production. *J Gen Virol* **83**, 2999–3002.

Rosenberg, I. M. (2006). *Protein Analysis and Purification*. Boston, MA: Birkhäuser Boston.

Rossiter, P. B. (1982). Attempts to protect rabbits against challenge with virulent, cell-associated, malignant catarrhal fever virus. *Vet Microbiol* **7**, 419–425.

Rovnak, J., Quackenbush, S. L., Reyes, R. A., Baines, J. D., Parrish, C. R., Casey, J. W., Bhv, J., Bhv, J., Ohv, J. & Act, J. (1998). Detection of a Novel Bovine Lymphotropic Herpesvirus. *J Virol* **72**, 4237–4242.

Russell, G. C., Stewart, J. P. & Haig, D. M. (2009). Malignant catarrhal fever: A review. *Vet J* **179**, 324–335. Elsevier Ltd.

Russell, G. C., Benavides, J., Grant, D. M., Todd, H., Thomson, J., Puri, V., Nath, M. & Haig, D. M. (2012a). Host gene expression changes in cattle infected with Alcelaphine herpesvirus 1. *Virus Res* **169**, 246–254. Elsevier B.V.

Russell, G. C., Benavides, J., Grant, D., Todd, H., Deane, D., Percival, A., Thomson, J., Connelly, M. & Haig, D. M. (2012b). Duration of protective immunity and antibody responses in cattle immunised against alcelaphine herpesvirus-1-induced malignant catarrhal fever. *Vet Res* **43**, 51.

Ryerson, M. R. & Shisler, J. L. (2018). Characterizing the effects of insertion of a 5.2 kb region of a VACV genome, which contains known immune evasion genes, on MVA immunogenicity. *Virus Res* **246**, 55–64. Elsevier.

Sadeghipour, S. & Mathias, R. A. (2017). Herpesviruses hijack host exosomes for viral pathogenesis. *Semin Cell Dev Biol* **67**, 91–100. Elsevier Ltd.

Samuelson, J. C. (2011). *Heterologous Gene Expression in E.coli*. *Methods*

Mol Biol, Methods in Molecular Biology (T. C. Evans, & M.-Q. Xu, Eds.). Totowa, NJ: Humana Press.

Sathiyamoorthy, K., Chen, J., Longnecker, R. & Jardetzky, T. S. (2017). The complexity in herpesvirus entry. *Curr Opin Virol* **24**, 97–104. Elsevier B.V.

Saura, H., Al-Saadi, M., Stewart, J. P. & Kipar, A. (2018). New Insights into the Pathogenesis of Vasculitis in Malignant Catarrhal Fever. *J Comp Pathol* **158**, 98. Elsevier Ltd.

Schleiss, M. R. (2016). Cytomegalovirus vaccines under clinical development. *J virus Erad* **2**, 198–207.

Schock, a. & Reid, H. W. (1996). Characterisation of the lymphoproliferation in rabbits experimentally affected with malignant catarrhal fever. *Vet Microbiol* **53**, 111–119.

Schock, A., Collins, R. A. & Reid, H. W. (1998). Phenotype, growth regulation and cytokine transcription in Ovine Herpesvirus-2 (OHV-2)-infected bovine T-cell lines. *Vet Immunol Immunopathol* **66**, 67–81.

Schultheiss, P. C., Collins, J. K., Austgen, L. E. & DeMartini, J. C. (1998). Malignant catarrhal fever in bison, acute and chronic cases. *J Vet Diagn Invest* **10**, 255–262.

Schultheiss, P. C., Collins, J. K., Spraker, T. R. & Demartini, J. C. (2000). Epizootic malignant catarrhal fever in three bison herds: differences from cattle and association with ovine herpesvirus-2. *J Vet Diagn Invest* **12**, 497–502.

Scott, F. M. M., Sharp, J. M., Angus, K. W. & Gray, E. W. (1984). Infection of specific-pathogen free lambs with a herpesvirus isolated from pulmonary adenomatosis. *Arch Virol* **80**, 147–162.

Silva.M, S., Weiblen, R., Irigoyen, L. ., Roehe, P. ., Sur, H. ., Osorio, F. . & Flores, E. . (1999). Experimental infection of sheep with bovine herpesvirus type-5 (BHV-5): acute and latent infection. *Vet Microbiol* **66**, 89–99.

Silva, M. L. C. R., Pituco, E. M., Nogueira, A. H. C., Martins, M. S. N., Lima, M. S. & de Azevedo, S. S. (2013). Serological evidence and risk factors associated with Caprine herpesvirus 1 in dairy goat flocks in a

semiarid region of northeastern Brazil. *J Vet Diagnostic Investig* **25**, 125–128.

Simon, S., Li, H., O'Toole, D., Crawford, T. B. & Oaks, J. L. (2003). The vascular lesions of a cow and bison with sheep-associated malignant catarrhal fever contain ovine herpesvirus 2-infected CD8+ T lymphocytes. *J Gen Virol* **84**, 2009–2013.

Sinzger, C. (2008). Entry route of HCMV into endothelial cells. *J Clin Virol* **41**, 174–179.

Slater, O. M., Peters-Kennedy, J., Lejeune, M., Gummer, D., Macbeth, B., Warren, A., Joseph, T., Li, H., Cunha, C. W. & Duignan, P. J. (2016). Sheep-Associated Malignant Catarrhal Fever–Like Skin Disease in a Free-Ranging Bighorn Sheep (Ovis canadensis), Alberta, Canada. *J Wildl Dis* **53**, 2016-05-103.

von Sonnenburg, F., Perona, P., Darsow, U., Ring, J., von Krempelhuber, A., Vollmar, J., Roesch, S., Baedeker, N., Kollaritsch, H. & Chaplin, P. (2014). Safety and immunogenicity of modified vaccinia Ankara as a smallpox vaccine in people with atopic dermatitis. *Vaccine* **32**, 5696–5702. Elsevier Ltd.

Sorel, O., Chen, T., Myster, F., Javaux, J., Vanderplasschen, A. & Dewals, B. G. (2017). Macavirus latency-associated protein evades immune detection through regulation of protein synthesis in cis depending upon its glycin/glutamate-rich domain. *PLoS Pathog* **13**, 1–30.

Spear, P. G., Manoj, S., Yoon, M., Jogger, C. R., Zago, A. & Myscofski, D. (2006). Different receptors binding to distinct interfaces on herpes simplex virus gD can trigger events leading to cell fusion and viral entry. *Virology* **344**, 17–24.

Spear, P. G., Eisenberg, R. J. & Cohen, G. H. (2000). Three Classes of Cell Surface Receptors for Alphaherpesvirus Entry. *Virology* **275**, 1–8.

Stahel, A. B. J., Baggenstos, R., Engels, M., Friess, M. & Ackermann, M. (2013). Two Different Macaviruses, ovine herpesvirus-2 and caprine herpesvirus-2, behave differently in water buffaloes than in cattle or in their respective reservoir species. *PLoS One* **8**, e83695.

Staib, C., Drexler, I. & Sutter, G. (2004). Construction and Isolation of Recombinant MVA. In *Vaccinia Virus and Poxvirology*, pp. 77–99. Totowa, NJ: Humana Press.

Stenglein, M. D., Schumacher, A. J., Larue, R. S. & Harris, R. S. (2009). *Viral Genome Replication* (K. D. Raney, M. Gotte & C. E. Cameron, Eds.). Boston, MA: Springer US.

Suzuki, T., Isobe, T., Kitagawa, M. & Ueda, K. (2010). Kaposi's sarcoma-associated herpesvirus-encoded LANA positively affects on ubiquitylation of p53. *Biochem Biophys Res Commun* **403**, 194–197. Elsevier Inc.

Tabery, H. M. (2010). *Herpes simplex virus epithelial keratitis: In vivo morphology in the human Cornea*. *Herpes Simplex Virus Epithel Keratitis Vivo Morphol Hum Cornea*. Berlin, Heidelberg: Springer Berlin Heidelberg.

Tang, Q., Wu, Y. Q., Chen, D. S., Zhou, Q., Chen, H. C. & Liu, Z. F. (2014). Bovine herpesvirus 5 encodes a unique pattern of microRNAs compared with bovine herpesvirus 1. *J Gen Virol* **95**, 671–678.

Taus, N. S., Traul, D. L., Oaks, J. L., Crawford, T. B., Lewis, G. S. & Li, H. (2005). Experimental infection of sheep with ovine herpesvirus 2 via aerosolization of nasal secretions. *J Gen Virol* **86**, 575–579.

Taus, N. S., Oaks, J. L., Gailbreath, K., Traul, D. L., O'Toole, D. & Li, H. (2006). Experimental aerosol infection of cattle (Bos taurus) with ovine herpesvirus 2 using nasal secretions from infected sheep. *Vet Microbiol* **116**, 29–36.

Taus, N. S., Herndon, D. R., Traul, D. L., Stewart, J. P., Ackermann, M., Li, H., Knowles, D. P., Lewis, G. S. & Brayton, K. A. (2007). Comparison of ovine herpesvirus 2 genomes isolated from domestic sheep (Ovis aries) and a clinically affected cow (Bos bovis). *J Gen Virol* **88**, 40–45.

Taus, N. S., Schneider, D. a., Oaks, J. L., Yan, H., Gailbreath, K. L., Knowles, D. P. & Li, H. (2010). Sheep (Ovis aries) airway epithelial cells support ovine herpesvirus 2 lytic replication in vivo. *Vet Microbiol* **145**, 47–53. Elsevier B.V.

Taus, N. S., O'Toole, D., Herndon, D. R., Cunha, C. W., Warg, J. V., Seal, B. S., Brooking, A. & Li, H. (2014). Malignant catarrhal fever in American bison (Bison bison) experimentally infected with alcelaphine herpesvirus 2. *Vet Microbiol* **172**, 318–322. Elsevier B.V.

Taus, N. S., Cunha, C. W., Marquard, J., O'Toole, D. & Li, H. (2015). Cross-reactivity of neutralizing antibodies among malignant catarrhal fever viruses. *PLoS One* **10**, 1–9.

Taylor, S., Wakem, M., Dijkman, G., Alsarraj, M. & Nguyen, M. (2010). A practical approach to RT-qPCR-Publishing data that conform to the MIQE guidelines. *Methods* **50**, S1–S5. Elsevier Inc.

Tempesta, M., Pratelli, A., Normanno, G., Camero, M., Buonavoglia, D., Greco, G. & Buonavoglia, C. (2000). Experimental intravaginal infection of goats with caprine herpesvirus 1. *J Vet Med Ser B* **47**, 197–201.

Tempesta, M., Camero, M., Sciorsci, R. L., Greco, G., Minoia, R., Martella, V., Pratelli, A. & Buonavoglia, C. (2004). Experimental infection of goats at different stages of pregnancy with caprine herpesvirus 1. *Comp Immunol Microbiol Infect Dis* **27**, 25–32.

Tempesta, M., Camero, M., Bellacicco, A. L., Tarsitano, E., Lorusso, A., Martella, V., Decaro, N., Del Giudice, G., Cassone, A. & other authors. **(2007).** Caprine herpesvirus 1 vaccine with the LTK63 mutant as a mucosal adjuvant induces strong protection against genital infection in goats. *Vaccine* **25**, 7927–7930.

Tempesta, M., Pratelli, A., Greco, G. & Martella, V. (1999). Detection of Caprine Herpesvirus 1 in Sacral Ganglia of Latently Infected Goats by PCR. *J Clin Microbiol* **37**, 1598–1599.

Tempesta, M., Camero, M., Greco, G., Pratelli, A., Martella, V. & Buonavoglia, C. (2001). A classical inactivated vaccine induces protection against caprine herpesvirus 1 infection in goats. *Vaccine* **19**, 3860–3864.

Thakker, S., Purushothaman, P., Gupta, N., Challa, S., Cai, Q. & Verma, S. C. (2015). Kaposi's Sarcoma-Associated Herpesvirus Latency-Associated Nuclear Antigen Inhibits Major Histocompatibility Complex

Class II Expression by Disrupting Enhanceosome Assembly through Binding with the Regulatory Factor X Complex. *J Virol* **89**, 5536–5556.

Thirion, M., Machiels, B., Farnir, F., Donofrio, G., Gillet, L., Dewals, B. & Vanderplasschen, A. (2010). Bovine herpesvirus 4 ORF73 is dispensable for virus growth in vitro, but is essential for virus persistence in vivo. *J Gen Virol* **91**, 2574–2584.

Thiry, J., Tempesta, M., Camero, M., Tarsitano, E., Bellacicco, A. L., Thiry, E. & Buonavoglia, C. (2006a). A live attenuated glycoprotein E negative bovine herpesvirus 1 vaccine induces a partial cross-protection against caprine herpesvirus 1 infection in goats. *Vet Microbiol* **113**, 303–308.

Thiry, J., Tempesta, M., Camero, M., Tarsitano, E., Muylkens, B., Meurens, F., Thiry, E. & Buonavoglia, C. (2006b). Clinical protection against caprine herpesvirus 1 genital infection by intranasal administration of a live attenuated glycoprotein E negative bovine herpesvirus 1 vaccine. *Vet Microbiol* **3**, 33.

Thiry, J., Saegerman, C., Chartier, C., Mercier, P., Keuser, V. & Thiry, E. (2008). Serological evidence of caprine herpesvirus 1 infection in Mediterranean France. *Vet Microbiol* **128**, 261–268.

Thonur, L., Russell, G. C., Stewart, J. P. & Haig, D. M. (2006). Differential transcription of ovine herpesvirus 2 genes in lymphocytes from reservoir and susceptible species. *Virus Genes* **32**, 27–35.

Torres, F. D., Almeida, S. R., Silva, M. S., Weiblen, R. & Flores, E. F. (2009). Distribution of latent bovine herpesvirus 2 DNA in tissues of experimentally infected sheep. *Res Vet Sci* **87**, 161–6.

Torres, F. D., Cargnelutti, J. F., Masuda, E. K., Weiblen, R. & Flores, E. F. (2010). Acute and latent infection by bovine herpesvirus type 2 in a guinea pig model. *Microb Pathog* **48**, 69–73.

Toth, Z., Papp, B., Brulois, K., Choi, Y. J., Gao, S.-J. & Jung, J. U. (2016). LANA-Mediated Recruitment of Host Polycomb Repressive Complexes onto the KSHV Genome during De Novo Infection. *PLOS Pathog* **12**, e1005878.

Traul, D. L., Elias, S., Taus, N. S., Herrmann, L. M., Oaks, J. L. & Li, H.

(2005). A real-time PCR assay for measuring alcelaphine herpesvirus-1 DNA. *J Virol Methods* **129**, 186–190.

Tryland, M., Das Neves, C. G., Sunde, M. & Mørk, T. (2009). Cervid herpesvirus 2, the primary agent in an outbreak of infectious keratoconjunctivitis in semidomesticated reindeer. *J Clin Microbiol* **47**, 3707–3713.

Vanderplasschen, A., Bublot, M., Pastoret, P. P. & Thiry, E. (1993). Restriction maps of the DNA of cervid herpesvirus 1 and cervid herpesvirus 2, two viruses related to bovine herpesvirus 1. *Arch Virol* **128**, 379–388.

Vanderplasschen, A., Goltz, M., Lyaku, J., Benarafa, C., Buhk, H. J., Thiry, E. & Pastoret, P. P. (1995). The replication in vitro of the gammaherpesvirus bovine herpesvirus 4 is restricted by its DNA synthesis dependence on the S phase of the cell cycle. *Virology* **213**, 328–340.

Vandevanter, D. R., Warrener, P., Bennett, L., Schultz, E. R., Coulter, S., Garber, R. L. & Rose, T. M. (1996). Detection and analysis of diverse herpesviral species by consensus primer PCR. *J Clin Microbiol* **34**, 1666–1671.

Verheust, C., Goossens, M., Pauwels, K. & Breyer, D. (2012). Biosafety aspects of modified vaccinia virus Ankara (MVA)-based vectors used for gene therapy or vaccination. *Vaccine* **30**, 2623–2632. Elsevier Ltd.

Verma, S. C., Lan, K. & Robertson, E. (2007). Structure and function of latency-associated nuclear antigen. *Curr Top Microbiol Immunol* **312**, 101–36.

Verna, A. E., Manrique, J. M., Pérez, S. E., Leunda, M. R., Pereyra, S. B., Jones, L. R. & Odeón, A. C. (2012). Genomic analysis of bovine herpesvirus type 4 (BoHV-4) from Argentina: High genetic variability and novel phylogenetic groups. *Vet Microbiol* **160**, 1–8.

Verna, A. E., Pérez, S. E., Manrique, J. M., Leunda, M. R., Odeón, A. C. & Jones, L. R. (2016). Comparative study on the in vitro replication and genomic variability of Argentinean field isolates of bovine herpesvirus type 4 (BoHV-4). *Virus Genes* **52**, 372–378.

Vikøren, T., Li, H., Lillehaug, A., Monceyron Jonassen, C., Böckerman, I. & Handeland, K. (2006). MALIGNANT CATARRHAL FEVER IN FREE-RANGING CERVIDS ASSOCIATED WITH OVHV-2 AND CPHV-2 DNA. *J Wildl Dis* **42**, 797–807.

Vinet, L. & Zhedanov, A. (2005). *Molecular Diagnostic PCR Handbook*. *J Phys A Math Theor*. Berlin/Heidelberg: Springer-Verlag.

Vogel, F. S. F., Caron, L., Flores, E. F., Weiblen, R., Winkelmann, E. R., Mayer, S. V. & Bastos, R. G. (2003). Distribution of Bovine Herpesvirus Type 5 DNA in the Central Nervous Systems of Latently, Experimentally Infected Calves. *J Clin Microbiol* **41**, 4512–4520.

Walker, J. M. (2012). *Protein Electrophoresis*. Methods in Molecular Biology (B. T. Kurien & R. H. Scofield, Eds.). Totowa, NJ: Humana Press.

Wambua, L., Wambua, P. N., Ramogo, A. M., Mijele, D. & Otiende, M. Y. (2016). Wildebeest-associated malignant catarrhal fever: perspectives for integrated control of a lymphoproliferative disease of cattle in sub-Saharan Africa. *Arch Virol* **161**, 1–10. Springer Vienna.

Wang, C. & Mei, L. (2013). *Neural Development*. *Methods Mol Biol*, Methods in Molecular Biology (R. Zhou & L. Mei, Eds.). Totowa, NJ: Humana Press.

Wang, Z., Martinez, J., Zhou, W., La Rosa, C., Srivastava, T., Dasgupta, A., Rawal, R., Li, Z., Britt, W. J. & Diamond, D. (2010). Modified H5 promoter improves stability of insert genes while maintaining immunogenicity during extended passage of genetically engineered MVA vaccines. *Vaccine* **28**, 1547–1557.

Wellenberg, G. J., Van Der Poel, W. H. M. & Van Oirschot, J. T. (2002). Viral infections and bovine mastitis: A review. *Vet Microbiol* **88**, 27–45.

Whitley, R. J. (2014). *Herpes Simplex Virus*. *Curr Treat Options Neurol*, Methods in Molecular Biology (R. J. Diefenbach & C. Fraefel, Eds.). New York, NY: Springer New York.

Winkler, M. T. C., Doster, A. & Jones, C. (2000). Persistence and Reactivation of Bovine Herpesvirus 1 in the Tonsils of Latently Infected Calves. *J Virol* **74**, 5337–5346.

Woods, J. A., Herring, J. A., Nettleton, P. F., Kreuger, N., Scott, F. M. M.

& Reid, H. W. (1996). Isolation of bovine herpesvirus-2 (BHV-2) from a case of pseudolumpy skin disease in the United Kingdom. *Vet Rec* **138**, 113–114.

Wüthrich, D., Boujon, C. L., Truchet, L., Selimovic-Hamza, S., Oevermann, A., Bouzalas, I. G., Bruggmann, R. & Seuberlich, T. (2016). Exploring the virome of cattle with non-suppurative encephalitis of unknown etiology by metagenomics. *Virology* **493**, 22–30. Elsevier.

Wyatt, L. S., Earl, P. L., Vogt, J., Eller, L. A., Chandran, D., Liu, J., Robinson, H. L. & Moss, B. (2008). Correlation of immunogenicities and in vitro expression levels of recombinant modified vaccinia virus Ankara HIV vaccines. *Vaccine* **26**, 486–493.

Xiao, B., Verma, S. C., Cai, Q., Kaul, R., Lu, J., Saha, A. & Robertson, E. S. (2010). Bub1 and CENP-F can contribute to Kaposi's sarcoma-associated herpesvirus genome persistence by targeting LANA to kinetochores. *J Virol* **84**, 9718–32.

Yeruham, I., Goshen, T., David, D., Brenner, J. & Perl, S. (2004). Malignant catarrhal fever in a Barbary sheep (Ammotragus lervia). *Vet Rec* **155**, 463–465.

You, J., Srinivasan, V., Denis, G. V., Harrington, W. J., Ballestas, M. E., Kaye, K. M. & Howley, P. M. (2006). Kaposi's Sarcoma-Associated Herpesvirus Latency-Associated Nuclear Antigen Interacts with Bromodomain Protein Brd4 on Host Mitotic Chromosomes. *J Virol* **80**, 8909–8919.

Zaldumbide, A., Ossevoort, M., Wiertz, E. J. H. J. & Hoeben, R. C. (2007). In cis inhibition of antigen processing by the latency-associated nuclear antigen I of Kaposi sarcoma Herpes virus. *Mol Immunol* **44**, 1352–1360.

Zhang, G., Chan, B., Samarina, N., Abere, B., Weidner-Glunde, M., Buch, A., Pich, A., Brinkmann, M. M. & Schulz, T. F. (2016). Cytoplasmic isoforms of Kaposi sarcoma herpesvirus LANA recruit and antagonize the innate immune DNA sensor cGAS. *Proc Natl Acad Sci* **113**, E1034–E1043.

ŽIAK, J., KOPTIDESOVÁ, D., OVEČKOVÁ, I., REJHOLCOVÁ, O., KOPÁČEK, J., KÚDELOVÁ, M. & ZELNÍK, V. (2014). Ovine

herpesvirus 1 (OVHV-1) thymidine kinase locus sequence analysis: evidence that OVHV-1 belongs to the Macavirus genus of the Gammaherpesvirinae subfamily. *Acta Virol* **58**, 190–193.

Zuo, J. & Rowe, M. (2012). Herpesviruses Placating the Unwilling Host: Manipulation of the MHC Class II Antigen Presentation Pathway. *Viruses* **4**, 1335–1353.